Developing Spatio-temporal Models of Schistosomiasis Transmission with Climate Change

Thesis submitted in accordance with the requirements of the University of Liverpool for the degree of Doctor in Philosophy by Tara Danielle Mangal

August 2009

Table of Contents

List of Figures

List of Tables

Abbreviations

AIC	Aikake's Information Criterion
ANOVA	Analysis of Variance
CIESIN	Center for International Earth Science Information Network
CLIMPAG	Climate Impact on Agriculture
DDC	Data Distribution Centre
ESIP	Earth Science Information Partner
FAO	Food and Agriculture Organization
GIS	Geographic Information Systems
GLM	Generalised Linear Model
GRID	Global Resource Information Database
IPCC	Intergovernmental Panel for Climate Change
IWLS	Iteratively Weighted Least Squares
LME	Linear Mixed Effects Models
LRM	Logistic Regression Model
LST	Land Surface Temperature
NCAR	National Center for Atmospheric Research
NDVI	Normalised Difference Vegetation Index
RS	Remote Sensing
UN	United Nations
UNEP	United Nations Environment Programme
WHO	World Health Organization

Acknowledgments

This thesis was carried out under the joint supervision of Dr Andy Fenton and Dr Steve Paterson. I would like to extend my thanks to my primary supervisor, Dr Fenton, for his valuable support and encouragement throughout my time at the University of Liverpool. Furthermore, I truly appreciate being given the freedom to develop my own research. My thanks also go to Dr Mike Doenhoff, formally at Nottingham University for the supplies of snails and parasites throughout my research period along with expert advice on culture methods and protocols. Dr David Atkinson and Dr David Montagnes were very supportive throughout my PhD, acting as internal referees and giving assistance whenever needed. I thank them both for useful comments on my thesis and guidance on developing my research priorities.

This thesis would not have been possible without the freely accessible data provided by the World Health Organization, the Food and Agriculture Organization of the United Nations, the United Nations Environment Programme, the Centre national d'études spatiales in France and Dr Xiangming Xiao, at the University of New Hampshire, EOS-WEBSTER Earth Science Information Partner.

On a personal note, I would like to thank my partner James for his patience, support and encouragement throughout the last three years. Finally, I would like to extend my deepest thanks to my parents, for their unending support and belief in me.

Abstract

Schistosomiasis is one of the most prevalent diseases in the world and a major cause of morbidity in Africa. Accurate determination of the geographical distribution of schistosomiasis in Africa along with the number of people affected is difficult, since reliable prevalence data are often not available for most of the African continent. Effective schistosomiasis control programmes rely on accurate statistics regarding the geographical distribution of disease, the population at risk, and the intensity of disease transmission. These estimates can be obtained using a number of statistical methods which relate prevalence and intensity of disease to risk factors, measured at the individual level and at the population level. *Schistosoma mansoni* is largely a climate-driven parasite, which relies on the availability of a suitable snail host. The survival of parasitic infection depends on climatic variables, such as temperature, rainfall and vegetation. Statistical models which incorporate spatial or individual heterogeneity are highly complex and require large numbers of parameters. Until recently, the most common approach was to use regression modelling to identify risk factors for disease transmission. However, this method has a number of limitations. In particular, it gives no information on the dynamics of transmission, e.g. will the disease reach an endemic state under a certain set of conditions or be subject to a periodic cycle?

The aim of this thesis was to a) develop mechanistic transmission models to study how schistosomiasis disease dynamics change with water temperature change and to parameterise these models to provide better estimates for a specific host-parasite combination; b) explore how the efficacy of control programmes changes with changing water temperature; c) produce continent-wide maps of schistosomiasis prevalence in Africa, using a combination of geospatial models and environmental data; d) to quantify

the impact of climate change over the next 50 years on the prevalence and intensity of disease.

A mechanistic model describing the transmission dynamics of schistosomiasis at a range of water temperatures was developed and showed that as the long-term mean temperature increases up to 29°C, the mean worm burden increases. At 34°C, the mean worm burden starts to taper, as the thermal limits of both the snail and the parasite are reached. Adding complexity to the models, such as snail density-dependence and adult parasite density-dependence, had no significant impact on the overall transmission patterns. However, a sensitivity analysis revealed subtle changes in the relative importance of certain parameters. The most detailed model showed that the parameters describing the transmission of schistosomes from snail to man were the most sensitive to change and therefore, provided a useful target point for control strategies. The effects of various control programmes were modelled using discrete time series models and manipulation of the individual parameters. The most effective control programme was repeated mass chemotherapy, although reducing contact with contaminated water also proved highly effective.

Producing maps of geo-referenced point prevalence data highlighted the areas in which no data currently exist. This provides an invaluable tool for determining which regions need further study. Four separate geospatial models were developed to predict the distribution of schistosomiasis over Africa, and each was validated using existing data. The ordinary kriging model provided the best estimates for prevalence data and the indicator kriging model provided the best estimates for the probability of infection within a population. These models are useful for determining high-risk populations and locating areas in which control efforts should be focussed. Two types of regression models were used to investigate associations between climatic variables and prevalence of disease. Monthly rainfall and mean annual temperature were shown to have

important roles in defining the limits of schistosomiasis transmission. Using these data, it is possible to define a threshold, outside which schistosomiasis transmission is unlikely to occur. These models were used to predict how the distribution of schistosomiasis would change with climate change. It was shown that over the next 50 years, there will be an increase in the number of areas able to support the intermediate vector. Without socio-economic development or intervention strategies, this will almost certainly be followed by an increase in disease transmission. The use of mathematical and geospatial models can greatly enhance our understanding of schistosome epidemiology and are an essential tool in the planning stages of any intervention strategy.

CHAPTER 1

Introduction

1.1 Biology and epidemiology of human schistosomiasis

Schistosomiasis is a parasitic disease caused by digenetic trematodes, belonging to the Schistosomatidae family. It is currently endemic in 74 developing countries, infecting an estimated 200 million people (Mascie-Taylor and Karim 2003; Vennervald and Dunne 2004). Schistosomiasis is a major public health problem, causing debilitating disease, including dysentery, fever, intestinal obstruction, widespread granulomas and bladder cancer (Mascie-Taylor and Karim 2003). It is primarily found in rural areas in tropical and subtropical countries and infects humans and other vertebrates, using freshwater snails of the genera *Biomphalaria, Bulinus* and *Oncomelania* as intermediate hosts. Transmission relies upon natural water polluted with human excreta, often found in areas of poverty or low income, where a lack of facilities forces people to use natural water bodies for domestic, recreational, occupational, or religious purposes.

The three species responsible for the majority of human infections are *Schistosoma mansoni, S. haematobium* and *S. japonicum*, which can give rise to heavy infections and severe pathology. *Schistosoma intercalatum* and *S. mekongi* are less well distributed but are also capable of causing significant morbidity in humans. *Schistosoma mansoni* infections are found in most countries in Sub-Saharan Africa, extending from the Nile Valley down to coastal regions of Mozambique, and spreading westwards to Gambia and Senegal. A range of mammals can be infected, although humans are the main reservoir of infection. The distribution of each species of schistosome depends upon the availability of susceptible intermediate snail hosts, resulting in an irregular distribution pattern, varying between communities even in endemic countries.

A number of control programmes have been implemented throughout Africa, including wide-scale applications of molluscicides and chemotherapy, but none so far

have achieved long-term control. Several promising schistosome antigens have been identified as candidates for vaccines but to date, high success rates in the field have not been documented (Gryseels 2000). Control programmes have reduced the incidence of schistosomiasis in some areas by limiting human contact with infected water, removing snail habitats by environmental, chemical or biological means, or by chemotherapy. However, the recent construction of water development projects for agricultural purposes and hydroelectric power has created new habitats for snails and attracted large numbers of people, forced there by lack of work, natural disasters, or civil disorder. This, combined with a lack of adequate sanitation and health education, has increased the transmission of schistosomiasis in developing countries as well as introducing it to previous unaffected areas (Hunter 1993).

1.2 Transmission of schistosomiasis

1.2.1 The schistosome life-cycle

Schistosome eggs are released in the faeces or urine of infected animals and humans (Fig. 1). If they are deposited in warm, fresh water, the egg will hatch to produce a motile, ciliated miracidium that has an average life span of 8-12 hours (Carter *et al.* 1982). Miracidia contain finite energy reserves, and their rate of activity determines the rate at which their food stores are exhausted. This is dependent upon external conditions and factors which influence their behaviour, including temperature, light, water currents, turbidity, and chemical stimuli (El Hassan 1974; Prah and James 1978). Miracidia are attracted to macromolecules emitted by *Biomphalaria* and other species of snails and alter their behaviour in a manner which suggests chemokinesis rather than

chemotaxis (Chernin 1970; Haas *et al.* 1994; Haas *et al.* 1995). The ability of miracidia to locate and penetrate compatible hosts is influenced by a number of variables, including light, gravity, and temperature, and is density-dependent, age-dependent and time/space-dependent (Sturrock and Upatham 1973; Carter *et al.* 1982).

Successfully infecting miracidia penetrate the soft tissue of the snail body and transform into primary sporocysts. Each sporocyst undergoes several cycles of asexual reproduction and produces thousands of secondary sporocysts, which migrate through the host tissue and develop into cercariae. These are released from the snail in vast numbers displaying diurnal periodicity, stimulated by light and temperature (Sturrock and Sturrock 1970; Theron 1984). The shedding pattern is related to the activity periods of the definitive hosts and can vary depending on the site of transmission and the most common definitive host (Theron 1984; Mouchet *et al.* 1992; Favre *et al.* 1995). For example, in sites where a murine host is common, cercariae are released late in the evenings, to coincide with the crepuscular / nocturnal activity of their hosts (Theron 1984). This adaptation favours transmission of the parasite and the chronobiology of cercarial emergence can be used as a marker for selection (Pages and Theron 1990). The prepatent period, from penetration to cercarial shedding, varies between 17-18 days to several months depending on temperature (Pfluger 1980; Lewis *et al.* 1986). Over several months, one miracidia is capable of producing hundreds of thousands of cloned cercariae under optimal conditions.

Cercariae have limited resources and their swimming behaviour is stimulated by changes in light intensity and vibrations in the water. They tend to swim in intermittent bursts, followed by periods of slow falling, often remaining passive to conserve energy until stimulated by a potential host. Some species of schistosome exhibit different swimming behaviour; *S. mansoni* and *S. japonicum* cercariae usually stay near the surface of the water whereas *S. haematobium* cercariae tend to accumulate near the

riverbed (Mahmoud 2001). The cercariae die within 48-72 hours, although infectivity drops after 24 hours (Purnell 1966). Their exact life span depends upon the rate at which they use up their glycogen stores, which in turn is dependent upon the frequency of stimulation and the ambient temperature (Lawson and Wilson 1980).

As cercariae penetrate the skin of the definitive mammalian host, they lose their tails and enter the blood stream as a schistosomulum. The immature flukes use the host's vascular system to migrate towards the liver where they develop in the hepatic sinusoids (Jordan 1993). There they mature to dioecious adults and mate for life, producing between 100 and 300 non-operculated eggs per day (Loker 1983). The miracidium develops within the egg as it moves through the tissues and the lumen of the intestines or urinary tract and out of the host. Most of the associated pathology caused by schistosomiasis is due to the immune response mounted against the trapped eggs (Cheever 1968; Jordan 1993).

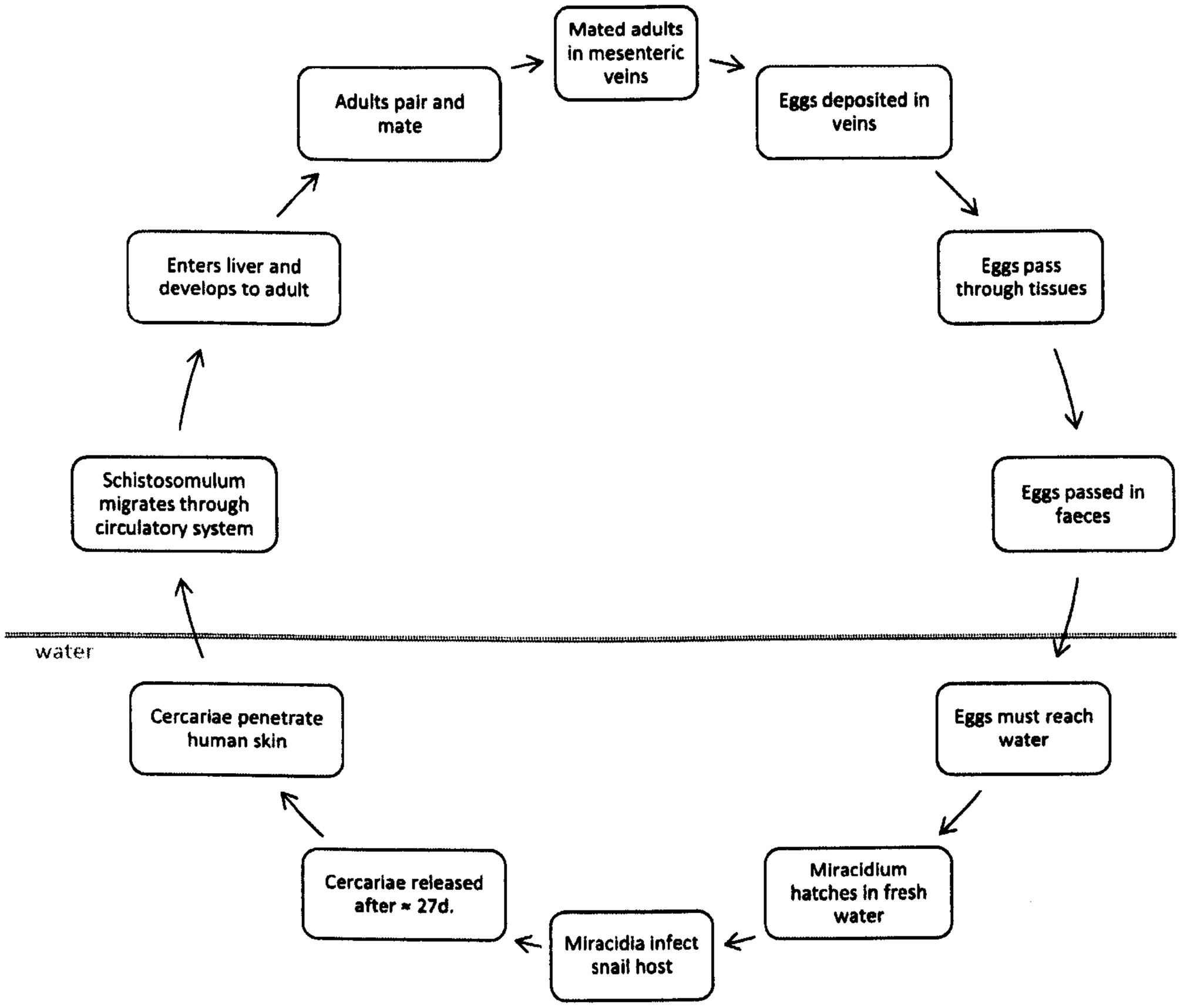

Figure 1.1. *Schistosoma mansoni*life-cycle.

1.2.1 Intermediate host snail ecology

Biomphalaria spp. snails are found throughout Africa, the Middle East and South/Central America, and all are susceptible to *S. mansoni* to varying degrees. These pulmonate snails are hermaphroditic and are capable of self-fertilisation, although cross fertilisation is more common (Jordan 1993). The rate of egg production is directly related to the size of the snail (Loker 1983). Egg masses are usually 1cm in length, containing an average of 15 eggs per mass. Hatching and development is temperature-dependent, and usually occurs within 5-10 days, producing snails of 0.5-1.0mm diameter. The snails reach sexual maturity in 4-12 weeks when they are approximately 5mm in diameter and they continue to grow throughout their lives.

Freshwater snails are able to thrive in a wide range of physiochemical conditions and a colony can become established in almost any body of water. The optimum water temperature for snails infected with schistosomiasis is 23-25°C and snails are adversely affected by temperature extremes either way (Stirewalt 1954; Loreau and Baluku 1987). As the temperature falls, growth rate and reproduction begin to slow, and mortality is increased when the temperature falls below 5°C (El Hassan 1974; Pimentel-Souza *et al.* 1990). Increasing temperature favours growth and development but fecundity is reduced as the temperature rises above 30°C. Snail mortality is also affected by high temperatures (>35°C), although they can survive short exposures to extreme temperatures (Foster 1964; El Hassan 1974; Appleton 1977).

Biomphalaria snails adapt to less stable environments by increasing their reproductive efforts earlier in life (Blair and Webster 2007). They are capable of surviving extreme conditions using behavioural changes such as aestivating during droughts, and due to their hermaphroditic nature, one surviving snail can repopulate an area. The snails can, therefore, tolerate most intervention programmes, such as drainage of irrigation canals and molluscicide treatment.

1.3 Impact of environmental variables on snail and parasite life-history traits

1.3.1 Temperature

Maintenance temperatures affect every stage of the *S. mansoni* and *Biomphalaria* life-cycle, and increases in temperature generally increase fitness up to a critical threshold, at which the fitness levels decline rapidly and death quickly follows (Kuntz 1947; Stirewalt 1954; Purnell 1966; Upatham 1973; El Hassan 1974; Woolhouse and Chandiwana 1990a). The optimal water temperature range for *Biomphalaria* spp. lies between 20-30°C (Sturrock 1993). Below 15°C, parasitic development is inhibited and they are unable to spread disease further. Above 30°C, reproductive activity is also reduced and mortality rates increase up to the thermal death point (approx. 40°C) (Pfluger 1980). High water temperatures may explain the absence of *Biomphalaria* spp. and consequently, schistosomiasis, from the East African coast (Sturrock 1966b). The effect of an increase in temperature is to accelerate development rates of the parasite and snail host, and consequently, increase transmission rate. The relationship between the infection rate of miracidia and temperature is linear up to the thermal death point of the snails (Martens *et al.* 1997). The change in miracidial infection rate due to temperature also influences the snail mortality rate, as parasitic infection reduces the life-expectancy of the snail. Higher temperatures reduce the survival rate of the intermediate host, so fewer of them will survive the pre-patent period of infection and release infective cercariae. Therefore, there are upper and lower temperature thresholds outside which schistosomiasis transmission is not viable.

1.3.2 Rainfall and vegetation

Rainfall is one of the most important factors affecting snail populations in tropical areas (Sturrock 1993). Seasonal variations in snail populations have been well documented throughout Africa (Shiff 1964; Webbe 1964; McCullough 1972) with the most pronounced effects seen in temporary breeding habitats (Sturrock 1993). During prolonged periods of low rainfall, snail populations temporarily diminish and only return when rainfall exceeds 4-8 inches per month (Sturrock 1973b). Low rainfall can cause small, standing water bodies to dry out, which will result in high snail mortality, although studies have shown that some species of snails can survive during prolonged dry periods. (Barbosa and Coelho 1955; Sturrock 1993). Reducing the water volume in larger water bodies will reduce the flow of water and may create new, favourable habitats for snails. These newly formed pools of standing water are also prone to drying out following a long period of drought. During episodes of high rainfall, snails can be washed out from their existing habitats and standing water bodies can become fast-flowing streams, unsuitable for habitation (Sturrock 1993). Conversely, rainfall can create new standing pools of water, ideal for snail populations. Increased levels of rainfall can increase the density of vegetation in water bodies, which will provide sheltered breeding sites and a food source for snails (Klumpp and Chu 1977).

1.4 Control programmes

As recently as 1970, most efforts to control schistosomiasis transmission were centred on the intermediate snail vector, with the belief that reducing the density of vectors would cause a substantial reduction in the prevalence and intensity of infection in the community (Hairston 1961; Webbe 1964; Webbe and Sturrock 1964). This targeted approach towards snail control was subsequently changed for two reasons. Firstly, reducing the density of snail intermediate hosts had only a transient effect on

disease transmission as the snails rapidly repopulated the area and so continued transmitting disease (Thomas 1987; Jordan 1993). Secondly, the high cure rates and low cost of chemotherapy changed the emphasis from snail host control to targeting the definitive human host (Asaolu and Ofoezie 2003). One of the main reasons for this change in control efforts stems from the availability of cheap, safe and effective drugs, principally praziquantel and oxamniquine (Magnussen 2003). Large-scale schistosomiasis control programmes depend heavily on external donor support. Even though drug costs have decreased over the past decade, many governments are still unable to meet the costs of a mass treatment programme. The current lack of an effective vaccine means that control of schistosomiasis is almost completely dependent on the availability and efficacy of cheap drugs. Initially, control programmes often show high success rates in reducing disease prevalence, but this success rate often decreases with successive assessments (Shuval *et al.* 1981). The early period of success gradually slows towards a saturation point, at which point investments in control programmes no longer deliver commensurate benefits.

1.4.1 Chemotherapy

Currently, large-scale chemotherapy programmes are the most commonly used intervention strategy for controlling schistosomiasis. The cost of a single dose of 600mg praziquantel has fallen to U$0.07 and causes a 60-90% reduction in egg numbers excreted in the faeces (Magnussen 2003; Scherrer *et al.* 2009) and so provides an affordable and cost-effective tool. Recently, concerns of resistance/tolerance to praziquantel have emerged following a number of low cure rates documented in high transmission areas (e.g. Egypt and Senegal) (Gryseels *et al.* 2001; Danso-Appiah and De Vlas 2002; Botros *et al.* 2005), leading to a renewed effort to develop new drugs for schistosomiasis. Artemether and artesunate are both highly effective against juvenile *S.*

japonicum (Utzinger *et al.* 2001) and may be successful in controlling *S. mansoni* and *S. haematobium* (Cioli 1998; Utzinger *et al.* 2000), although the widespread use of these artemisinine derivatives cannot be recommended in malaria endemic regions as it may induce drug resistance in malaria parasites (TDR 2000).

1.4.2 Molluscicide

The use of molluscicides in the control of schistosomiasis transmission is now less common than 30 years ago, when it was the control programme of choice. This is due to the relatively high costs of molluscicides coupled with the low long-term efficacy and the advent of cheaper, effective drugs. The use of molluscicides is generally limited to areas with focal transmission. Only one organic molluscicide, Niclosamide, is currently used in control programmes and results in 100% snail mortality when applied to small water bodies (Greer *et al.* 1996). Initial concentrations of 0.3 p.p.m. of Niclosamide are sufficient to kill 100% of *Bulinus coulboisis*, *Biomphalaria pfeifferi*, and *Limnaea natalensis* in ponds, and the treatment remains stable in the water for a considerable time, dropping between 5-10% within 24 hours (Sturrock *et al.* 1974). This treatment has no impact on snail eggs, and the reappearance of snails 10 weeks after Niclosamide application suggests that repeated treatment is necessary for sustained control of the snailpopulation. However, costs for the chemical and its application come to around $0.23 per person per year for a single treatment and so repeated application is neither practical nor affordable in many endemic regions. One application would suppress the snail population and would undoubtedly cause a transient but unsustainable reduction in transmission levels. Another disadvantage of using Niclosamide is its toxicity to fish and other aquatic animals. In a community dependent on fishing for their livelihood and sustenance, this method cannot be advocated.

1.4.3 Health education and sanitation

Programmes that improve sanitation in a community usually combine provision of clean water supplies along with health education. It is, therefore, difficult to directly quantify the impact of improvements in sanitation alone. Huttly (1990) proposed that sanitation has an inverse relationship with environmental contamination and disease transmission, both of which are directly related to each other. A lack of adequate sanitary facilities means that infective human faecal matter may remain in open, communal areas. It therefore follows that low income communities with little or no sanitation may be continually exposed to faecal-borne pathogens, such as *Ascaris*, *Trichuris* and *Schistosoma* species. In areas without adequate sanitation, water bodies may easily become contaminated with parasites. This is supported by several studies, which show an association between use of bucket and pit latrines with high prevalence and intensity of helminth infections (Elkins *et al.* 1986; Asaolu and Ofoezie 2003). When sanitation and improvements in water supply have been introduced into a community, schistosomiasis prevalence dropped by 25.6-69.9% (Asaolu and Ofoezie 2003). Although the increased availability of flush toilets should have a positive impact of the rate of helminth infection in a community, this is not always the case (Holland *et al.* 1988; Huttly 1990). This is because local attitudes to western-style toilets differ, many communities do not have sufficient water available for the latrines to function properly and some prefer not to use the newer facilities. Health education alone has resulted in an 86% reduction in the prevalence of schistosomiasis in Mauritius (Dhunputh 1994). The role of sanitation combined with health education cannot be underestimated as it is a feasible and low-cost approach with a sustainable outcome. It should, therefore, be recommended as the first option in disease control and will additionally facilitate the use of alternative control strategies, such as chemotherapy.

1.5 Global warming and schistosomiasis

There is evidence of temperature-related shifts in the distribution of schistosomiasis in China (Confalonieri 2007). China is experiencing an increase in *S. japonicum* infections despite 50 years of control programmes against the snail vector, *Oncolmelania hupensis*, and against the parasite using mass praziquantel administration (Mas-Coma 2009). This resurgence could be due to anthropogenic changes, such as the construction of the Three Gorges Dam, or environmental changes, e.g. flooding. The impact of climate change has also been considered (Zhou *et al.* 2005). The effects of flooding on snail distribution in the Lower Yangtze River basin were studied using remote sensing (Seto *et al.* 2002; Zhou *et al.* 2002). However, predictive spatial models were complicated by the presence of *O. hupensis* subspecies that varied in their habitat preferences. Predicting the distribution of *O. hupensis* in China using remote sensing proved difficult, as seasonal flooding complicated identification of snail habitats.

Currently, it is thought that an increase in annual water temperature will increase the extent and intensity of schistosomiasis transmission (Yang *et al.* 2006). There will be an expansion in regions able to support the snail hosts, and the number of parasite generations will increase as development rates increase (Brooker *et al.* 2000; Yang *et al.* 2005b). To date, there have been no attempts to quantify the impact of temperature increases on the distribution of *Schistosoma mansoni* throughout Africa. This is made particularly difficult by the lack of comprehensive prevalence data throughout this continent and the inconsistent availability of accurate climate data.

Clearly, global warming will directly affect aquatic environments and the presence of suitable water bodies for the intermediate host of schistosomiasis. Increasing the number of suitable habitats could increase the risk of infection to humans

and expand the current distribution of disease (Bergquist 2001a; Bergquist 2001b). Temperature, rainfall, vegetation density, and altitude can significantly alter both the parasite and the intermediate host life-cycle (Bavia *et al.* 2001; Kristensen *et al.* 2001; Zhou *et al.* 2001). Changes in the suitability of habitats able to support the intermediate host and parasite are becoming increasingly important as increased temperatures brought about through anthropogenic climate change may allow the spread of this parasite into previously uninfected areas.

Schistosomiasis population dynamics and the impact of disease burden have been well studied and extensively documented (Anderson and May 1979a; Anderson and Crombie 1984; Woolhouse and Chandiwana 1990b; Anderson 1991; Woolhouse 1991; Woolhouse 1992; Woolhouse 1994), but these models focus only on the temporal changes in transmission. These models are invaluable to understanding the epidemiology of disease and the impact of control programmes. However, an understanding of the spatial distribution is fundamental to understanding the epidemiology of disease.

1.6 General transmission models of schistosomiasis

Modelling the transmission of an infectious disease requires a balance between including enough detail to model the complex dynamics of the system in question and obtaining enough relevant data to accurately determine the key parameters. The value of the model lies both in its ability to accurately predict scenarios given a defined set of parameter values and its ease of use to field workers. One of the most difficult choices in developing a model is determining how much detail to include, making the model user-

friendly but still as accurate as possible. The first transmission model of schistosomiasis was developed by MacDonald (1965) and was used to provide predictions for schistosomiasis control. Since then, numerous schistosomiasis models have been developed, with varying degrees of complexity (Cohen 1977; Griffin 1988; Woolhouse 1991; Woolhouse 1992; Feng *et al.* 2002; Yang 2003; Das *et al.* 2006). Woolhouse (1991) reviewed existing schistosome transmission models and added a number of modifications, including reservoir hosts, population dynamics of miracidia and cercariae, seasonality and heterogeneous transmission. The importance of including snail dynamics was noted in this paper. Density-dependence within the snail population was modelled by Feng *et al.* (2002), and differences between this model and existing models have important implications for establishing effective treatment programmes. The stabilising effect of acquired immunity in the human population and age-structured water contact patterns have been discussed by Yang and Yang (1998; 2003).

Predicting the effects of control programmes in a community setting is extremely complex and involves a large number of parameters. Using a model, these parameters can be repeatedly manipulated to explore the various control approaches and determine the level of coverage needed for a significant reduction in morbidity. One issue in this type of modelling is the validity of the model in relation to the specific ecology of the area (Williams *et al.* 2002). The effects of various control programmes and the criteria for eradication of disease have been discussed previously (Woolhouse 1992; Allen and Victory 2003; Das *et al.* 2006; Zhao 2008). These models highlight important features of the schistosome transmission model but draw different conclusions. Models of control programmes for *S. japonicum* in China have simulated the effects of vaccines, mass treatment programmes and improvements in sanitation (Williams *et al.* 2002; Ishikawa *et al.* 2006). These models were based on field observations and include seasonal variations and heterogeneity in transmission to humans. Many of the countries with

endemic schistosomiasis have limited funds for healthcare resources, so it is essential that only the most effective and cost-efficient programmes are used. The complex nature of these decisions necessitates the use of mathematical models in exploring the various choices of control programmes. Each model has limitations and decisions must be made on which parameters are important in determining the trends in transmission dynamics and which have a relatively small impact.

1.7 Spatial epidemiology of schistosomiasis

Spatial epidemiology is the study of the geographical distribution of a disease and its relationship to potential risk factors. The origins of spatial epidemiology date back to 1855, with the seminal work of Snow on cholera transmission in London (Snow 1856). Modern methods make use of data derived from satellite sensors along with statistical modelling to provide an integrated approach to risk mapping. These methods allow us to establish risk factors for disease transmission, determine the spatial auto-correlation in disease occurrence, and predict prevalence at new locations. Spatial epidemiology can identify areas at high risk of infection and ascertain which potential environmental and socio-behavioural risk factors explain spatial heterogeneity. Defining the relationship between environmental variables and schistosomiasis risk allows prediction of the effects of environmental changes on disease, including the impact of human interventions (irrigation schemes, urbanisation, etc.) and global warming. Understanding the significance of environmental variables is important for successful control efforts, which are targeted at both the parasite within the human host and the

snail hostand the snail habitat. Maps of disease distribution and burden are essential in planning intervention programmes.

1.7.1 GIS and remote sensing

A geographic information system (GIS) is a tool for capture, analysis, and display of georeferenced datasets. Data from different sources are georeferenced and stored as layers within a geodatabase. The spatial relationship between data in each dataset can be analysed and used to produce maps highlighting the feature of interest. Geographic information systems can be used to study both natural and human factors affecting the spatial distribution of schistosomiasis and analyse them along with co-infections and changes in environmental variables. GIS-based mapping is particularly useful in highlighting areas in which little or no data exist. Previous studies have investigated statistical correlations between environmental variables and the spatial distribution of diseases to identify significant relationships (Rogers and Randolph 1991; Rogers and Williams 1993; Hay *et al.* 1998). The most significant variables may vary from place to place (Rogers and Randolph 1993), so it becomes difficult to generalise predictions on disease dynamics. Schistosome parasites have a more focal spatial distribution than infectious diseases passed from person to person due to the need for intermediate hosts and the narrow range of temperatures which support the external parasite life-stages. The climatic effects on schistosomiasis, and other vector-borne diseases, are likely to be more significant than on direct life-cycle helminths. The first use of GIS in schistosomiasis epidemiology was attempted by Cross *et al.* (Cross and Bailey 1984; 1984) in the Philippines and the Caribbean using data from the Landsat Multispectral Spectral Scanner and local weather to predict the risk of disease. This study predicted the absence or presence of disease with 87.1% accuracy in the Caribbean and 93.2% accuracy in the Philippines (Cross and Bailey 1984). A disease distribution map was then

produced that estimated the probability of schistosomiasis infection. Further schistosomiasis risk models have been developed using climate and satellite-derived data on temperature and vegetation coverage, respectively, in China (Zhou *et al.* 2001; Seto *et al.* 2002; Yang *et al.* 2005a), Ethiopia (Kristensen *et al.* 2001; Malone *et al.* 2001b), Egypt (Malone *et al.* 1997; Abdel-Rahman *et al.* 2001), Uganda (Kabatereine *et al.* 2004), Tanzania (Clements *et al.* 2006) and Brazil (Bavia *et al.* 1999). Kazibwe *et al* (2006) identified associations in field data between air temperature, rainfall, water temperature, and snail density dynamics. Kristensen *et al.* (2001) found a relationship between vegetation density, land surface temperature, and disease prevalence. Distance to water bodies and annual minimum temperature were significantly correlated with prevalence in Tanzania (Clements *et al.* 2006). The thresholds for schistosomiasis transmission in Uganda were elevation >1400m and annual rainfall <900mm (Kabatereine *et al.* 2004). These findings show the importance of environmental factors on the transmission of schistosomiasis. To date, no studies have correlated continent-wide environmental variables with the risk of schistosomiasis over the African continent. Furthermore, few studies have quantified the impact of climate change on *Schistosoma mansoni* transmission dynamics. Those studies to date that examine the effect of climate change on schistosomiasis, describe either general trends of temperature on *Schistosoma* spp. or focus only on *S. japonicum* in China (Martens *et al.* 1995; Martens *et al.* 1997; Zhou *et al.* 2008).

1.8 Objectives of this thesis

The main objectives of this thesis were to a) develop parameterised mathematical models to analyse the effects of temperature change on schistosomiasis prevalence and intensity and b) to use spatial modelling techniques to assess associations between prevalence and climate variables and produce smoothed maps of schistosomiasis transmission in Africa with climate change.

The specific objectives were:

- development of a schistosome transmission model that explicitly incorporates snail population dynamics over a range of temperatures and analysis of this model to evaluate the efficacy of control programmes over a range of temperatures. This model is described in Chapter 2.
- accurate determination of the effects of temperature change on *Schistosome mansoni* and *Biomphalaria alexandrina* life-history traits to parameterise the transmission model. This is addressed in Chapter 3.
- experimental investigation of the density-dependent constraints within the *B. alexandrina* population. This is examined in Chapter 4.
- development of further models that incorporate density-dependence in the snail and adult parasite populations and comparison of these models with the original model developed in Chapter 2. This forms the first part of Chapter 5.
- evaluation of the efficacy of three control programmes, chemotherapy, molluscicide, and sanitation, at different temperatures using the models described above. This forms the second part of Chapter 5.

- geostatistical modelling of point-prevalence data to produce smoothed maps of schistosomiasis risk in Africa. These maps are presented in Chapter 6.
- identification of the climatic factors associated with schistosomiasis prevalence in Africa and use of these climatic data to predict the prevalence in areas where no prevalence data are available. This analysis is described in Chapter 6.
- predictions of the change in distribution of schistosomiasis with climate change and production of smoothed maps for future schistosomiasis risk in Africa. These maps are presented in Chapter 6.

CHAPTER 2

Predicting the Impact of Long-Term Temperature Changes on the Epidemiology and Control of Schistosomiasis: A Mechanistic Model

This paper has been published in PLoS ONE 3(1): e1438, 2008

2.1 Introduction

Global climatic changes alter the equilibrium of many ecosystems and the distribution of species they support (Ottersen *et al.* 2001; Stenseth *et al.* 2002). In particular, the potential effects of climate change on the distribution and severity of human diseases are of major interest (Martens *et al.* 1995; Martens *et al.* 1997; Patz *et al.* 2000; Hales *et al.* 2002; Patz *et al.* 2005). These changes can arise through both direct effects of climate change, e.g. alterations in the geographic areas able to support disease vectors, and indirect effects, such as changes in human migration patterns affecting disease distribution. Furthermore, the impacts of climate change may occur over several time scales, ranging from increasing the amplitude and stochasticity of diurnal or seasonal fluctuations in temperature and precipitation, particularly in temperate regions, to more stable increases in mean ambient temperatures over longer periods, particularly in tropical regions where many of the more concerning human diseases are endemic. The regions most vulnerable to the disease-related impacts of climate change are the temperate latitudes and the countries in the Indian and Pacific Oceans and sub-Saharan Africa, which will be disproportionately affected by extremes in temperature, and where public health programmes may be unable to cope with the changes in disease transmission (WHO 2003).

Of particular concern is the impact climate change will have on the prevalence of vector borne infectious diseases, including malaria, schistosomiasis, and dengue. The prevalence and abundance of these vector-borne diseases are particularly sensitive to changes in mean ambient temperature since their transmission relies principally on the survival and reproduction of their invertebrate vector or intermediate host, and the

parasite's incubation and survival rates therein. Since these vectors and intermediate hosts are incapable of thermoregulation, and their reproduction and survival rates are strongly influenced by temperature, small changes in temperature could greatly alter their distribution and abundance, resulting in a shift in disease patterns. Predicting how the long-term distribution and prevalence of such important human diseases will change in the face of global warming is a key challenge facing humans in the near future.

There are three main methods of examining the relationship between mean ambient temperature and infectious diseases. The first is to study current variations in climate and monitor the short-term effects on disease transmission. The second - a phenomenological approach - is to analyse past and current disease patterns and extrapolate these patterns into the future. The third method, which will form the focus of this chapter, is to use mechanistic models to predict the changes in prevalence and the burden of infectious diseases in response to forecasted global warming scenarios. This mechanistic approach has the advantage that it allows greater confidence in extrapolating beyond current conditions into a range of possible future climate scenarios. Here, such an approach is adopted to predict the impact of long-term temperature changes on the prevalence and abundance of human schistosomiasis, caused by the trematode *Schistosoma mansoni*. Currently, 600 million people are at risk of infection by schistosome species and current research predicts that vector-borne diseases such as schistosomiasis will be particularly affected by changes in temperature (Martens *et al.* 1995; Chitsulo *et al.* 2000). The model specifically focuses on long-term changes in mean ambient temperature, rather than short-term diurnal or seasonal temperature fluctuations, and concentrates on the impact of increasing mean ambient temperatures on the snail-schistosome interaction within a region in which schistosomiasis is already endemic, rather than the spread of the disease into new areas. Ultimately, however, this approach can be extended to include geographical and

ecological factors using a geographic information systems (GIS) approach to predict how the distribution of schistosomiasis will change in response to increased temperatures. Similar approaches have been developed for malaria, showing that increasing the average global temperature by 2-3°C, would increase the number of people at risk of infection worldwide by several hundred million (WHO 2003).

A number of mathematical models have been developed to understand the epidemiology, transmission dynamics and impact of control strategies on schistosomiasis (Cohen 1977; May and Anderson 1979; Woolhouse 1991; Woolhouse 1992; Williams *et al.* 2002; Allen and Victory 2003). The life-cycle of schistosomes is complex, involving two free-living stages and two host populations (Fig. 1.1). Briefly, paired male and female adults in the (human) definitive hosts produce eggs which pass into the environment in the host's faeces. These eggs hatch into miracidia, which seek out and infect the snail intermediate host where they undergo asexual reproduction. After a period of development, thousands of free-swimming infective cercariae are released, which actively seek out and penetrate a new human host, where they develop into adults. There are a number of stages of the schistosome and snail life cycles that will be highly dependent on ambient temperatures, affecting the distribution and prevalence of schistosomiasis and the likely response to global warming. A recent review of the effects of temperature on cercarial emergence found that a 10°C temperature increase resulted in an average 8-fold increase in cercarial output (Poulin 2006). From this, a large increase in the number of humans infected following a large increase in cercarial production is expected. However, Poulin focussed on only one stage of the parasite life-cycle (cercarial emergence) and ignored other key stages and potential sources of density dependent regulation within the parasite life-cycle. It is likely that different stages will respond in different ways to temperature increases, making it necessary to develop an explicit epidemiological model

to predict how these factors combine to affect the overall impact of temperature changes on the host-parasite system.

This chapter addresses three important questions regarding the impact of temperature on schistosomiasis: What effect does temperature have on the prevalence of schistosomiasis in a population? How do long-term temperature increases affect the mean worm burden in the population? What are the implications of long-term temperature increases on the optimal control strategy of schistosomiasis in the field?

2.2 Methods

The schistosomiasis epidemiological model is modified from those developed by Woolhouse (1991; 1992) and Anderson and May (1979b) and is shown schematically (Fig. 2.1). Mated adult schistosomes within infected human hosts produce eggs which hatch and develop to free-swimming miracidia at a net rate λ_M. These miracidia either die at rate δ_M or infect uninfected snails (U) at rate β_S. Due to the intense density dependence acting on schistosome development within snails, I follow previous models of schistosome epidemiology (Woolhouse 1991; Woolhouse 1992) by ignoring the burden of infection within snails, and simply class snails as uninfected (U), latently (pre-patent) infected snails (L) and patent infected snails (I). Pre-patent infections develop to patency at rate σ, after which they release cercariae (C) at a constant rate λ_C, which either die at rate δ_C or infect human hosts (H) at rate β_H. Successfully infecting schistosomes are assumed to mature immediately to adult parasites (P), which die at rate δ_P and produce new eggs throughout their life to begin the life-cycle again. Based on empirical data from the literature, this basic model is modified to incorporate more

details on the snail life-cycle. Specifically, the density of snail eggs (E) and the density of juvenile snail stages (J) in the environment are considered. All adult snails may lay eggs, although infected snails may lay eggs at a different rate (a') from uninfected snails (which lay at rate a), but overall egg production of the population is limited by density dependent regulation by a carrying capacity, K. Snail eggs die at rate δ_E and hatch at rate δ_E and juvenile snails die at rate δ_J and mature to adult, uninfected snails at rate δ_S. All adult snails die at background rate δ_S and infected adult snails also die due to parasite-induced mortality at additional rate α. All parameters are defined in Table 2.1.

This detailed model is simplified by recognising that the dynamics of external stages of the schistosome life-cycle tend to be far quicker than those of the infecting stages, or their hosts (Woolhouse 1994). Therefore, it is assumed that the miracidia and cercariae are at 'pseudo-equilibrium' and are not modelled explicitly. Similarly, the dynamics of the egg and juvenile stages of the snail life-cycle are relatively fast and are not modelled explicitly. The snail population is modelled at three levels, uninfected, latently and patently infected which implies that the level of infection has no effect on the resulting number of cercariae produced. This assumption is supported by experimental evidence (Christie 1978 ; Touassem 1989). Finally, the important assumption that the size of the definitive host population (humans) is constant is made, allowing us to consider the risk of infection to a static host population of a given size.

This results in the final model comprising four state variables describing the adult size of the adult parasite population within humans (P), the density of uninfected snails (U), the density of latently infected snails (L) and the density of patently infected snails (I):

$$\frac{dP}{dt} = \frac{\beta_H H \lambda_C I}{\delta_C + \beta_H H} - P\delta_P \tag{2.1}$$

$$\frac{dU}{dt} = \left(a_S U + a'(L+I)\right)\left\{1 - \frac{U+L+I}{K}\right\} - \frac{\beta_S \lambda_M P U}{\delta_M + \beta_S(U+L+I)} \tag{2.2}$$

$$\frac{dL}{dt} = \frac{\beta_S \lambda_M P U}{\delta_M + \beta_S(U+L+I)} - L(\delta_S + \alpha + \sigma) \tag{2.3}$$

$$\frac{dI}{dt} = \sigma L - I(\delta_S + \alpha) \tag{2.4}$$

This model was parameterised at different temperatures using data from the literature that explored the effects of temperature on various life-history traits of both parasites and hosts (see Appendix A1). These values were used to generate predictions of how the mean number of parasites per human host ($m = P/H$) and the prevalence of infection (p) change with temperature. For this latter measure, it is assumed that adult parasites are distributed among hosts in an aggregated manner, according to a negative binomial distribution with aggregation parameter k.

Given the predicted mean burden of parasites per host, m, the predicted prevalence is given by:

$$p = 1 - \left(1 + \frac{m}{k}\right)^{-k} \tag{2.5}$$

The data from the literature were not consistent for all life-history traits and may have been collected for different species under different conditions, but they are used as a first approximation of parameter values. To explore how robust the predictions are to variations in parameter values, a sensitivity analysis was conducted, where the value of each parameter in turn was increased and decreased up to 10 times from the baseline value and the relative impact on the predicted mean parasite burden and prevalence was calculated. This allows us to qualitatively determine the key parameters that need to be estimated accurately to obtain reasonable predictions of the impact of temperature on schistosomiasis. Furthermore, this process reveals 'leverage points' in the epidemiology, highlighting traits that may be targeted by control measures to bring about the greatest reduction in disease. Once again, it is emphasised that a broad brush approach is taken, concentrating on the impact of changes in long-term mean ambient temperature on the abundance and control of schistosomiasis, rather than the impact of short-term diurnal or seasonal fluctuations in temperature. Hence, in what follows, the ambient temperature was assumed to remain constant throughout each simulation.

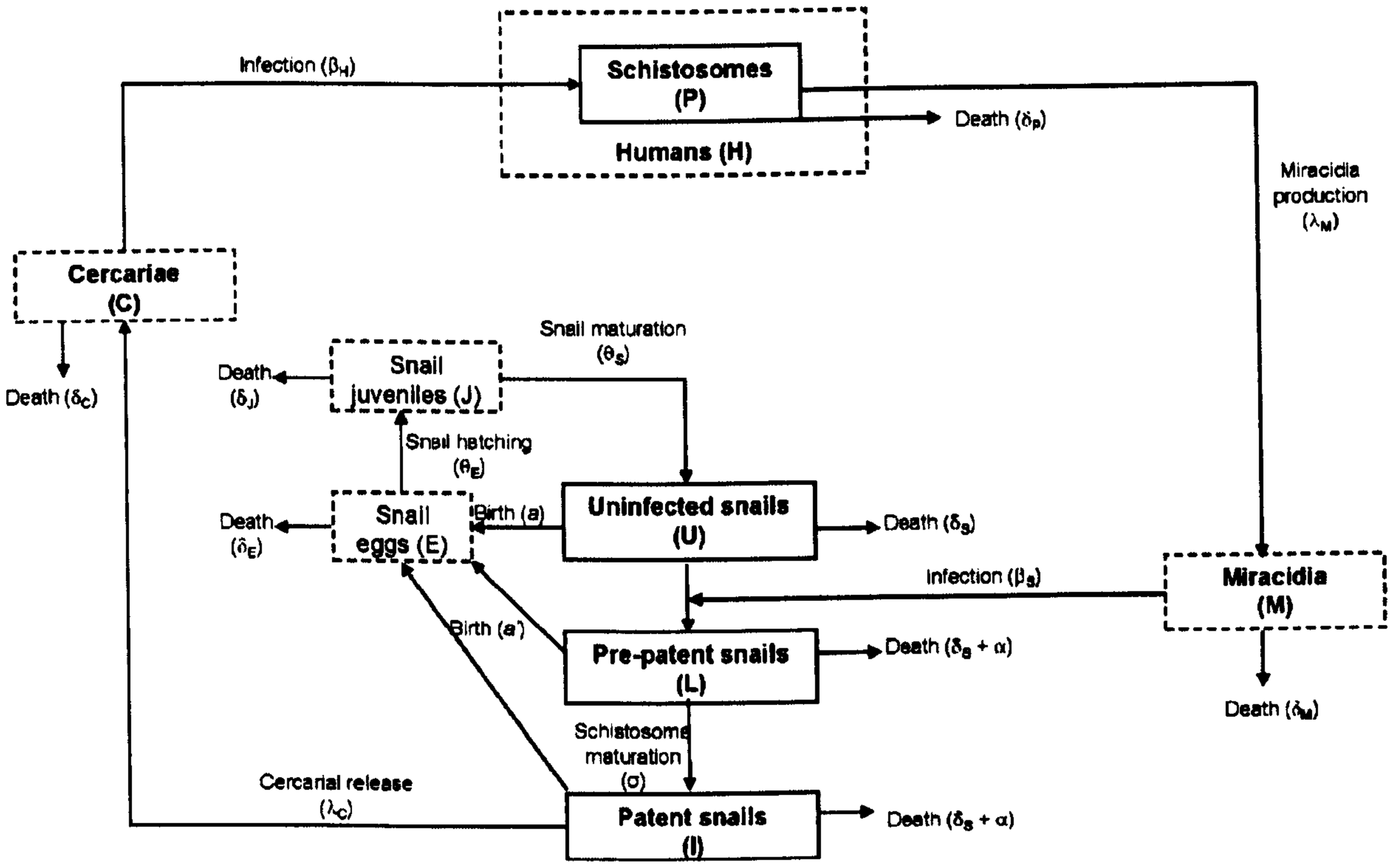

Figure 2.1. Schematic diagram of the schistosome disease model. The dashed boxes show stages of the life-cycle that are not modelled explicitly.

Table 2.1. Estimates of each parameter at baseline temperatures of 20, 25, 30 and 35°C.

Parameter	Definition	20°C (d^{-1})	25°C (d^{-1})	30°C (d^{-1})	35°C (d^{-1})
λ_C	Cercarial production rate	2476	4128	6103	8400
δ_C	Cercarial mortality rate	1	1	1	1
β_H	Cercarial infection rate	0.028	0.059	0.091	0.122
δ_P	Adult schistosomes death rate	0.0309	0.02	0.01	0.008
λ_M	Net miracidial production rate	500	500	500	500
δ_M	Miracidia death rate	2	2.526	4.364	4.444
β_S	Miracidia infection rate	$1.27x10^{-4}$	$9.1 x10^{-5}$	$1.4 x10^{-3}$	$1.2 x10^{-3}$
σ	Within-snail schistosome maturation rate	0.0216	0.036	0.05	0.065
α_S	Snail egg laying rate	0.663	0.849	0.057	0.010
a'	Infected snail egg laying rate				
θ_E	Snail hatching rate	0.08	0.1	0.118	0.128
θ_S	Snail maturation rate	0.02	0.029	0.012	0.0075
δ_E	Snail egg mortality rate	0.001	0.001	0.001	0.001
δ_J	Snail juvenile mortality rate	0.002	0.0038	0.0071	0.0207
δ_S	Snail adult mortality rate	0.004	0.003	0.008	0.0182
α	Additional snail mortality due to infection	0.002	0.0145	0.0295	0.05
K	Snail carrying capacity	100 L^{-1}	100 L^{-1}	100 L^{-1}	100 L^{-1}

2.3 Results

2.3.1 The impact of ambient temperature on schistosome dynamics

The model predicts that mean worm burdens in humans are affected by ambient temperature, rising to a peak at 30°C and then falling sharply at 35°C (Fig. 2.2). This decline in worm burdens at 35°C may be explained by the increasing mortality of both the intermediate hosts and the parasite at higher temperatures (see Appendix A1). However, the disease prevalence in humans remains almost constant over the temperature range of 20 - 35°C (Fig. 2.2), suggesting that although increases in long-term mean ambient temperature may lead to an increase in mean worm burdens and associated increases in morbidity and even mortality of infected hosts, the number of infected people is unlikely to change greatly.

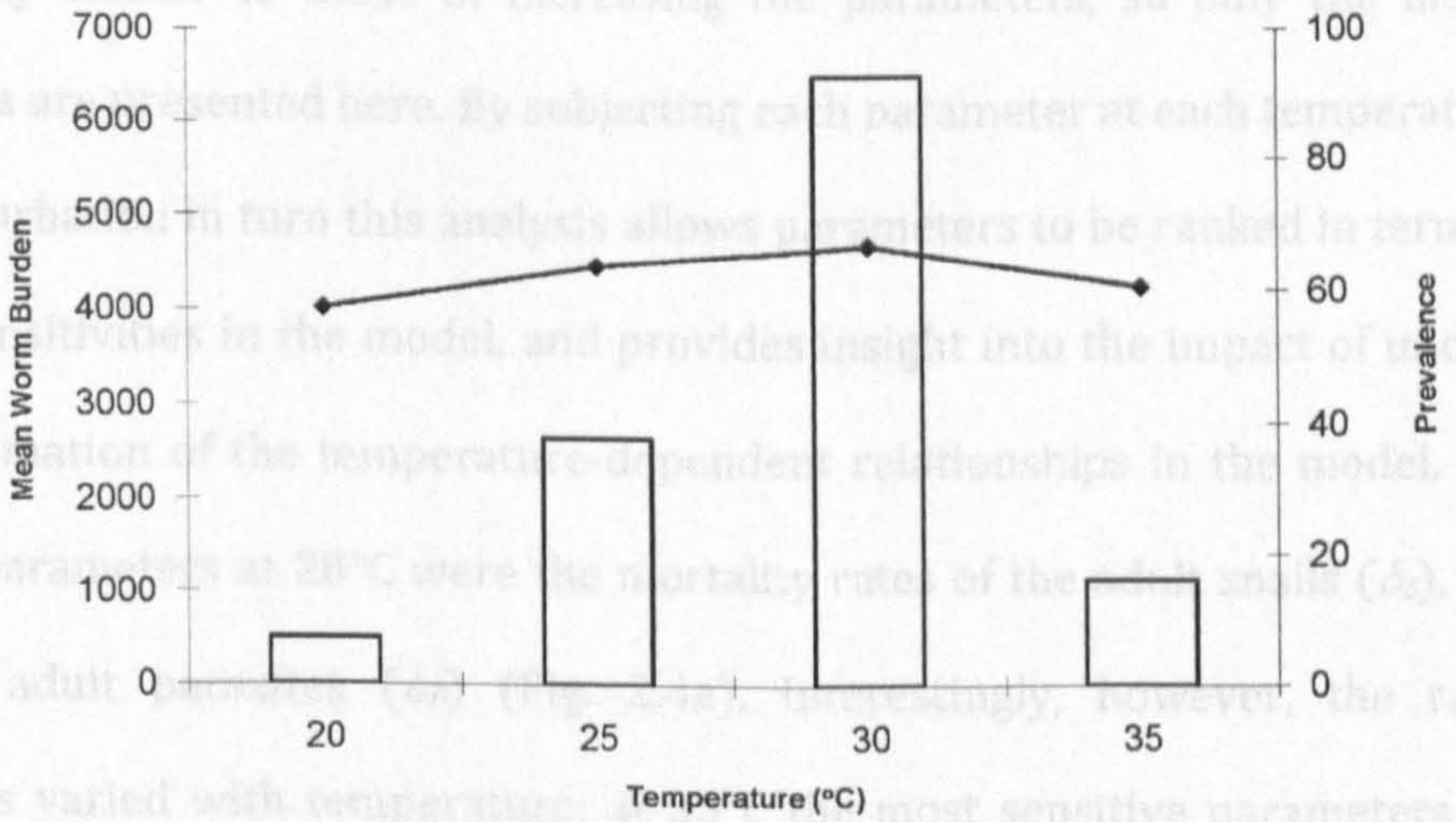

Figure 2.2. Variations in mean worm burden (bars) and prevalence (lines) of *Schistosoma mansoni* as a function of temperature.

Interestingly, increased temperatures also lead to changes in disease dynamics (Fig. 2.3). At 20°C, disease dynamics are stable, with mean burdens and prevalence remaining constant over time. However, at 35°C the dynamics switch from endemic to epidemic, with repeated oscillations in worm burdens and disease prevalence over time. A previous model of schistosome dynamics showed that density-dependent regulation of the intermediate host (snail) population could allow such cyclical dynamics (Feng *et al.* 2002) and this parameterised model shows that the interaction between such regulation and the increased snail birth rates at higher temperatures make such dynamics more likely.

A sensitivity analysis was conducted where each parameter at each temperature was increased and decreased by up to a factor of 10 and the impact on mean worm burden per individual and prevalence measured. The results for prevalence are qualitatively similar to those of the mean worm burden, so only the results for mean worm burden are presented here. Similarly, the results for decreasing parameters were qualitatively similar to those of increasing the parameters, so only the increases in parameters are presented here. By subjecting each parameter at each temperature to the same perturbation in turn this analysis allows parameters to be ranked in terms of their relative sensitivities in the model, and provides insight into the impact of uncertainties in our estimation of the temperature-dependent relationships in the model. The most sensitive parameters at 20°C were the mortality rates of the adult snails (δ_S), miracidia (δ_M) and adult parasites (δ_P) (Fig. 2.4a). Interestingly, however, the ranking of parameters varied with temperature; at 35°C the most sensitive parameters were the mortality rate of juvenile snails (δ_J), the infection rate of snails (β_S) and the birth rate of snails (a) (Fig. 2.4b). All of these parameters involve snail life stages, highlighting the importance of the intermediate host in determining the dynamics and abundance of schistosomes, suggesting that control methods that target the snails will prove highly

effective at increased ambient temperatures. Overall, these results show that the optimal control approach will vary depending on the ambient temperature and the degree of temperature change.

(a)

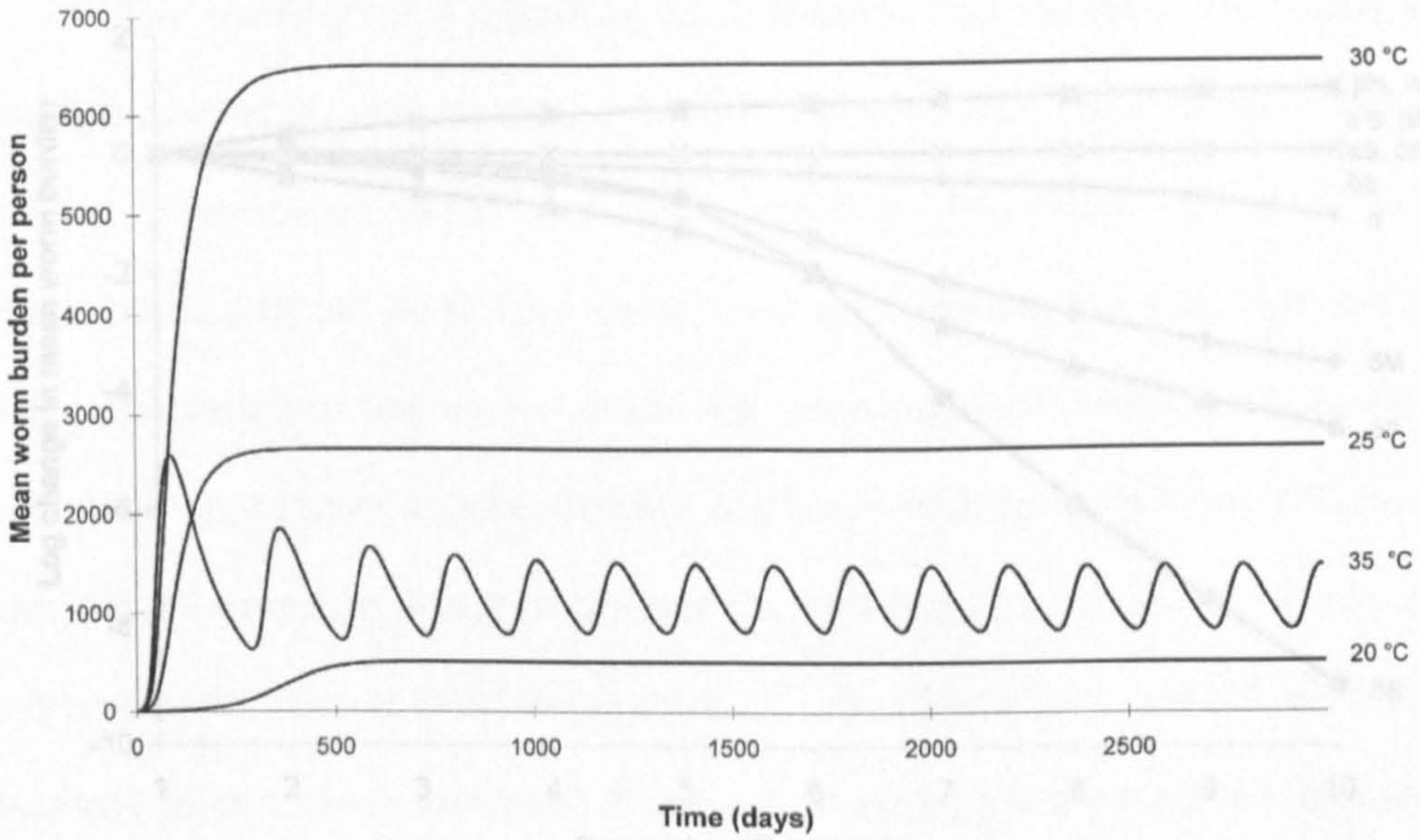

(b)

Figure 2.3. Dynamics of mean worm burden per individual (a) and prevalence of infection (b) over time at 20°C, 25°C, 30°C and 35°C.

(a)

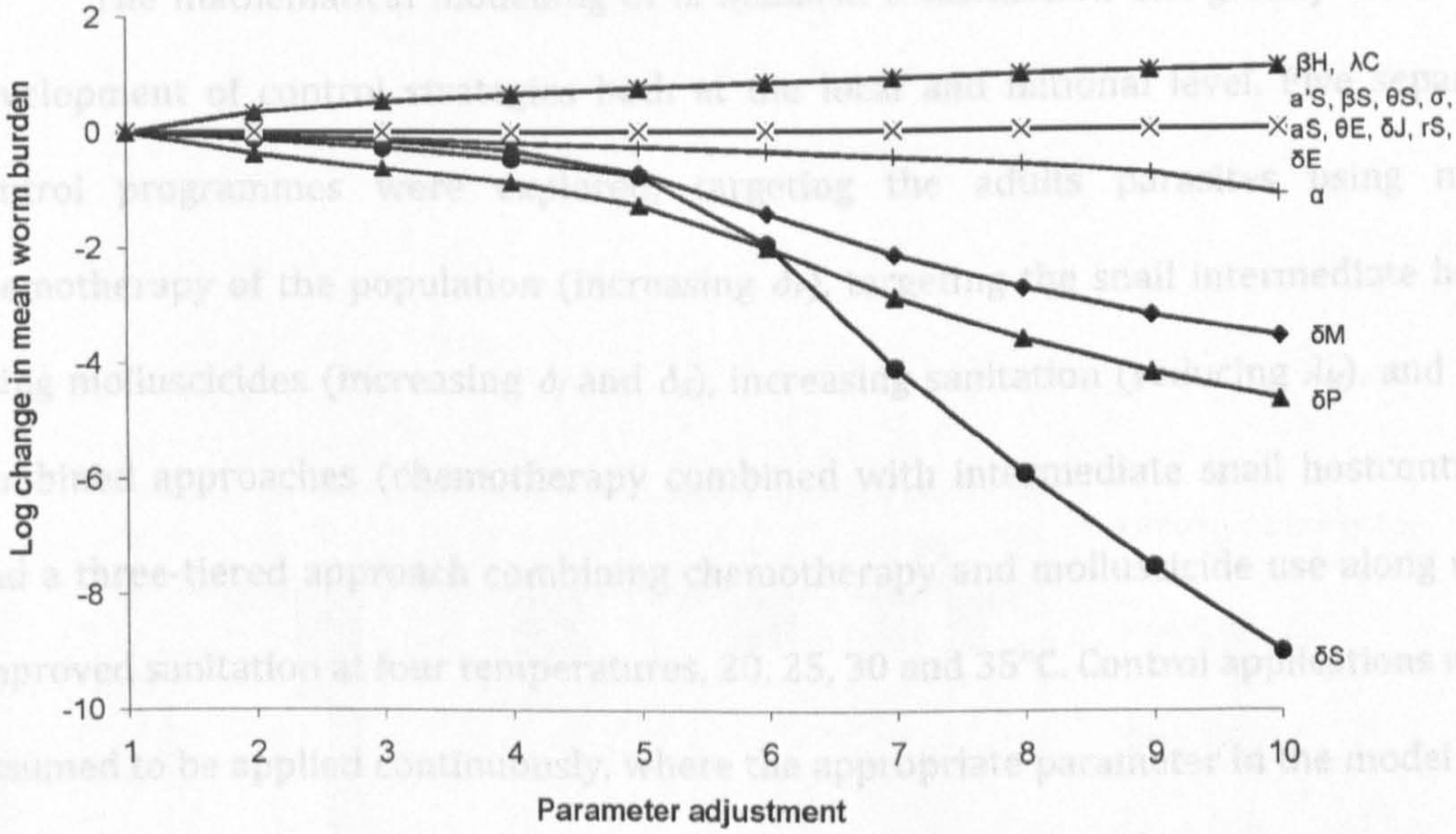

(b)

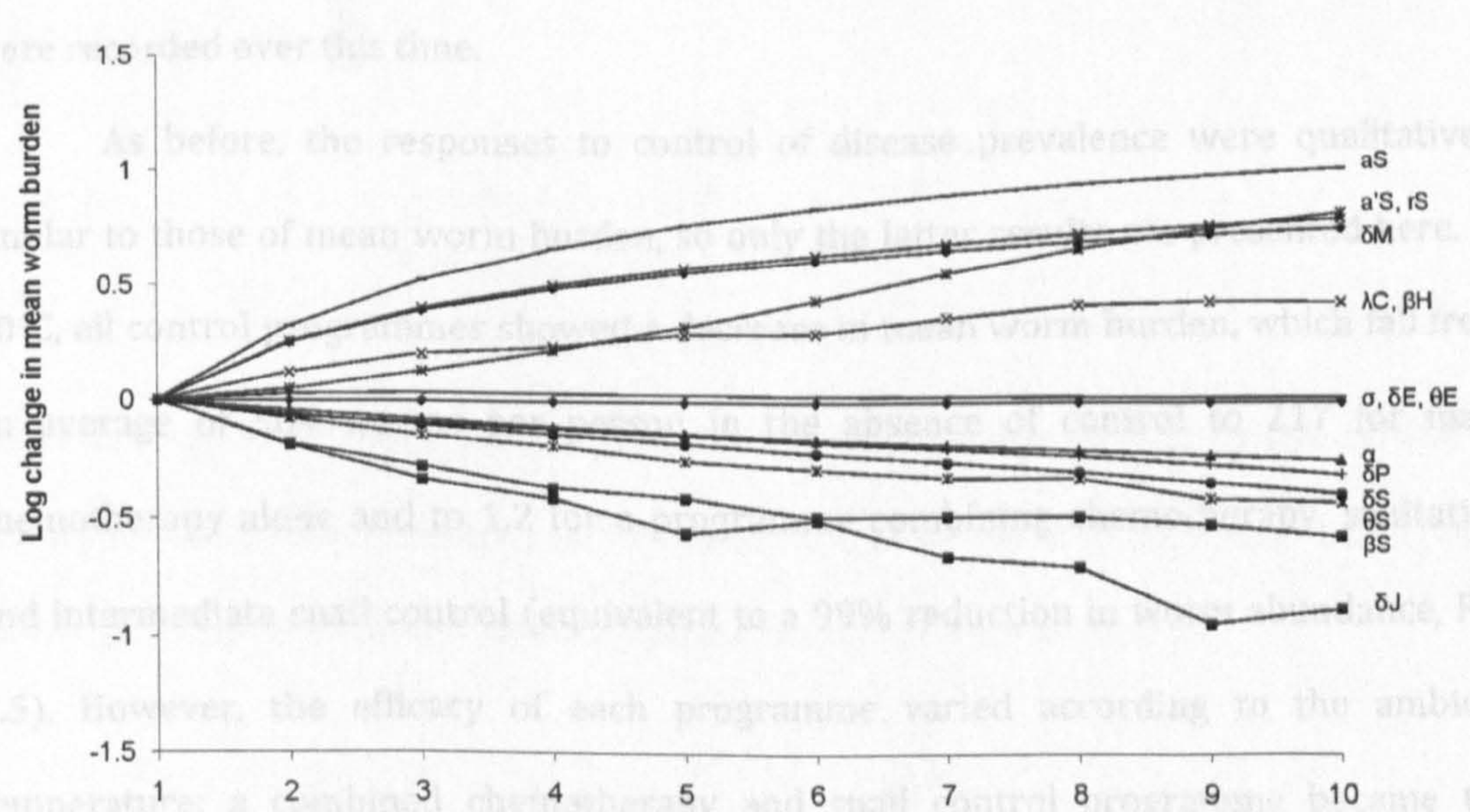

Figure 2.4. Results of the sensitivity analysis of the mean worm burden per individual at 20°C (a) and 35°C (b).

2.3.2 The impact of ambient temperature on the optimal control strategy

The mathematical modelling of *S. mansoni* transmission can greatly aid in the development of control strategies both at the local and national level. Five separate control programmes were explored; targeting the adults parasites using mass chemotherapy of the population (increasing δ_P), targeting the snail intermediate hosts using molluscicides (increasing δ_I and δ_S), increasing sanitation (reducing λ_M), and two combined approaches (chemotherapy combined with intermediate snail hostcontrol), and a three-tiered approach combining chemotherapy and molluscicide use along with improved sanitation at four temperatures, 20, 25, 30 and 35°C. Control applications were assumed to be applied continuously, where the appropriate parameter in the model was altered by a factor of 2 (i.e., δ_P, δ_I and δ_S were doubled and λ_M was halved). The model was run for 3000 days and the mean prevalence and mean parasite burdens in humans were recorded over this time.

As before, the responses to control of disease prevalence were qualitatively similar to those of mean worm burden, so only the latter results are presented here. At 20°C, all control programmes showed a decrease in mean worm burden, which fall from an average of 504 worms per person in the absence of control to 217 for mass chemotherapy alone and to 1.2 for a programme combining chemotherapy, sanitation and intermediate snail control (equivalent to a 99% reduction in worm abundance, Fig. 2.5). However, the efficacy of each programme varied according to the ambient temperature; a combined chemotherapy and snail control programme became the optimal strategy at 25-35°C, whereas targeting adult parasites alone had a negligible effect at 35°C. Surprisingly, sanitation appeared to have a detrimental effect, almost doubling the burden of disease at 35°C. Overall, these results show a clear advantage to targeting both intermediate vectors and the human population over treating humans alone; indeed, it appears adopting a human-only treatment is very unlikely to be

effective in reducing either the regional prevalence or mean worm burden of schistosomiasis at increased temperatures.

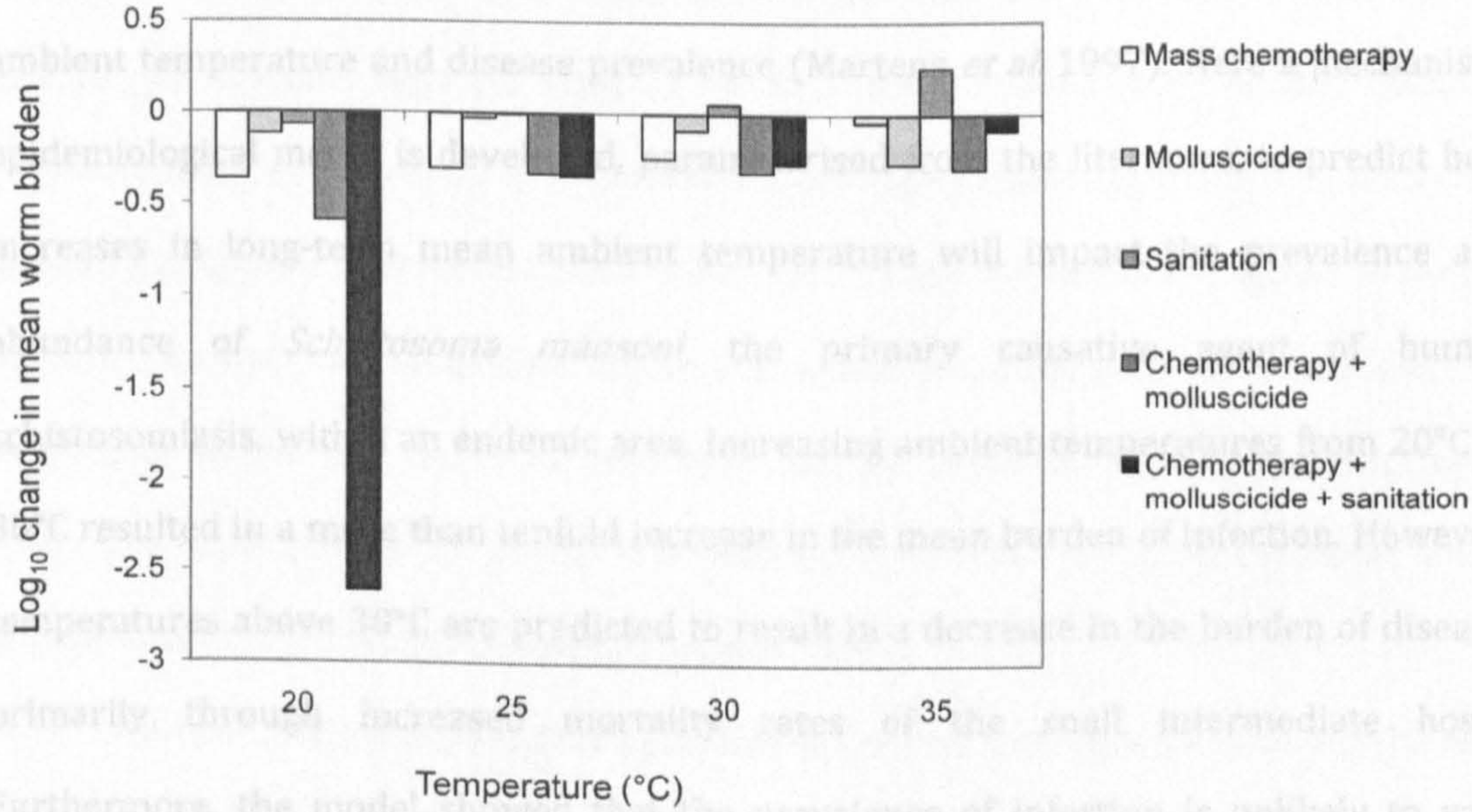

Figure 2.5. Impact of temperature on the efficacy of different control programmes. The efficacy of control was measured as the Log_{10} of the mean parasite abundance during the control phase divided by the mean abundance in the absence of control.

2.4 Discussion

Predicting the impact of climate change on the epidemiology of infectious disease is a pressing challenge. However, extrapolating from current scenarios into the future is unlikely to be straightforward. Due to the differential impact of temperature on each of the life-history stages of a parasite there is unlikely to be a simple relationship between ambient temperature and disease prevalence (Martens *et al.* 1997). Here a mechanistic epidemiological model is developed, parameterised from the literature, to predict how increases in long-term mean ambient temperature will impact the prevalence and abundance of *Schistosoma mansoni*, the primary causative agent of human schistosomiasis, within an endemic area. Increasing ambient temperatures from 20°C to 30°C resulted in a more than tenfold increase in the mean burden of infection. However, temperatures above 30°C are predicted to result in a decrease in the burden of disease, primarily through increased mortality rates of the snail intermediate hosts. Furthermore, the model showed that the prevalence of infection is unlikely to vary greatly regardless of the ambient temperature. Therefore, although the burden of infection will increase substantially within infected people, the number of people infected is unlikely to change. This is consistent with earlier models which predict large increases in worm burdens with little change in prevalence levels (Anderson 1982). Nevertheless, the increased morbidity will have severe consequences, ranging from reduced birth rates, neurological complications and high economic costs through lost work days and the need for medical care.

The model quantifies human disease burden by predicting the mean number of worms harboured in an individual in the population. It would be interesting to validate the model's predictions by comparing existing worm burdens from regions with

different ambient temperatures. However, this is not possible at present for two reasons. Firstly, patterns of worm burden from different regions will be influenced by a range of factors such as differences in human, snail and parasite genotypes, variations in microclimate and other environmental variables, and differences in human behaviour and exposure (Jones *et al.* 1989; Malone *et al.* 2001b; Yang 2003). Secondly, it is accepted that direct quantification of worm loads is impossible and so many studies use faecal egg counts to estimate the intensity of infection. While this is a very useful measure, the relationship between eggs per gram of faeces and worm load is continually disputed (Gryseels and deVlas 1996). It is therefore extremely difficult to directly validate the model's predictions of worm load but rather the data are used as an indication of disease burden. The only available data containing actual measurements of worm pairs in individuals shows that counts of over 1000 may be rare, although this study includes only older age groups in a low transmission area, and so generalising to other populations or regions is not feasible (Cheever 1968).

Current estimates state that a global temperature increase of 2-3°C over the next 100 years is likely (WHO 2003). However, exploring a wider range of temperature values (20-35°C) shows that the impact of even a small rise in temperature on both prevalence and burden of infection will depend greatly on the initial, baseline temperature. In particular, an important result to emerge from the sensitivity analyses is that changes in mean ambient temperature will alter the relative sensitivities of the parameters in the model. Therefore, the optimal disease control strategy will change as temperatures increase. In particular, at 20°C increasing adult parasite mortality rates, for example through chemotherapy, may have a large impact on the prevalence and abundance of disease, whereas at 35°C parameters relating to the snail stages become more important, suggesting that snail eradication programmes may be more successful. Indeed, the model showed that a combined approach integrating chemotherapy

treatment with snail control had a larger impact on schistosome prevalence and abundance than chemotherapy alone. Macdonald (1965) suggested that very high sanitation levels (i.e. reducing the number of eggs reaching water), has a negligible effect on mean worm load compared to the combined effects of treating infected people and keeping them out of infected water. This was because the water that the snails live in is typically saturated with miracidia and nearly all snails are infected. This is supported by the model, which predicts that prevalence in the snails typically approaches 100%, and so reducing human contact with the water is crucial for breaking the transmission cycle. The increase in mean worm burden following sanitation improvements at 35°C arises due to the complex interaction between the strong density dependent constraints acting on cercarial production and the negative impact of schistosome infection on the snail population. Reducing the input of miracidia into environment has little impact on the total number of cercariae released, since the same number are released per infected snail regardless of the number of infecting miracidia. However, reducing the number of miracidia also reduces the number of snails dying due to infection, allowing the snail population to build up to large numbers. This provides more susceptible snails for infection, resulting in an overall increase in the total number of cercariae being released into the environment and a subsequent increase in human infections.

A number of control programmes, such as mass chemotherapy, molluscicide applications and improvements in sanitation and water supplies have been used in a combined effort to control schistosomiasis worldwide. These programmes have been successful in Brazil, the Middle East, and parts of the Far East, but the disease has remained endemic in many regions of sub-Saharan Africa (Chitsulo *et al.* 2000). Many countries with endemic levels of schistosomiasis did not implement control programmes, believing the costs required for control would be disproportionately high compared with the health benefits. A number of control programmes were initiated in

sub-Saharan Africa but local and national health authorities were unable to maintain the high costs involved. These programmes enjoyed short-term success but infection levels soon returned to pre-intervention states. In particular, Sturrock noted that chemotherapy alone does not have a lasting effect on transmission, and suggested that re-infection rates largely depend on ecological factors affecting the snail population (Sturrock *et al.* 1994). The model supports this suggestion, particularly in regions with high ambient temperatures.

Clearly, the design of any control programme needs to take into account a wide range of social, medical, and environmental factors beyond the scope of this model (for example, the occurrence of adverse side effects to chemotherapy or the knock-on effects of mass molluscicide treatment on the wider ecological community). Furthermore, the model omits a number of biological complications, such as heterogeneous transmissions rates, the presence of alternative reservoir hosts and the build-up of acquired immunity (Woolhouse 1991; Woolhouse 1992; Yang and Yang 1998). One important simplification is that the model is restricted to considering the impact of long-term changes in mean ambient temperature on schistosome abundance and control. However, climate change is likely to have a number of impacts on the environment, including increased fluctuations in temperature over shorter time scales (e.g., diurnal or seasonal), and will impact on the distribution and longevity of suitable water bodies for the snails. Such complications will modify the finer predictions of the model, but this approach is appropriate for providing an initial insight into the broader consequences of climate change. Further studies, building on this existing framework and incorporating some of these factors would be invaluable. In particular, to improve the accuracy of the model, it is essential to conduct a series of experiments using one specific host-parasite combination over a range of temperatures. These could then be compared with field studies conducted in different regions with different ambient temperatures to validate

the model. A fascinating next step would be to place this mechanistic model within a spatially explicit GIS framework with realistic migration patterns and predicted temperature regimes. This could further extend the work of Malone *et al.* (Malone *et al.* 1997; Malone *et al.* 2001a; Malone *et al.* 2001b) who have used satellite imagery and geographic information system to develop area suitability maps and environmental risk models for schistosomiasis. It would then be possible to predict with greater confidence than current, extrapolation-based approaches how the spatial distribution of schistosomiasis will change under global warming. However, the current model provides an important mechanistic insight into how the complex interactions between the various life-history stages and ambient temperature will determine the impact of schistosomiasis and the success of future control programmes in the face of global climate change.

CHAPTER 3

The impact of temperature on *Schistosoma mansoni* – *Biomphalaria alexandrina* interactions: estimating the parameters for a transmission model

3.1 Introduction

The geographic distribution of the human parasite *Schistosoma mansoni* is bounded by the range of the intermediate host, freshwater snails of the genera *Biomphalaria*. The development of *S. mansoni* within its intermediate host is directly affected by environmental and endogenous factors, with temperature being one of the most important (Stirewalt 1954; Anderson and May 1979a; Anderson *et al.* 1982). Given concerns over global climate change and the relationship between temperature and host distribution, climate changes are likely to influence the prevalence of schistosomiasis and the epidemiology of human disease (Woolhouse 1991). The model presented in Chapter 2 highlights the importance of temperature in determining the prevalence and burden of disease. The most influential parameters related to the stages most susceptible to changes in environmental conditions, the intermediate and free-living stages. The aim of this study was to quantify how the impact of the parasite on the life-history of its snail intermediate host changes with ambient temperature.

Various aspects of the impact of ambient temperature on snail-schistosome life-histories have been described for a variety of host and parasite species. Snail development and survival are restricted to well-defined thermal limits of 12.5°C – 37.0°C, with temperature affecting all stages of the snail life-cycle (Etges and Gresso 1965; El Hassan 1974). In particular, above 30°C, snail mortality increases and fecundity decreases due to inhibition of gametogenesis and gonad development and below 15°C, snails hibernate, or die (Appleton and Eriksson 1984). Therefore, the distribution of suitable snail host species can be limited by local temperatures.

Temperature can also alter the impact that schistosomes have on their snail hosts, with epidemiological consequences. Schistosomes have detrimental impacts on their snail hosts, and depending on how the parasite sequesters the host's resources, and how the host responds to these demands, the consequences of parasite infection can differ widely. Schistosomes can be pathogenic, raising snail mortality rates compared to uninfected controls (Woolhouse 1989; Webster and Woolhouse 1999; Davies *et al.* 2001; Webster *et al.* 2004). Furthermore, both stunting of growth (Pan 1965; Sturrock and Sturrock 1970; Fernandez and Esch 1991) and gigantism have been documented in infected snails (Ballabeni 1995).

Aspects of the thermal responses of snails and schistosomes have been quantified (El Hassan 1974; Pfluger 1980; Anderson *et al.* 1982; Appleton and Eriksson 1984; Coelho and Bezerra 2006). However, these studies have tended to be conducted on several combinations of host and parasite species and strains over a range of temperatures, making it difficult to determine how they may respond to changes in ambient temperature. In Chapter 2, I combined these studies to obtain a standardised set of temperature responses for a 'generic' snail host-schistosome interaction. These data were then used to parameterise an epidemiological model to predict the impact of temperature changes on schistosomiasis transmission dynamics. Chapter 2 showed that the dynamics, intensity and prevalence of infection in humans are unlikely to change in a simple way with increases in ambient temperature, due to different stages of the snail and schistosome life-cycles responding to temperature in different ways. These different thermal responses result in fundamentally different outcomes of imposed management programmes, suggesting that the optimal control strategy is likely to vary as temperatures change. However, due to the diverse species and conditions under which the data used for this model were based, it is difficult to determine the reliability of these

predictions. Current estimates for global temperature changes range from 0.8 – 2.6°C by 2050, and 1.4 – 5.8°C by 2100, so a realistic model must identify the impact of temperature changes up to at least 5°C from the baseline (Carter 2007).

The impact of climate change on the distribution of vector-borne diseases requires the use of quantitative modelling techniques. These models depend on accurate estimates of every contributing parameter and variable. When no estimates exist for a parameter, it is given an arbitrary value. The importance of the parameter can then be explored using a sensitivity analysis. In the previous chapter, some parameter estimates were derived from different host-parasite combinations and the methods varied between studies. To directly quantify the effects of temperature change on schistosomiasis transmission, it is necessary to accurately determine every parameter using the same host-parasite combination under the same conditions. In this chapter, I have experimentally quantified the complete set of temperature responses for a single host-parasite pair, *Schistosoma mansoni* and its invertebrate host, *Biomphalaria alexandrina*, under controlled conditions.

3.2 Methods

3.2.1 Study system

Stock colonies of *Biomphalaria alexandrina* (originating from Egypt), were maintained in the laboratory for approximately 20 generations without parasite pressure. The parasite was a mixed strain *Schistosoma mansoni* line, developed over 10 generations using isolates from Brazil, Egypt and Puerto Rico and routinely passaged

through *Biomphalaria alexandrina* and CBA/CA mice (supplied by Professor Mike Doenhoff, University of Bangor / University of Nottingham). This combination of host and parasite ensured a high degree of compatibility (>85%) whilst minimising potential heterosis effects, which may occur with novel parasite-host combinations (Blair and Webster 2007). All snails were kept in plastic, 5L tanks in a 12L:12D photoperiod room (using 6W fluorescent bulbs) at 23-25°C with <10 snails L^{-1} water. The snails were fed high protein rabbit food pellets daily (Pascoe's Bunny Balance, Driffield, UK), and water was supplemented with 1g calcium carbonate once every two weeks (see Lewis *et al.* (1986) for cultivation methods).

3.2.2 Experimental design

Temperatures within the thermal limits of *B. alexandrina* were investigated, 18, 23, 29, and 34°C. These temperatures lie within the thermal limits of the snail and parasite and have not been thoroughly explored by existing studies (see Appendix A1). Two tanks of infected snails and one tank of uninfected snails were incubated at each temperature and each tank contained 20 snails. Two weeks before exposure juvenile snails (4 - 7mm) were size introduced into their tanks at their optimum temperature (24°C). The incubator temperature was altered by 1°C every day until the desired temperatures were reached.

Schistosoma mansoni were maintained in a murine host, and the infected liver was removed 49 days post-infection. The liver was homogenised, forced through a wire mesh, sedimented in 1.8% NaCl for one hour, and washed repeatedly to isolate the parasite eggs. These eggs were left to hatch into miracidia under an artificial lamp for one hour at 25°C. Uninfected snails were individually exposed to five freshly hatched miracidia each for 2 hours, sufficient time for maximal miracidial infection success (Lewis *et al.* 1986). The snails were examined weekly from one week post-exposure to

12 weeks post-exposure, to determine growth rate (measured as wet weight – a biologically relevant indicator of snail fitness in terms of its relationship to snail survival and reproduction), net reproductive rate (measured as the number of eggs produced per snail over the duration of the experimental period), and mortality. The experiment was ended after 12 weeks. After 21 days, all snails exposed to miracidia were individually isolated in 6-well plates and examining aliquots of the water stained with Lugol's solution to check for cercarial production. Lugol's solution consists of 5g iodine (I_2), 10g potassium iodide (KI) in 85ml distilled water, which produces a 130mg/mL solution. Each week cercarial samples were taken individually from snails every two hours over 8 hours to produce a profile of cercarial shedding at every temperature, over the life span of the snail. Control snails were isolated in an identical manner and kept in temperature-controlled incubators alongside the infected snails.

3.2.3 Statistical analysis

Repeated measure and survival analyses were performed using the statistical package R (http://www.r-project.org). Linear mixed effects models (LME) were used to analyse snail weight and fecundity, using the lme4 package in R. The LME models were appropriate in this study due to temporal pseudoreplication, as observations were grouped on each tank. Time, temperature, infection status, and the interactions between these terms were modelled as fixed effects and the tanks were fitted as random effects to control for pseudoreplication, as the repeated measures were temporally correlated with one another. The maximum likelihood method was used to fit the models containing all variables, and then a stepwise deletion process using AIC methods was used to eliminate the highest order interactions first. For the survival analysis model, a Weibull error distribution ($\alpha\lambda\,(\lambda t)^{\alpha-1}$) was used, which allows for non-constant hazard with age along

with censoring as some individuals outlived the length of the experiment (Crawley 2007).

3.3 Results

3.3.1 Biomphalaria alexandrina *survival analysis*

The minimal survival model contained significant terms for temperature and infection status (Table 3.1). *Biomphalaria alexandrina* survivorship was associated with temperature ($P < 0.001$), and temperature*infection status ($P < 0.05$). Time post-infection (p.i.) was included as an explanatory variable in the full model but remained non-significant as the effects of time on snail survival rates are accounted for with the Weibull error distribution. There was a noticeable reduction in survival of infected snails around day 49 p.i. at all temperatures (Fig. 3.1). This coincided with the start of cercarial shedding (section 3.3.5), whereas survival for uninfected snails declined at a constant rate throughout the experiment consistent with earlier studies (El Hassan 1974; El-Emam and Madsen 1982). The survival rates of uninfected snails at 12 weeks (the end of the experiment) peaked at 29°C and began to decline at 34°C, which approached the reported thermal limit for *Biomphalaria sp* (El Hassan 1974). However, as suggested by the significant interaction between temperature and infection status (Table 3.1), infected snails showed a different response to temperature with survival rates decreasing as the temperature reached 29°C and then increasing slightly at 34°C.

(a)

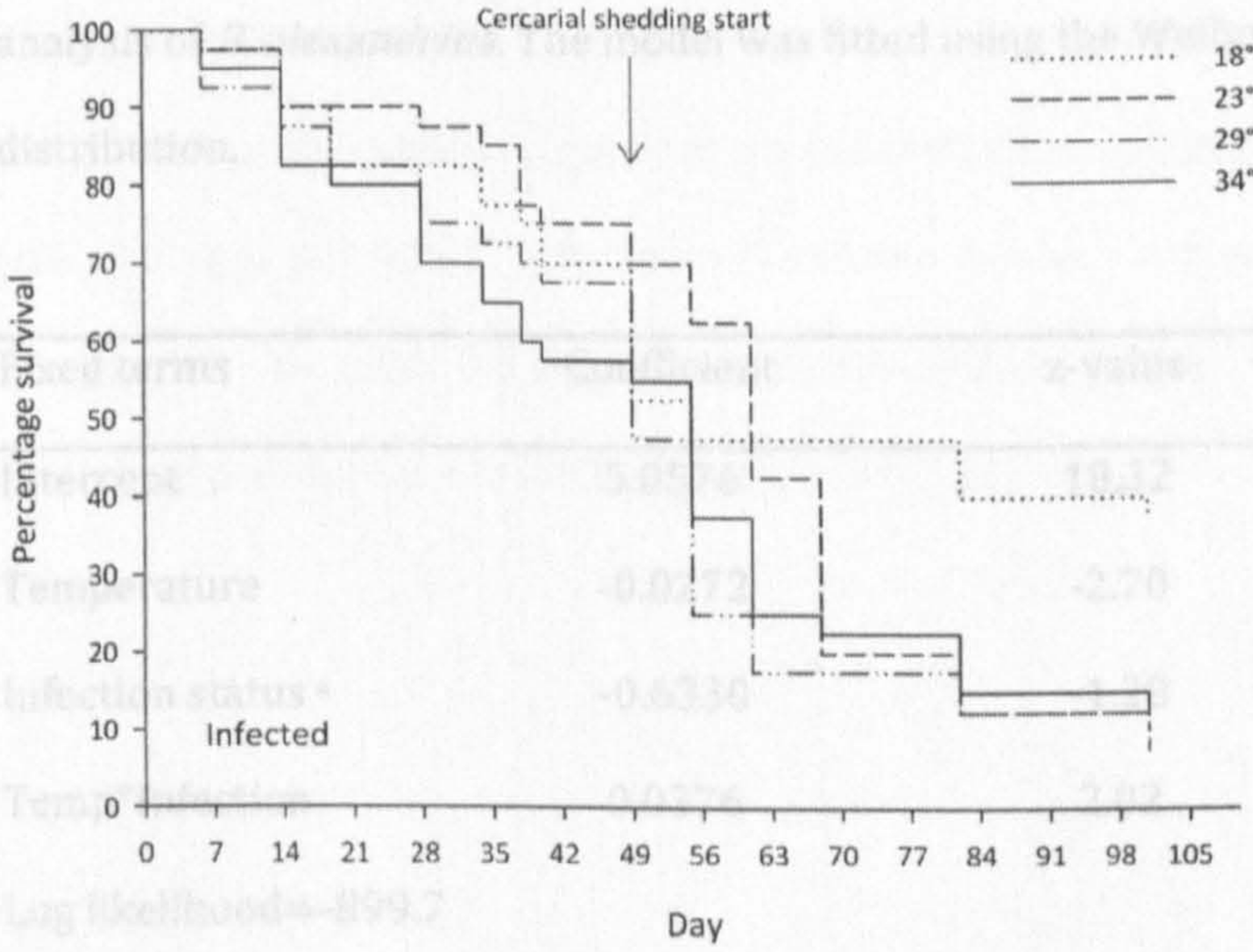

(b)

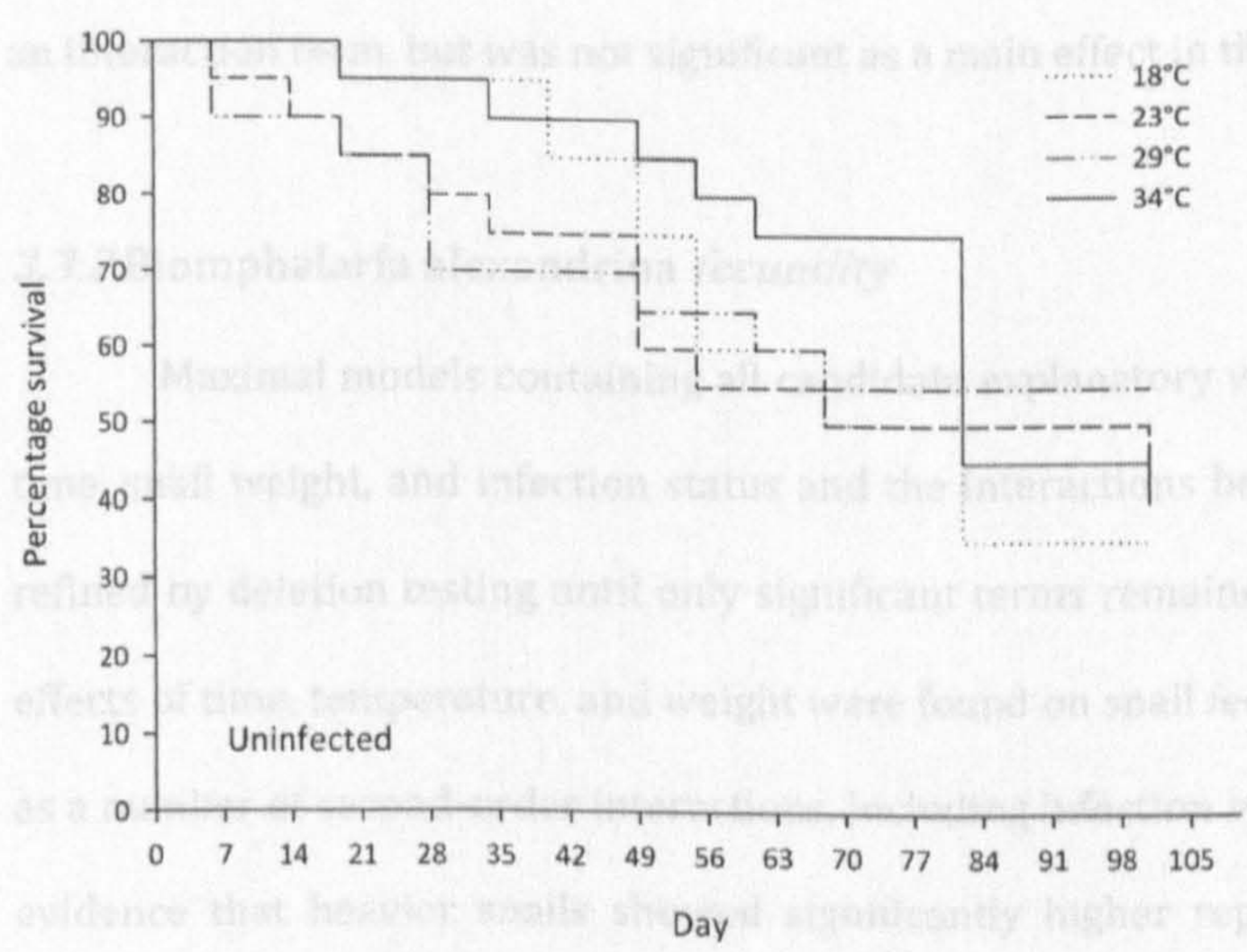

Figure 3.1. Percentage observed survival for infected (a) and uninfected *B. alexandrina* (b) over four temperatures.

Table 3.1. Coefficients and significance for estimated effects in the survival analysis of *B. alexandrina*. The model was fitted using the Weibull error distribution.

Fixed terms	Coefficient	z-value	P-value
Intercept	5.0576	18.32	< 0.001
Temperature	-0.0272	-2.70	< 0.001
Infection status [a]	-0.6330	-1.28	0.202
Temp*Infection	0.0376	2.02	0.0438
Log likelihood=-899.7			

Response variable = time to death; random variable = tank.

[a] Infection status is included as an explanatory variable because it was involved in an interaction term, but was not significant as a main effect in the minimal model.

3.3.2 Biomphalaria alexandrina *fecundity*

Maximal models containing all candidate explanatory variables, i.e. temperature, time, snail weight, and infection status and the interactions between these terms, were refined by deletion testing until only significant terms remained (Table 3.2). Significant effects of time, temperature, and weight were found on snail fecundity ($P < 0.05$) as well as a number of second-order interactions, including infection status. The model provides evidence that heavier snails showed significantly higher reproductive activity in the uninfected groups but not in the infected groups.

By week 7, there was a decrease in reproductive activity by infected snails at every temperature that was not observed in uninfected snails (Fig. 3.2). Egg-laying did not resume throughout the period of cercarial shedding, which may be due to the hosts resources being continually used by the parasite. Infected snails at 18°C and 23°C

stopped laying after week 7, whereas snails at 29°C and 34°C laid between 14 and 30 eggs per snail per week. Uninfected snails maintained at 18°C stopped laying eggs at week 7, whereas uninfected snails at the other three temperatures produced between 10 and 120 eggs per week. This value fluctuated but showed no strong trend for either temperature or time. All eggs were removed from tanks after counting to prevent crowding, preventing any further study on hatching rates.

Table 3.2. Coefficients and significance for estimated effects in the minimal adequate model for fecundity of *B. alexandrina* using the maximum likelihood method.

Fixed terms	Coefficient (SE)	t-value	P-value
Intercept	3.338 (1.592)	2.097	0.0381
Time	0.028 (0.014)	2.047	0.0427
Temperature	-0.126 (0.050)	-2.530	0.0353
Weight	4.339 (0.669)	6.489	<0.0001
Infection status [a]	-0.436 (2.840)	-0.154	0.8818
Time*Weight	-0.151 (0.029)	-5.245	<0.0001
Time*Infected	0.349 (0.067)	5.205	<0.0001
Temp*Infected	0.237 (0.094)	2.513	0.0362
Weight*Infected	-5.636 (1.179)	-4.782	<0.0001
Log-likelihood = -252.8187			

Time is measured in days post-infection.

[a] Infection status was involved in significant higher-order interactions and so was retained as an explanatory variable despite being non-significant as a main effect.

(a)

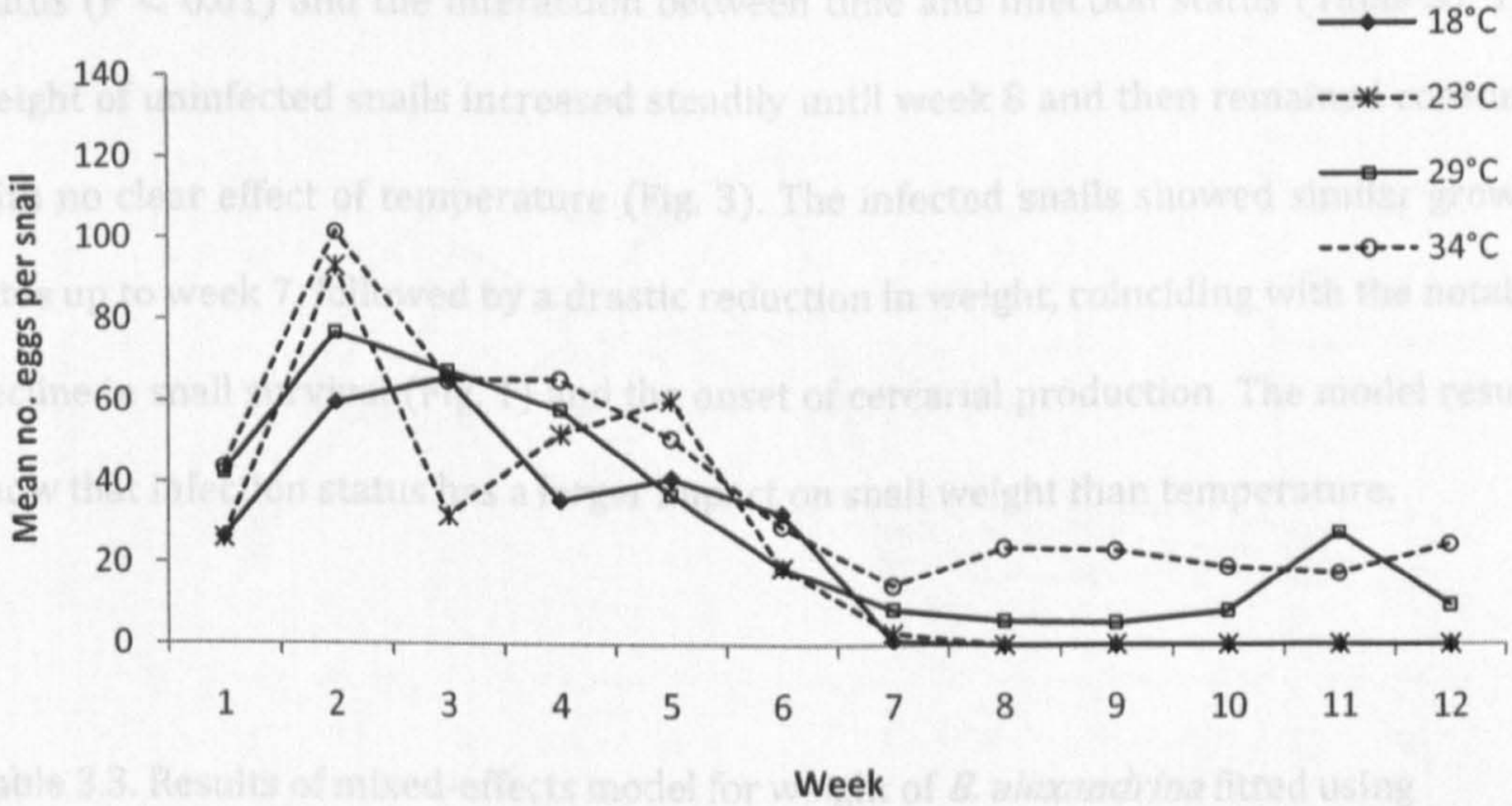

(b)

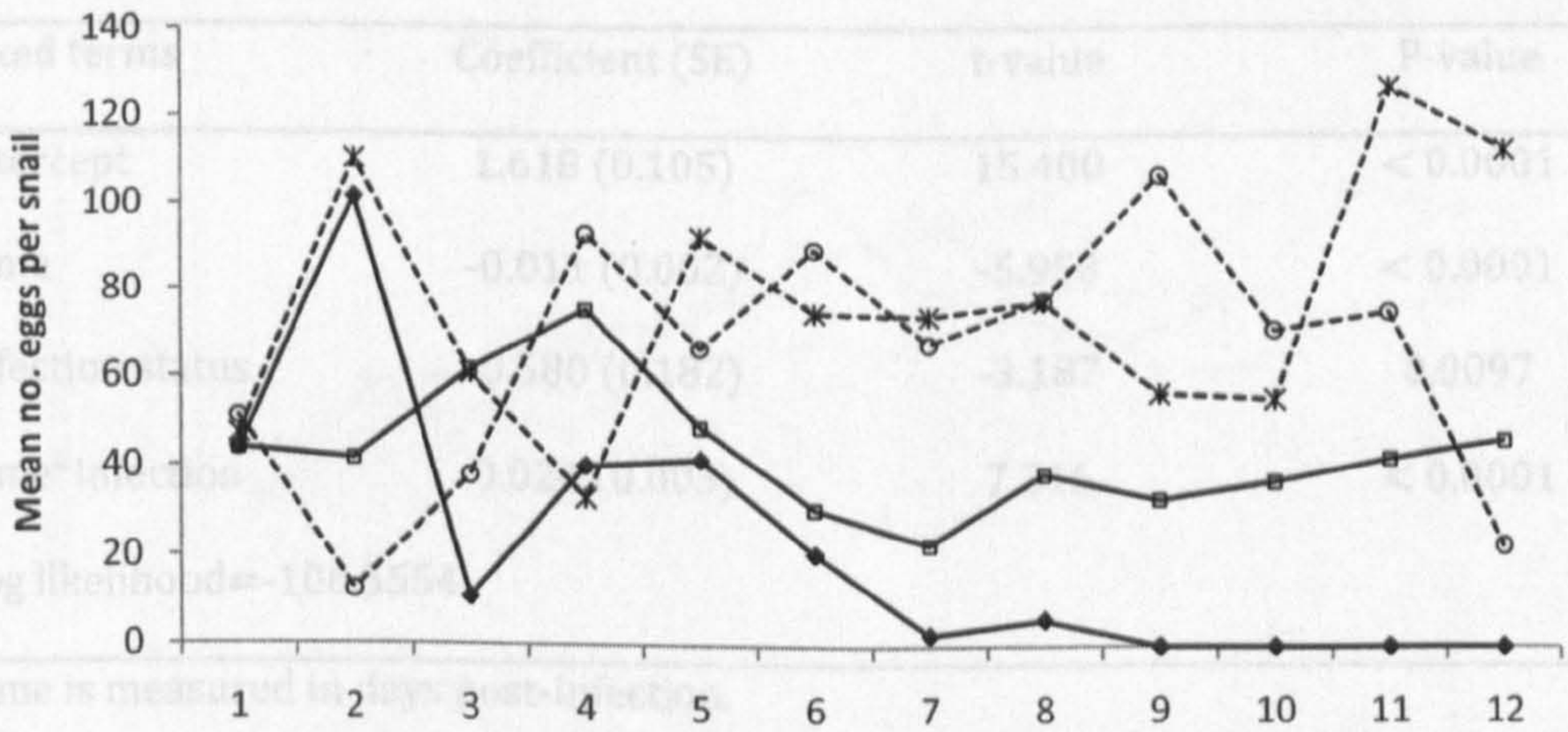

Figure 3.2. Fecundity, measured as mean number of eggs produced per snail per week over the fourteen week experimental period for infected (a) and uninfected *B. alexandrina* (b).

3.3.3 Biomphalaria alexandrina *weight*

Significant effects on snail weight were observed for time ($P < 0.0001$), infection status ($P < 0.01$) and the interaction between time and infection status (Table 3). The weight of uninfected snails increased steadily until week 8 and then remained constant, with no clear effect of temperature (Fig. 3). The infected snails showed similar growth rates up to week 7, followed by a drastic reduction in weight, coinciding with the notable decline in snail survival (Fig. 1) and the onset of cercarial production. The model results show that infection status has a larger impact on snail weight than temperature.

Table 3.3. Results of mixed-effects model for weight of *B. alexandrina* fitted using maximum likelihood.

Fixed terms	Coefficient (SE)	t-value	P-value
Intercept	1.618 (0.105)	15.400	< 0.0001
Time	-0.011 (0.002)	-5.958	< 0.0001
Infection status	-0.580 (0.182)	-3.187	0.0097
Time*Infection	0.024 (0.003)	7.316	< 0.0001
Log likelihood=-106.5554			

Time is measured in days post-infection.

(a)

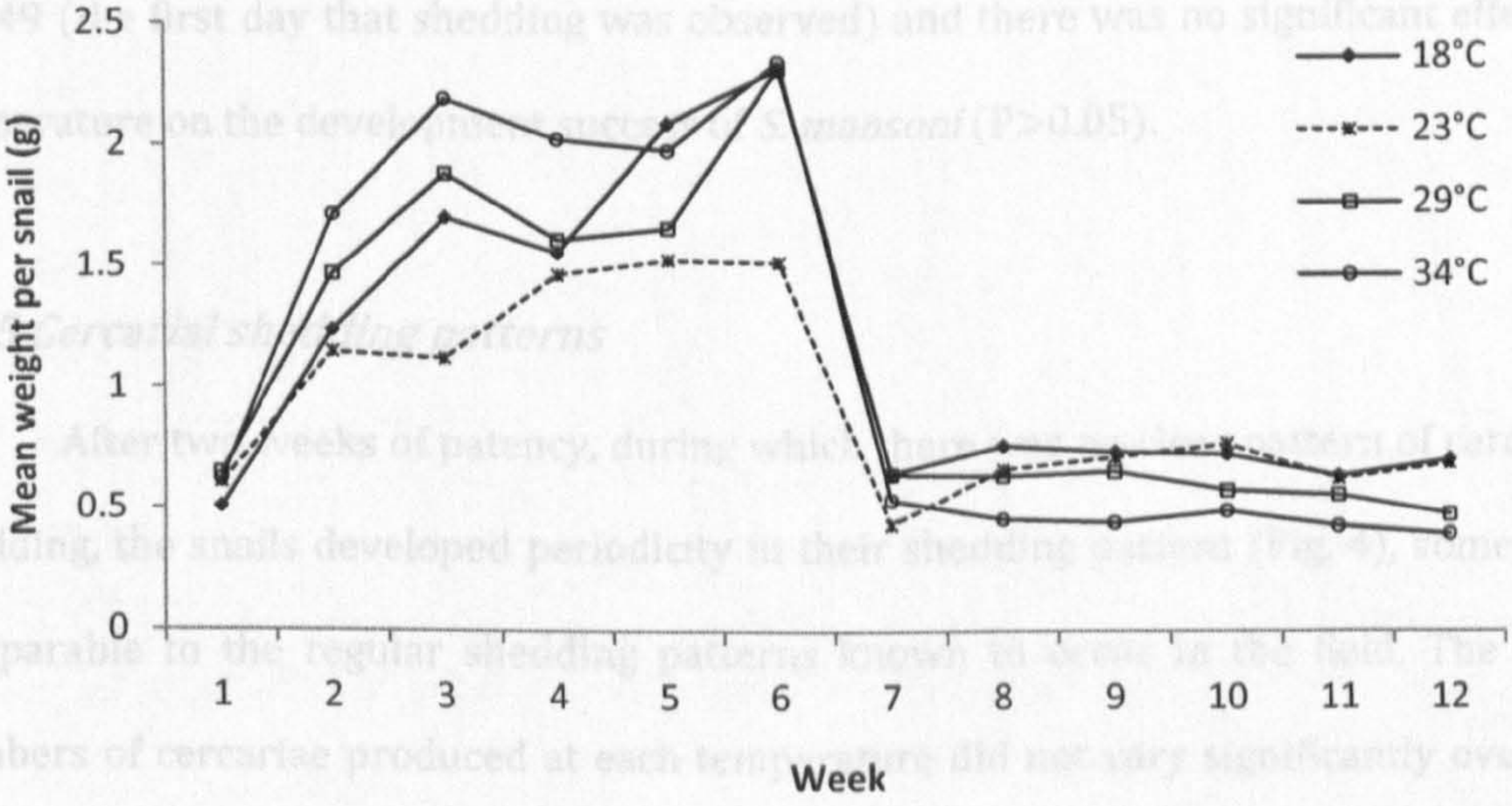

(b)

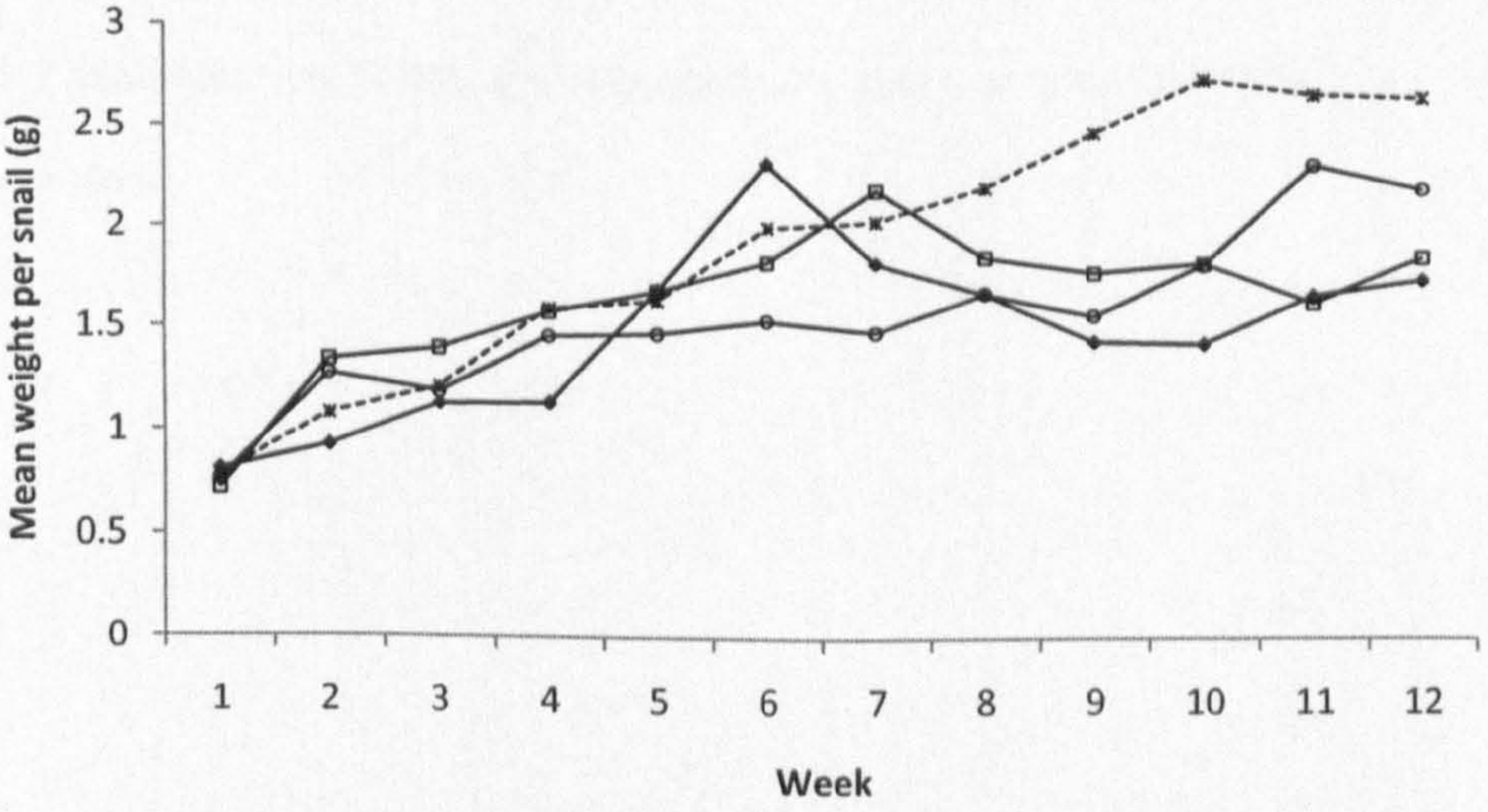

Figure 3.3. Mean weight per snail for infected (a) and uninfected *B. alexandrina* (b) over fourteen weeks at each temperature.

3.3.4 Schistosoma mansoni *development within* Biomphalaria alexandrina

From the 160 snails exposed to *S. mansoni* miracidia, 113 were still alive when cercarial shedding was recorded at day 49. Every infected snail produced cercariae on day 49 (the first day that shedding was observed) and there was no significant effect of temperature on the development success of *S. mansoni* ($P>0.05$).

3.3.5 Cercarial shedding patterns

After two weeks of patency, during which there was no clear pattern of cercarial shedding, the snails developed periodicity in their shedding pattern (Fig. 4), somewhat comparable to the regular shedding patterns known to occur in the field. The daily numbers of cercariae produced at each temperature did not vary significantly over the course of the experiment ($P>0.05$).

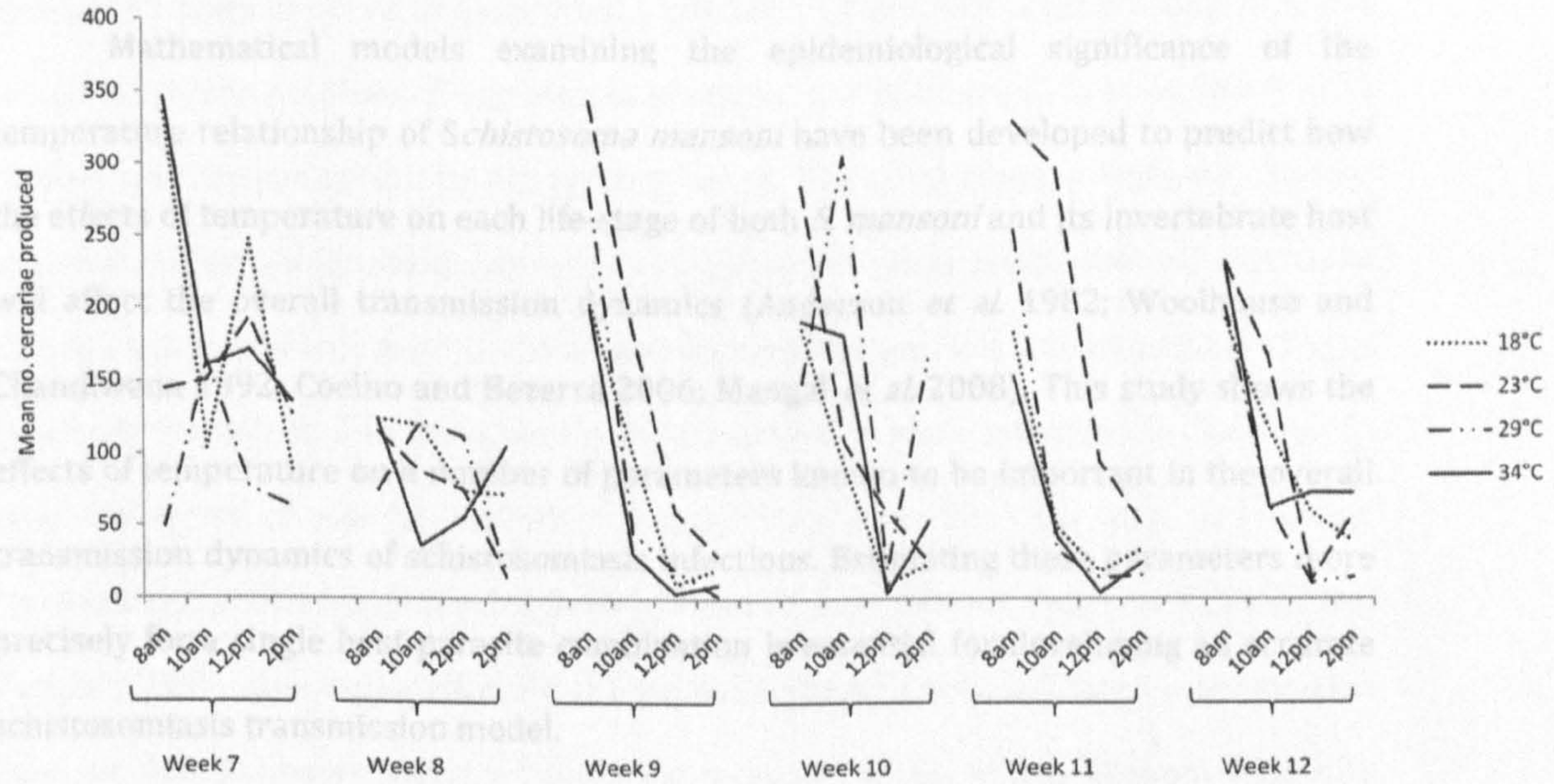

Figure 3.4. Daily production of S. mansoni cercariae for each temperature from week 7 post infection. Values are averaged over each time-point for each temperature.

3.4 Discussion

Mathematical models examining the epidemiological significance of the temperature relationship of *Schistosoma mansoni* have been developed to predict how the effects of temperature on each life-stage of both *S. mansoni* and its invertebrate host will affect the overall transmission dynamics (Anderson *et al.* 1982; Woolhouse and Chandiwana 1992; Coelho and Bezerra 2006; Mangal *et al.* 2008). This study shows the effects of temperature on a number of parameters known to be important in the overall transmission dynamics of schistosomiasis infections. Estimating these parameters more precisely for a single host-parasite combination is essential for developing an accurate schistosomiasis transmission model.

The survival data from this experiment supports earlier studies (Foster 1964; Lewis *et al.* 1986); the lowest survival rates of *B. alexandrina* occur at the two temperature extremes, 18°C and 34°C, with an optimum around 29°C. However, snails infected with *S. mansoni* exhibit a different trend, with survival rates dropping as temperature rises. This may be explained by the increases in fitness of the parasite at warmer temperatures, which would have a detrimental effect on the host's fitness. Furthermore, the drop in survival of infected snails but not uninfected snails at day 49, coinciding with the start of cercarial shedding, suggests that the onset of schistosome patency may be detrimental to the survival of infected snails. Indeed, the mortality rate of snails infected with schistosomes may not be directly dependent on the miracidial exposure dose but on the development and reproduction of the parasite within the host (Woolhouse 1989; Dekock 1993; Blair and Webster 2007). These values are similar to the previous model estimates (in Chapter 2) which show the lowest mortality rates for uninfected snails and the highest additional mortality due to parasitic infection at 30°C.

The most marked effect of infection on fecundity also occurred at day 49, coinciding with the first emergence of cercariae. This is consistent with the reduction in fecundity known to occur in parasitized snail hosts (Etges and Gresso 1965). At every temperature, the numbers of egg masses produced per snail dropped to almost zero at patency and did not return to pre-patency levels. The early stages of infection had no significant effect on fecundity, agreeing with an earlier study which showed that snails that became patent before or just after maturity did still produce a small number of eggs (Sturrock 1966a). In this study, nearly all snails with mature infections became sterile after the onset of patency, differing slightly from previous work that saw almost complete cessation of egg-laying between 14 and 21 days following exposure (Crews and Yoshino 1989). One explanation for the small numbers of eggs still seen with infection may be due to lower levels of infection in some snails. There was no fecundity compensation during the pre-patent period which has been previously documented (Thornhill *et al.* 1986); the rates of egg-laying among pre-patent snails paralleled those of uninfected control snails. It is possible that the differences in reproductive strategies seen here compared to those previously reported are due to differences in host or parasite strains. These data will have a definite impact on the outcome of the model as the egg-laying term (a_S) is influential in disease transmission. Hence, differential fecundity values for uninfected and infected snails at each temperature will be added to the model (Chapter 5).

Stressors such as starvation and low oxygen levels are known to affect the weight of snails (Ishak 1970; Ohlweiler and Kawano 2002), and I was interested to see if parasitism would have a similar effect. A large number of studies have documented the effects of *S. mansoni* infection on growth rates of snails and some conflicting results have arisen. Some papers describe a significant increase in growth rate of infected snails known as gigantism (Sturrock 1966a), whilst others have found that digenean infection

had no effect on snail growth rates (Crews and Yoshino 1989). The data presented here show no significant difference in weight between infected and control snails until patency, where a reduction in the weight of infected snails coincided with the onset of cercarial shedding. The discrepancies between some studies may be due to the different methods of measuring growth. In this experiment, growth was measured as wet weight whereas some studies use shell diameter as an indicator of growth. Wet weight was used as it is a more biologically relevant measure, representing the actual volume of snail tissue, with direct implications for its reproductive capacity.

The peak cercarial shedding times occurred at 8-10am daily, earlier than previous studies which have documented a peak at 11am, thought to coincide with human water contact patterns (Theron 1984). This is most likely to be due to the continued maintenance of parasite strains in the lab for a number of generations, which may have lead to the chronobiological variation noted here. Daily cercarial counts were performed once a week and under these experimental conditions. They do not directly indicate the mean number of cercariae that would be shed daily at these temperatures in natural conditions. The results of the patency at different temperatures showed a lack of variation. These results differ from studies by Lewis (1986) that state that the majority of snails shed cercariae within 32-35 days and snails kept up to 33°C may shed as early as 18 days. However, this value is still within the normal range of a 31-52 day patency previously documented in NMRI and PR-1 strains and may be due to differences in lab strains (Lewis *et al.* 1986). Nevertheless, there was a trend in the data, with total cercariae production peaking around 23°C and declining at higher temperatures. Poulin (2006) suggested that, on average, cercarial output from a range of trematode species increases almost 8-fold when the temperature rises by 10°C. However, the data presented here show a different trend, concurrent with the study by Pfluger *et al.* (1980), where the geometric mean number of cercariae produced increased up to 25°C,

and then decreased as the temperatures rose to 32°C with infected snails failing to shed cercariae at temperatures above 35°C. The discrepancy may also be due to authors using light or heat to stimulate cercarial production (Pfluger 1980), which would invariably lead to higher counts. As high mortality rates were seen at 34°C, these results seem consistent with this being the upper threshold for both development and survival of the parasite and host. Cercarial production was not an influential parameter in the transmission model (Chapter 2) and it is expected that changing the cercariae numbers will not have a significant impact on the outcome of the model.

As transmission is a function of the number of cercariae in the water frequented by humans, continuous periods of low temperatures may affect transmission due to alterations in human behaviour along with physiological changes in the intermediate host or parasite (Pfluger 1980). However, the relationship between cercarial shedding rates and exposure risk is not straightforward since changes in cercarial numbers may only have a minimal effect on the overall transmission dynamics of schistosomiasis as a single infecting miracidium can give rise to a large number of cercariae through a succession of asexual divisions.

These experiments were performed under controlled temperatures, and snails were maintained at a constant water temperature. In the natural environment, diurnal and seasonal temperatures can vary dramatically. This may affect both the parasite and the snail host life history traits and would result in small changes in the data, although this is unlikely to significantly alter the long-term patterns determined here. The validity of these laboratory data for other strains or species of schistosomes and snails needs further substantiation. Likewise, the reliability of lab strains when compared with field isolates would require additional studies. Nevertheless, this study highlights the importance and potential implications of long-term temperature change on snail and schistosome fitness and dynamics.

Overall these results support the previous suggestion that the various key biological processes determining snail and schistosome fitness (snail survival and reproduction, and parasite fecundity) are affected differentially by environmental temperature. Therefore, predicting the consequences of temperature changes on the prevalence, severity and distribution of schistosomiasis is unlikely to be straightforward, and requires a mechanistic framework such as the one presented in Chapter 2 and further developed in Chapter 5. By using a single species of both host and parasite, it is hoped that these parameter estimates will determine a more accurate picture of the potential effects of climate change.

CHAPTER 4

Estimating parameters for density-dependent constraints on the snail *Biomphalaria-alexandrina*

4.1 Introduction

Density-dependence affects the behaviour and fitness of every organism, which in turn alters the life-history of that organism and the dynamics of the whole population (Thomas and Benjamin 1974; Brown *et al.* 1994; Lande 2002). Such factors become important for controlling host-parasite systems where the presence and magnitude of population regulatory factors are crucial for disease dynamics and the design of effective long-term control strategies (Feng *et al.* 2002). In particular, control efforts may be negated if there is strong density-dependence acting within the host-parasite system (Feng *et al.* 2002). For example, one proposed method of controlling schistosomiasis is to treat water bodies with a molluscicide to reduce the number of snail intermediate hosts, thereby breaking the disease transmission cycle (McCullough 1980; Greer *et al.* 1996). However, such control efforts may prove ineffective if the snail population is regulated by density dependent constraints that buffer it against the additional imposed mortality.

Both laboratory and *in situ* studies have shown that snail density can greatly affect population growth, by reducing either snail survival or fecundity at high densities (Sturrock 1973a; Thomas and Benjamin 1974). These studies show that these fitness reductions are likely to arise through resource competition (either through exploitation or possibly, interference competition) rather than the increase of water-borne excretory/secretory products at high densities (Brown *et al.* 1994). However, few studies have quantified the form of these density-dependent relationships to inform mathematical models to predict their consequences for schistosome epidemiology. Few schistosome models have explicitly included density-dependence acting on the snail intermediate host population, despite the likely importance of such factors for the

spread and control of this parasite (Anderson 1978; Woolhouse 1991; Feng *et al.* 2002). Furthermore, those models that have incorporated density-dependence in the snail population are uninformed by empirical studies.

Here the density-fitness relationships for the schistosome intermediate host *Biomphalaria alexandrina* are quantified, for both naïve (unexposed) snails and snails exposed to miracidia of *Schistosoma mansoni*. Data on survival, fecundity, and weight were recorded and used to determine whether density-dependence affects fitness of snails. These data will be incorporated into a mathematical model (see Chapter 5) to explore the impact of temperature on the epidemiology and control of *Schistosoma mansoni*.

4.2 Methods

4.2.1 Study system

Biomphalaria alexandrina is a freshwater snail that is an intermediate host for *Schistosoma mansoni* in shallow parts of the Nile, Egypt. The strains used in this study were from Egypt and maintained in laboratories for approximately 20 generations. None of the experimental snails had been exposed to S. *mansoni* miracidia. Before the experiment, snails were kept in aerated 5L tanks at <10 snails L^{-1}, as detailed in Chapter 3.

4.2.2 Experimental design

One hundred and sixty juvenile snails (4-7mm) were randomly assigned to 8 experimental tanks containing water at 25°C. The tanks were equally divided into four density treatments, 5, 15, 25 and 35 snails in 2L water, and each treatment was replicated twice. An additional 80 juvenile snails were individually exposed to 5 freshly hatched *S. mansoni* miracidia in 2ml water for 2h and assigned to one of the four treatments. These snails were monitored weekly for development of infection.

All snails were transferred to incubators with a fluorescent low-light system (6W) set to 12L:12D. Water temperature stayed at 25°C ± 1°C throughout the experiment and was changed weekly. Before the experiment, all snails had received rabbit food (Pascoe's Bunny Balance, Driffield, UK) *ad libitum*, and any excesses of food were removed daily. They were all, therefore, in similar states of health before introduction to the experimental tanks. During the experiment, each tank received 2 pellets of food at 6am, daily. Fecundity, measured as the number of eggs produced per week was recorded weekly, and eggs were removed from the tanks after counting. This was to control for any possible effects associated with a reduced surface area available for the snails to lay eggs. Growth, measured as wet weight, and weekly mortality rates were also recorded throughout the study. All dead snails were removed from tanks. After ten weeks, all snails were removed, weighed, and final mortality rates were recorded.

4.2.3 Statistical analysis

Survival rates were modelled using two-way ANOVA using the "aov" function in R (http://www.r-project.org) to detect any significant differences between treatment groups. Linear mixed effects (LME) models were used to analyse the effects of exposure to miracidia and density on the weight and fecundity of snails using the lme4 package in R. LME models were used as the variance was not constant and the errors were not

normally distributed; this allows the specification of different error structures, e.g. poisson, binomial or Gaussian. This technique also controlled for pseudoreplication by adding a random factor. The model fit was assessed using the deviance, which is defined as -2 times the difference in log-likelihood between the current model and a saturated model and using ANOVA.

4.3 Results

4.3.1 Development of infection

Eighty snails were exposed to *Schistosoma mansoni* miracidia at the start of the experiment, but none developed full infections. The impact of exposure to infecting miracidia was studied as an additional stressor, and the responses were measured as stated previously.

4.3.2 Survivorship

The survival rates for the unexposed snails were higher in the low density tanks; no snails in the lowest density group died until day 60, whereas the other three treatment groups had lower survival rates from week 1 (Fig. 4.1). The snails exposed to *S. mansoni* miracidia showed lower survival rates than the control snails: 17% of exposed snails survived the ten week study period whereas 60% of control snails survived. Survival was significantly affected by exposure to infection (two-way ANOVA; $P < 0.0001$). In contrast, the differences between density groups did not produce a statistically significant result (two-way ANOVA; $P = 0.072$ for density group). However, there was a significant interaction between exposure and density group ($P < 0.05$)

suggesting that the survival of snails exposed to miracidia responded to population density in a different manner to unexposed snails.

4.3.3 Weight of snails

The initial mean weights of both the unexposed and exposed snails did not significantly differ (Fig. 4.2). When the density of snails in each tank was increased, the relative growth rate slowed in both treatment groups. The minimal adequate model developed by deletion testing using linear mixed effects models included all the variables measured throughout the experiment; treatment group, time and exposure to parasitic infection (Table 4.1). Over time, snails exposed to *S. mansoni* in the higher density groups increased their growth to eventually approach that of the lowest density group, although the average weight in the highest density group remained lower (Fig. 4.2b).

Exposure to parasite did not have a significant effect on snail weight but became significant when combined with time.

(a)

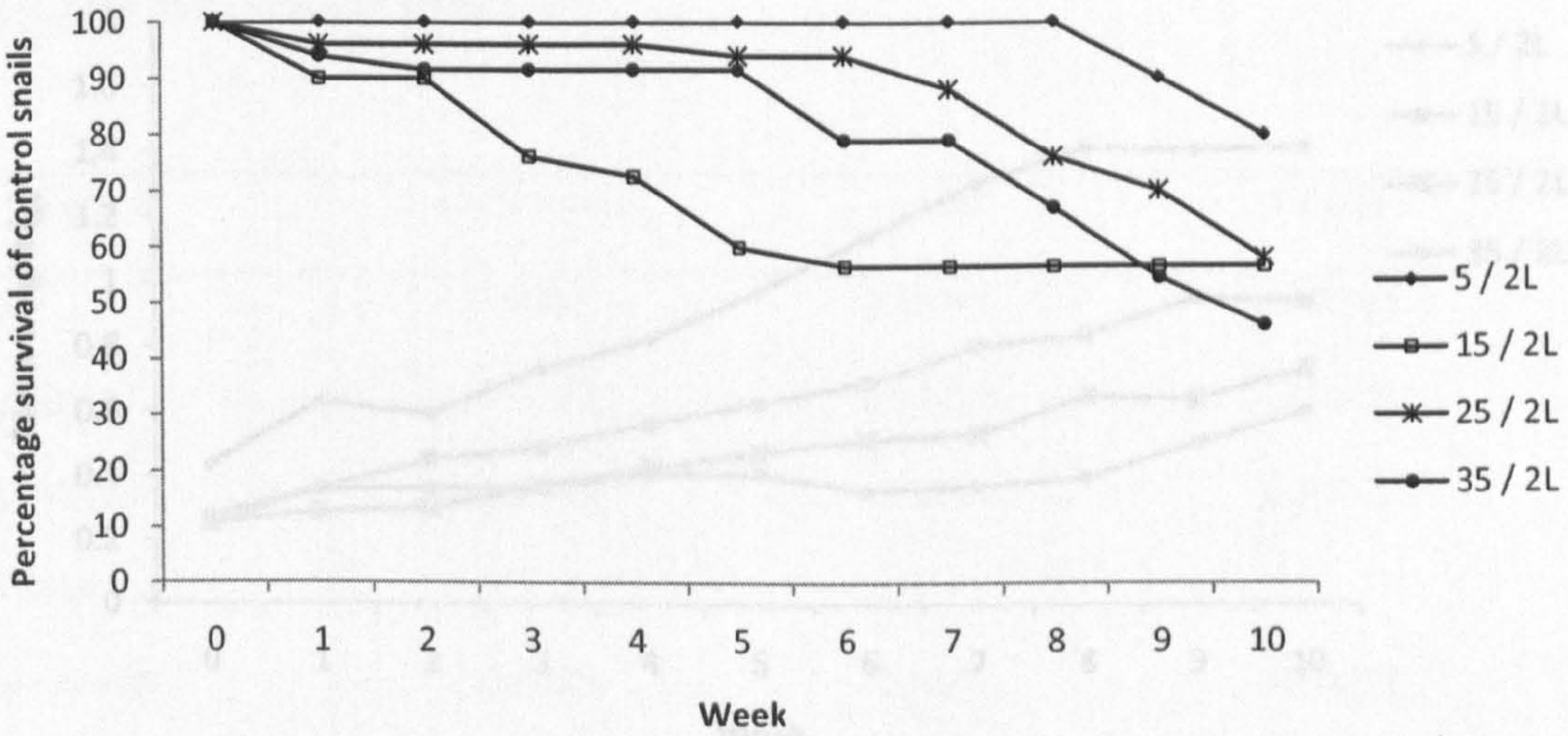

(b)

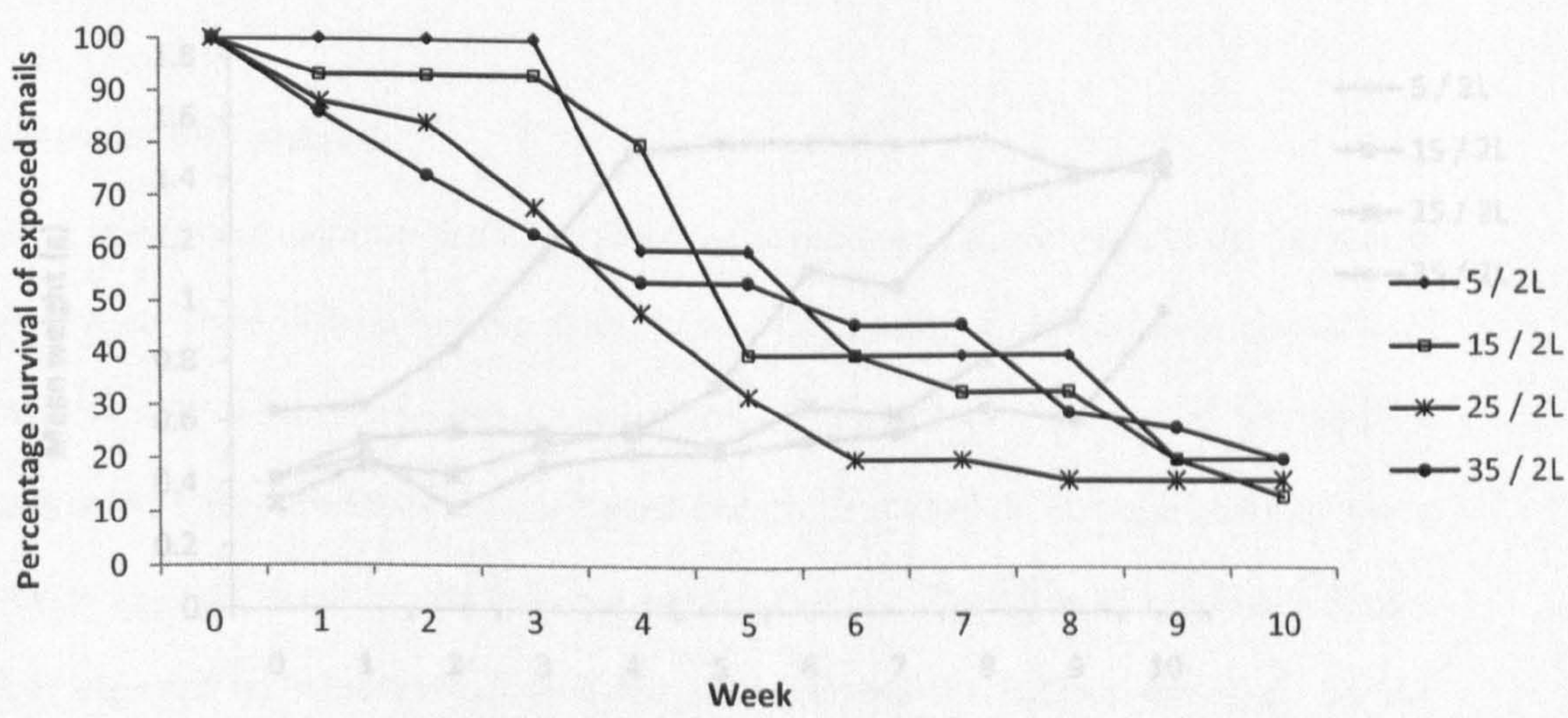

Figure 4.1. Percentage survival of unexposed snails (a) and snails exposed to miracidia (b).

(a)

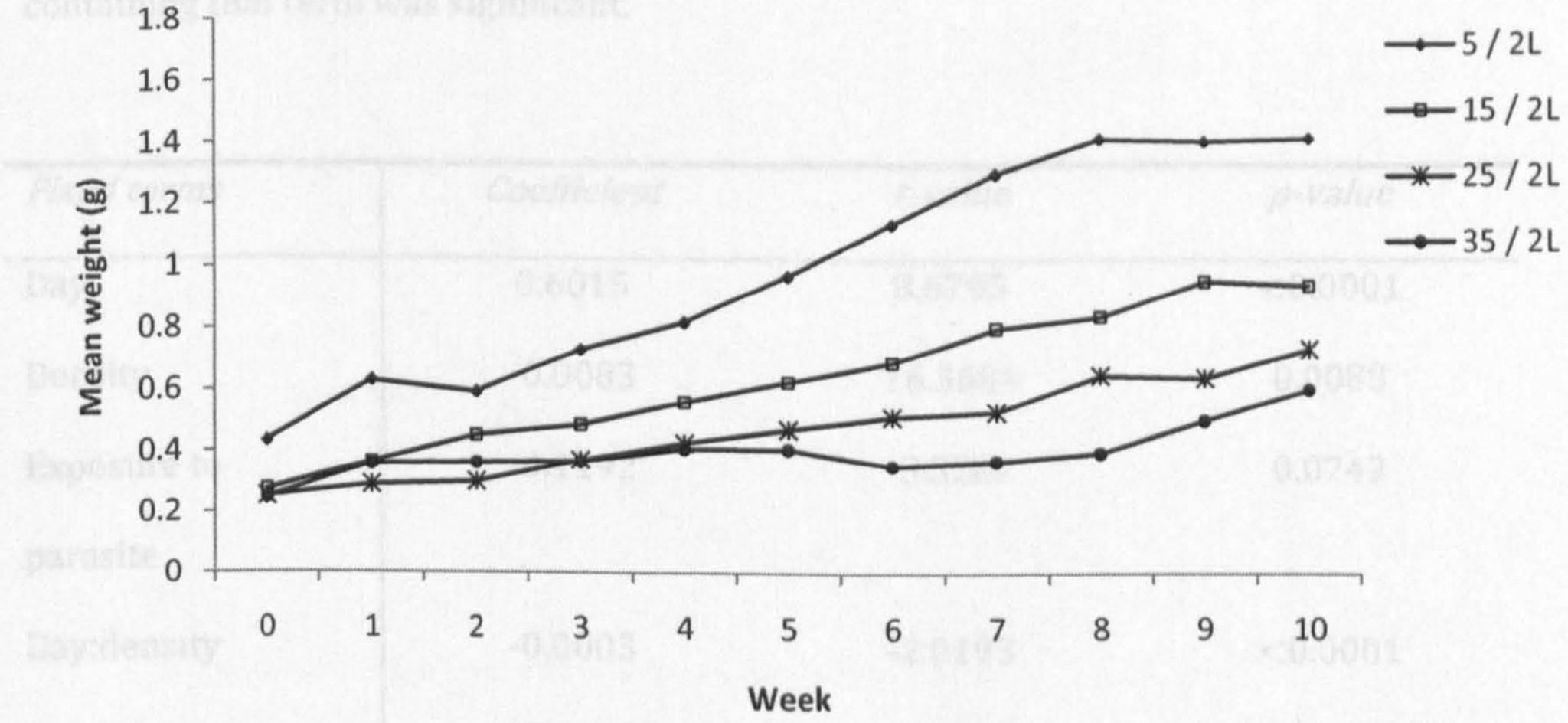

(b)

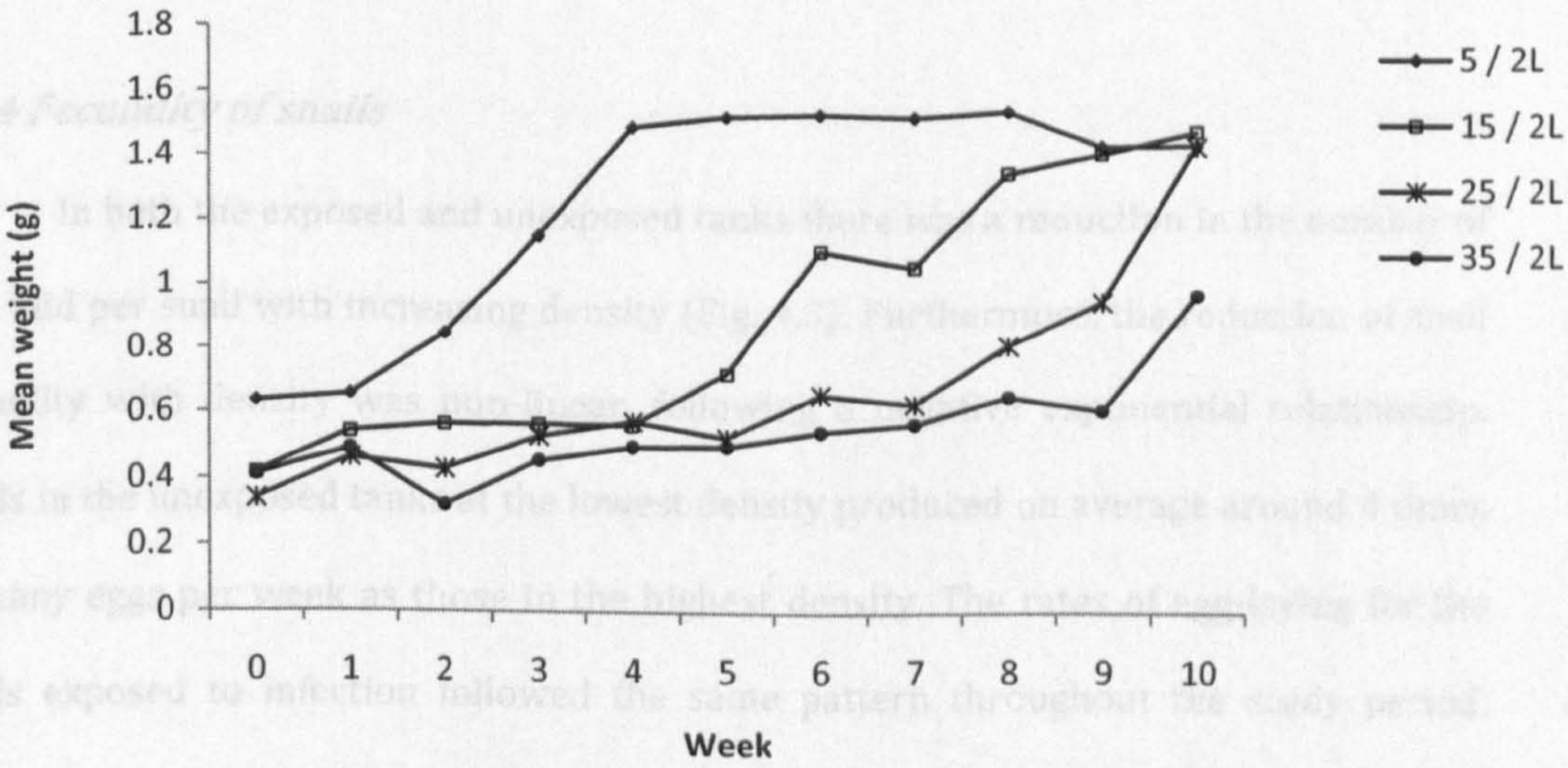

Figure 4.2. Mean weight per unexposed (a) and exposed snail (b) over ten weeks.

Table 4.1. Minimal adequate model for weight of snails containing all significant terms. Insignificant first-order terms were retained only if a second-order interaction containing that term was significant.

Fixed terms	*Coefficient*	*t-value*	*p-value*
Day	0.6015	8.6795	<0.0001
Density	-0.0083	16.3684	0.0088
Exposure to parasite	-0.1192	-3.3267	0.0742
Day:density	-0.0003	-2.0193	<0.0001
Day:exposure	-0.0027	-3.0038	0.0033

4.3.4 Fecundity of snails

In both the exposed and unexposed tanks there was a reduction in the number of eggs laid per snail with increasing density (Fig. 4.3). Furthermore, the reduction of snail fecundity with density was non-linear, following a negative exponential relationship. Snails in the unexposed tanks at the lowest density produced on average around 4 times as many eggs per week as those in the highest density. The rates of egg-laying for the snails exposed to infection followed the same pattern throughout the study period, although the unexposed snails consistently laid higher numbers of eggs (20-69% higher). Day, density and exposure to parasitic infection all reduced the number of eggs produced by snails (Table 4.2).

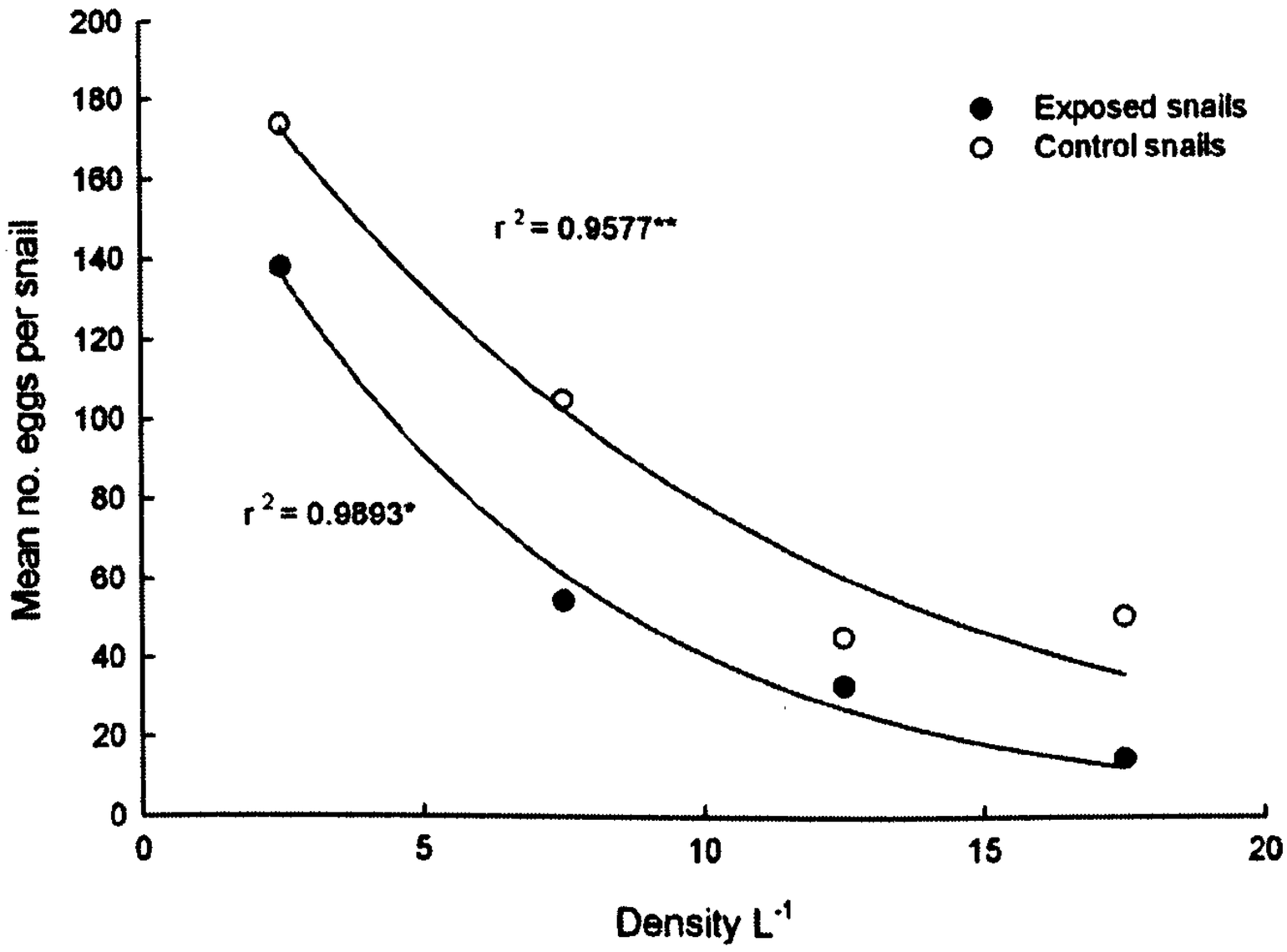

Figure 4.3. Regression analyses of the mean number of egg masses produced by each snail per week over the 10 week study period. Regression analysis was performed using an exponential decay model;

*, *y=208.7*exp(-0.0797*x)*;

**, *y=231.03*exp(-0.0524*x)*.

Table 4.2. Minimal adequate model for snail fecundity, determined using deletion testing as before.

Fixed terms	*Coefficient*	*t-value*	*p-value*
Day	-0.1666	8.8414	<0.0001
Density	-0.4885	-6.2137	<0.001
Exposure to parasite	-2.8598	3.2336	0.0103
Day:density	0.005	2.9615	0.0038

3.4 Discussion

Exposing juvenile snails to *S. mansoni* miracidia had a negative impact on *Biomphalaria alexandrina* survival, which became more pronounced as density increased, reducing the survival rates in every group by 20-60%. Although the miracidia did not mature within many of the snail hosts, the impact of exposure alone on host survival was significant. The lowest density group showed the highest rate of growth and achieved the highest rates of oviposition per week, contradicting other studies where the highest density groups showed the highest rates of growth and reproduction (Thomas and Benjamin 1974). The snails exposed to miracidia were the same weight in each treatment group at the end of the study. This is likely to be due to the higher mortality rates within the exposed groups reducing the density of snails throughout the experiment. Therefore, although snail growth was initially inhibited in the high density

treatments, the snails retained the potential for growth and, as densities reduced over time, were able to compensate for deficiencies early in life to catch up with their maximal attainable size as observed in the lowest density treatments.

The biological explanations for the effects of density dependence were not investigated in this study. However, there are three plausible explanations for the negative feedback effects seen in the highest density groups; competition for food resources, depletion of oxygen and/or calcium, and the production of growth inhibitory or toxic factors. By giving each tank the same amount of food daily, competitive pressure may have forced some individuals to experience a food shortage. This could be explored further to determine whether food would be a limiting factor. The tanks were continually aerated to provide sufficient oxygen for snail growth and calcium carbonate was added weekly. *Biomphalaria glabrata* remove calcium from the water at a rate proportional to the absolute growth of the snails; it can, therefore, become a limiting factor if the concentration drops below 40-80µg ml^{-1} (Thomas *et al.* 1974). However, 80% of the calcium required by the snails is taken directly from the water (Thomas and Benjamin 1974). Under these circumstances, it may be possible that calcium was limited in the higher density tanks and growth was restricted. The third factor that may affect growth is the production of various factors by the snails themselves. Waste products or specific growth inhibitory factors may be released by snails and concentrated in the high density tanks. As these inhibitory factors in the tanks become more concentrated, the limiting effect would increase. Consequently, the water in each tank was replaced weekly to reduce any adverse effects of waste product. Further study is necessary to determine the mechanisms which drive these responses.

The density-dependent reduction of snail fecundity observed in both the exposed and unexposed groups of snails followed a non-linear, negative exponential relationship. This pattern is different from the traditional linear relationship indicative of logistic

growth assumed by the majority of population models. A recent review of a wide range of taxa, spanning mammals, birds, fish and insects, showed that such non-linear, decelerating density-dependent relationships are likely to be the norm (Sibly 2005). Furthermore, these relationships are likely to have important implications for population dynamics, potentially slowing population growth, driving large fluctuations in population size and altering the population's response to perturbations. From an applied perspective, such non-linear density dependent relationships are likely to have important implications for parasite control; the response of the parasite population to the additional mortality imposed through a control programme will greatly depend on the functional form of such density-dependent regulating processes.

The diversity of potential effects of density-dependence on vectors of human disease makes it difficult to predict how the overall transmission of infection within a host population will be affected. If the density-dependence succeeds in reducing a population of disease vectors, the disease may not be able to persist. It is, therefore, clear that the effects of density-dependence on infectious disease dynamics are not as straightforward as expected. The implications of non-linear density-dependent relationships have yet to be examined using mathematical models. It may be that by incorporating these empirically derived relationships into an existing model framework, the responses of schistosomes to a range of imposed control methods can be better predicted.

CHAPTER 5

Modelling schistosome dynamics with a comparison of control strategies

5.1 Introduction

Several studies have modelled the dynamics of schistosomiasis infections in humans (May and Anderson 1979; Anderson 1991; Woolhouse 1991) using a similar framework to the model described in Chapter 2. This model focussed on one host-parasite combination, *Schistosoma mansoni* and its invertebrate host *Biomphalaria alexandrina*. The model describes the key features of the host-parasite system using parameter values derived from an extensive literature search. As far as possible, the model was parameterised using the host-parasite combination *B. alexandrina* – *S. mansoni*. However, the paucity of data on specific host-parasite combinations resulted in a model that used data from a number of different species. To address this shortcoming, data on temperature (Chapter 3) and density-dependent effects on the snail intermediate host (Chapter 4) were collected in the laboratory and used to refine this earlier model.

In this chapter, I present a series of more comprehensive models incorporating the data collected in Chapters 3 and 4, with the addition of density-dependence in the adult parasite population. These models will each be subjected to a sensitivity analysis to determine whether each modification to the model changes the relative sensitivities of each parameter. By comparing these models, I will develop an improved model that will capture biologically important features of this system based on the sensitivity analysis and provide more accurate predictions on the impacts of temperature on human disease. The second part of this chapter uses this final model to assess the impact of various control strategies on an endemic community. This chapter is organised as follows. Section 5.2.1 presents a modification of the initial model, developed in Chapter 2 and parameterised in Chapter 3 (and Appendix A2). From this, two further models are

derived (Sections 5.2.2 and 5.2.3); in Section 5.3 the results of each of these models along with the sensitivity analyses are presented. Section 5.4 contains the discussion of these analyses and presents the definitive schistosomiasis model, which will be used for examining the control programmes. Section 5.5 deals with the various control approaches and examines each in turn to determine how the optimal control programme may change with temperature change.

5.2.1 Model 1 – the baseline model

The basic structure of this epidemiological model is slightly modified from that described previously (Chapter 2) and is based on earlier models of schistosome population dynamics by Anderson and May (1979b) and Woolhouse (1991; 1992). Key aspects of this basic model are: (i) the size of the human host population is assumed to be constant and hence the risk of infection to a static host population of a given size is modelled; (ii) due to the intense density-dependence acting on schistosome development within snails, previous models are followed (Woolhouse 1991; Woolhouse 1992) by ignoring the burden of infection within snails and simply classing snails as uninfected (U), latently (pre-patent) infected (L) and patently infected (I); (iii) all infected snails shed cercariae at a constant rate λ_C regardless of the number of miracidia they were challenged with; (iv) based on the results in Chapters 3 and 4, latently and patently infected snails may lay eggs at different rates (a_L and a_I, respectively) from uninfected snails (which lay at rate a_S); (v) overall egg production of the snail population is limited through density-dependent competition of strength (q). The probability of the snail eggs hatching (ν) rather than an explicit death rate is included in the model; hence the model effectively describes the number of viable eggs laid, rather than the total number. This eliminates the need for the egg mortality term δ_E from the model in

Chapter 2, which is set to 0. The model describes the rate of spread of infection into a previously uninfected area and is run until both prevalence and mean worm burden reach equilibrium.

All parameters are defined in Table A2.10, together with their baseline values, as obtained from the literature and the experiments in Chapter 3 (see Appendix A2 for details). The final model comprises four differential equations, describing the adult parasite population within humans (P), and the density of uninfected (U), latently infected (L) and patently infected (I) snails:

$$\frac{dP}{dt} = \frac{\beta_H H \lambda_{C'} I}{\delta_{C'} + \beta_H H} - P\delta_P \qquad 5.1$$

$$\frac{dU}{dt} = \varepsilon(1 - qN)(a_s U + a_L L + a_I I) - \delta_s U - \frac{\beta_S \lambda_M U(P/2)}{\delta_M + \beta_S N} \qquad 5.2$$

$$\frac{dL}{dt} = \frac{\beta_S \lambda_M U(P/2)}{\delta_M + \beta_S N} - L(\delta_S + \sigma) \qquad 5.3$$

$$\frac{dI}{dt} = \sigma L - I(\delta_S) \qquad 5.4$$

where $N = U + L + I$ and $\varepsilon = \upsilon\left(\frac{\theta_S}{(\delta_J + \theta_S)}\right)$ 5.5 and 5.6

The parameter ε describes the maturation of snails from eggs to adulthood. The derivation of the mean worm burden per human host and the prevalence of infection in the population are explained in Chapter 2 (Equation 2.5).

For a dioecious, monogamous parasite like schistosomes, it is important to consider the probability of each infecting parasite to find a mate within the host (May 1977). This probability will be influenced by the mean worm burden per person and the degree of aggregation of the parasites. The relationship between the mean number of worms in an individual host and the probability of finding a mate assuming monogamous pairing is described by May (1977) as:

$$\phi(m,k) = 1 - \frac{(1-\alpha)^{1+k}}{2\pi} \int_0^{2\pi} \frac{(1-\cos\theta)}{(1+\cos\theta)^{1+k}} d\theta \qquad 5.7$$

where φ is the probability that a female will mate and produce eggs, m is the mean number of worms per person, k is the clumping parameter and $\alpha = m/(m+k)$.

The mating probability is affected by changes in k and m (Fig. 5.1). Clearly, at moderate to high worm burdens (>30 worms per person), the mating probability approaches 1, with little difference between the four k values. Almost all worms found in individuals harbouring over 100 worms are expected to be mated (mating probability of 0.95 when k=1, and 0.99 when k=0.01). The mating probability only becomes important with mean worm burdens (m)<10. Therefore, the mating probability for these models is assumed to be 1 and the aggregation parameter is kept at 0.1 (Gryseels and deVlas 1996).

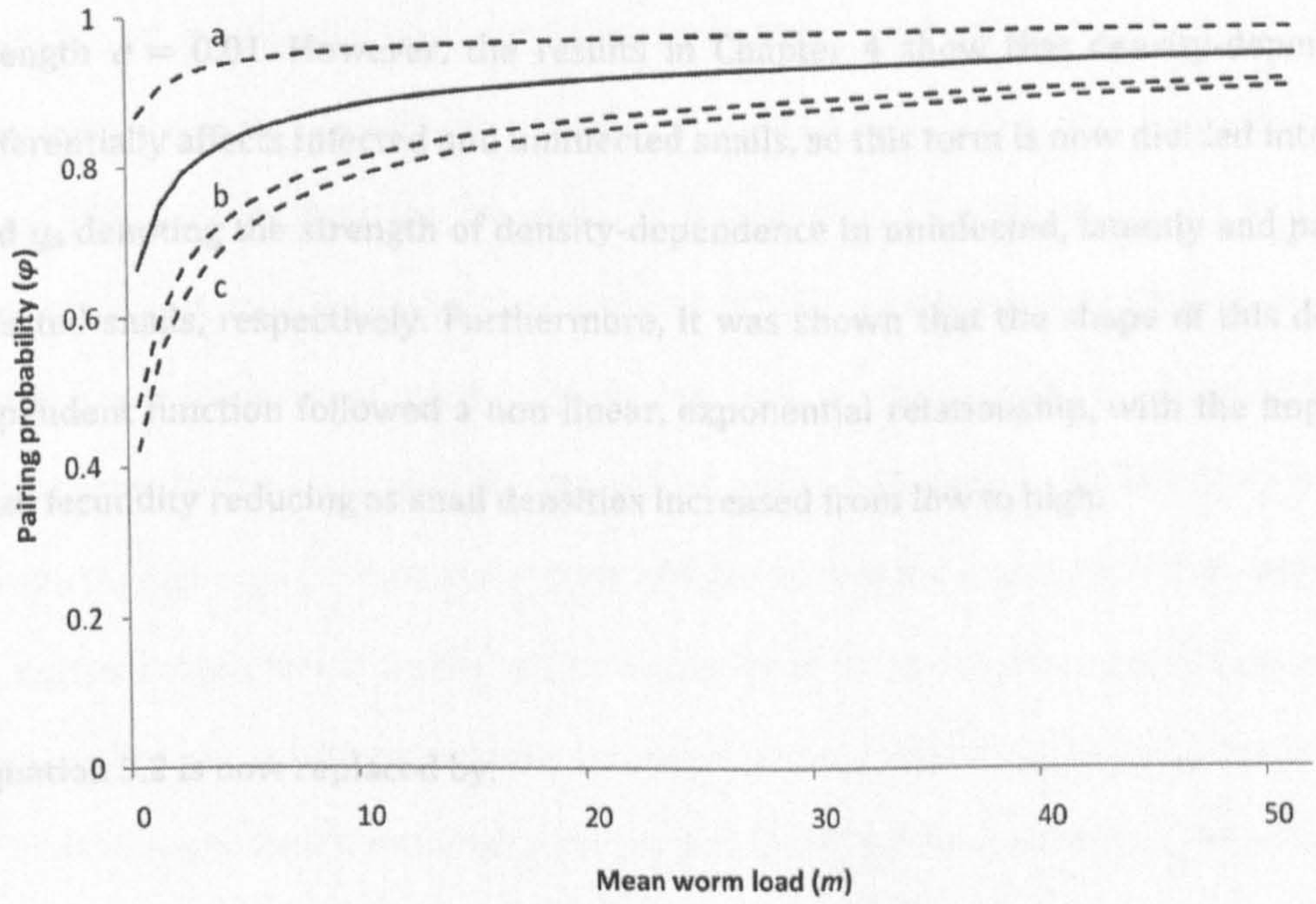

Figure 5.1 The pairing probability (φ) of adult worms as a function of the mean worm burden per person (m) assuming monogamy.

The four lines relate to a negative binomial distribution with an aggregation parameter k of various values. The solid line is the commonly used aggregation parameter (k) of 0.1, which is used in these models and is based on empirical data observed in the field (Sturrock 1973b). The dashed lines represent (a) $k = 0.01$, (b) $k=0.5$ and (c) $k=1$.

5.2.2 Model 2 – incorporating realistic density-dependent effects within the snail host

In the absence of empirical data, Model 1, described above, assumed that all snails were subject to a linear density-dependent constraint on fecundity, of arbitrary strength $q = 0.01$. However, the results in Chapter 4 show that density-dependence differentially affects infected and uninfected snails, so this term is now divided into q_U, q_L and q_I, denoting the strength of density-dependence in uninfected, latently and patently infected snails, respectively. Furthermore, it was shown that the shape of this density-dependent function followed a non-linear, exponential relationship, with the impact on snail fecundity reducing as snail densities increased from low to high.

Equation 5.2 is now replaced by:

$$\frac{dU}{dt} = \varepsilon(va_S Ue^{-qU_N} + va_L Le^{-qLN} + va_I Ie^{-qIN}) - \delta_S U - \frac{\beta_S \lambda_M PU}{\delta_M + \beta_S N} \qquad 5.8$$

5.2.3 Model 3 – density-dependent effects on the adult parasite

Density-dependent effects on the adult parasites within a heavily infected human host may arise as a result of limitations in space or nutrients or as a consequence of acquired immunity. These effects can manifest themselves as changes in parasite mortality or fecundity and will be sensitive to the worm burden in each individual. These mechanisms can limit schistosome growth and may decrease the sensitivity of the model to perturbations in the other parameter values (Griffin 1988; Woolhouse 1991).

Medley and Anderson (1985) presented an analysis of autopsy data (Cheever 1968) showing significant density-dependent fecundity in *S. mansoni* worms. This paper developed a number of models to describe the decrease in per capita fecundity of the schistosomes at high density within the human host. A subsequent paper that used a murine host model also concluded that there was significant evidence for a density-dependent reduction in parasite fecundity in animals with high levels of infection (Jones *et al.* 1989). Estimating the fecundity of mated pairs of schistosomes is biologically important and may have significant effects on the transmission of disease. However, there are a number of complications involved in experimentally determining the relationship between parasite density and fecundity, including the difficulty of retrieving all worms and eggs present in the body and faeces and the assumption that the number of eggs in a single faecal sample will be indicative of the average number of eggs excreted per day. The impact of host immune responses and the effect of parasite age on fecundity are unknown, further complicating the picture. Despite these limitations, the influence of parasite density-dependence in the model is investigated and its impact on the dynamics of disease is discussed. Furthermore, a sensitivity analysis will be conducted as before and the results are compared to the two models above.

This model does not explicitly model schistosome egg production, rather the term λ_M is used to denote the number of miracidia produced per mated schistosome pair, per day. This assumes that all excreted eggs are viable and develop into miracidia and ignores eggs trapped within the host tissue, as they will not contribute to the next generation. Medley and Anderson (1985) consider the negative exponential model to be the most reliable and robust method of parameter estimation for the data presented by Cheever (1968), although the power function provided the best fit. Hence, I use the parameterised negative exponential function to describe this relationship. This gives the equation:

$$\lambda_M = \lambda_0 e^{-\gamma_M} \qquad 5.9$$

Where λ_0 is the maximum possible fecundity and γ is a constant that determines the strength of constraint on egg production. However, it is not viable to simply replace λ_M in the previous equations with Eq. 5.9, since the degree of density-dependence will depend on the distribution of parasites across the host population. Smith (1993) showed how this relationship may be used to describe the rate of parasite egg production, within a similar modelling framework to the one presented here, assuming a negative binomial distribution in the number of worms per host. Here I follow his approach, replacing the λ_M term in equations 5.2, 5.3 and 5.8 by:

$$\lambda_M = \lambda_0 e^{-\gamma}\left(1+\frac{P(1-e^{-\gamma})}{Hk}\right)^{-(k+1)} \qquad 5.10$$

5.3 – Results

In this section I present the mean worm burden per person and the overall prevalence in a population as predicted by each model. The main goal here is to determine whether there is any advantage in adding the extra complexities of density-dependence within the snail and parasite population. The behaviour of the models was explored over a 10^4 days, allowing the dynamics to stabilise. The model was run with a constant human population size (H) of 10^4 and an initial parasite population (P_0) of 20. This allows us to see the early behaviour of the model as the disease spreads throughout

an uninfected population. The long-term model output is insensitive to the initial parameter values.

The results for Model 1 show a stable, endemic state for all four temperatures (Fig. 5.2). There is a clear effect of temperature on the mean worm burden per person (Fig. 5.2a) with the highest mean worm burden of 150 worms per person at 34°C, decreasing to 53 worms as the temperature decreases to 18°C. The model predicts that prevalence will quickly reach a steady-state at which approximately half of the population is infected in the absence of any interventions (Fig. 5.2b). Long-term variations in the temperature do not significantly affect the overall prevalence level although they do influence the initial rate of spread of the disease. This model supports earlier models which use an aggregated negative binomial distribution and show large increases in worm burdens can be accompanied by relatively small changes in prevalence (Anderson 1982). Uninfected human hosts remain uninfected but those human hosts that are infected have higher worm burdens.

(a)

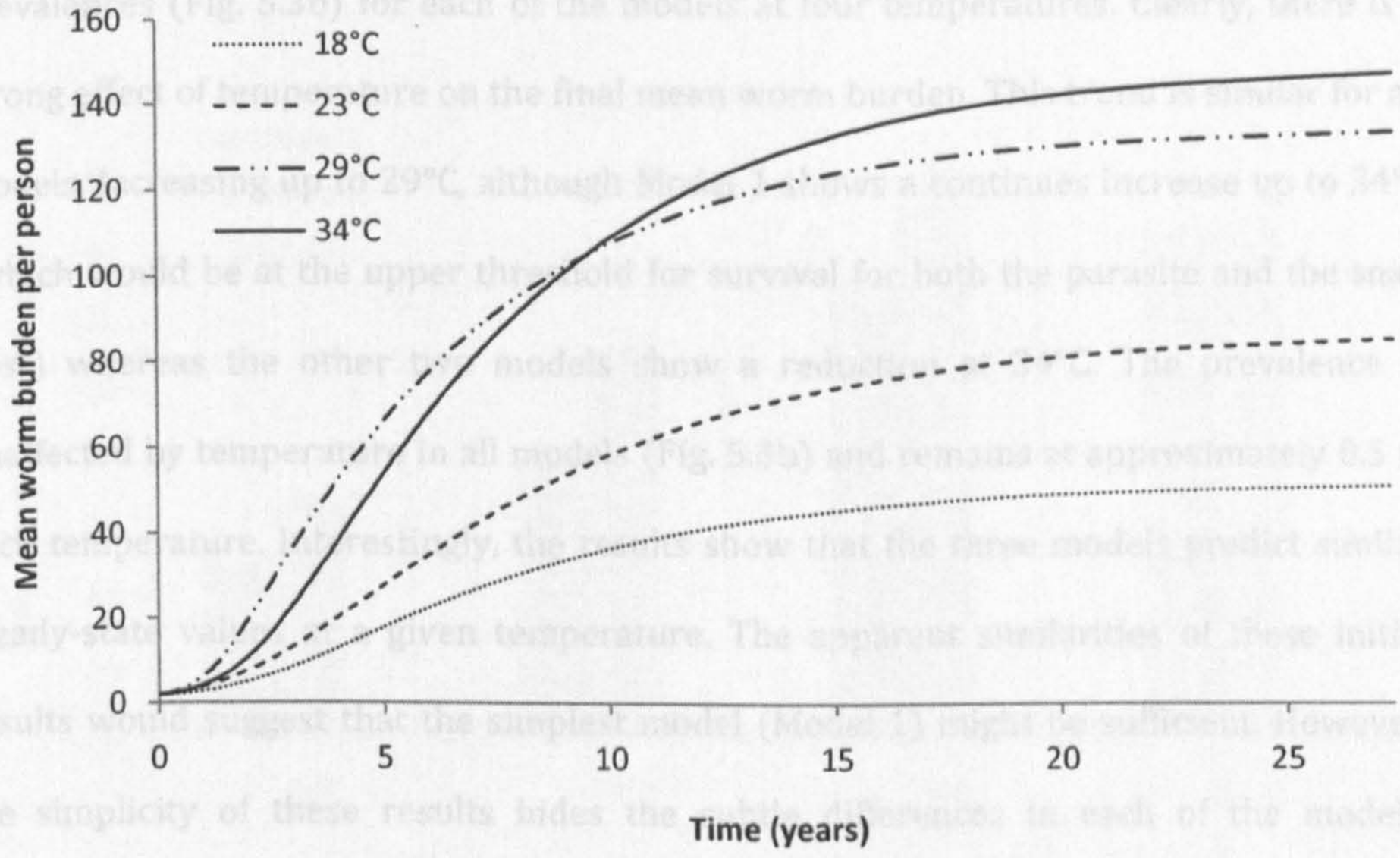

(b)

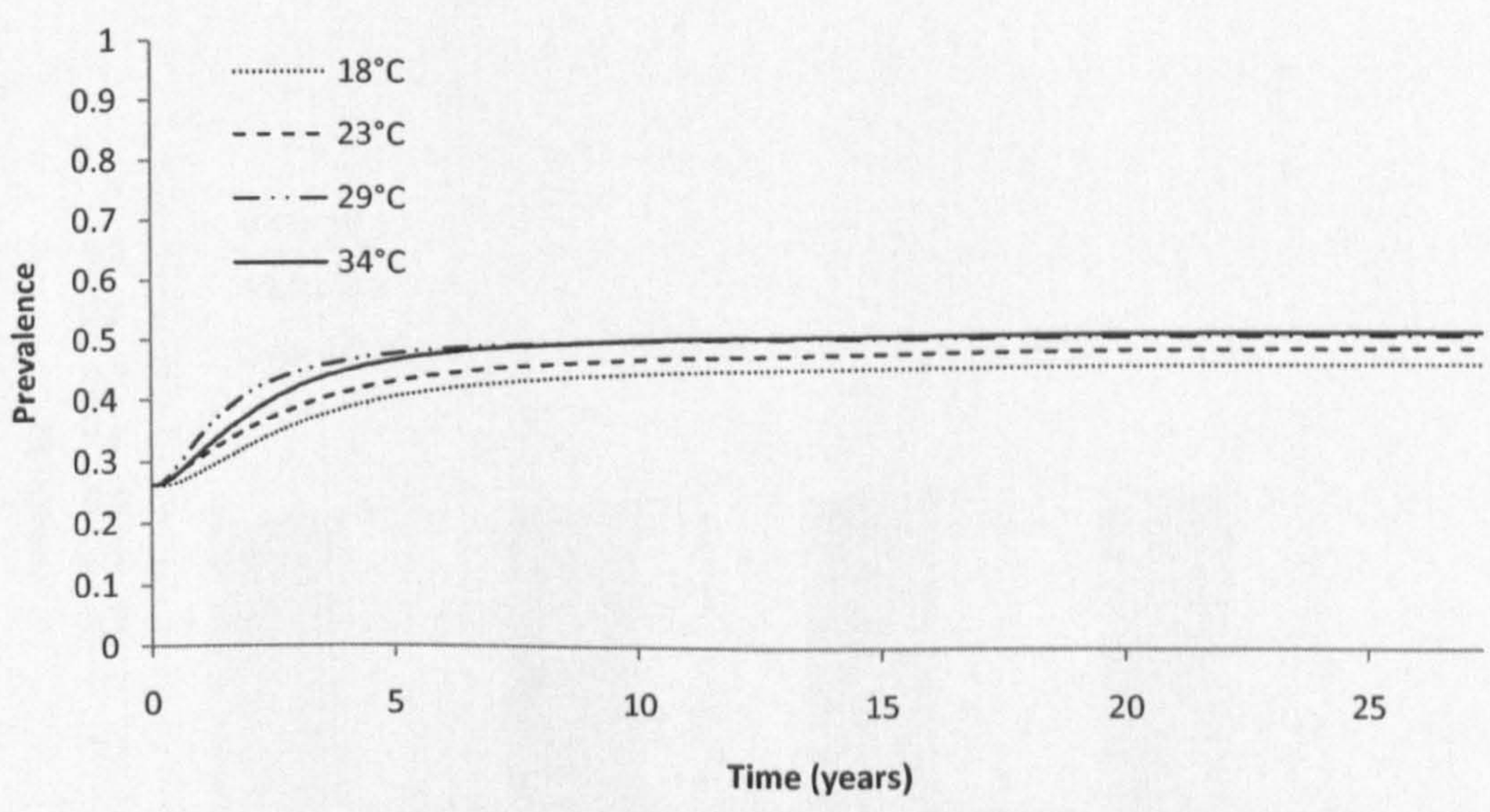

Figure 5.2. Temporal dynamics of model simulations using Model 1 results showing (a) mean worm burden per person and (b) prevalence at each temperature.

Figure 5.3 shows the steady-state mean worm burdens (Fig. 5.3a) and prevalences (Fig. 5.3b) for each of the models at four temperatures. Clearly, there is a strong effect of temperature on the final mean worm burden. This trend is similar for all models, increasing up to 29°C, although Model 1 shows a continues increase up to 34°C (which would be at the upper threshold for survival for both the parasite and the snail host) whereas the other two models show a reduction at 34°C. The prevalence is unaffected by temperature in all models (Fig. 5.3b) and remains at approximately 0.5 at each temperature. Interestingly, the results show that the three models predict similar steady-state values at a given temperature. The apparent similarities of these initial results would suggest that the simplest model (Model 1) might be sufficient. However, the simplicity of these results hides the subtle differences in each of the model's behaviour. This will be investigated further in the next section.

(a)

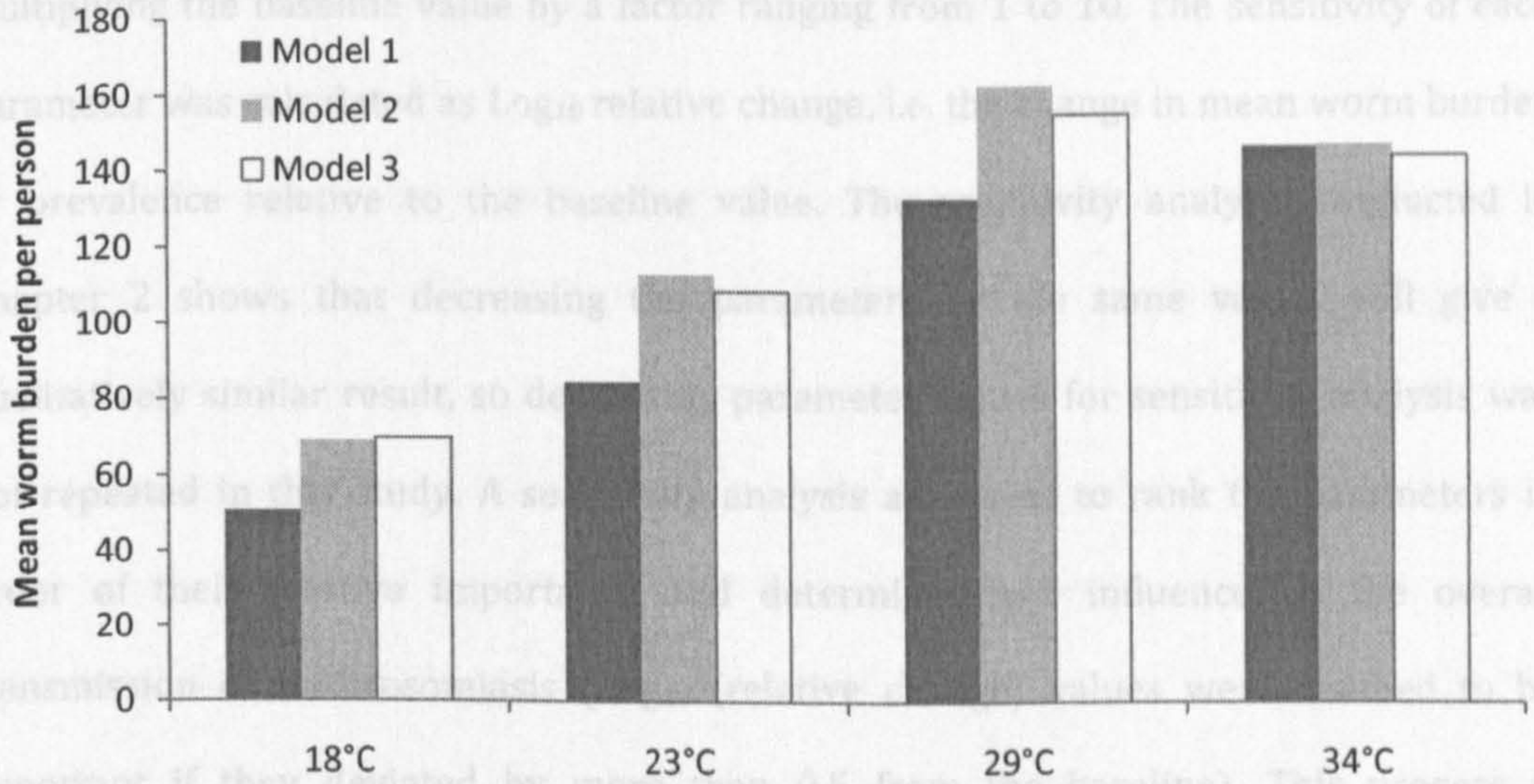

(b)

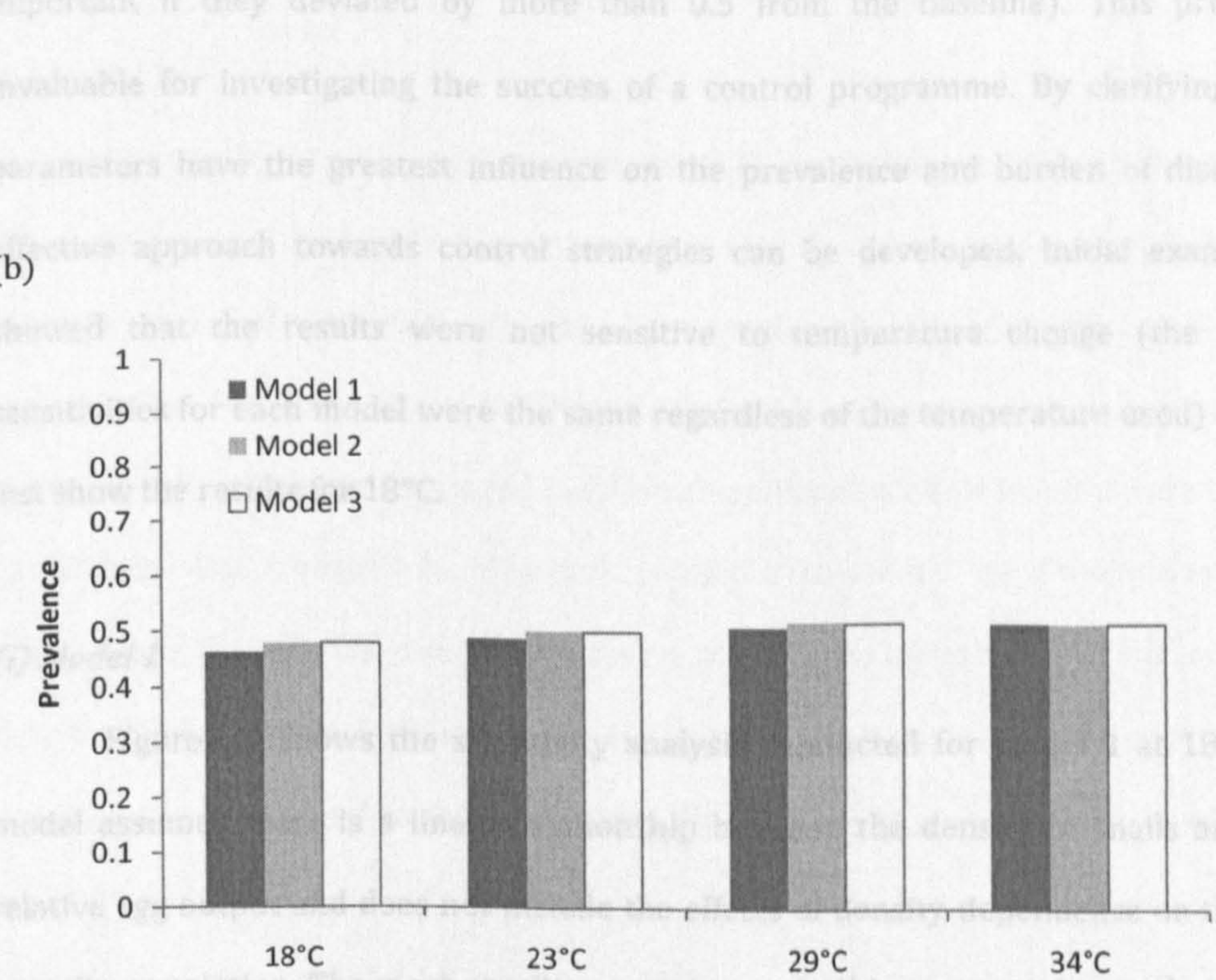

Figure 5.3 Simulation results comparing the endpoints of the three models showing (a) the predicted mean worm burden per person and (b) the prevalence at each temperature.

5.3.1 Sensitivity analysis

A sensitivity analysis was conducted where each parameter was increased by multiplying the baseline value by a factor ranging from 1 to 10. The sensitivity of each parameter was calculated as Log_{10} relative change, i.e. the change in mean worm burden or prevalence relative to the baseline value. The sensitivity analysis conducted in Chapter 2 shows that decreasing the parameters by the same values will give a qualitatively similar result, so decreasing parameter values for sensitivity analysis was not repeated in this study. A sensitivity analysis allows us to rank the parameters in order of their relative importance and determine their influence on the overall transmission of schistosomiasis (Log_{10} (relative change) values were deemed to be important if they deviated by more than 0.5 from the baseline). This process is invaluable for investigating the success of a control programme. By clarifying which parameters have the greatest influence on the prevalence and burden of disease, an effective approach towards control strategies can be developed. Initial examination showed that the results were not sensitive to temperature change (the relative sensitivities for each model were the same regardless of the temperature used) and so I just show the results for 18°C.

(i) Model 1

Figure 5.4 shows the sensitivity analysis conducted for Model 1 at 18°C. This model assumes there is a linear relationship between the density of snails and their relative egg output and does not include the effects of density-dependence on the adult parasite population. The most sensitive parameters in this case are the production and transmission rates of cercariae (λ_C and β_H respectively), death rates of the uninfected and infected snails (δ_S and δ_I), and the death rates of the three stages of the parasite (δ_M, δ_P and δ_C). This suggests that a control strategy which targets the snail population and

the free-living parasite population will have a significant effect on the overall disease transmission. The adult stages of the parasite also appear to be important in the transmission dynamics, suggesting chemotherapy would also be a very effective tool in controlling disease.

In addition, the parameter q emerged as important, highlighting the importance of snail density-dependence in this model. This parameter was assumed to be equal for all three groups of snails, such that there was no effect of infection status on the strength of density-dependence in these populations. As detailed in Chapter 4, this is not the case, so, given the apparent importance of this term in this analysis, modelling this aspect more carefully will provide a more accurate model.

(ii) Model 2

The results of the sensitivity analysis on Model 2 show similar results (Fig. 5.5); the death rates of the three stages of parasite (δ_M, δ_P and δ_C) and the production and infection rates of cercariae (λ_C and β_H respectively) strongly influenced disease transmission. The death rate of uninfected snails (δ_S) has become less important, whilst the death rate of infected snails (δ_I) remained significant. Models 1 and 2 were expected to produce similar results as they both contain a parameter for density-dependence within snails, the only difference being that in model 1 the trend is linear, and in Model 2 it is a negative exponential trend. As the negative exponential trend mimics what is actually seen in the snail population, Model 2 is the more biologically realistic of the two models.

(iii) Model 3

Once density-dependence is introduced into the adult parasite population (Model 3), the results of the sensitivity analysis change (Fig. 5.6). The most influential

parameters on the transmission of schistosomiasis are now the four parameters that describe the transmission of parasites from snail to man, i.e. β_H, δ_C, δ_P, and λ_C, together with the parameter describing the strength of density-dependence acting on infected snail reproduction (q_I). These results provide recommendations for reducing the burden and prevalence of schistosomiasis. Both β_H and λ_C determine the probability of an individual being infected by a cercaria, which can be blocked by changing people's attitudes and behaviour towards water contact through health education and improved sanitation. Reducing the probability of contact with an infective cercaria will have a considerable impact on the overall prevalence in a population. Furthermore, parameters relating to the production of miracidia and transmission to the snails are less important. Consequently, the focus of control efforts should be blocking transmission to humans (e.g., improved sanitation), rather than preventing contamination of water bodies (i.e., the provision of latrines) or targeting the snail population. The death rate of the adult worm population is also of importance in this model, so a wide-spread chemotherapy campaign may be highly effective.

Overall the differences in these results for the different models highlight subtle changes in the dynamics of each model that were hidden in the initial, steady-state results (Figs. 5.2 and 5.3).

(a)

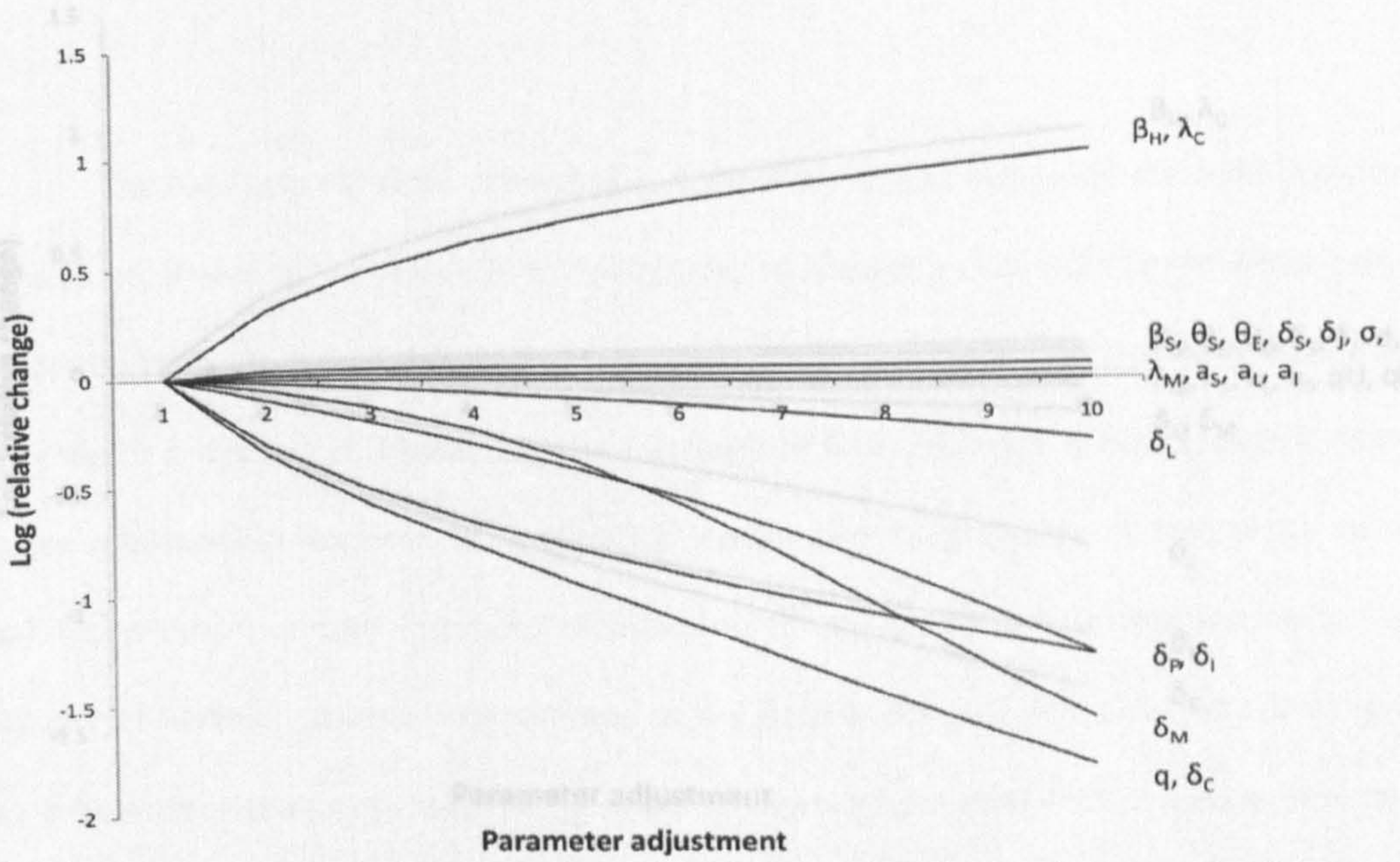

(b)

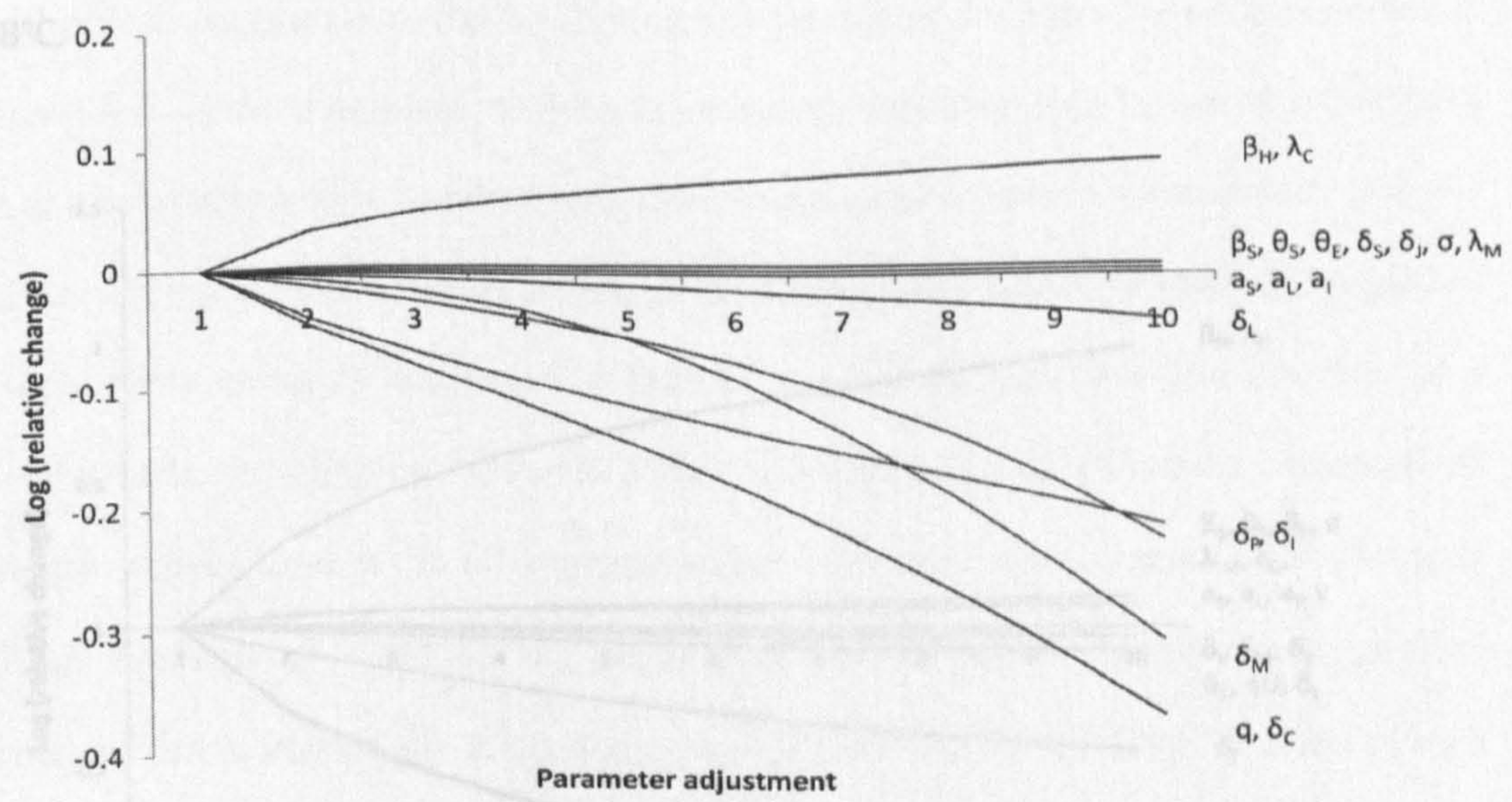

Figure 5.4 Results for the sensitivity analysis using Model 1. The output is plotted as the $\log_{10}$ (relative change) and each parameter is increased by a factor of up to 10. The results for mean worm burden (a) and prevalence of infection (b) are qualitatively similar so from this point, only the results of the sensitivity analysis on the mean worm burden will be presented.

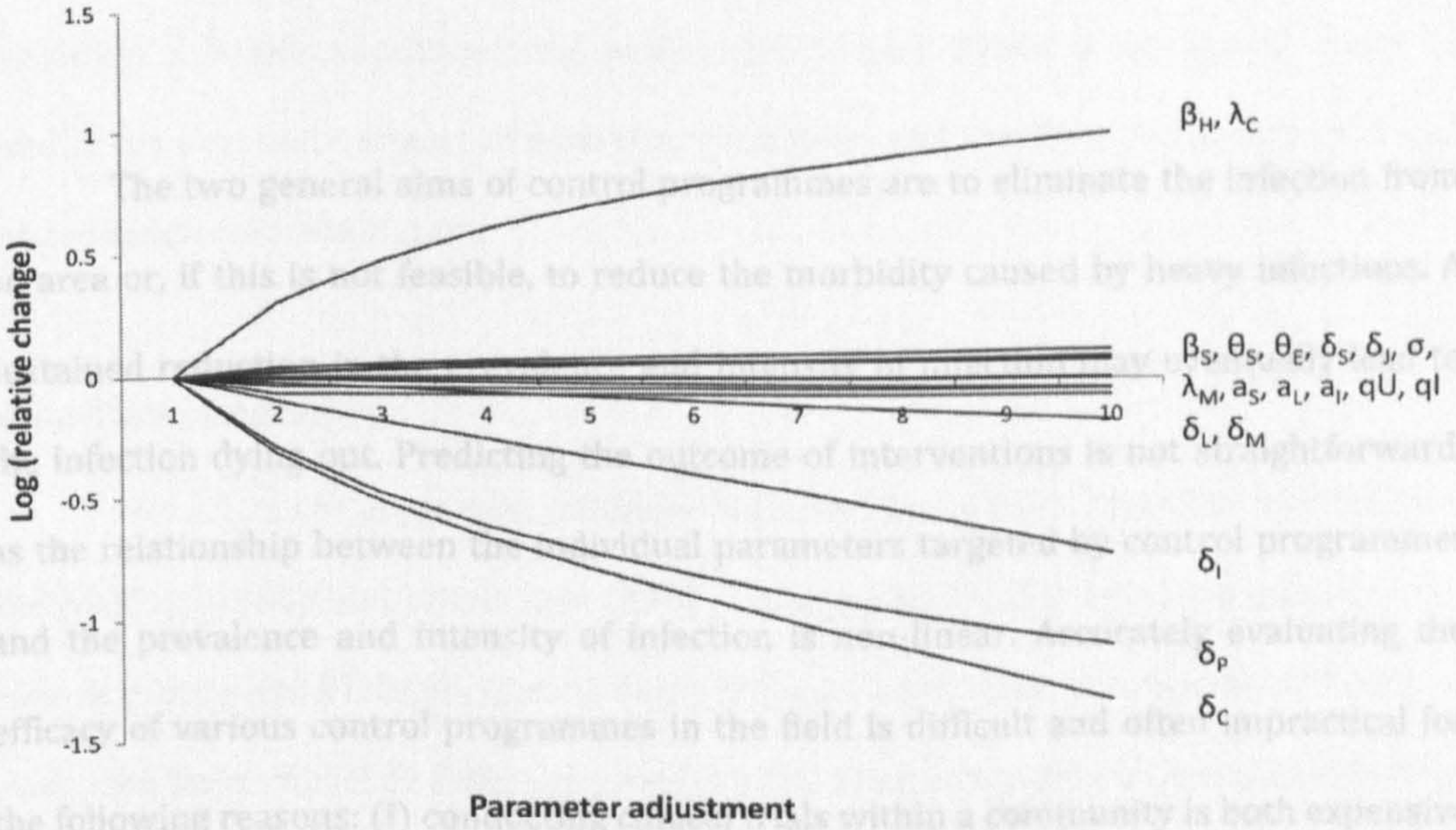

Figure 5.5 Results of the sensitivity analysis using Model 2 on the mean worm burden at 18°C.

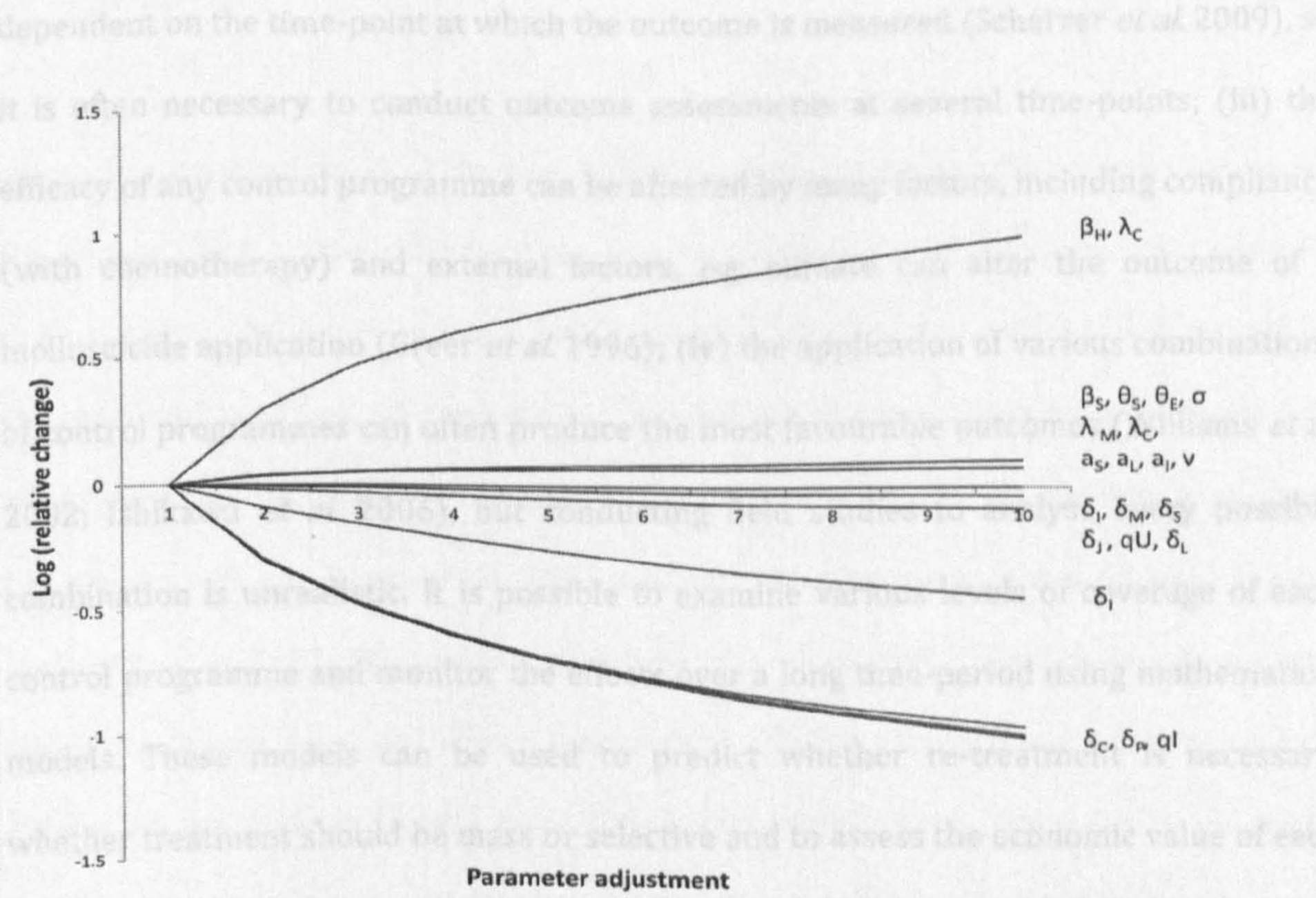

Figure 5.6 Results of the sensitivity analysis using Model 3 on the mean worm burden at 18°C.

5.5 - Evaluating the impact of different control programmes

The two general aims of control programmes are to eliminate the infection from an area or, if this is not feasible, to reduce the morbidity caused by heavy infections. A sustained reduction in the prevalence and intensity of infection may eventually lead to the infection dying out. Predicting the outcome of interventions is not straightforward, as the relationship between the individual parameters targeted by control programmes and the prevalence and intensity of infection is non-linear. Accurately evaluating the efficacy of various control programmes in the field is difficult and often impractical for the following reasons: (i) conducting clinical trials within a community is both expensive and time-consuming, long-term studies (5-10 years) of interventions are rarely feasible and ethical considerations can be limiting; (ii) measuring the impact of an intervention is dependent on the time-point at which the outcome is measured (Scherrer *et al.* 2009), so it is often necessary to conduct outcome assessments at several time-points; (iii) the efficacy of any control programme can be affected by many factors, including compliance (with chemotherapy) and external factors, e.g. climate can alter the outcome of a molluscicide application (Greer *et al.* 1996); (iv) the application of various combinations of control programmes can often produce the most favourable outcomes (Williams *et al.* 2002; Ishikawa *et al.* 2006), but conducting field studies to analyse every possible combination is unrealistic. It is possible to examine various levels of coverage of each control programme and monitor the effects over a long time-period using mathematical models. These models can be used to predict whether re-treatment is necessary, whether treatment should be mass or selective and to assess the economic value of each programme.

In this section, I model the effects of three control programmes, chemotherapy, sanitation / health education, and molluscicides using Model 3 developed above to predict the long-term impact of each intervention strategy as the infected is introduced into an uninfected population.

4.5.1 Chemotherapy

The effects of mass chemotherapy have previously been modelled by Anderson and Medley (1985) and Woolhouse (1992) amongst others, but few have modelled the control programmes using empirical data (Williams *et al.* 2002; Hisakane *et al.* 2008) or evaluated their impact at different temperatures. Chemotherapy can be modelled as an instantaneous reduction in the size of the parasite population (P) and is described by:

$$\Delta P = -\log[1 - gh] \qquad 5.11$$

where g is the proportion of the population (chosen at random) that receive treatment ("coverage") and h is the efficacy of the drug, i.e. the proportion of schistosomes killed by one treatment (Anderson and May 1982). Usually, the efficacy of a drug is determined by the reduction in egg output per person. The analysis presented here is based on the use of praziquantel, randomly administered to a population within an endemic area. Here the efficacy (h) has been set at 80%, a conservative estimate based on field studies (Gryseels *et al.* 1987; Magnussen 2003; Scherrer *et al.* 2009). This value incorporates treatment failure, i.e. cases where treatments with the standard dose of praziquantel fails to kill the parasite (Hagan *et al.* 2004). Treatment failure occurs due to the stage-specificity of praziquantel, where immature parasites tolerate usually therapeutic doses, or where drug-resistant parasites exist. In this case, the parameter h is assumed to be independent of the number of worms in an individual and ΔP is equally sensitive to both

g and *h* (Woolhouse 1992). Firstly, simulations exploring an annual mass chemotherapy programme with three coverage rates: 30%, 50%, and 70% were conducted. Secondly, the effects of a repeated 6-month programme were compared at each coverage rate. All programmes were run for 10 years until a stable state had been reached. All control programmes were modelled at both 18°C and 34°C to explore whether temperature had a significant impact on the success of each control strategy.

At 18°C, the implementation of chemotherapy at each coverage level immediately reduced the mean worm burden per person and the prevalence of infection (Fig. 5.7). The efficacy of the treatment was set to 80%, so some positive cases remained after each treatment. There is a rise in worm burden and prevalence following each treatment, which is due to the remaining cases not cured by the drug and reinfection from the environment. Assuming regular, repeated administrations of praziquantel, the saw-tooth behaviour of the model gradually falls to very low levels. With 70% coverage, the final prevalence is 0.01 after 10 years. This model shows that running a control programme for 5 years, as is often the case, will not result in elimination of the disease, with around 5% of the population remaining infected, even with 70% coverage. Once treatment is withdrawn, the parasite may recover to pre-treatment levels as the population would not have developed immunity.

(a)

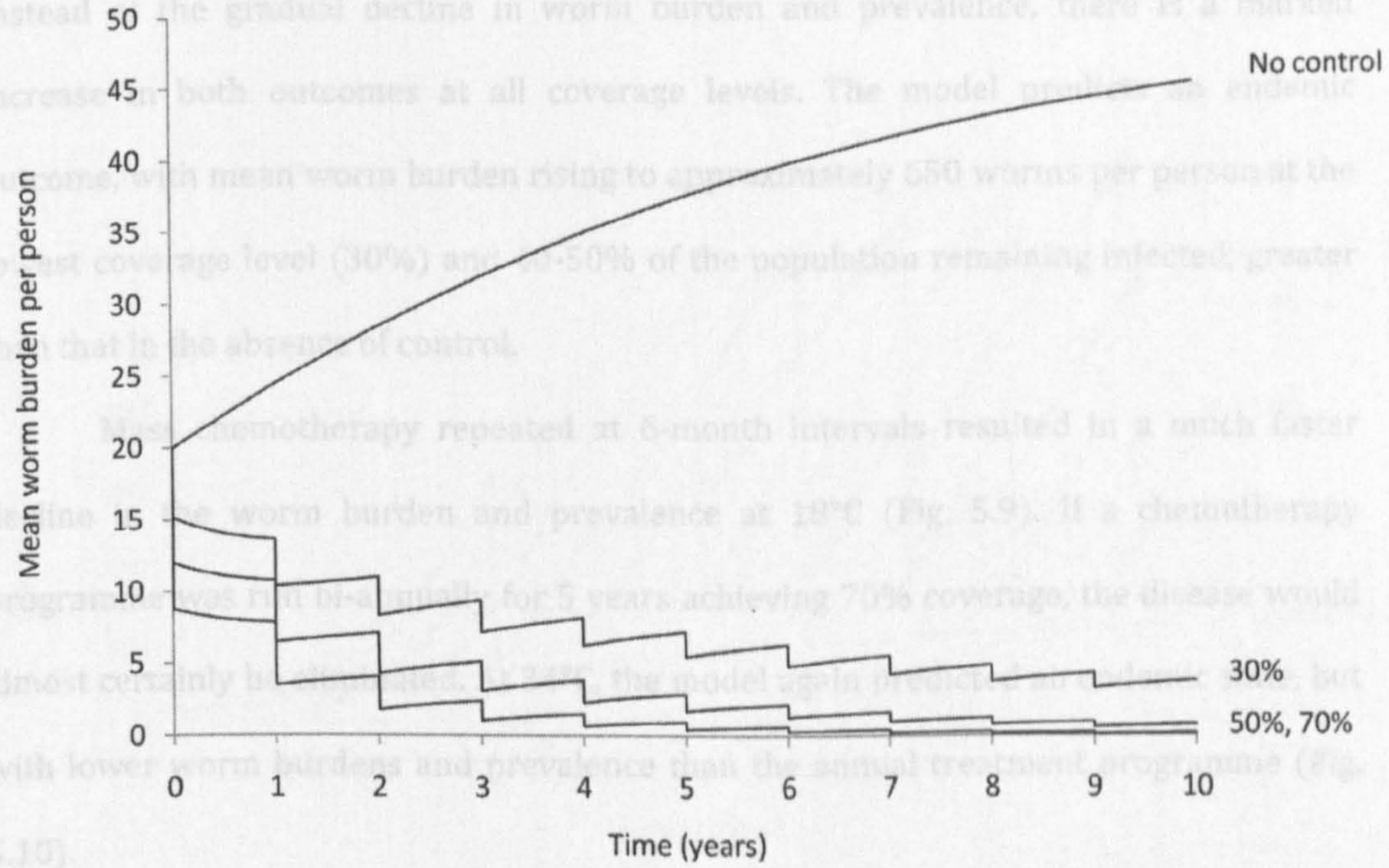

(b)

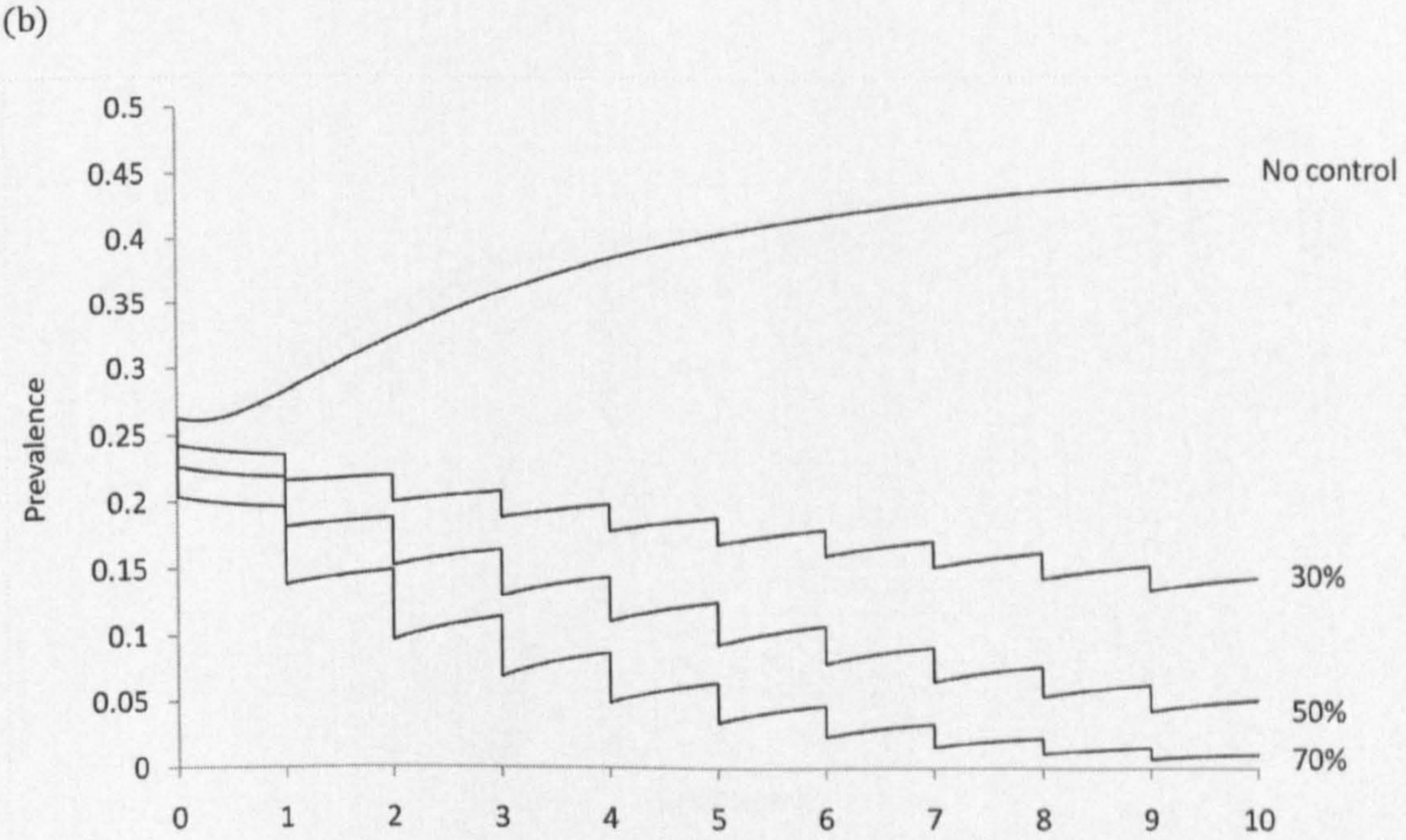

Figure 5.7 Variations in the mean worm burden (a) and prevalence (b) for the human chemotherapy models at 18°C with random mass treatment at a 1 year interval with three coverage rates, 30%, 50% and 70%.

Running the same model at 34°C produced strikingly different results (Fig. 5.8). Instead of the gradual decline in worm burden and prevalence, there is a marked increase in both outcomes at all coverage levels. The model predicts an endemic outcome, with mean worm burden rising to approximately 650 worms per person at the lowest coverage level (30%) and 40-50% of the population remaining infected, greater than that in the absence of control.

Mass chemotherapy repeated at 6-month intervals resulted in a much faster decline in the worm burden and prevalence at 18°C (Fig. 5.9). If a chemotherapy programme was run bi-annually for 5 years achieving 70% coverage, the disease would almost certainly be eliminated. At 34°C, the model again predicted an endemic state, but with lower worm burdens and prevalence than the annual treatment programme (Fig. 5.10).

(a)

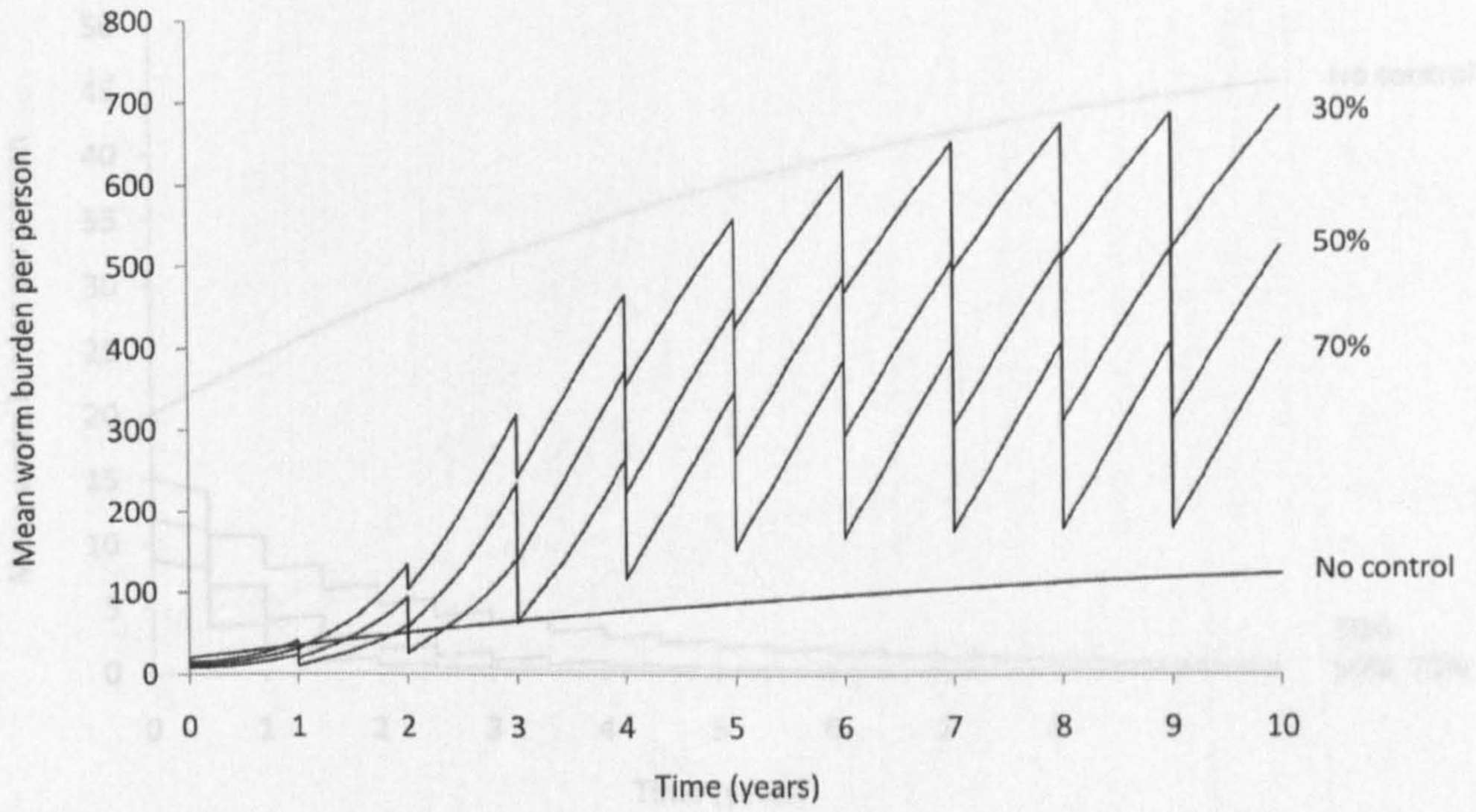

(b)

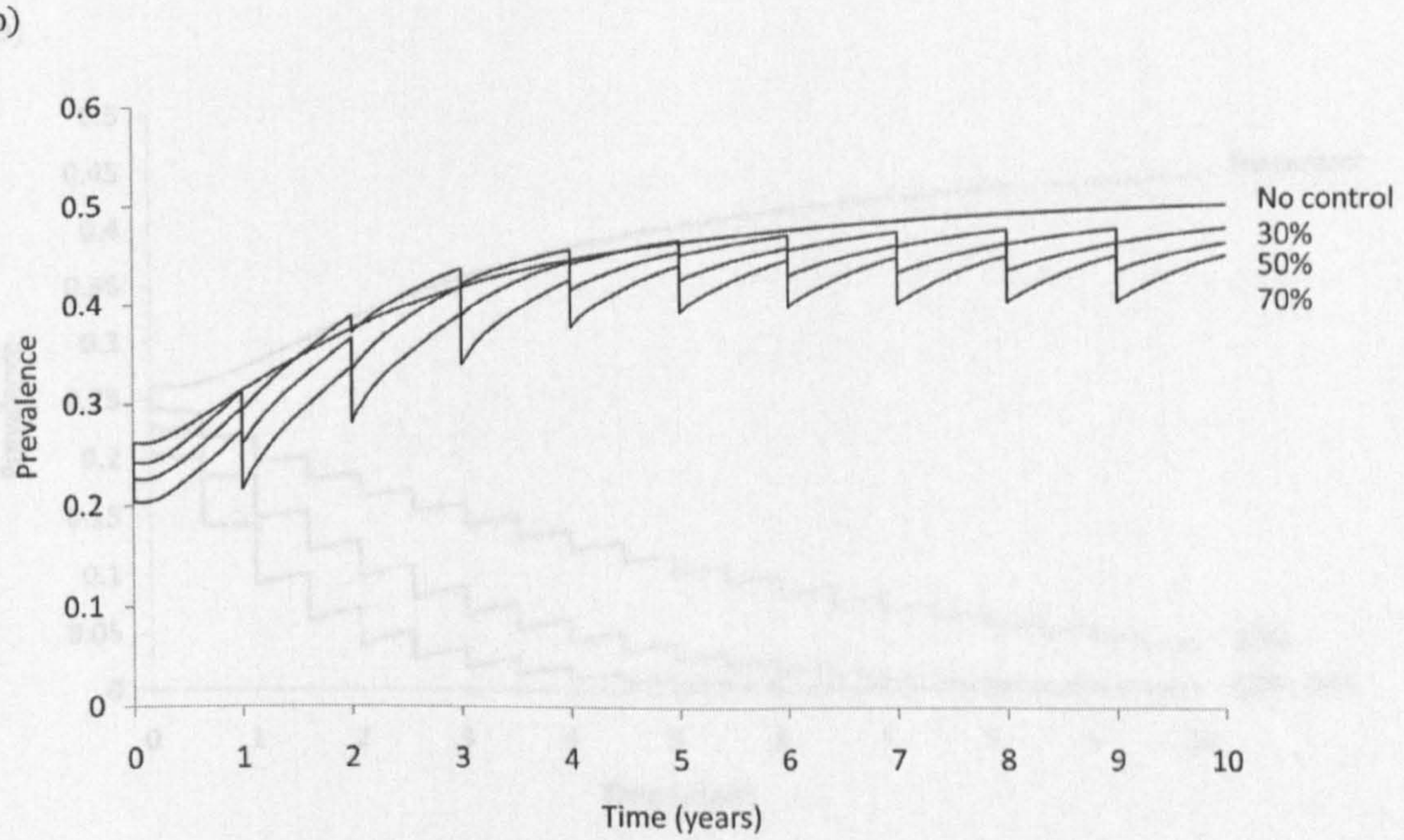

Figure 5.8 Variations in the mean worm burden (a) and prevalence (b) for the human chemotherapy models at 34°C with random mass treatment at a yearly interval with three coverage rates, 30%, 50% and 70%.

(a)

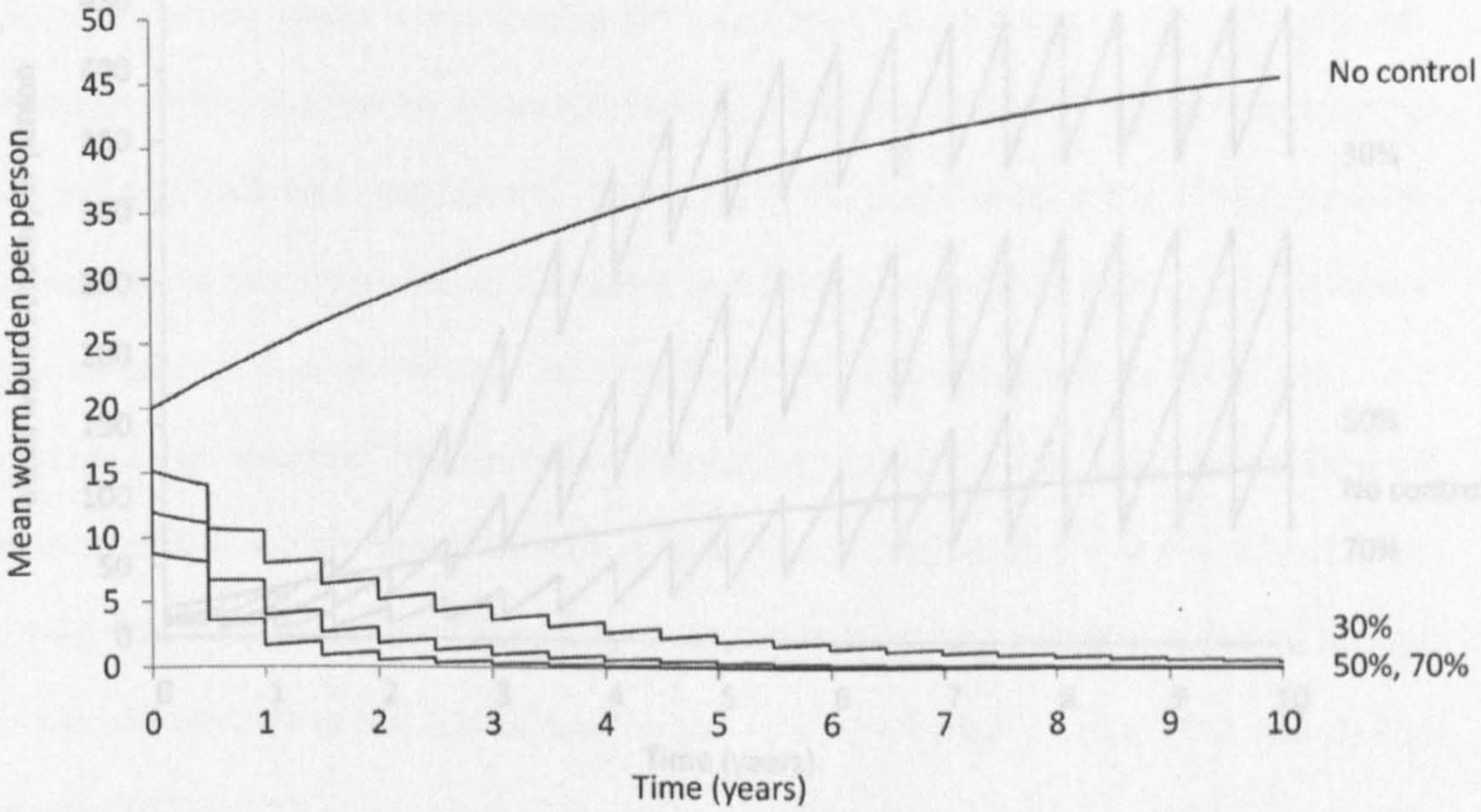

(b)

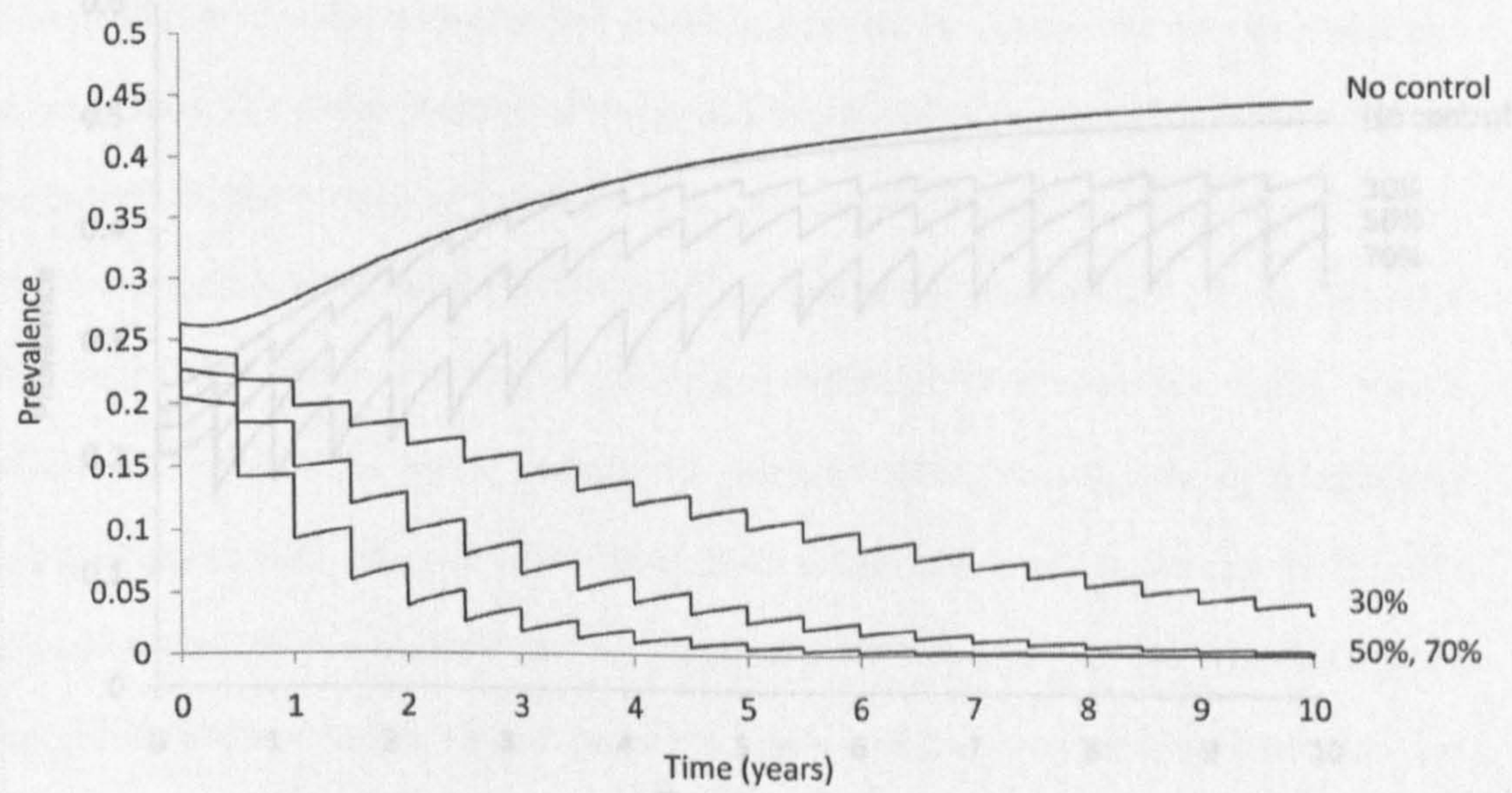

Figure 5.9 Variations in the mean worm burden (a) and prevalence (b) for the human chemotherapy models at 18°C with random mass treatment at a twice-yearly interval with three coverage rates, 30%, 50% and 70%.

(a)

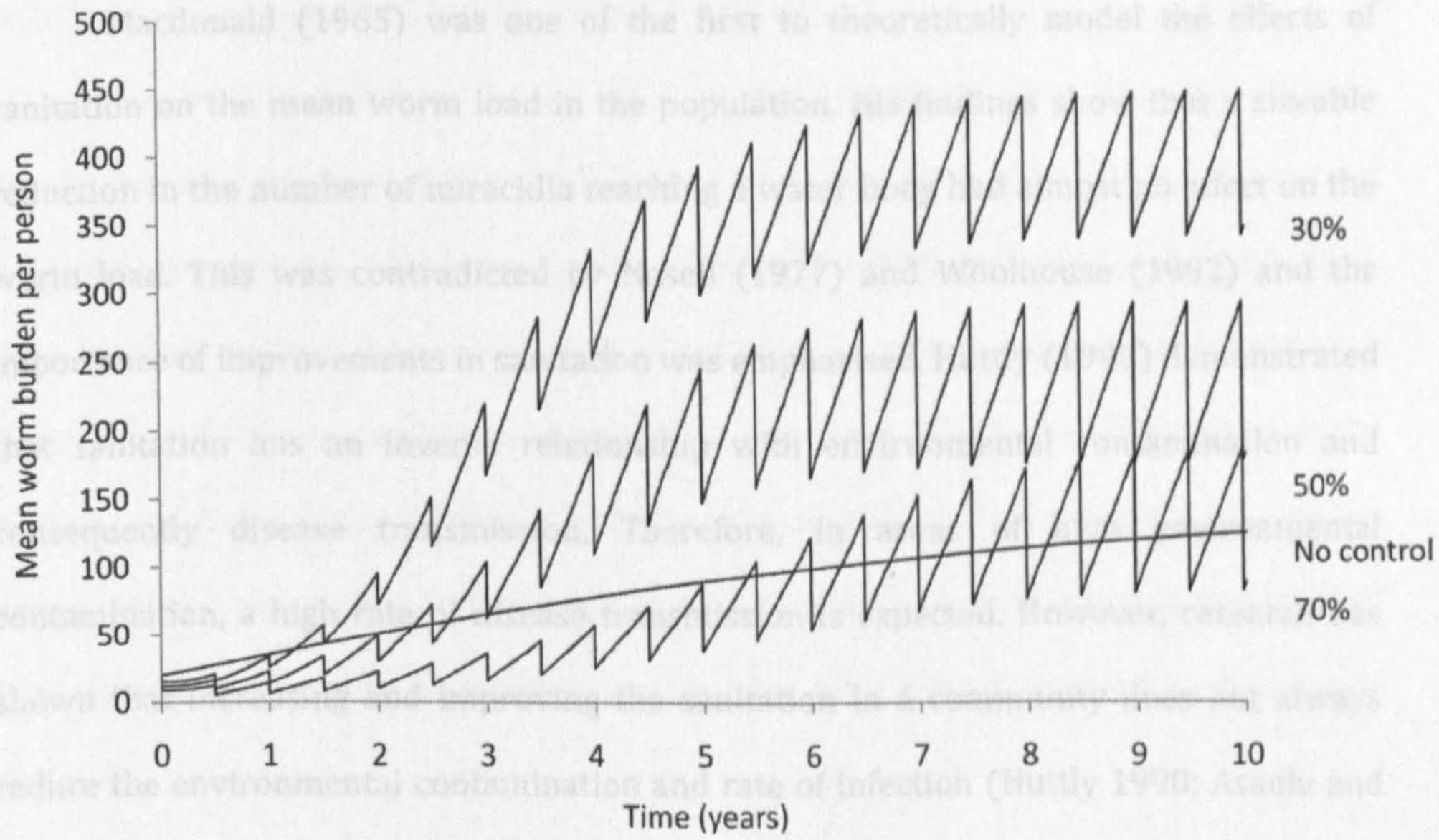

(b)

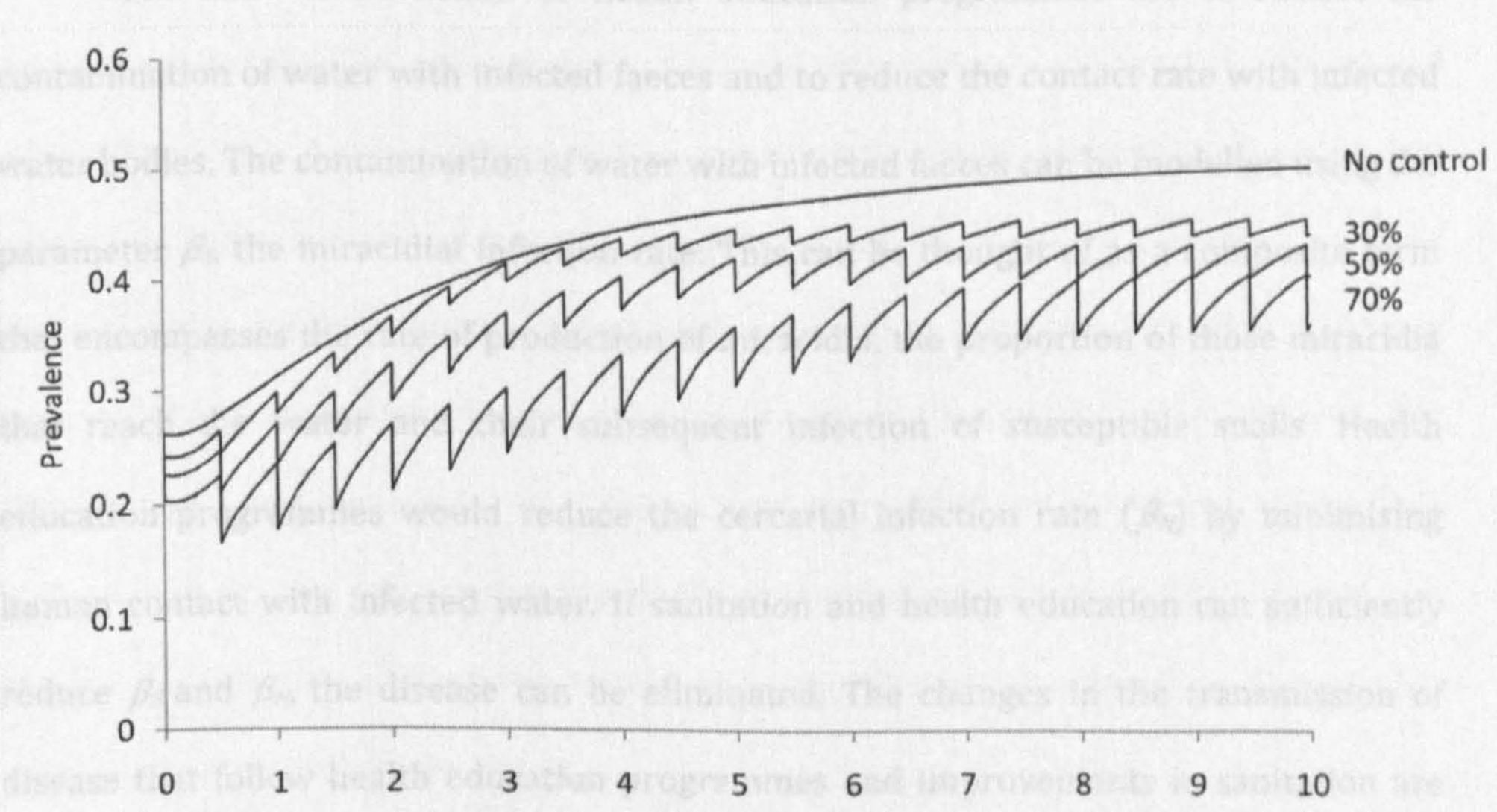

Figure 5.10 Variations in the mean worm burden (a) and prevalence (b) for the human chemotherapy models at 34°C with random mass treatment at a twice-yearly interval with three coverage rates, 30%, 50% and 70%.

5.5.2 Sanitation and health education

Macdonald (1965) was one of the first to theoretically model the effects of sanitation on the mean worm load in the population. His findings show that a sizeable reduction in the number of miracidia reaching a water body had almost no effect on the worm load. This was contradicted by Nasell (1977) and Woolhouse (1992) and the importance of improvements in sanitation was emphasised. Huttly (1990) demonstrated that sanitation has an inverse relationship with environmental contamination and consequently disease transmission. Therefore, in areas of high environmental contamination, a high rate of disease transmission is expected. However, research has shown that increasing and improving the sanitation in a community does not always reduce the environmental contamination and rate of infection (Huttly 1990; Asaolu and Ofoezie 2003).

The aims of sanitation or health education programmes are to reduce the contamination of water with infected faeces and to reduce the contact rate with infected water bodies. The contamination of water with infected faeces can be modelled using the parameter β_S, the miracidial infection rate. This can be thought of as a composite term that encompasses the rate of production of miracidia, the proportion of those miracidia that reach the water and their subsequent infection of susceptible snails. Health education programmes would reduce the cercarial infection rate (β_H) by minimising human contact with infected water. If sanitation and health education can sufficiently reduce β_S and β_H, the disease can be eliminated. The changes in the transmission of disease that follow health education programmes and improvements in sanitation are difficult to quantify, as the outcome is dependent on human behaviour, which is both unpredictable and highly variable. To explore the effects of sanitation, the transmission parameter β_S was reduced by 30%, 50%, 70%, and 90% over 55 years. This end-point was chosen due to the stable states of worm burden and prevalence at this point. It is

assumed that this control programme represents a permanent change in infrastructure or behaviour and is applied continuously through time.

The results presented below refer to the programmes running at 18°C. The results for 34°C are very similar and are not presented here (Fig. 5.11). The effect of control on the worm burden is most pronounced with a 90% reduction in β_S as expected. This level of control slowed the rate of increase in mean worm burden, but each intervention level eventually reached a similar end-point. There was little change in the overall prevalence with 30-70% reductions, and even at 90% the prevalence reached the same final end-point. This finding supports those of the sensitivity analysis, that showed that changes in the miracidial infection rate have little impact on the transmission of disease.

Alternatively, health education and behavioural changes could cause a constant reduction in the exposure to cercariae. Reducing the human contact rate with infected water was modelled by decreasing the cercarial infection rate (β_H) by 30, 50, 70 and 90% (Fig. 5.12). Again, I assumed this control programme represents a permanent change in behaviour and was run continuously over 55 years. This approach proved more effective than preventing contamination of water by miracidia. Reducing the rate of cercarial infection reduced the mean worm burden in the population by between 30 - 90% although the prevalence of infection was only significantly reduced with a 90% reduction in β_H. This was consistent with the sensitivity analysis, indicating that reducing the rate of infection of cercariae would be more effective in controlling disease than reducing the miracidial infection rate.

(a)

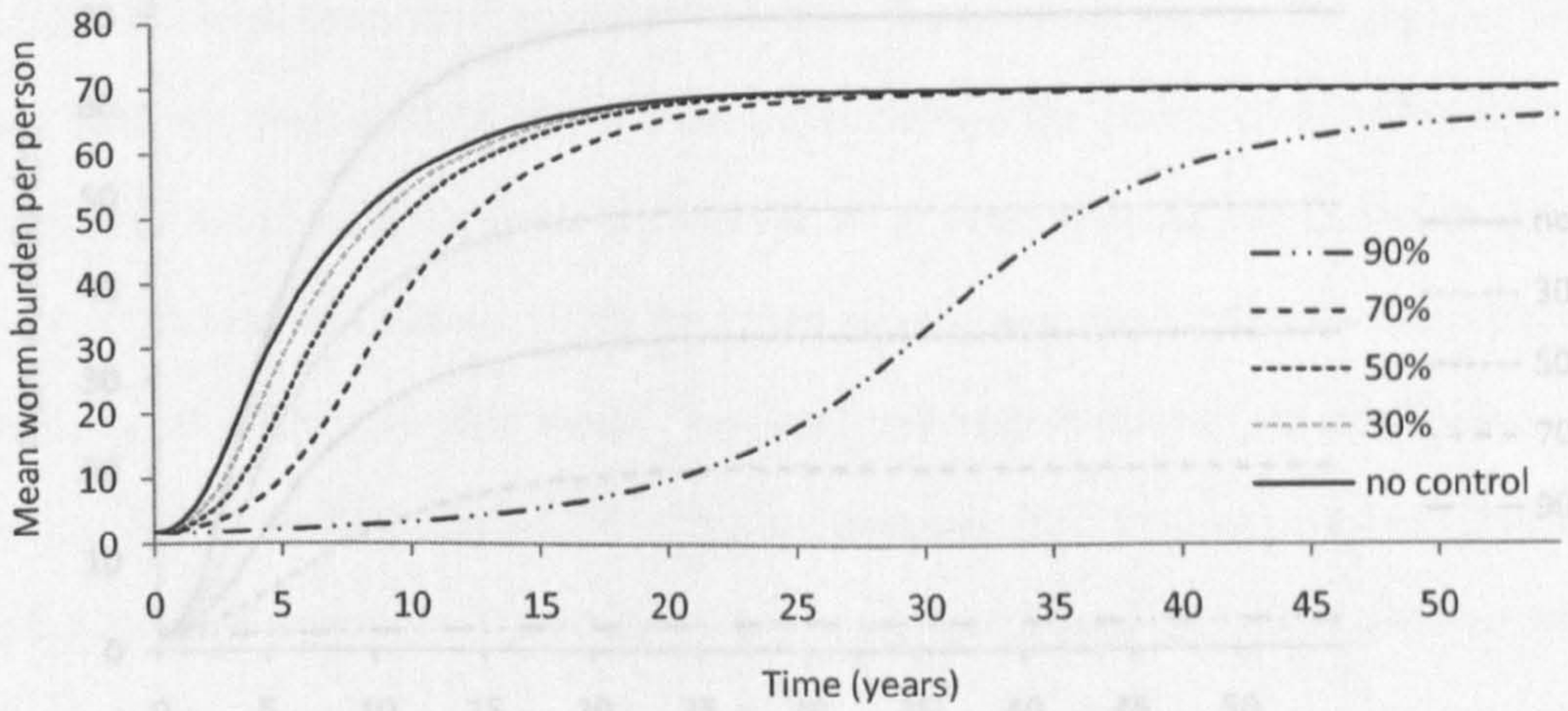

(b)

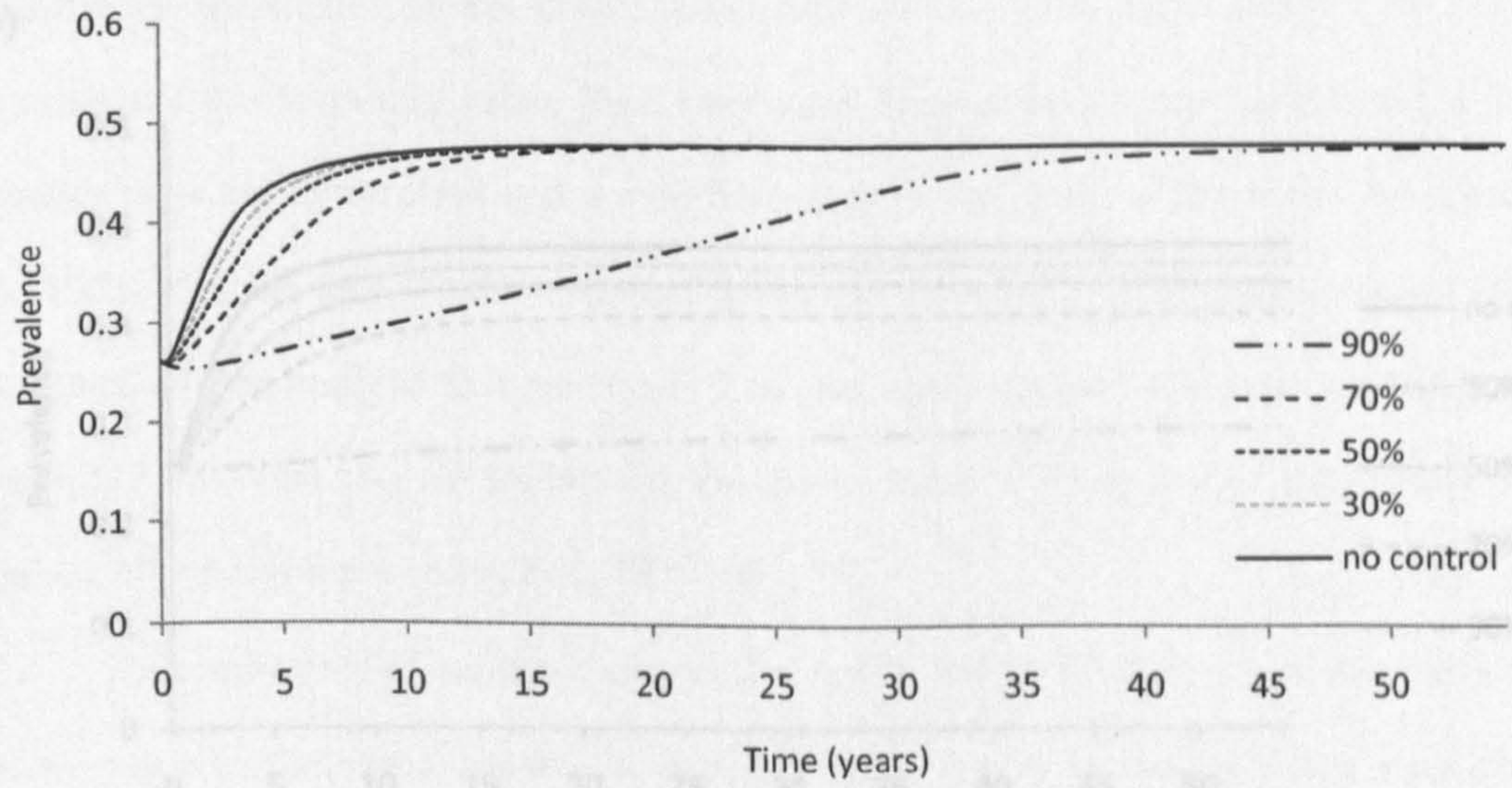

Figure 5.11. The mean worm burden (a) and prevalence (b) over 55 years at 18°C with reductions in the miracidial infection rate (β_S).

(a)

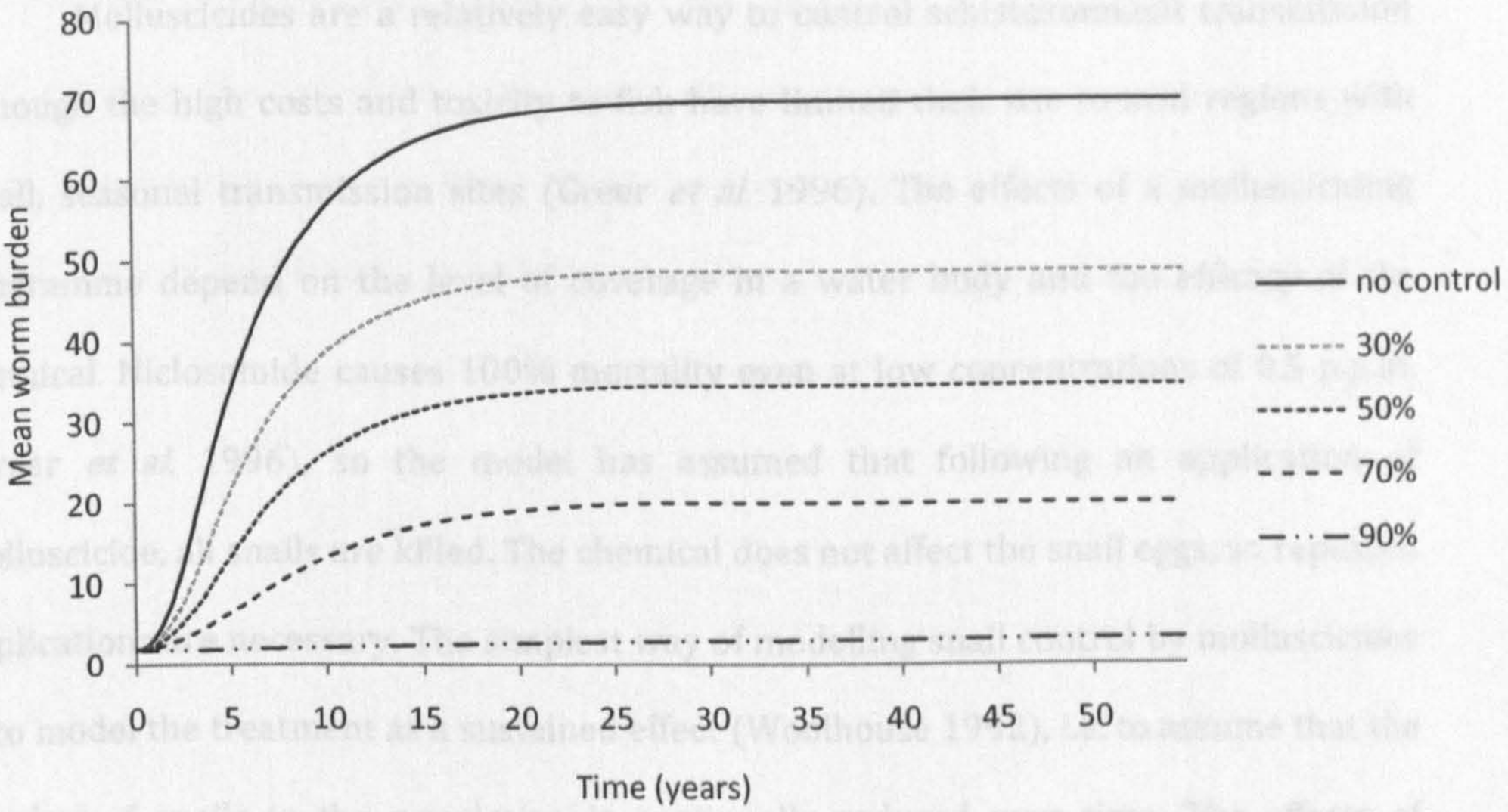

(b)

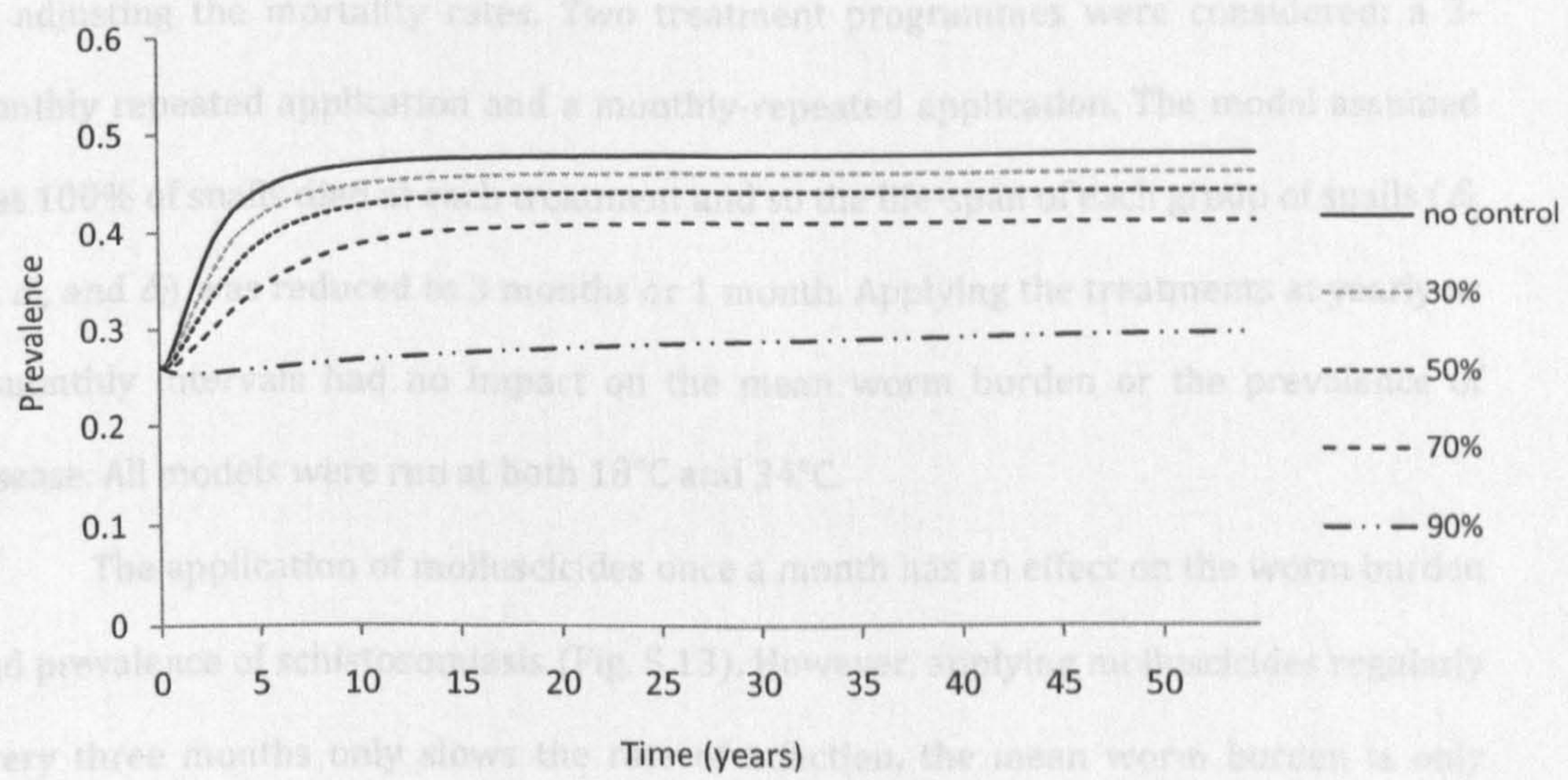

Figure 5.12 The mean worm burden (a) and prevalence (b) over 55 years at 18°C with decreases in cercarial infection rate (β_H).

5.5.3 Molluscicides

Molluscicides are a relatively easy way to control schistosomiasis transmission although the high costs and toxicity to fish have limited their use to arid regions with small, seasonal transmission sites (Greer *et al.* 1996). The effects of a mollusciciding programme depend on the level of coverage in a water body and the efficacy of the chemical. Niclosamide causes 100% mortality even at low concentrations of 0.5 p.p.m. (Greer *et al.* 1996), so the model has assumed that following an application of molluscicide, all snails are killed. The chemical does not affect the snail eggs, so repeated applications are necessary. The simplest way of modelling snail control by molluscicides is to model the treatment as a sustained effect (Woolhouse 1992), i.e. to assume that the number of snails in the population is continually reduced over time. The effects of molluscicide application on the snail population were modelled continuously over time by adjusting the mortality rates. Two treatment programmes were considered: a 3-monthly repeated application and a monthly-repeated application. The model assumed that 100% of snails died at each treatment and so the life-span of each group of snails (δ_I, δ_S, δ_L and δ_I) was reduced to 3 months or 1 month. Applying the treatments at yearly or 6-monthly intervals had no impact on the mean worm burden or the prevalence of disease. All models were run at both 18°C and 34°C.

The application of molluscicides once a month has an effect on the worm burden and prevalence of schistosomiasis (Fig. 5.13). However, applying molluscicides regularly every three months only slows the rate of infection, the mean worm burden is only reduced by approximately 10 worms per person and the final prevalence is almost equal to that of no control. However, monthly applications appear able to greatly reduce the mean worm burden and prevalence of disease, although the feasibility or cost-effectiveness of such regular treatments may greatly limit the achievability of this approach. At 34°C, both treatment plans slow the rate of infection and the mean worm

burden is significantly reduced using monthly applications. The prevalence of infection is not affected by 3-monthly applications and, although it is reduced by monthly molluscicidings, the prevalence rates eventually reach near pre-intervention levels (Fig. 5.14). These results support those of the sensitivity analyses above (section 5.3.1, Fig. 5.6) that treatment of snails is unlikely to be a feasible way of control schistosomiasis.

(a)

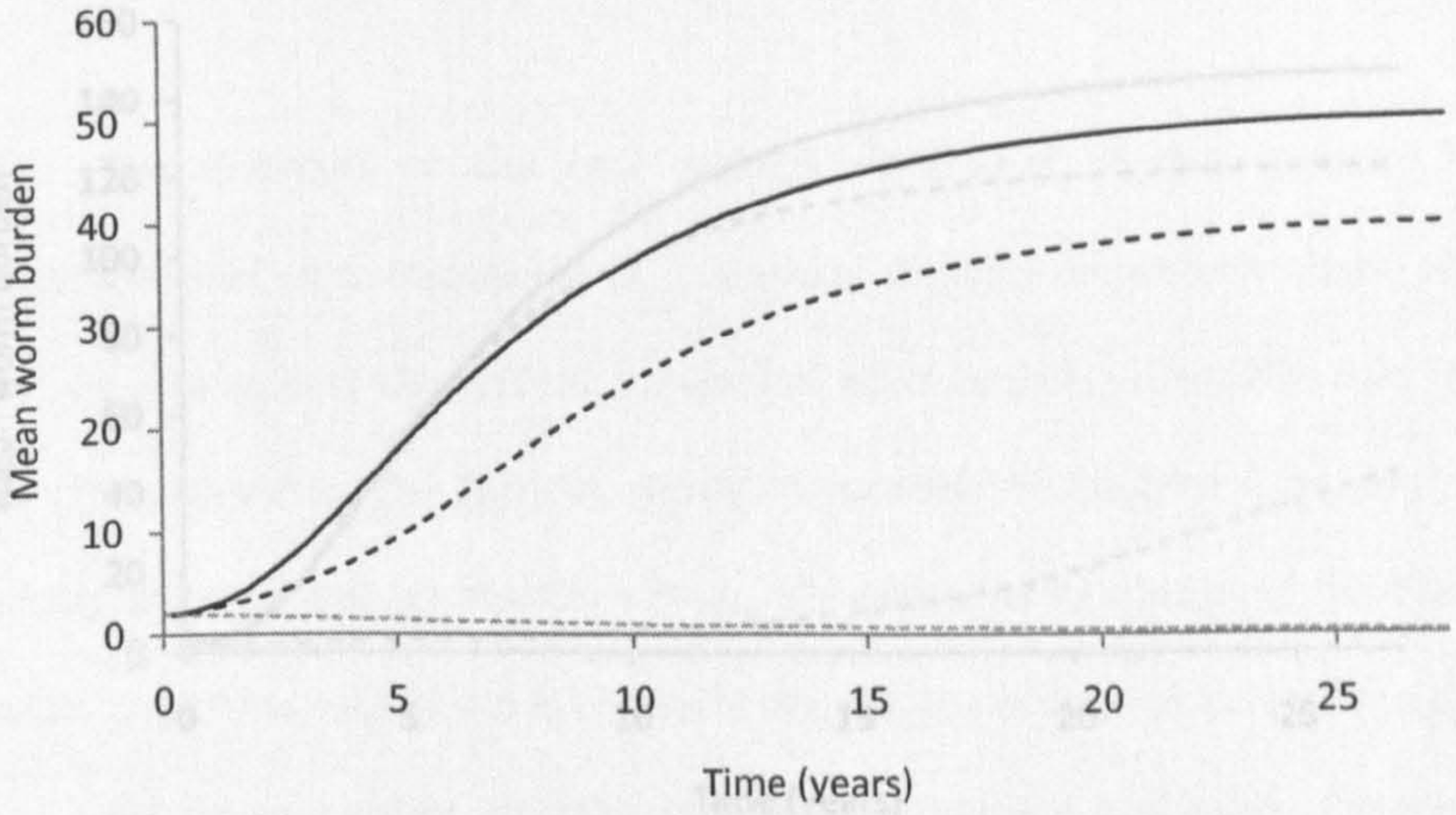

(b)

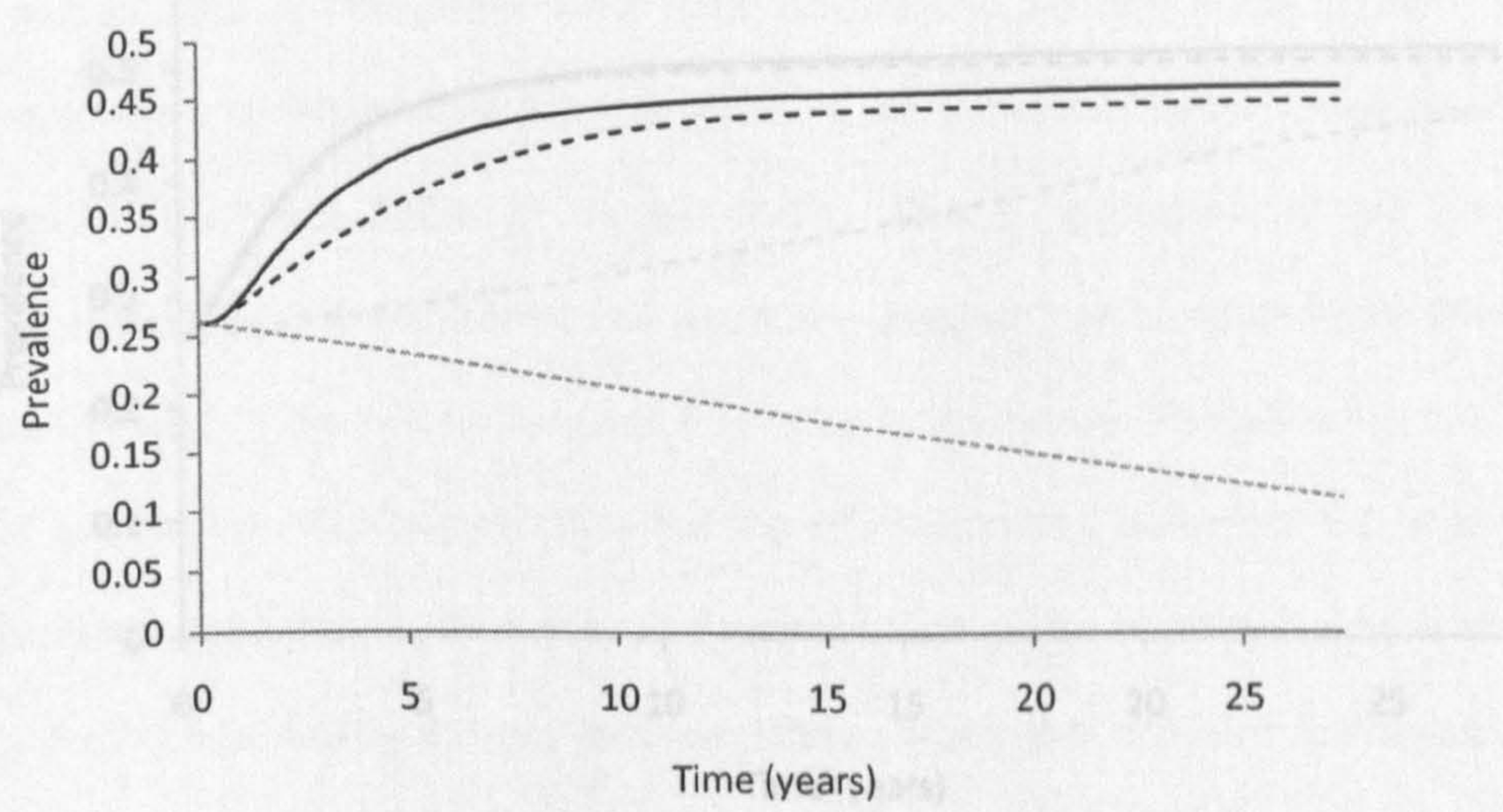

Figure 5.13 Variations in the mean worm burden (a) and prevalence (b) of disease with molluscicide application at 18°C. The levels of infection without control (solid line) and with molluscicide applications every 3 months (black dashed line) and one month (grey dashed line) are presented.

(a)

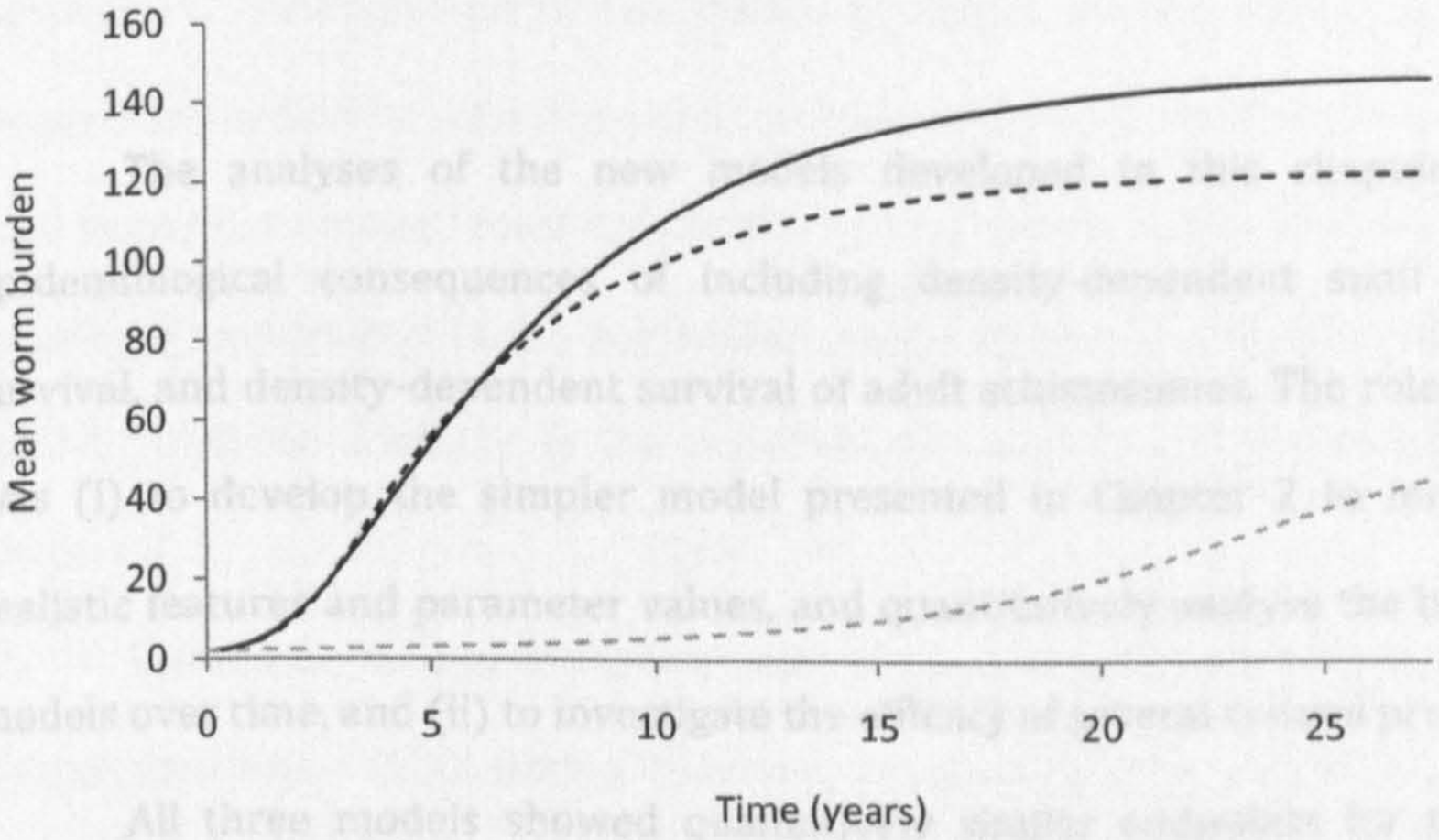

(b)

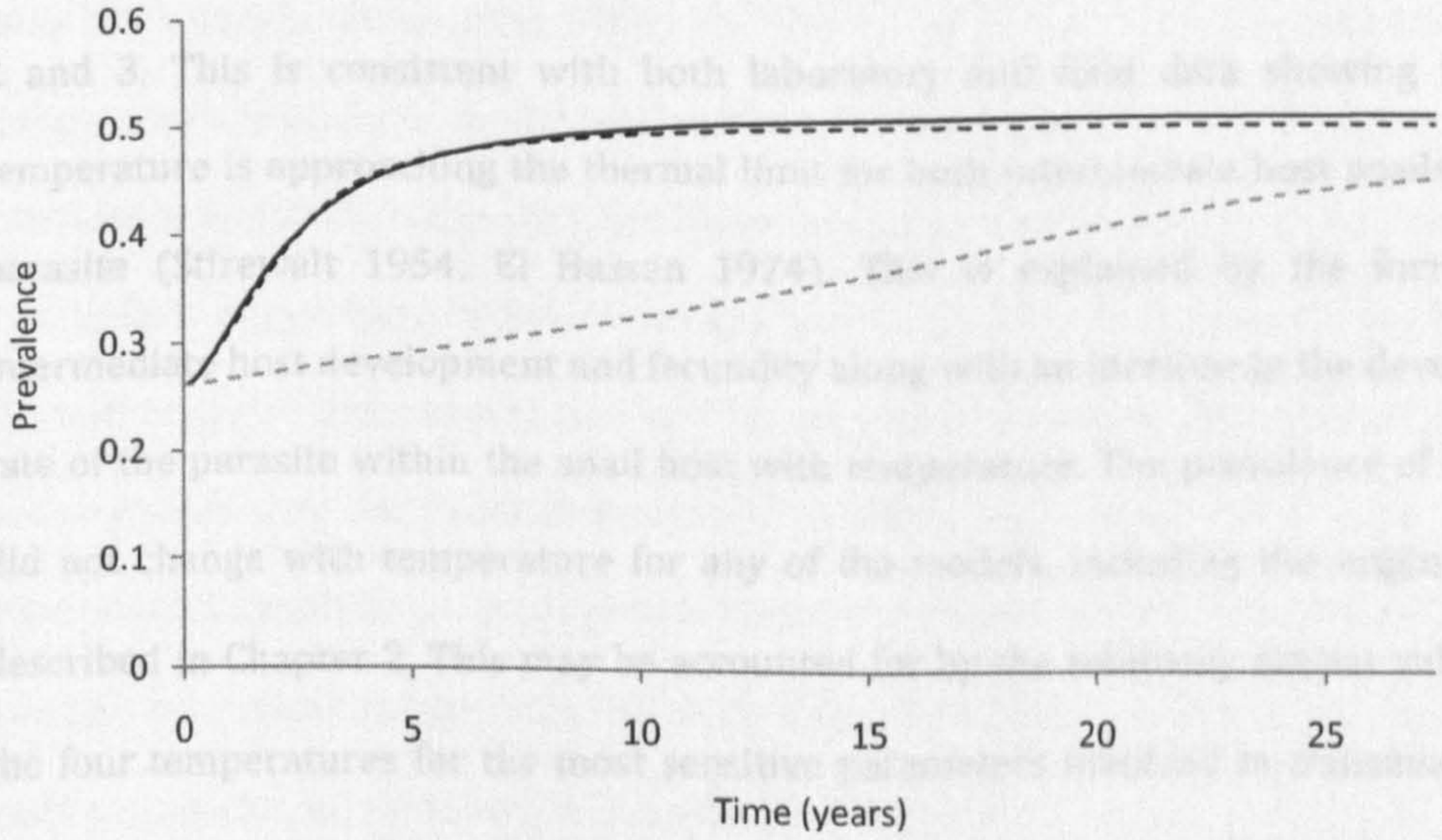

Figure 5.14 Variations in the mean worm burden (a) and prevalence (b) of disease with molluscicide application at 34°C. The levels of infection without control (solid line) and with molluscicide applications every 3 months (black dashed line) and one month (grey dashed line) are presented.

5.6 Discussion

The analyses of the new models developed in this chapter highlight the epidemiological consequences of including density-dependent snail fecundity and survival, and density-dependent survival of adult schistosomes. The role of this chapter was (i) to develop the simpler model presented in Chapter 2 to incorporate more realistic features and parameter values, and quantitatively analyse the behaviour of the models over time, and (ii) to investigate the efficacy of several control programmes.

All three models showed qualitatively similar endpoints for the intensity of infection (measured as mean worm burden per person) and prevalence of disease in the population. The worm burden increased up to 29°C and then tapered at 34°C for Models 2 and 3. This is consistent with both laboratory and field data showing that this temperature is approaching the thermal limit for both intermediate host snails and the parasite (Stirewalt 1954; El Hassan 1974). This is explained by the increases in intermediate host development and fecundity along with an increase in the development rate of the parasite within the snail host with temperature. The prevalence of infection did not change with temperature for any of the models, including the original model described in Chapter 2. This may be accounted for by the relatively similar values over the four temperatures for the most sensitive parameters involved in transmission, e.g. the parameters describing the transmission from snail to humans and the death rates of adult parasites. As shown in the sensitivity analyses, these parameters are very influential in the overall outcome of the models.

The inclusion of density-dependence in snails and adult parasites is clearly important in modelling the overall transmission dynamics of schistosomiasis and evaluating the potential of various control programmes. The absence of these

biologically important parameters leads to false estimations of the sensitivities of some parameters. Although overall the models produced similar results in terms of their steady-state behaviour, this disguised the finer, dynamical details within each model that have important consequences for control success. For example, Model 3 highlighted the overriding importance of the parameters depicting the transmission of infection from snail to humans, contrary to the previous two models and the model developed in Chapter 2.

Direct comparison of the outcomes of the chemotherapy programmes shows the clear superiority of the bi-annual treatment programme over the annual programme (for the same coverage levels). This finding is substantiated by findings in Zaire where the effects of mass treatment disappeared within 20 months even when supplemented with focal molluscicide (Polderman 1984). At 50% coverage levels, the bi-annual treatment programme is successful in eliminating disease after 8 years at 18°C. However, if some individuals remain infected after the treatment programme has ended, the disease may re-establish and return to pre-treatment levels. At 34°C, both annual and bi-annual chemotherapy programmes caused an increase in worm burden. The sensitivity analysis demonstrates that the production rate of miracidia (λ_M) does not strongly influence transmission dynamics as snails produce the same number of cercariae regardless of the number of miracidia that infected them (Fig. 5.6). The complex density-dependent mechanisms that explain this are discussed in Chapter 2.

Improvements in sanitation, modelled as a reduction in the miracidial infection rate, slowed the transmission of disease, although long-term, these levels eventually reached those with no control. This was not surprising, as the miracidial infection rate (β_S) did not influence mean worm burdens or prevalence in the sensitivity analysis (Fig. 5.6). This is explained by the intense density-dependence at the intermediate host stage. Decreasing the number of miracidia infecting each snail does not reduce the number of

cercariae produced. With improvements in sanitation usually comes provision of safe water for drinking and washing which would reduce the contact rate of humans with cercariae. Therefore, a general improvement in living standards would impact the transmission of disease more substantially than described here. Monthly molluscicide treatment constantly reduced the prevalence of infection over the duration of the study period and reduced the mean worm burden to <2 worms per person. However, if the treatment is applied every 3 months, there is no significant impact on transmission. Niclosamide, the most commonly used molluscicide, only kills snail eggs when it is present at 0.01mg/L for a period of two weeks (McCullough 1980). Therefore, the snail population can build up following an application of molluscicide and continue to transmit the disease. The costs of repeated administration of molluscicide make this a prohibitively expensive programme to recommend (Greer *et al.* 1996). This is consistent with previous findings in the Philippines, which showed a snail control programme alone was insufficient to maintain long-term control (Ishikawa *et al.* 2006).

Overall, the most effective strategy is mass chemotherapy, but a combination of two or more control programmes may have better success in eliminating the disease. Further study on combinations of control programmes would be useful and has previously been done for *S. japonica* (Williams *et al.* 2002). This showed that the most effective strategy in reducing prevalence of disease was a combination of a vaccination targeting the reservoir host, selective chemotherapy and a reduction in water contact. These results are not directly applicable to *S. mansoni* but indicate where future work can be directed. Many other refinements can be made to these models, including age-dependent acquired immunity, seasonal heterogeneity, age-structure contact rates, and animal reservoir hosts. One of the main advantages of theoretical modelling is that it highlights areas in which comprehensive data are lacking. It is clear from this study that

a more detailed model is critical to understanding the complex nature of schistosomiasis transmission and for determining the efficacy of control programmes.

CHAPTER 6

A spatial statistical approach to schistosomiasis mapping

6.1 Introduction

Schistosomiasis is found across the African continent in highly variable geographic surroundings and its distribution is influenced by climatic and human characteristics. The distribution of disease is limited by conditions which support the survival of both the snail intermediate host and parasite. Predicting the risk of schistosomiasis depends on an understanding of the environmental and sociological risk factors that affect transmission. However, these predictions are often complicated by the complex nature of the interactions between variables and the unpredictable nature of human behaviour. Two important climatic determinants of the snail population are temperature and rainfall (Brooker 2007). Schistosomes are more sensitive to lower temperatures than snails, so uninfected snails can be found at high altitudes in endemic countries, where larval development is inhibited (Brooker 2007). It is difficult to quantify the relationship between rainfall and schistosome transmission dynamics as the effects of rainfall on the snail population can vary. High rainfall in some areas can create additional habitats for snails, whilst other areas may be prone to flooding, thereby destroying habitats. It is unclear how important seasonal fluctuations in snail population dynamics may be in the overall transmission of disease, as these fluctuations are typically of a much shorter duration than the adult parasite life-span (Anderson 1987). The distribution of snail habitats is also influenced by numerous other factors, including the presence of temporary water bodies, water velocity, and pH (Sturrock 1993). However, these small-scale heterogeneities are impossible to include in a large-scale spatial model.

The first comprehensive maps of the distribution of schistosomiasis were created by WHO twenty years ago (Doumenge 1987). The WHO Global Atlas of Schistosomiasis

collated every known source of data on schistosomiasis to that date and produced a series of maps to be used as tools in the control of disease. This now outdated resource remains the only comprehensive survey of schistosomiasis on a continent-wide scale. This report documents the presence of *S. mansoni* in 39 countries in continental Africa. In many endemic African countries, comprehensive data showing the prevalence and intensity of infection are not available. The limited data available often do not define the intensity of disease or identify the true 'foci' of disease, which are blurred by population movement. The prevalence of infection, based on the presence of *S. mansoni* eggs in stool samples, is the most widely used indicator of infection status, although the mean worm burden per person is more indicative of morbidity (Sukwa 1986; Wilkins 1989). The heterogeneity of the data may be explained by the data collection techniques, some studies use parasitological data, whilst others present only immunodiagnostic results. Furthermore, many surveys present results from samples of the population that may not be representative of the entire population. A more current atlas is being developed with aims to produce prevalence maps at the second administrative level for the whole of sub-Saharan Africa using geographic information systems (GIS) (Brooker *et al.* 2000). Accurately mapping the distribution of disease relies on modelling to predict the risk of infection for the whole population, as prevalence studies usually only exist at a limited number of locations. Furthermore, studies of schistosomiasis are often clustered in areas of high transmission and focus on high-risk sub-sections of the community, e.g. schoolchildren or hospital admissions. Consequently, data are often highly spatially correlated (Clements *et al.* 2006). Finally, the current literature on the epidemiology of schistosomiasis is strongly biased towards positive findings; there is a considerable lack of negative data, which confounds our understanding of the diversity of transmission.

The implications of spatial heterogeneity to the overall spread and intensity of disease are poorly understood. Likewise, the significance of spatial heterogeneity in

predicting the efficacy of control programmes needs further study (Gurarie 2005). A number of studies have mapped schistosomiasis over large areas of Africa but few have considered the effects of spatial autocorrelation between foci (Brooker and Michael 2000; Malone *et al.* 2001b; Moodley *et al.* 2003). An infectious disease that is correlated with environmental variables is likely to be spatially clustered even when the human population is not clustered (Kleinschmidt *et al.* 2000). GIS and remote sensing (RS), along with geostatistical techniques, allow the quantification of such spatial heterogeneity in distribution patterns. Geostatistics can establish whether the patterns in prevalence are caused by specific environmental conditions, or due to random stochastic variability. At the community-level, semi-variograms can be used to reveal spatial correlation between study sites by measuring the mean-squared difference of pairs of observations separated by the same distance (Chiles 1999).

The purpose of this study was twofold. Firstly, predictions of schistosomiasis risk in regions where data are not available were generated by measuring the degree of spatial autocorrelation between existing data sets. Smoothed risk maps of schistosomiasis distribution for Africa were then produced using Bayesian kriging. Secondly, statistical models were developed using a number of environmental and ecological variables obtained from RS and GIS. These models were used to create both current risk maps and future risk maps given a defined temperature change using an IPCC climate change scenario (IPCC 2001).

6.2 Methods

6.2.1 Data Collection and Preparation

(i) Disease data

The data used in this study were obtained from the WHO Atlas of the global distribution of schistosomiasis (Doumenge 1987) which includes all published prevalence data available from 1930 – 1985. Altogether 1639 surveys were documented with suitable estimates of schistosomiasis prevalence due to *S. mansoni*. If two or more values existed for one location, the value pertaining to the most representative sample of the population was used, i.e. surveys of schoolchildren were excluded in favour of surveys from the general population. If both surveys represented the general population, the average value was calculated. If the region only was specified, the mid-point was taken as the survey focus. Each location was georeferenced using Google Earth which uses the Simple Cylindrical projection with a WGS84 datum. The longitude and latitude in decimal degrees, along with the elevation at the mid-point of each location was recorded.

(ii) Environmental variables

The lack of environmental data recorded at a fine spatial scale can be overcome by using remotely sensed satellite data. To reduce the effects of cloud contamination in satellite imagery, composite images are produced from which we can derive long-term mean values or select the data from the most cloud-free day (Hay 2000). Environmental data can be also estimated at locations for which no observations are available using spatial interpolation. Environmental variables were initially chosen for inclusion in the model based on biological plausibility. Low levels of precipitation may reduce the

availability of snail habitats whilst high precipitation levels may washout snail populations. Consequently, precipitation levels are a conceivable factor in the transmission of disease and were included as both a linear and a quadratic term. The level of vegetation can be used as an indicator of rainfall or humidity, so normalised difference vegetation index (NDVI) was also included in the model. The host snail and the free-living parasite stages have optimal temperature ranges outside which survival is inhibited. Land surface temperature (LST) and water temperature were, therefore, included in the model as both linear and quadratic terms. Transmission intensity is thought to be restricted by high altitude (Ostfeld 2009), so elevation was included after being checked for colinearity with LST and precipitation (Clements *et al.* 2008). The initial model variables included elevation, water temperature, mean LST, minimum and maximum LST, NDVI, precipitation, and human population density.

The minimum, maximum and mean LST along with the average monthly precipitation were obtained from the Climate Impact on Agriculture (CLIMPAG) division of the Food and Agriculture Organization (FAO) of the United Nations and georeferenced using ArcGIS Version 9 (ESRI, Redlands, CA) to match the projection of the prevalence data. Prevalence data were collected over many decades, so it was not possible to accurately match each survey with the corresponding climate data. Long-term average climate values (over a 12-month period) were used where possible to compensate for this. The paucity of accurate historical climate data for most African countries meant that the choice of data was restricted. Water temperature estimates were obtained from the FAO's Geonetwork (http://www.fao.org/geonetwork/srv/en/main.home) and averaged for the period of 1920 to 1980. NDVI was used as a numerical indicator of the type of land cover and was derived from the VGT sensor aboard the SPOT-4 satellite. These data consist of 10-day composites aggregated into 0.5 degree grid-cells where values lie between -1 (barren areas) and +1 (rainforest cover). Estimated figures for the

population density in Africa during 1980 were obtained from the United Nations Environment Programme / Global Resource Information Database (UNEP/GRID) and the Center for International Earth Science Information Network (CIESIN) World Data Center (http://na.unep.net/globalpop/africa/part1.html#pop). The full methods concerning the derivation of population density values and a detailed description of each of the data sources mentioned here are presented in Appendix A3. Climate and population data were linked to the prevalence data using the Spatial Analysis tool in ArcMap.

(iii) The Koeppen classification system

Due to the amount of data needed from different sources for the previous analysis, a more practical approach may be to characterise a location according to a simple, discrete classification system. Hence, an alternative approach to using the climate variables listed above is to use one indicator of climate as a predictor variable for schistosomiasis. The associations between climate and disease were separately analysed using the Koeppen climate classification system, one of the most widely used classification systems (Peel *et al.* 2007). This system is based on the concept that vegetation is the best indicator of climate and so categorises climate boundaries based upon vegetation distribution. It combines average monthly and annual temperatures and precipitation, along with the seasonality of precipitation (Table 6.1). Data were obtained from CLIMPAG, projected in ArcGIS and re-coded using R v2.8.1 (http://www.r-project.org/). Each code was assigned a unique numerical value for analysis.

Table 6.1 A definition of the Koeppen classification system.

T corresponds to the long term monthly mean temperature in °C and *P* is the long term monthly precipitation in mm. The subscripts min and max represent the lowest and highest monthly values of the year, and the subscript *ann* represents the annual sum. Subscripts *S* and *W* stand for the summer and winter. *Pth* is the threshold precipitation for aridity which is defined as 2(*Tann*) if $PW \geq 2PS$; 2(*Tann*) + 28 if $PS \geq 2PW$; or 2(*Tann*) + 14 otherwise.

Code	Numerical code	Description	Criterion
A	1-50	Equatorial climates	$T_{min} \geq 18°C$
Af	13	Equatorial full humid rainforest	$P_{min} > 60mm$
Am	23	Equatorial monsoon	$P_{ann} \geq 25\ (100mm - P_{min})$
As	33	Equatorial savannah with dry summer	$P_{min} < 60mm$ in summer
Aw	43	Equatorial savannah with dry winter	$P_{min} < 60mm$ in winter
B	51-100	Arid climate	$P_{ann} < 10\ P_{th}$
Bw	83	Desert climate	$P_{ann} \leq 5\ (P_{th})$
Bs	63	Steppe climate	$P_{ann} > 5\ (P_{th})$
C	101-150	Warm temperate climates	$-3°C < T_{min} < 18°C$
Cf	112	Warm temperate fully humid climate	Neither Cs nor Cw
Cw	122	Warm temperate climate, dry winter	$P_{Wmin} < P_{Smin}, P_{Smax} > 10\ (P_{Wmin})$
Cs	132	Warm temperate climate, dry summer	$P_{Smin} < P_{Wmin}, P_{Wmax} > 3\ (P_{Smin}), P_{Smin} < 40mm$
D	151-200	Snow climate	$T_{min} \leq -3°C$
Df	162	Snow climate, fully humid	Neither Ds nor Dw
Dw	172	Snow climate with dry winter	$P_{Wmin} < P_{Smin}, P_{Smax} > 10\ (P_{Wmin})$
Ds	182	Snow climate with dry summer	$P_{Smin} < P_{Wmin}, P_{Wmax} > 3(P_{Smin}), P_{Smin} < 40mm$
E	201-230	Polar climates	$T_{max} \leq 10°C$
Et	213	Frost climate	$T_{max} \leq 0°C$
Ef	223	Tundra climate	$0°C \leq T_{max} < 10°C$

Source: (Grieser 2006)

6.2.2 Testing spatial autocorrelation using kriging

First, I describe the procedure used to determine the spatial distribution of schistosomiasis across Africa, and quantify the spatial autocorrelation in prevalence. This is important because the prevalence data documented by the WHO highlight many areas of Africa where data are limited or non-existent. In order to predict prevalences for these undocumented locations it is important to establish whether the data display any spatial autocorrelation, i.e. do study sites that are close together have similar values of schistosomiasis prevalence, in contrast to study sites that are far apart. Data that are highly spatially correlated cannot be classified as independent observations. Hence, to examine the spatial distribution of disease and create a continuous distribution map over the African continent, it is necessary to use spatial interpolation methods to describe the spatial behaviour between locations. First, a semivariogram was established to measure the degree of spatial dependence between the data points. The value of the semivariance (γ_h) for a separation distance h (known as the lag) is the average squared difference in Z-value (prevalence) between a pair of data points, h distance apart, as described below:

$$\gamma_h = \frac{1}{2n}\sum_{i=1}^{n}(Z(x_i) - Z(x_i + h))^2 \qquad 6.1$$

where n is the number of pairs of data points separated by h and $Z(x)$ is the prevalence value at location x. Larger distances between two points will yield a larger value of semivariance, and the magnitude of γ_h describes how different the prevalences are between locations of distance h apart; high values indicate locations that differ greatly in their prevalences. This value increases as the distance between data points increases until it reaches a critical value (known as the sill, C), at which the semivariance will equal

the variance of the whole data set. The distance to this point is the effective range (r) and within this range, it is assumed that all data points are related to each other. The semivariogram plots the variance between points (γ_h) against the distance (h) at which the variance was calculated. Depending on the type of semivariogram selected, a model formula is then fitted to the data. The most common models include spherical, exponential, Gaussian, and power, and model choice depends on which model curve best represents the variance in the data. There is no significance test associated with the semivariogram, so model selection is done by eye. The spherical model was determined as the most appropriate model for this data set. This model rises to the sill more quickly than the exponential and Gaussian models, showing a shorter effective range which fits the data well. The spherical semivariogram model is described in Equations 6.2-6.4:

$$\gamma_h\{0\}\ if\ h = 0 \qquad 6.2$$

$$\gamma_h\left\{C_0 + C\left[\frac{3}{2}\left(\frac{h}{r}\right) - \frac{1}{2}\left(\frac{h}{r}\right)^3\right]\right\}\ if\ 0 < h < r \qquad 6.3$$

$$\gamma_h\{C_0 + C\}\ if\ h \geq r \qquad 6.4$$

The intercept (C_0 – also known as the nugget) represents the variance due to data variation at a fine scale and/or spatial dependence which has not been explicitly modelled. This occurs when sampling locations are very close together but show different prevalence levels. It is not possible to detect variation at such a fine-scale and discontinuity at the origin arises; C is the value of semivariance at the sill and $C + C_0$ denotes the error variance at the sill, i.e. when the data points are no longer spatially correlated.

The semivariogram assigns a weight to each data point that determines its relative influence in predicting the unknown values. Ordinary kriging uses these weighted values to predict unknown values within the calculated effective range (r) assuming no directional trends in the data. This method assumes that the data have a stationary variance but a non-stationary mean value within the effective range. Outside the effective range, the model will make predictions based on the nearest 5 neighbours, but these predictions may be less accurate than those within range. However, one of the main assumptions in spatial modelling is that the spatial dependency is isotropic, that is, the spatial structure is not influenced by direction (Deng 2006). This assumption reduces the complexity of spatial models but disregards the reality that effects of spatial dependency may vary between study sites and in different directions. To examine the effects of directional trends in the data set, anisotropic modelling is used. This creates a separate model for each directional trend identified using trend analysis. When predicting values in one direction the kriging weights can be influenced to use the parameters of one model, whilst values positioned in another direction will be differentially influenced by a separate model. Both models, with and without directional influences, were compared and cross-validated with the existing data set.

Two types of kriging are investigated here, each using two different approaches. Firstly, ordinary kriging with and without directionality are used to estimate the prevalence of disease. Secondly, ordinary probability and indicator kriging are used to estimate the probability that the disease is present in an area. Indicator kriging uses an indicator function in order to estimate the probability of the unknown value exceeding a pre-defined threshold. This converts the existing data into a binary variable (see Equation 6.5) and calculates the probability of the unknown variable being above the threshold.

$$I_x = I(Z_x < threshold) = \begin{cases} 0, Z_x < threshold \\ 1, Z_x \geq threshold \end{cases} \quad 6.5$$

The indicator value is set to 0 if the prevalence value is less than the threshold, defined as 0.1. This is an arbitrarily low threshold, used to separate the disease data into two categories, present and absent. All prevalence values over 0.1 are coded as 1. This model follows the same method as ordinary kriging and produces a continuous surface output containing probability values that the prevalence at location x exceeds the threshold level. Predictions made by kriging are more accurate if the data follow a Gaussian distribution. To normalize the data and make the variance more constant, lognormal kriging is often used. As the prevalence data contain zeros, the data were transformed using log (prevalence +1).

To summarise the procedures carried out to describe the distribution of schistosomiasis prevalence across Africa, four maps were produced using the methods described, two predictive maps using ordinary and directional kriging and two probability maps using ordinary and indicator kriging.

6.2.3 Climate model development

Here I describe the procedures to relate the observed distribution of schistosome to local climatic variables. All statistical models were developed and validated using R. Colinearity was explored amongst all pairs of predictor variables (temperature, rainfall, elevation, NDVI, water temperature and population density), and if any pair had a correlation coefficient > 0.9, the least biologically relevant variable of that pair was excluded. Two separate models were developed using the variables described above; (1) a binomial logistic regression model (or generalised linear model – GLM) using the MASS

package and (2) a proportional odds ordinal logistic regression model (LRM). These two modelling approaches were compared using Akaike's information criterion (AIC) to determine which model provided the most accurate predictions of prevalence. The GLM model (Model 1) uses a continuous response variable and can produce actual predictions of prevalence whereas the LRM model (Model 2) divides the prevalence into categories and produces a series of probabilities of the predicted prevalence lying within one of those categories.

Non-linear relationships were explored univariately and polynomial terms up to second order were included for any variables which exhibited non-linear behaviour. Model 1 included the predictor variables above as fixed effects with a binomial error structure using iteratively reweighted least squares (IWLS) to fit the model. A backwards stepwise progression procedure simplified the model based on deletion testing (using Chi-squared tests) until the minimal adequate model was achieved which contained only significant terms ($P \leq 0.05$). Model 2 was developed using the Design package with the prevalence classified into 4 categories (0, <20%, 20 - 70% and >70%). The model was fitted using maximum likelihood estimation and a stepwise deletion process was done as before. The minimum adequate model for both Model 1 and Model 2 were used to create a current risk map, which was compared to the observed data, and a future risk map using the climate change scenario described in Section 6.2.5.

The Koeppen climate data were analysed using ANOVA. Each location was designated a two-letter code describing the climatic conditions (Table 6.1). For the analysis, the first letter of each code was used because the two-letter code resulted in some categories having insufficient data. Therefore, the analysis examined the influence of three Koeppen classes (A – C) on the prevalence of disease.

6.2.4 Climate model validation

Both models were validated by dividing the data into two random sets, containing ¼ and ¾ of the original data respectively. The ¾ dataset was used to run the model and the output was validated using the ¼ dataset. The accuracy of the predictions of Model 1 was determined in terms of the ability to discriminate between a true prevalence of 0 versus >0 (i.e. absence versus presence), and two thresholds of 0.2 and 0.7. Model 2 was validated using optimal threshold analysis, which calculates the probability that the predicted value (x) is present above a defined threshold ($\tilde{x}$) (Robinson 2000).

6.2.5 Climate change scenario and future disease risk predictions

The climate change model used was the SRA1B model with projections from 2040-2069, which predicts an average global temperature increase of 2.9°C by 2100 (Carter 2007). This climate change scenario assumes very rapid economic growth, with a global population that peaks at 2050. This model also incorporates rapid introduction of new and more efficient technologies balanced across energy sources. The model data were acquired from the National Center for Atmospheric Research's (NCAR) Community Climate System Model 3.0. This model was chosen as a worst-case scenario model, with rapid population growth and high estimates for future CO_2 concentrations. The climate change data were obtained from the IPCC Data Distribution Centre (DDC) and projected in ArcMap at 0.5 degree cell resolution using the WGS84 datum as before. The study sites described previously were overlaid onto this map and the predicted temperatures were extracted at each location. These data were then input into the GLM and LRM models and the predicted prevalence values were modelled using the "predict" function in R. The predicted prevalence values were imported back into ArcMap and ordinary kriging was used to produce a smoothed map over Africa.

6.3 Results

The first part of this analysis involved examining the spatial pattern in prevalence using kriging and producing smoothed prediction maps for the whole continent. Secondly, the ecological predictors of schistosomiasis were extracted at each of the study sites and analysed using generalised and ordered logistic regression. Once a minimal adequate model had been obtained, this was then used to produce another map of predicted prevalence using the model output and compared with the original data. The statistical models were used to produce risk maps predicting future distribution of schistosomiasis given the current estimates of global warming.

6.3.1 Summary of prevalence data

The location and prevalence values at each of the study sites show large areas in the north, central and south-west of Africa which have no data available (Fig. 6.1). There was a high concentration of points along the eastern side of the continent, particularly in Ethiopia (222 sites) and Tanzania (114 sites). Highest prevalence rates were seen in the eastern region (Ethiopia, Uganda, Tanzania) and in the far western region (Sierra Leone, Guinea, Mali). The high prevalence rates appeared to be clustered in these areas, with the exception of one study site in Angola. The prevalence data were examined for normality using a Q-Q plot, which showed significant deviation from normality (Fig. 6.2a). Log-transformation of the data improved the normality although at high prevalence levels, the data did still deviate from the plot (Fig. 6.2b).

A trend analysis was conducted to check for directionality in the dataset. Each data point was projected onto two perpendicular planes, an east-west plane and a north-south plane. The line of best fit was drawn through the points on each plane and the

shape of this line indicates trends in specific directions (a flat line suggests that there is no directional trend in the data). Initially, the trend analysis showed a small increase in prevalence values in the east-west direction as the trend line increased linearly as it moved east (Fig. 6.3). The trend line running north-south was flat, indicating no trend in this direction. Rotating the graph shows the east-west plane more clearly, the graph now shows that the trend on the east-west projection plane actually runs northwest to southeast. The reasons for this trend are unknown, it may be due to the large amount of data available for southeast Africa that has skewed the trend analysis, but this can be statistically quantified and removed using anisotropy. Once the trend was removed from the data, the model used the residuals to analyse the variation in the data.

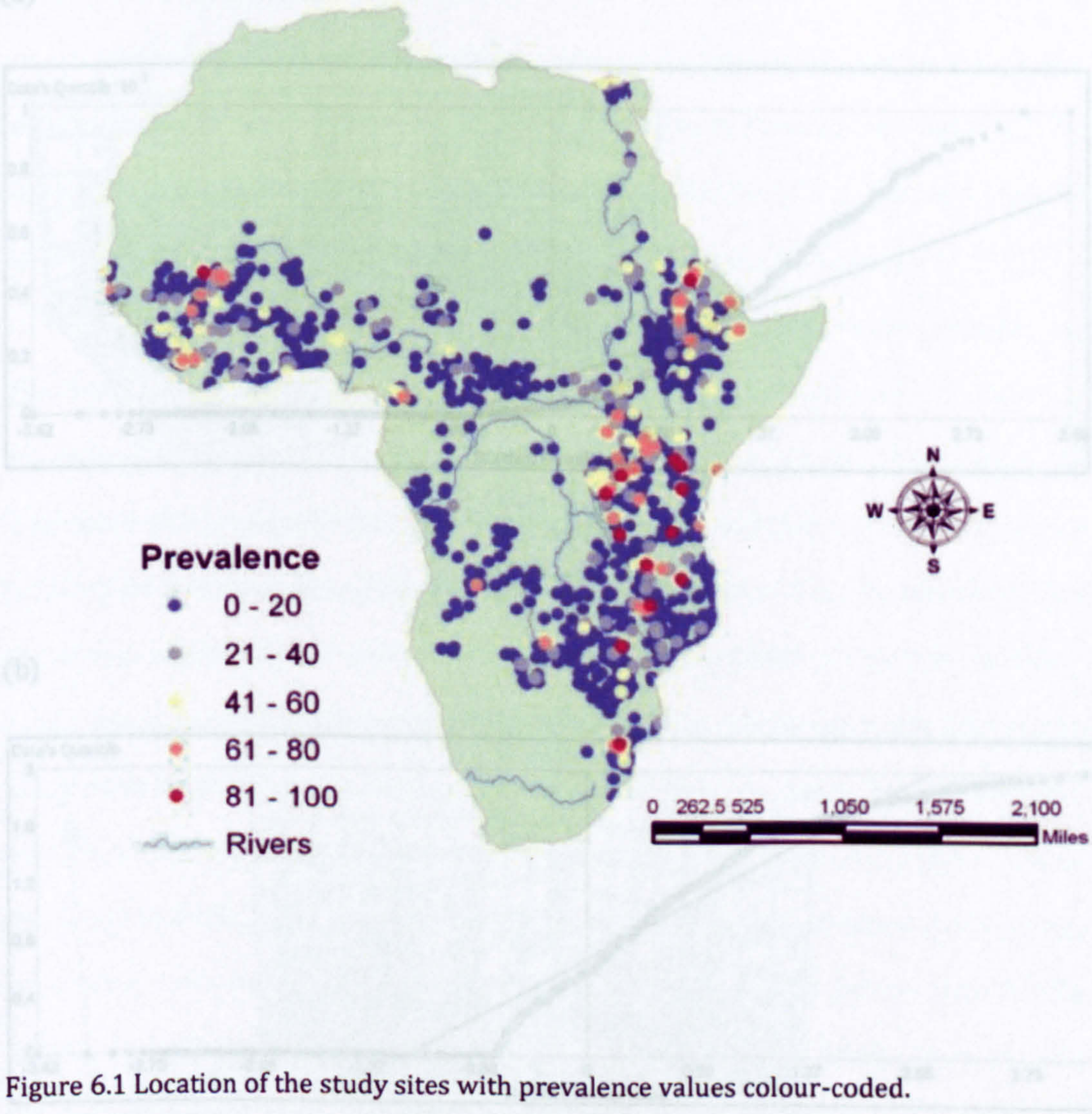

Figure 6.1 Location of the study sites with prevalence values colour-coded.

(a)

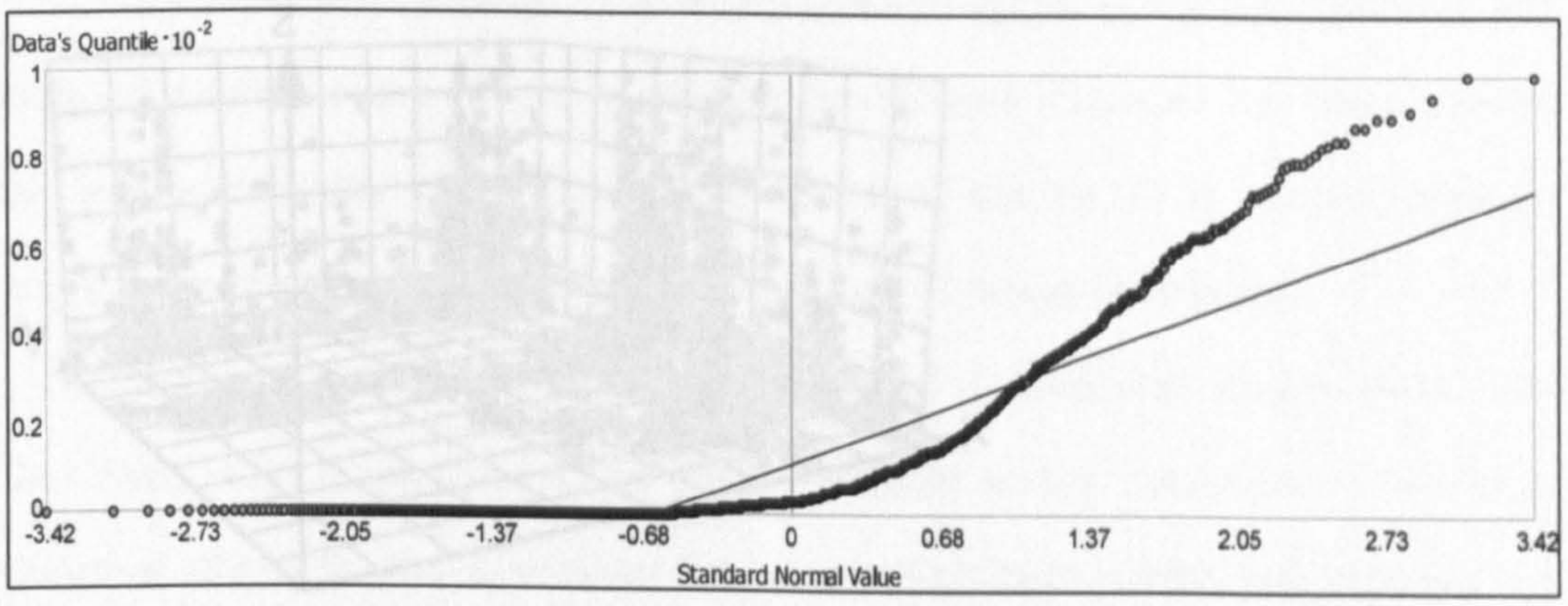

(b)

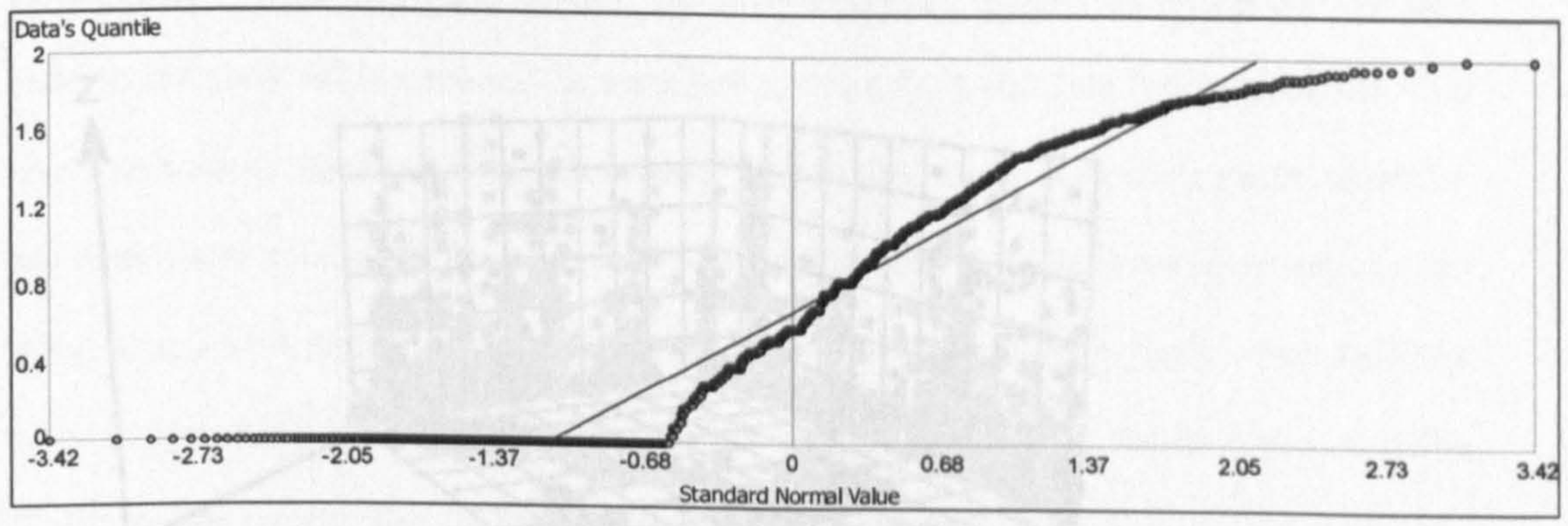

Figure 6.2 Q-Q plot of prevalence data without transformation (a) and subjected to a log-normal transformation (b).

(a)

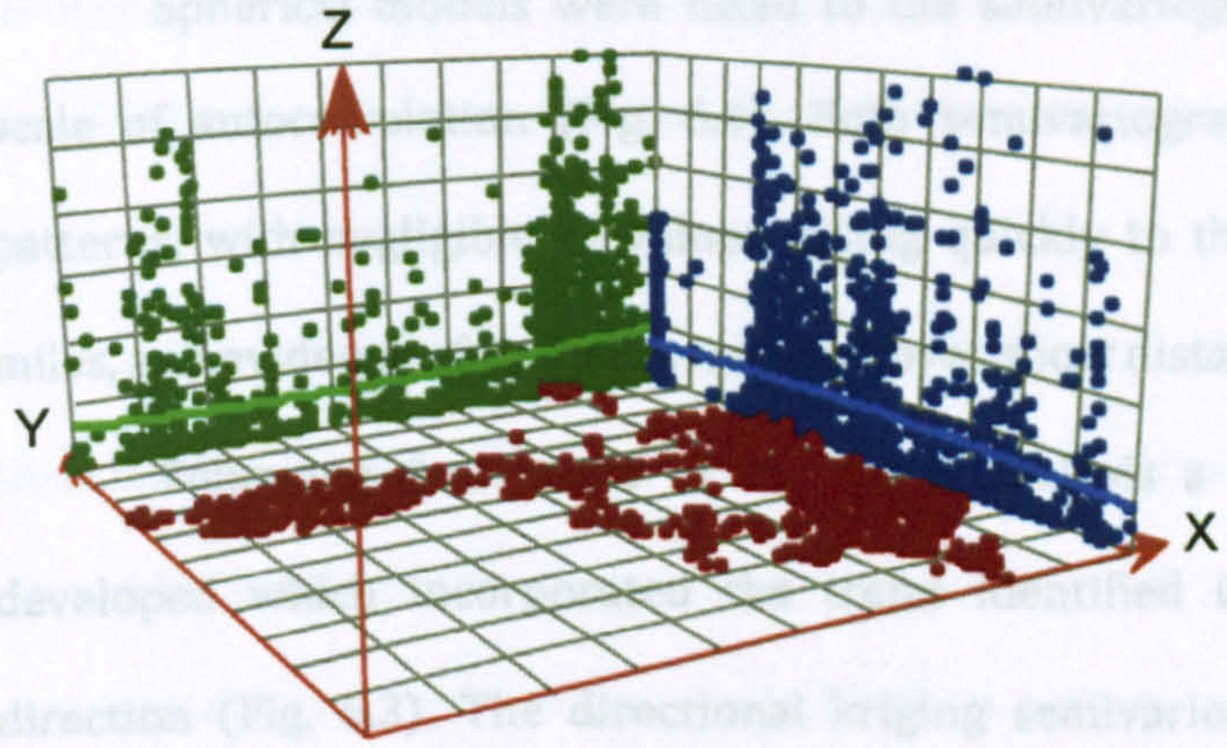

(b)

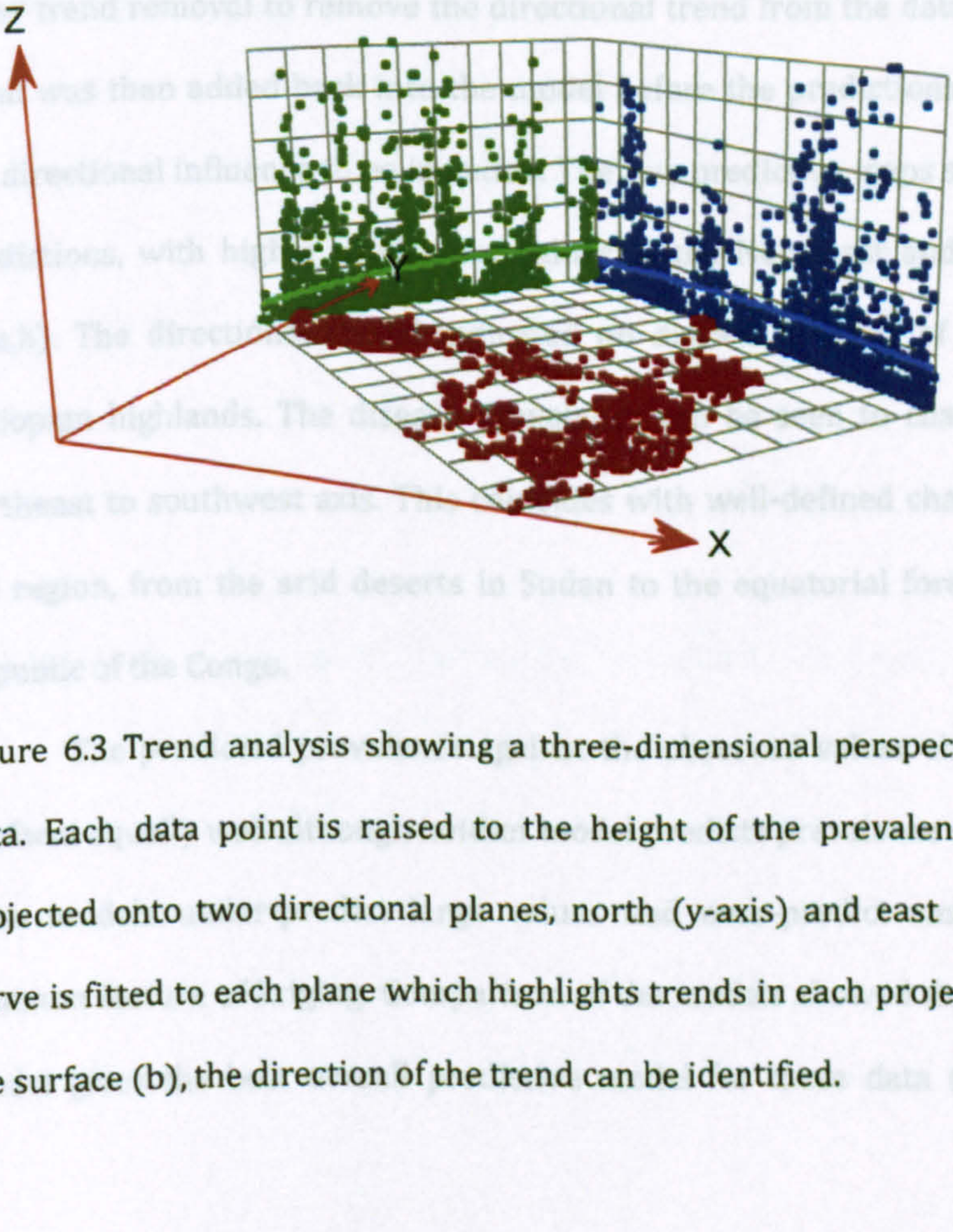

Figure 6.3 Trend analysis showing a three-dimensional perspective of the prevalence data. Each data point is raised to the height of the prevalence value (Z-axis) and projected onto two directional planes, north (y-axis) and east (x-axis). A polynomial curve is fitted to each plane which highlights trends in each projected plane. By rotating the surface (b), the direction of the trend can be identified.

6.3.2 Spatial autocorrelation models

Spherical models were fitted to the semivariograms to quantify the level and scale of autocorrelation (Fig. 6.4). Both semivariograms showed the same general patterns, with negligible C_0 values, rising quickly to the sill (C) at approximately 10 miles, and evidence of spatial correlation over short distances (<10 miles).

Following the results of the trend analysis a directional kriging model was developed which incorporated the trend identified in the northwest to southeast direction (Fig. 6.3). The directional kriging semivariogram, which had removed the large-scale directional influence, showed a longer range than the ordinary model, with locations further apart displaying spatial autocorrelation (Fig. 6.4b). Both ordinary and directional kriging models were used to predict the prevalence in unknown locations across Africa, producing a smoothed continuous map. The directional model used second order trend removal to remove the directional trend from the data before analysis. This trend was then added back into the model before the predictions were made, allowing the directional influence to be included. The two predictive maps show relatively similar predictions, with higher prevalence values in the Northeast and Central regions (Fig. 6.5a,b). The directional model indicated no disease in parts of South Africa and the Ethiopian highlands. The disease prevalence can be seen to change rapidly along the northeast to southwest axis. This coincides with well-defined changes in the ecology of the region, from the arid deserts in Sudan to the equatorial forests of the Democratic Republic of the Congo.

The predicted prevalence against the observed values shows that both models perform equally well although neither model predicts prevalence values >0.25 (Fig. 6.6). Both models under-predict large values and over-predict small values which is a common feature of kriging. Comparison of the models showed that the ordinary kriging model gives the best overall predictive model for these data (Table 6.2). The mean

prediction error is smaller for the ordinary kriging model, indicating smaller differences between the fitted and observed values than the directional kriging model. The standardised root mean squared prediction error is closer to 1, proving a better model fit.

The probability maps show the likelihood of the prevalence exceeding a threshold of 0.1 using the ordinary kriging method and the indicator kriging method (Fig. 6.5). Both models show similar results for high probability of disease in central regions of Africa and a lower probability in eastern and southern coastal areas. The indicator model predicts areas where schistosomiasis is unlikely to occur, e.g. Namibia, Gabon, Mauritania and Senegal. Data are not available for many of these locations and so it is not possible to confirm these findings. The ordinary probability model is likely to over-estimate the probability of disease, it predicts that every region has ≥ 50% chance of having a prevalence >0.1.

(a)

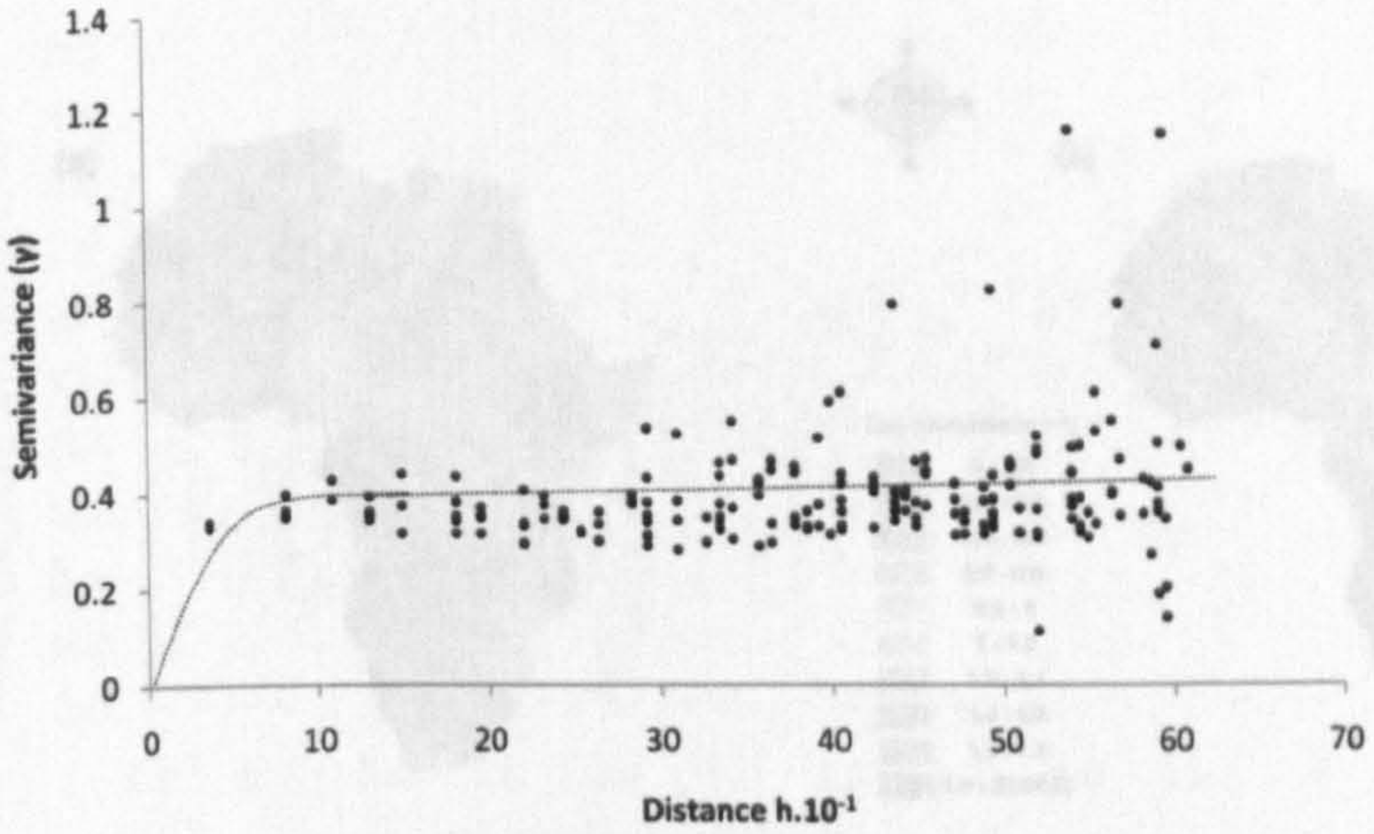

(b)

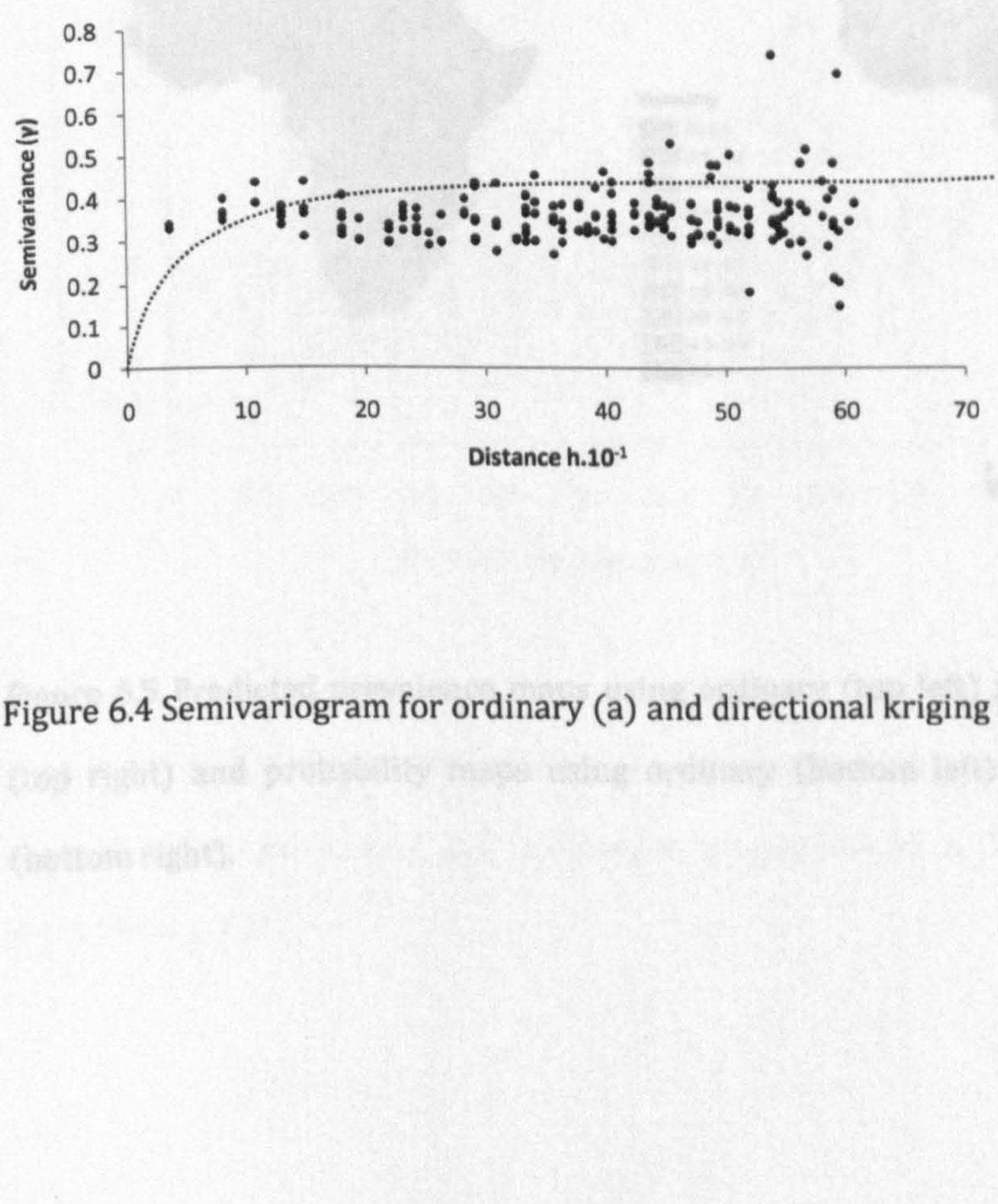

Figure 6.4 Semivariogram for ordinary (a) and directional kriging (b).

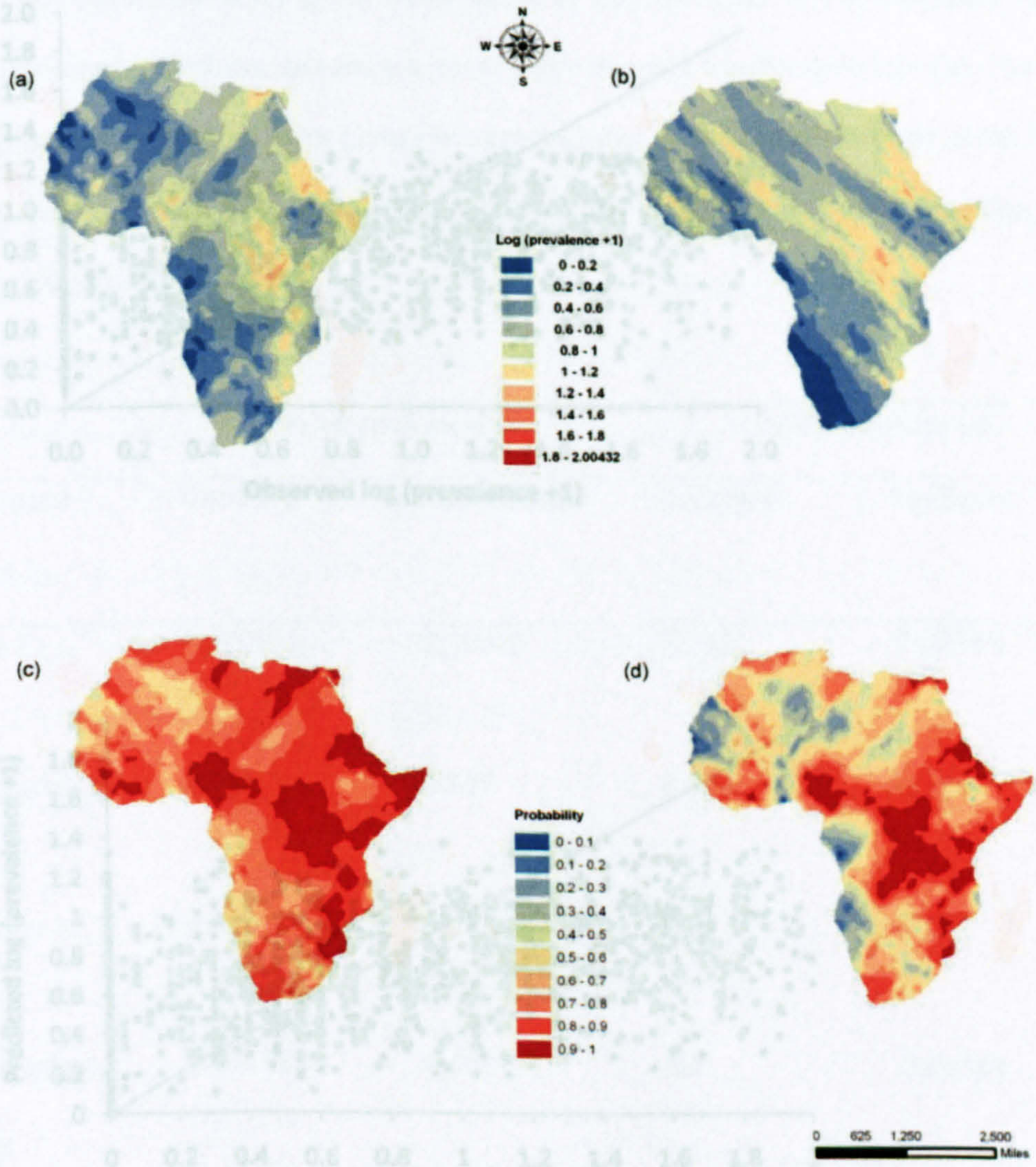

Figure 6.5 Predicted prevalence maps using ordinary (top left) and directional kriging (top right) and probability maps using ordinary (bottom left) and indicator kriging (bottom right).

(a)

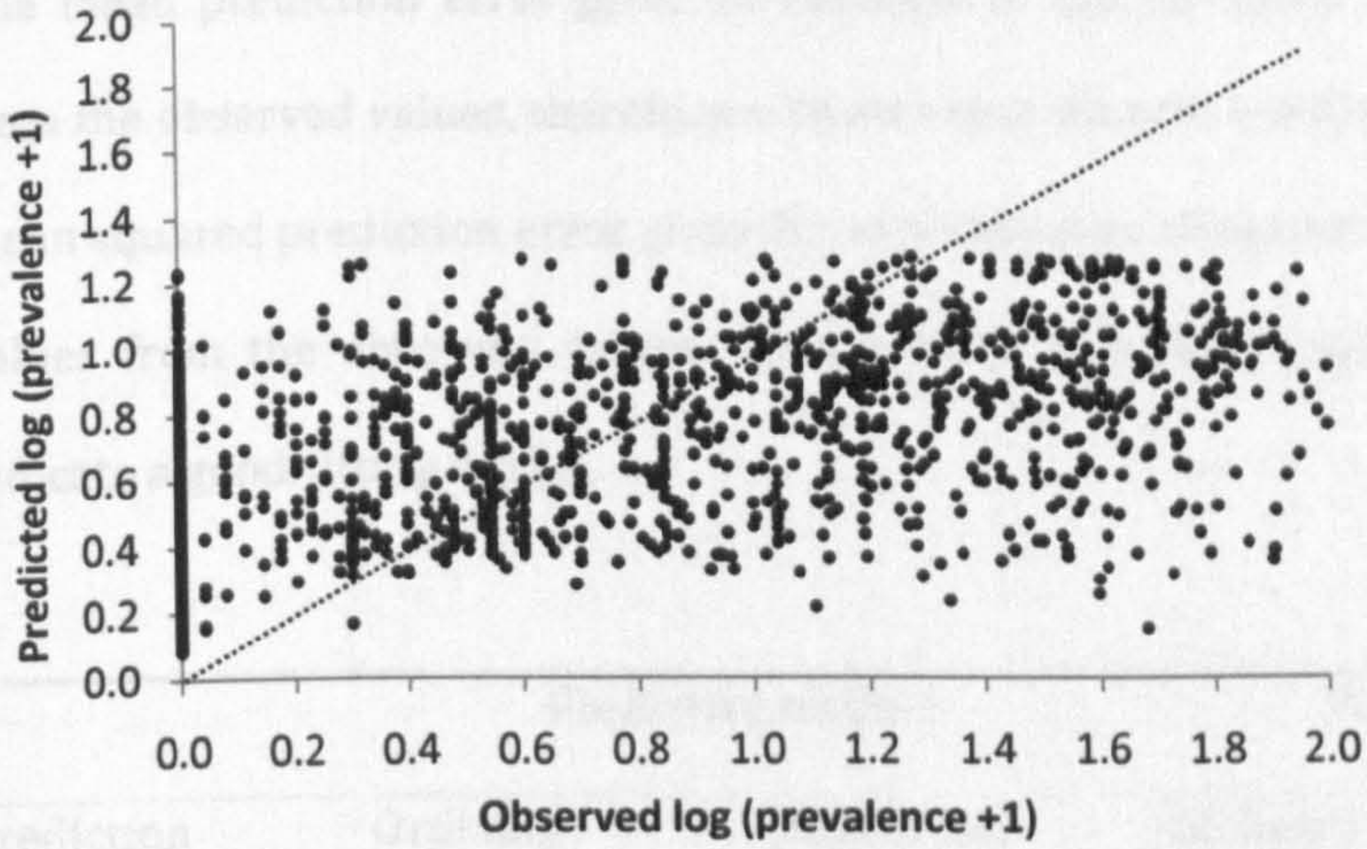

(b)

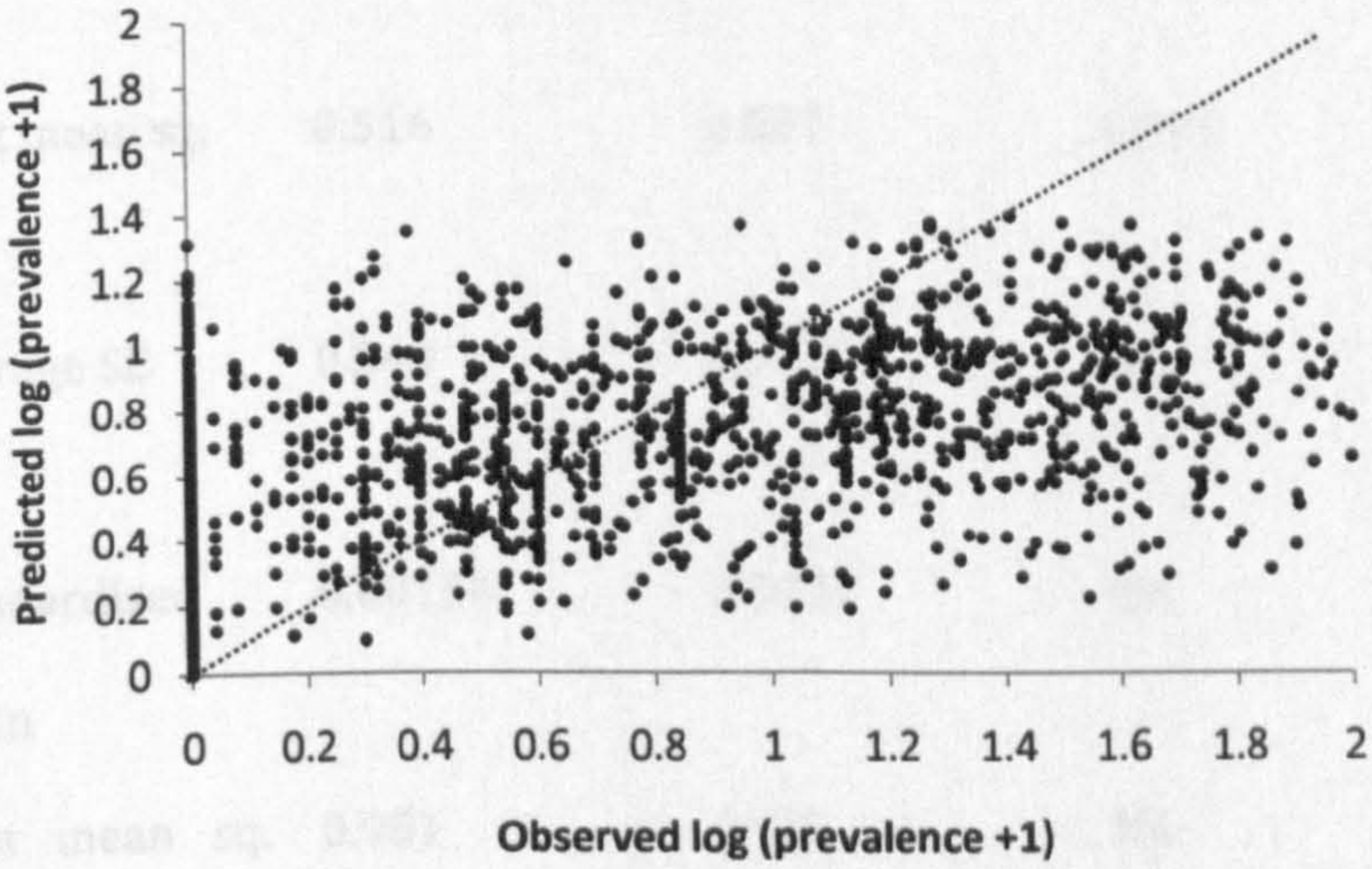

Figure 6.6 Predicted $\log_{10}$ (prevalence) against observed $\log_{10}$ (prevalence) for ordinary (a) and directional kriging (b). Ordinary kriging model $R^2 = 0.29$, directional kriging model $R^2 = 0.252$.

Table 6.2 Comparison of kriging methods.

The mean prediction error gives an estimate of the deviation of the predicted values from the observed values, therefore a lower value denotes a better fitted model. The root mean squared prediction error gives the expected sum of squared deviations of the fitted values from the observed values. Standardised root mean squared values close to 1 indicate a good-fitting model.

	Predictive models		Probability models	
Prediction errors	Ordinary	Directional	Ordinary	Indicator
Mean	0.000883	0.00745	0.121	0.00144
Root mean sq.	0.516	0.507	0.431	0.394
Average SE	0.543	0.547	NA	0.432
Standardised mean	0.00154	0.0137	NA	0.00331
Root mean sq. standardised	0.951	0.926	NA	0.913

6.3.3 Predicting the distribution of schistosomiasis using climate models

The values for the climate variables were extracted from the maps for each of the study sites. Examination of the climate maps demonstrates a clear relationship between the climate predictors and prevalence of schistosomiasis. The lack of available prevalence data for the northern regions of Africa means that no definite associations can be drawn from these areas. The data show that the approximate mean monthly temperature cut-off point for schistosomiasis transmission is around 28-30°C, whilst the precipitation data show that schistosomiasis is unlikely to occur in regions with a very low monthly rainfall (Fig. 6.7a,b). Low temperature may be a limiting factor in schistosomiasis distribution, the disease is absent in large areas of southern Africa and the eastern highlands. In areas with an NDVI value of <0 (i.e. barren areas), very little schistosomiasis has been reported (Fig. 6.7c).

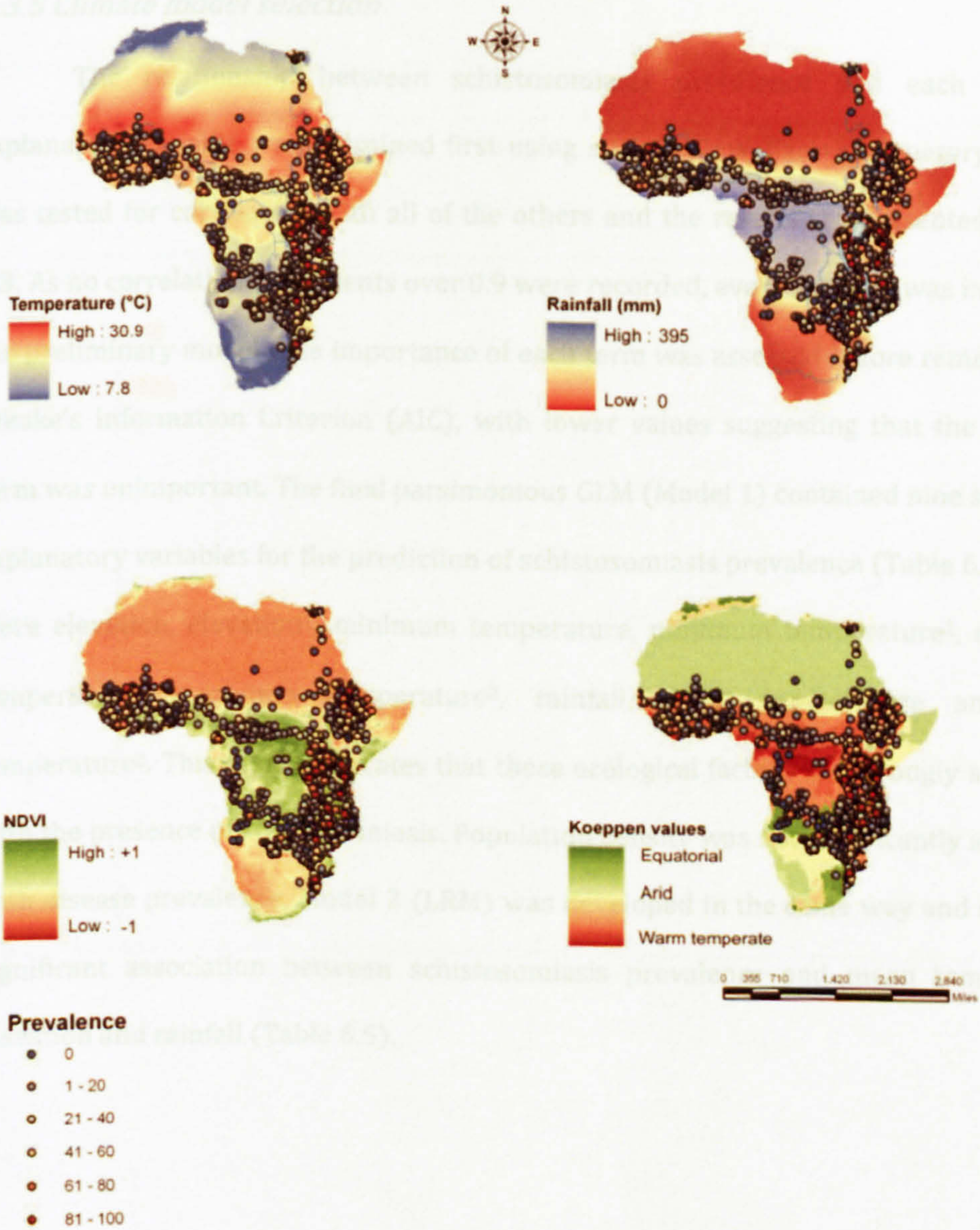

Figure 6.7 Predictor variables used to develop environmental models of schistosomiasis prevalence in Africa.

6.3.5 Climate model selection

The relationship between schistosomiasis prevalence and each potential explanatory variable was examined first using scatter plots. Each explanatory variable was tested for correlation with all of the others and the results are presented in Table 6.3. As no correlation coefficients over 0.9 were recorded, every variable was included in the preliminary model. The importance of each term was assessed before removal using Aikake's Information Criterion (AIC), with lower values suggesting that the excluded term was unimportant. The final parsimonious GLM (Model 1) contained nine significant explanatory variables for the prediction of schistosomiasis prevalence (Table 6.4). These were elevation, elevation^2, minimum temperature, minimum temperature^2, maximum temperature, maximum temperature^2, rainfall, water temperature and mean temperature^2. This model indicates that these ecological factors are strongly associated with the presence of schistosomiasis. Population density was not significantly associated with disease prevalence. Model 2 (LRM) was developed in the same way and showed a significant association between schistosomiasis prevalence and mean temperature, elevation and rainfall (Table 6.5).

Table 6.3 Correlation coefficients for environmental variables.

	Mean temp	Min temp	Max temp	Rainfall	Water temp	NDVI
Elevation	-0.717	-0.523	-0.616	-0.119	-0.0312	-0.077
Mean temp		0.771	0.851	0.0523	-0.0202	0.0954
Min temp			0.411	0.0754	0.0992	0.0433
Max temp				0.0248	-0.092	0.128
Rainfall					0.165	0.584
Water temp						-0.0322

Table 6.4 Minimum adequate Generalised linear model (Model 1) for schistosomiasis prevalence.

Variable	Coefficient	SE	Z-value	*P*
(Intercept)	-3.169e+00	5.754e-01	-5.508	< 0.0001
Elevation	-2.200e-04	4.335e-05	-5.075	< 0.0001
Min. temp	-5.075e-01	1.532e-02	-33.131	< 0.0001
Max. temp	4.253e-01	3.273e-02	12.996	< 0.0001
Rainfall	9.028e-04	1.909e-04	4.728	< 0.0001
Elevation ^2	2.746e-07	1.847e-08	14.867	< 0.0001
Min. temp ^2	1.837e-02	5.571e-04	32.969	< 0.0001
Mean temp ^2	2.517e-03	2.237e-04	11.251	< 0.0001
Max. temp ^2	-6.293e-03	4.835e-04	-13.016	< 0.0001
Water temp ^2	-2.924e-04	5.464e-05	-5.352	< 0.0001

Table 6.5 Minimum adequate ordinal logistic regression model (Model 2) for schistosomiasis prevalence.

Variable	Coefficient	SE	Z-value	*P*
Mean temp	-0.1402092	0.0204967	-6.84	< 0.0001
Rainfall	-0.0022741	0.0011433	-1.99	0.0467
Elevation	-0.0004076	0.0001026	-3.97	0.0001

The GLM (Model 1) and LRM (Model 2) were used to predict prevalence and probability of schistosomiasis in locations in Africa where data were not observed (Fig. 6.8). Model 1 predicts actual prevalence of schistosomiasis at each location whereas Model 2 gives a predicted probability that the prevalence level will fall into one of four categories. These maps reveal the differences in predictive outputs between the two modelling techniques. A threshold prevalence of 0.7 was used for the output of Model 2 to highlight the areas that were most at risk of infection, therefore the map shows the probability of each area experiencing a prevalence of >0.7 (Fig. 6.8b). The most obvious differences between the two models are found in the regions that are predicted to have a very low probability of schistosomiasis (South Africa, Botswana and Zimbabwe). This may have occurred due to differences in the method of predictions although both models over-estimate the level of infection compared with the empirical data. Model 2 predicts that northern Egypt, parts of Uganda and Kenya, and most of southern Africa will experience a low probability of disease. Both models predict that northern regions of Africa will experience high prevalence / probability of infection. This is likely to be an over-estimation as very dry regions will not be able to support the snail host.

The association between Koeppen classes and prevalence levels was analysed using ANOVA ($P = 0.07$) (Table 6.6). Although the overall test was non-significant, it indicated differences in prevalence between the equatorial climate (class A) and the warm temperate climate (C) ($P = 0.029$). No differences were found between the arid climate (B) and classes A and C ($P = 0.96$). The differences in coefficient values for A and C show that prevalence in temperate climates was on average 2% lower than in equatorial climates. As the overall result was non-significant, this model was not used to create a predictive map of prevalence.

Table 6.6. Analysis of Koeppen classification using ANOVA.

	Coefficients	SE	t-value	Pr(>|t|)
(Intercept)	12.46251	0.60312	20.664	<2e-16
Class B	-0.05474	1.22594	-0.045	0.9644
Class C	-2.37777	1.08637	-2.189	0.0288

6.3.6 Climate model validation

Model 1 was validated using three threshold values, 0 versus >0, then thresholds of 0.2 and 0.7 were used. Model 1 failed to identify any areas with a prevalence <0.2. Validation of Model 1 using an observed prevalence threshold of 0.7 gave an accuracy rate of 55% although it performed less well in predicting sites with prevalence <0.7 (21%). Model 2 gave the probability that the prevalence values lay within four categories, 0, 0-0.2, 0.2-0.7 and >0.7. This model correctly predicted the prevalence category for 51% of study sites and correctly identified study sites using a threshold of 0.2 in 100% of cases, indicating highly accurate predictive performance.

A sub-set of data which comprised Ethiopia, Kenya and Tanzania only, was used to create and validate a GLM. This was done to determine whether the predictive power of the model would increase with a smaller, more localised data set. The minimal adequate model was identical to the initial GLM containing all study sites and the predictive power of the model remained at 50%.

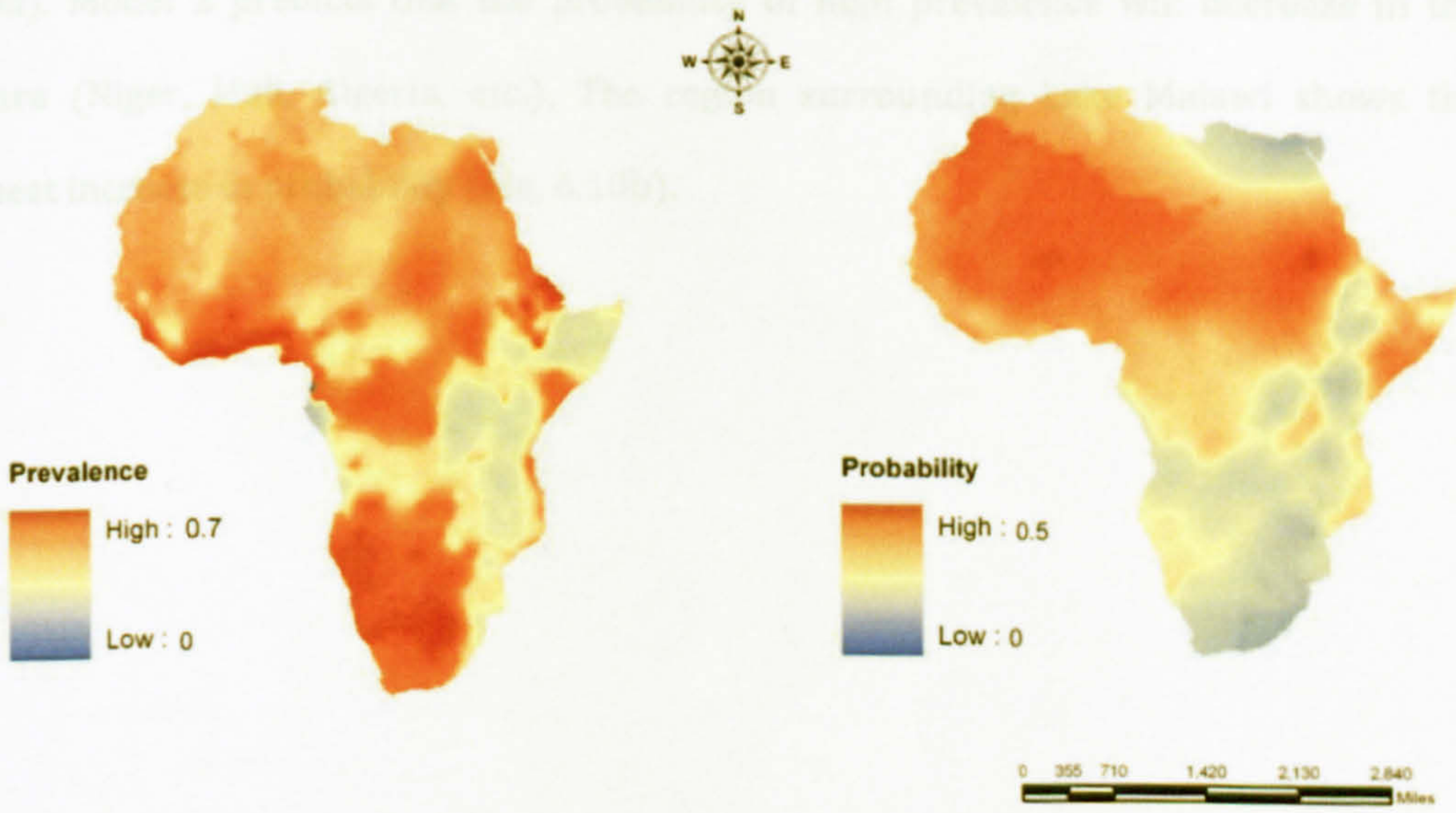

Figure 6.8 Spatial predictions of the GLM (Model 1) showing predicted prevalence (a) and the LRM (Model 2) showing probability of prevalence ≥ 0.7 (b).

6.3.7 Predicting future risk of disease using climate models

Model 1 (GLM) and Model 2 (LRM) were used to make predictions of disease risk using the climate data obtained from IPCC. The climate change model predicted a global temperature increase of 1.6°C by 2050 and 2.9°C by 2100 (Carter 2007). Model 1 predicted an average prevalence of 0.88 over the continent compared with the observed current data average of 0.12 (Fig. 6.9a). No regions were predicted to have prevalence <0.5, indicating that no area would be completely free from the disease. Model 2 shows the predicted probability of prevalence >0.7 (Fig. 6.9b). This map shows that the probability of a high prevalence is between 0.4-0.5 for most areas. Both maps show a high prevalence of disease in areas currently unaffected by schistosomiasis, e.g. the Sahara, Niger and Chad. The relative change in disease distribution predicted by Models 1 and 2 is shown in Fig. 6.10. Model 1 predicts increases in prevalence between 0.05 and 0.25 throughout Africa, with the highest increases seen in Namibia and Angola (Fig.

6.10a). Model 2 predicts that the probability of high prevalence will decrease in the Sahara (Niger, Mali, Algeria, etc.). The region surrounding Lake Malawi shows the highest increase in probability (Fig. 6.10b).

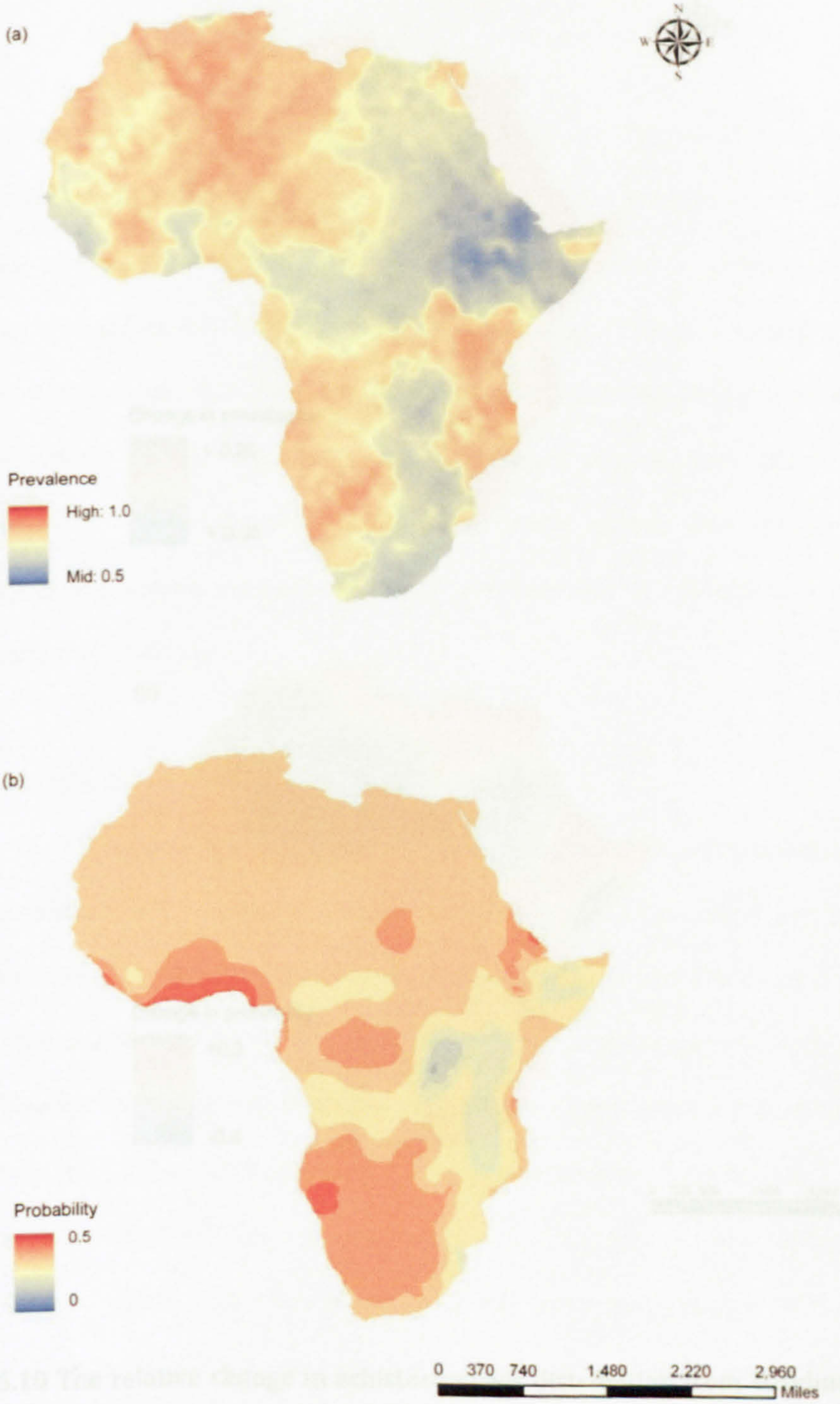

Fig. 6.9 The predicted distribution of schistosomiasis by 2040-2069 given the SRA1B climate change scenario using Model 1 which predicts future prevalence (a) and Model 2 which predicts the probability of prevalence >0.7 (b).

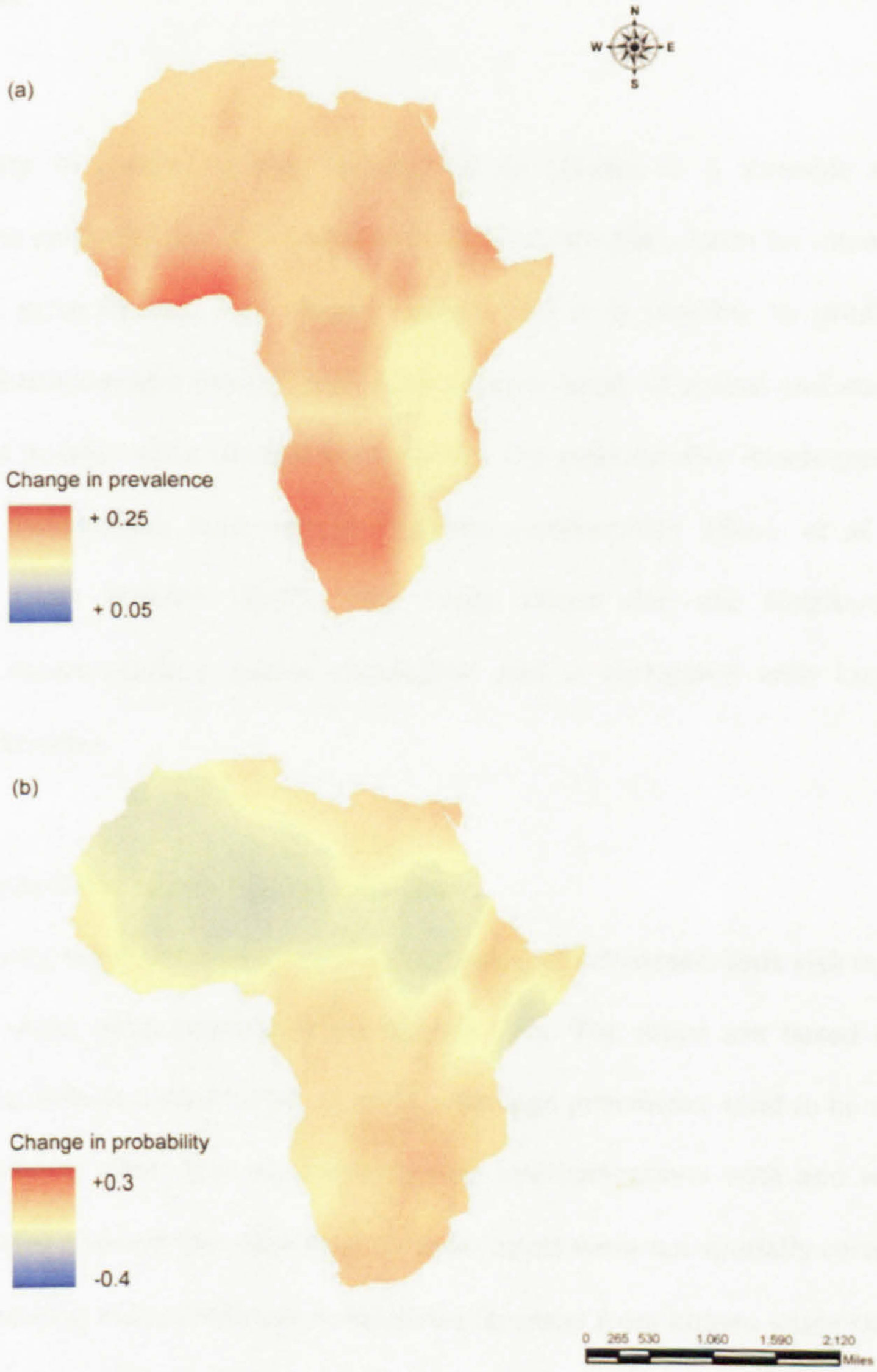

Figure 6.10 The relative change in schistosomiasis distribution from baseline (Fig. 6.8) to future estimates with temperature change (Fig. 6.9). This shows the change in prevalence predicted by Model 1 (a) and the change in probability of prevalence >0.7 predicted by Model 2 (b).

6.4 Discussion

The ability to predict spatial distribution of disease is a valuable tool in understanding the epidemiology of transmission and can provide a basis for introducing targeted control programmes. This chapter shows that it is possible to predict the prevalence of schistosomiasis over a large-scale using a range of spatial and statistical models. Previous smaller-scale models have shown the considerable heterogeneity in schistosomiasis distribution, even within endemic communities (Raso *et al.* 2005; Clennon *et al.* 2006; Brooker 2007). This study shows that the distribution of schistosomiasis shows marked spatial correlation and is correlated with long-term environmental variables.

6.4.1 Spatial interpolation of point-prevalence data

In this study, maps showing the spatial variation of schistosomiasis risk in Africa were produced using point-referenced prevalence data. The maps are based on the spatial correlation between study sites, i.e. sites with high prevalence tend to be near to other high prevalence sites. This was tested using semivariograms with and without directionality, which showed that sites over 10 miles apart were not spatially correlated. Therefore, it is unlikely that prevalence in locations far away from known study sites can be accurately estimated. This suggests that prevalence is driven by highly localised (< 10 mile) factors, which may explain the relatively poor performance of the large-scale spatial models. Spatial clustering in human disease data is inevitable, as human populations generally live in spatial clusters rather than a random distribution (Kleinschmidt *et al.* 2000).

Kriging is a useful method for predicting schistosomiasis risk in areas with a high density of study sites. However, given that the data used for obtaining the model are not homogeneously distributed, caution must be taken in extrapolating predicted risk outside the effective range. The ordinary and directional kriging maps show that the distribution of schistosomiasis is highly variable, with high prevalence in Kenya and Ethiopia (Fig. 6.5a,b). The directional kriging model showed a strong trend in the Southeast – Northwest direction, consistent with the data observed. However, this trend may have been due to the distribution of study sites, which has the potential to bias the model predictions. Both risk maps predicted high prevalence of disease in central and eastern parts of Africa with the highest prevalence values clustered around Lake Victoria and Lake Albert, two regions known to experience high levels of schistosomiasis (Dunne *et al.* 2006; Malenganisho *et al.* 2008). The ordinary kriging model provided the best estimates for prevalence based on the analyses.

The two probability kriging maps showed differences in their predictions of low risk areas, the indicator kriging model predicted that areas of the Eastern coast, Algeria and Niger have a very low probability of disease whereas the ordinary probability kriging map predicted that these had a probability of 0.5-0.6 (Fig. 6.5c,d). It is not possible to statistically compare the two probability models, as they use different techniques to predict the risk of infection. Generally, the indicator kriging agreed with the observed data more than the ordinary probability model, which over-estimated the risk of infection throughout Africa. Both of these maps over-estimate the probability of disease in Africa, showing high risk of infection in regions known to be unaffected by schistosomiasis, e.g. South Africa and the Sahara. The current absence of disease in South Africa is likely to be due to the high socio-economic status and availability of high-quality healthcare. They also show a high risk of infection in countries with little or no schistosomiasis prevalence data, such as Libya and Algeria. These countries may be at

risk of disease as neighbouring countries Egypt, Mali and Chad have previously documented the presence of infection (Doumenge 1987).

One problem with this method is that some of the predicted values are outside the effective range for the spatial model to provide accurate predictions. There are insufficient data points with which to estimate some locations, particularly in the northern parts of Africa. The frequency of surveys tends to be higher in areas which experience high levels of infection, and so a paucity of data may indicate absence or low levels of infection. Therefore, the maps are likely to be most accurate where it matters most, e.g. in areas of high schistosomiasis prevalence. These maps are useful for focussing schistosomiasis control efforts. They highlight areas that are most likely to experience high disease burden and identify gaps where our knowledge is limited.

6.4.2 Predicting risk of disease using climate models

These models are based on statistical methods that incorporate the impact of climatic variables on the prevalence of disease. Some say this may be a better approach than using GIS and spatial statistical methods although both methods are subject to limitations (Diggle *et al.* 1998; Kleinschmidt *et al.* 2000; Diggle *et al.* 2002; Boyd *et al.* 2005; Kazembe *et al.* 2006). Predicting prevalence based on climatic variables reflects the ecology of the intermediate and definitive host population. The advantages of using either spatially interpolated or remotely-sensed climate values has been discussed previously (Hay and Lennon 1999). Following their analysis, the land surface temperatures used in the climate models were derived using spatial interpolation of data recorded at meteorological stations. Precipitation levels were derived using RS, which provides a more accurate measure of this spatially stochastic variable.

An important finding in this study is that large-scale environmental factors influence large-scale infection patterns. This is similar to other studies documenting

spatial distribution of helminth infections in general (Brooker *et al.* 2004) and schistosomiasis in particular (Malone *et al.* 2001b). Temperature plays an important role in establishing the boundaries of disease distribution. The biological explanation for this is provided in Chapters 2 and 3, which show the thermal limits to schistosome and snail populations. In addition to temperature, rainfall and elevation influence the transmission of disease. There is a correlation between elevation and mean land surface temperature, although the correlation coefficient was not high enough to justify removing it from the model. Areas with low monthly rainfall (<50mm) are not able to support snail habitats. In these areas, alternate habitats may be created by irrigation dams or water projects. Human population density was not correlated with prevalence of schistosomiasis. This is likely to be due to the presence of disease in both highly and sparsely populated communities.

Predicting schistosomiasis prevalence using only generalised linear regression tends to produce predicted values that are pulled towards the mean (Kleinschmidt *et al.* 2000). For example, different levels of prevalence may be seen in two distinct locations in Africa with similar climatic conditions. Generalised regression modelling would predict similar values for these two locations based on the climate data alone, which would produce large residuals. Including a spatial factor in the model may adjust these values to better reflect the actual prevalence observed. Spatial correlation between the data points may arise due to unknown factors, and so incorporating a spatial random effect in the model would account for these and may provide a better model fit.

Using the Koeppen classification system as an alternative measure of climate did not produce a statistically significant model. There was a significant difference between the prevalence recorded in the tropical climates (Class A) and the temperate climate (Class C), possible due to the cooler winter temperatures in these climates. This alternative climate model may become more effective in predicting disease risk as more

disease data are collected. Indeed the distribution of data in this case may have biased the model. The majority of study sites were recorded in Class A (928) compared with Class B (296) and Class C (412). Taking an equal, random sample from each class may improve the model fit and would be an interesting next step. If a larger dataset were available, the more detailed Koeppen classification system could be used, which divides the data into more categories. This finer resolution may detect differences in schistosomiasis prevalence not identified by the coarse-scale system.

6.4.3 Using climate data to predict future risk of disease

Predicting the future risk of disease is difficult, as the transmission of disease is dependent on numerous factors other than climate. However, it is interesting to see how long-term climatic changes may change the distribution of disease in the absence of any intervention programmes. Using a climate change scenario which incorporates high rates of CO_2 increase gives a "worst-case scenario" of future climate conditions. Model 1 predicted a prevalence of 0.5-1.0 for the whole continent, with no areas left unaffected. Model 2 predicted that the probability of a high prevalence of disease (>0.7) would be approximately 0.4 for most of Africa. The only area with a low probability was found around Lake Victoria, which currently experiences high prevalence. As these maps are based on climate models, they provide good indicators for which areas may experience a change in temperature suitability over the next 50 years. As cool areas become warmer, and dry areas become wetter, there may be an increase in the number of areas able to support the intermediate host snail. An expansion in intermediate host distribution is likely to be followed by an expansion in parasite distribution (Kristensen *et al.* 2001).

6.4.4 Conclusions and further study

This study shows the importance of integrating spatial correlation with climate factors in the prediction of schistosomiasis risk. Generally, the climate models showed that temperature, rainfall and elevation have an important role in defining schistosomiasis risk in Africa. The results presented here have some limitations. Firstly, the data points used for the analysis were irregularly distributed over Africa and tended to be clustered in more politically stable countries. Some countries such as Algeria and Libya, had no data available. It is not known whether this is due to an absence of the disease, as studies are often biased towards positive findings. This has the potential to bias the data. Using a climate model may have reduced this bias as disease prevalence is correlated with environmental predictors. Without any empirical data at these sites, it is not possible to validate the predictions for these areas. Secondly, the data used here have been compiled over 30 years and the prevalence of disease may not have been constant over this time. For example, shifts in populations, changes in socio-economic development and advances in irrigation may all have changed the distribution of disease. These effects are more likely to be important in previously unaffected areas in which the disease is introduced, or areas with low prevalence, in which the disease may be able to die out with effective interventions. The new atlas of human helminth infection currently being developed will provide a useful tool in defining the risk of disease in Africa (Brooker *et al.* 2000). This database will provide an up-to-date resource collating all known sources of disease data throughout Africa, along with the study methods and study population.

Schistosomiasis transmission is complex and is determined by more than large-scale topographical and climatic factors. Socio-demographic factors, economic development and micro-variations in climate will all affect transmission. Adding these

data to a model is very complicated, but it would be worthwhile exploring how the addition of independent covariates improves the model fit.

Another useful approach to modelling distribution of disease is universal kriging. This is an extension of ordinary kriging and incorporates regression modelling along with spatial modelling (Diggle *et al.* 1998). This method would be appropriate for any infectious disease known to be associated with climate variables as it incorporates the climate covariables with the position of the location and its relation to other study sites. Essentially, this technique combines the two separate modelling approaches described earlier into one comprehensive model. This approach would avoid breaching the assumptions of the ordinary kriging model, which assumes the data have a constant mean. In universal kriging, the mean is a function of the covariates, rather than a constant. Currently, universal kriging applied to a generalised linear model is not available, but will provide an invaluable tool in the future (Kleinschmidt *et al.* 2000).

Despite the limitations, the maps of predicted current and future risk of schistosomiasis in Africa provide an indispensable portrayal of geographical variation of disease risk. This is the only study which examines the predictions of both spatial and climate models on the risk of schistosomiasis over the whole continent and, as such, provides a baseline model which can be continually updated. This work can be extended to include precipitation and snail distribution as a limiting factor.

CHAPTER 7

Conclusions

7.1 Conclusions

The main aim of this thesis was to develop models to describe schistosomiasis transmission and the impact of climate change on the distribution and intensity of disease. New mechanistic models have been developed in this thesis to incorporate snail population dynamics and density-dependence in the parasite and snail populations into the models. Parameter estimates for these models were obtained for a number of key parameters in the model using a single host-parasite combination, *Biomphalaria alexandrina* – *Schistosoma mansoni*. Geospatial models were then developed to predict risk of disease in areas where no data are available and risk of disease in the future, given current concerns for global warming. These methods have been applied to address several important epidemiological questions, such as 1) will schistosomiasis transmission dynamics change with changing temperature?; 2) what is the most effective intervention strategy and how is this affected by temperature?; 3) can the risk of disease be estimated for unknown locations using data from known study sites?; and 4) how will the distribution of schistosomiasis in Africa change with climate change? A detailed discussion of the findings was provided in each chapter. Here I present a summary of the key findings along with their epidemiological significance. Recommendations for future research are also discussed.

7.2 Development of schistosomiasis models

In this thesis, three principal modelling techniques were used. A series of increasingly complex mechanistic models were developed to describe the biological processes of schistosomiasis transmission. Generalised linear models (GLM) and ordered regression models (LRM) were used to relate climate data to schistosomiasis

prevalence data over the African continent. Finally, geospatial (kriging) models were developed to study the spatial correlation between study sites and predict the risk at other locations.

The sensitivity analysis performed in Chapter 2 highlighted the importance of snail population dynamics in the transmission of schistosomiasis. This provided the impetus for accurate estimation of these parameters in a controlled set of experiments, using one host-parasite combination. Clearly, controlled laboratory experiments cannot mimic the conditions in the field, but these results provided a baseline set of parameter values. Seasonal dynamics and diurnal temperature fluctuations may affect the life-history traits measured in these experiments, but the temporal scale of the models was years, rather than weeks or days. The paucity of data concerning the effects of density-dependence in the snail population prompted the studies detailed in Chapter 3. Inclusion of the density-dependent relationships described in Chapter 3 emphasised the importance of transmission from snail to man. This has important epidemiological significance; an intervention strategy that targets the most sensitive parameters will have the most successful outcome. This model showed that stopping cercarial infection, by reducing contact with contaminated water, would have the greatest impact on reducing morbidity (Chapter 5). If the disease can be controlled by improving access to safe water and changing behavioural patterns, this would eliminate the need for mass treatment campaigns and molluscicide programmes. The high sanitation levels in South Africa may explain the absence of disease from an area which has a suitable climate for transmission (Chapter 6). Similarly, low prevalence rates in Botswana may reflect the high socio-economic standards of this country compared with its neighbours (Doumenge 1987).

Many existing models make unrealistic assumptions which alter the behaviour of the model. Firstly, the common assumption of identical mortality and fecundity rates for

uninfected, latently and patently infected snails. This assumption will lead to false estimates of snail population dynamics, which were among the most sensitive parameters in the models presented here. Inclusion of additional mortality due to infection has been done by Zhao and Milner (2008), however the model was not parameterised using empirical data. Previous models, which lack this feature, are likely to overestimate the abundance of snail hosts and therefore, the prevalence and intensity of disease. Including snail population dynamics in a transmission model can change the behaviour of the model from an endemic equilibrium state to a cyclical periodic state (Feng *et al.* 2002). Secondly, the absence of density-dependence in the snail population and the adult parasite population cannot be justified. Parasitic regulation of snail host mortality and fecundity is well documented and the addition of this feature in the model significantly changes the dynamics of the system (Chernin and Michelson 1957; Baudoin 1975; Anderson 1978; Feng *et al.* 2002).

Further parameters that could be incorporated into a transmission model include heterogeneous water contact patterns, acquired immunity and seasonality. Modelling water contact patterns is complex; it relies on an understanding of the availability and accessibility of water sources for each household, along with the variability in water use in space and time (Watts *et al.* 1998). Heterogeneity in water contact patterns do not significantly alter the behaviour of a model (Yang 2003) and so were not considered in this thesis. However, when acquired immunity was added, this partly explained the robust transmission of schistosomiasis, showing that a very low worm burden per person is sufficient to maintain the disease in a community (Yang 2003). Seasonal dynamics of environmental risk factors will certainly affect short-term schistosomiasis transmission and this approach has previously been studied for malaria transmission (Mabaso *et al.* 2007). Further study on seasonality in schistosomiasis is

required and would prove useful in non-endemic areas which experience seasonal peaks in transmission.

The effects of temperature on schistosome transmission dynamics have been explored in Chapters 2, 3, and 5. Clearly, ambient temperature will be an important regulatory factor in transmission, a point reinforced by the climate models presented in Chapter 6 and previous studies (Pfluger 1980; Malone *et al.* 2001b; Brooker 2002; Stensgaard *et al.* 2005). Other potential ecological risk factors were monthly rainfall and elevation. One interesting question arises: why is schistosomiasis transmission currently limited to defined foci, when the suitable climate range extends the full length of Africa? This study shows that the predominant ecological factors go some way to defining the distribution of disease, but there exists an unexplained amount of variability, which cannot be attributed to climate (Ostfeld 2009). This will be dependent on socio-economic factors, human behaviour, treatment programmes, etc., which are beyond the scope of this modelling approach. "Environmental niche"-based models fail to take into account other potential drivers of species abundance / distribution. Localised variation in socio-economic status and other risk factors need to be considered when predicting schistosomiasis distribution. These factors may explain some of the limitations in my predictive models.

To accurately predict future disease distribution, it is necessary to consider each of these factors in turn and its relative importance in transmission. The maps showing how the distribution of disease may change with climate change in Chapter 6, consider the worst-case scenario, i.e. what would happen in the absence of control interventions. Clearly, schistosomiasis has the potential to spread throughout Africa and increase in intensity in current endemic areas.

A review paper summarising the current uses of GIS in schistosomiasis epidemiology found that in East Africa, schistosomiasis transmission rarely occurs

where annual maximum land surface temperatures exceed 33°C (Malone *et al.* 2001b). In Cameroon, West Africa, the upper threshold value for transmission was >45°C. This discrepancy could be attributed to the different snail species, *Bulinus senegalensis*, present in West Africa (Greer *et al.* 1990). In addition, the arid conditions of West Africa concentrates communities around the few water bodies available, increasing the risk of transmission (Brooker 2002). There is a need for a multi-faceted modelling approach which characterises the changing ecology of snail hosts in different regions of Africa. For vector-borne diseases such as schistosomiasis with relatively weak spatial patterns, models that include a spatial component will improve predictions by capturing geographical shifts in the principal ecological risk factors.

The fundamental objective of these models was to provide information on the risk of infection so effective prevention and control programmes could be designed. Although large-scale models cannot identify foci of high transmission, they are useful in identifying at-risk populations, and, conversely, populations that are unlikely to be infected. Smaller-scale national or sub-national studies can identify risk factors in local populations, such as irrigation schemes and distance to nearest water body (Brooker *et al.* 2001; Leonardo *et al.* 2005). These models can also estimate the burden of infection within a community and therefore provide policy-makers with essential information to guide their decision on targeted intervention strategies. Simulations of control measures (in Chapter 5) predicted that the optimal control strategy would be to reduce human contact with infective cercariae, either through health education or through improvements in sanitation. The highest rates of infection are usually found in children aged 5-15 (WHO 2002). Using risk models combined with population data enables us to quantify the target population and direct resources towards the highest risk group. Using this approach also allows direct estimation of the costs involved in each intervention strategy.

7.3 Summary of findings

- Three specific population processes were shown to be particularly important in determining the dynamical behaviour of the schistosomiasis transmission model; the differing mortality and fecundity rates of infected snails, the non-linear density-dependent constraints on snail populations, and the density-dependent fecundity of adult parasites.

- Temperature significantly alters the dynamics of the transmission model and the efficacy of control programmes through variations in both host and parasite life-history traits.

- The distribution of schistosomiasis is directly influenced by climatic factors. Temperature, rainfall and elevation provide defined thresholds for transmission, outside which, schistosomiasis is unlikely to occur.

7.4 Future work

Studies using GIS and remote sensing of schistosomiasis in Africa are remarkably lagging behind those of malaria studies (Craig *et al.* 1999; Kleinschmidt *et al.* 2000; Diggle *et al.* 2002; Rogers *et al.* 2002; Tanser *et al.* 2003; Kazembe *et al.* 2006; Mabaso *et al.* 2007; Abellana *et al.* 2008). Although progress has been made in developing predictive risk models, there remain some important issues which need to be investigated. Firstly, the paucity of data in many regions of Africa hinders progress in developing accurate models over a large-scale. Current attempts to combine all recorded sources of infection data to date will provide an invaluable tool for future research (Brooker *et al.* 2000). Gaps in our knowledge often result from political instability within

an endemic region and without these data, future risk of disease must be interpolated from neighbouring countries. Secondly, the use of the basic reproductive ratio, R_0, as a measure of the potential of a disease to spread would be a logical next step (Dobson 2009). This mechanistic approach can incorporate explicit relationships between environmental variables (predominantly temperature) and key host-parasite life-history parameters. This has previously been used for malaria (Rogers *et al.* 2002) and a similar approach would provide further insight into the important parameters involved in schistosomiasis transmission. Thirdly, further study needs to be done on the socio-economic and behavioural traits which determine transmission. Inclusion of these factors in a transmission model will improve the accuracy of predictions. These factors may be parameterised for each ecological zone, or for each endemic community, to provide distinct models based on the ecology of each particular area. A final point to note is that few studies explicitly quantify the impact of health education and sanitation on schistosomiasis prevalence and intensity. This was the most effective intervention strategy in the models, and as this would prove a more cost-effective strategy than mass chemotherapy and molluscicide, the efficacy of this type of intervention programme should be thoroughly tested in the field.

Appendix A1

Estimating the parameters for the schistosomiasis transmission model

The model in Chapter 2 was parameterised using all available data from the literature, where laboratory experiments were conducted at a range of temperatures (described below). The parameter estimates were then extrapolated at the range of temperatures shown to obtain estimates of parameter values at the baseline temperatures of 20, 25, 30 and 35°C. Clearly, these studies were conducted under a range of conditions, sometimes using different snail or parasite species. It would therefore be invaluable to conduct comprehensive experiments using specific host-parasite species combinations at the full range of temperatures to obtain more accurate parameter estimates. However, the present data is used as a baseline with which to parameterise the model, fully acknowledging their limitations.

A1.1 Estimating mortality rates

1) Snail mortality rates (δ_I and δ_S)

El-Hassan (1974) presented mortality rates for juvenile and adult snails at a range of temperatures over a two-week period. These can be converted into mortality rates per day using the following equation:

$$\delta = -\frac{\ln(N_t/N_0)}{t} \qquad \text{A1.1}$$

where N_t is the number alive at time t. This resulted in the following estimates:

Table A1.1 Adult and juvenile snail mortality rates over 10-35°C.

Temperature (°C)	Juvenile mortality rate day^{-1} (δ_j)	Adult mortality rate day^{-1} (δ_s)
10	0.0080	0.0038
15	0.0046	0.0062
20	0.0022	0.0038
25	0.0038	0.0030
30	0.0071	0.0080
35	0.0207 day^{-1}	0.0182 day^{-1}

2) Additional snail mortality due to infection (α)

Foster (Foster 1964) also produced similar data to that of El-Hassan (El Hassan 1974), showing percentage mortality after 60 days for both infected and uninfected snails. Using equation A1.1, δ_s and the additional mortality due to infection (α) were calculated, producing the following data:

Table A1.2 Additional mortality of snails due to parasitic infection.

Temperature (°C)	Uninfected mortality day^{-1} (δ_S)	Infected mortality day^{-1} (δ_I)	Additional mortality day^{-1} ($\alpha = \delta_I - \delta_S$)
22.85	0.0031	0.0067	0.0036
24.01	0.0033	0.0116	0.0082
26.26	0.0039	0.0260	0.0221
28.07	0.0085	0.0368	0.0283

3) Miracidial mortality rate (δ_M)

Anderson *et al* (1982) presented data on the mean miracidial life expectancy (in hours) over a range of temperatures. These were converted to daily mortality rates (1/life expectancy) to give the following values:

Table A1.3 Miracidial mortality rates over 10-40°C.

Temperature (°C)	Miracidial mortality rate day^{-1} (δ_M)
5	4.90
10	2.18
15	1.50
20	2.00
25	2.53
30	4.36
35	4.44
40	4.80

4) Adult parasite mortality rate (δ_P)

Stirewalt (1954) presented data on the proportion of mice containing a varying initial number of worms seven weeks post-infection, which can be used to calculate the mean number of worms per mouse at the end of the seven weeks. In addition, Stirewalt also presented the average number of cercariae that penetrated each mouse at time $t=$ 0. Using equation A1, with $t=$ 49 days, N_0 the initial number of cercariae infecting and N_t the mean number of worms per mouse at the end of the seven weeks gives the following estimates of adult parasite mortality (δ_P):

Table A1.4 Adult schistosome mortality rates.

Temperature (°C)	Adult schistosome mortality rate day^{-1} (δ_P)
23-25	0.022
26-28	0.015

A1.2 Estimating developmental rates

1) Schistosome maturation rate (patency, σ)

Foster (1964) presented data on the time of development to cercarial shedding for *Schistosoma mansoni* in *Biomphalaria pfeifferi*. Based on the minimum and maximum periods to shedding presented, the mean maturation rates are:

Table A1.5 The maturation rates of *Schistosoma mansoni* in *Biomphalaria pfeifferi.*

Temperature (°C)	Average days to shedding	Maturation rate day^{-1} (σ)
18	57	0.018
21	37	0.027
23	34	0.029
24	32	0.031
26	24.5	0.041
28	21.5	0.047
30	20	0.050
32	17.5	0.057

2) Snail maturation rate (θ_S)

El-Hassan (El Hassan 1974) determined the minimum and maximum incubation periods of *Biomphalaria alexandrina* eggs between 15°C and 30°C. Based on the average number of days to hatching the mean hatching rate for each temperature is:

Table A1.6 Maturation rates of *Biomphalaria alexandrina.*

Temperature (°C)	Incubation period (days)	Hatching rate day^{-1} (θ_E)
15	23.5	0.042
20	12.5	0.080
25	10	0.100
30	8.5	0.118

A1.3 Estimating birth (production) rates

1) Snail egg-laying rates (a)

El-Hassan (1974) measured the number of eggs laid per snail per day for *B. alexandrina* over 60 days, resulting in daily *per capita* egg production rates of:

Table A1.7 The egg-laying rates of *Biomphalaria alexandrina* per day.

Temperature (°C)	Eggs per snail day^{-1} (a_S)
10	0
12.5	0.06
15	0.16
20	0.66
25	0.85
28	0.23
30	0.57
35	0

Infected snails were assumed to be castrated following miracidial infection, i.e. $a' \approx 0$ (Crews and Yoshino 1989).

2) Cercarial production (λ_C)

Fried *et al* (2002) presented data on the number of cercariae released during one hour under various conditions. Based on their standard (incandescent light) conditions, at different temperatures, the daily cercarial production rates (per infected snail) are:

Table A1.8 The number of *S. mansoni* cercariae produced per day at 12-35°C.

Temperature (°C)	Number of cercariae (λ_C)
12	504 day^{-1}
25	4128 day^{-1}
35	8400 day^{-1}

A1.4 Estimating infection rates

1) Miracidial infection of snails (λ_S)

Stirewalt (Stirewalt 1954) presented data on the percentage of snails becoming infected following exposure to 1 miracidium in 1 ml water for 24 hours. The dynamics of this experiment can be described by the equations:

$$\frac{dU}{dt} = -MU\beta_S \qquad \text{A1.2}$$

$$\frac{dI}{dt} = MU\beta_S \qquad \text{A1.3}$$

$$\frac{dM}{dt} = -MN\beta_S \qquad \text{A1.4}$$

where U are the number of uninfected snails, I the number of infected snails, N the total number of snails $(U+I)$ and M the number of miracidia. Solving these equations provides the following expression for the number of infected snails at time t:

$$I_t = 1 - e^{\frac{M_0\left[1-e^{-\beta_S Nt}\right]}{N}} \quad \text{A1.5}$$

which can be rearranged to provide an expression for β_S:

$$\beta_S = -\frac{ln\left[M_0 + N\ ln(1-I_t)\right]}{M_0 Nt} \quad \text{A1.6}$$

Given M_0 (the initial number of miracidia) = 1, t = 1 day and I_t is the final number of infected snails at the end of the experiment, this equation provides the following estimates of miracidial infections rates:

Table A1.9 The infection rates of miracidia from 23-33°C.

Temperature (°C)	Miracidial infection rate (β_S)
23-25	0.487 day^{-1} ml^{-1}
26-28	1.498 day^{-1} ml^{-1}
31-33	1.324 day^{-1} ml^{-1}

2) Cercarial infection of definitive host (β_H)

Stirewalt (Stirewalt 1954) presented data on the number of worms infecting mice following exposure to 50 cercariae for 1 hour. As before, this experiment can be described by the equation:

$$\frac{dC}{dt} = -\beta_H CM \quad \text{A1.7}$$

where C is the number of cercariae in the water and M the number of mice (which remained constant at 1). This equation can be solved to give the expression:

$$\beta_H = -\frac{\ln\left(C_t / C_0\right)}{t} \qquad \text{A1.8}$$

where C_t is the number of cercariae that did not infect and C_0 is the initial number of cercariae. Applying this equation to Stirewalt's data provides the following estimates of miracidial infections rates:

Table A1.10 The *S. mansoni* cercarial transmission rate over 23-28°C.

Temperature (°C)	Cercarial transmission rate (β_H)
23-25	52.97 day^{-1} ml^{-1}
26-28	71.90 day^{-1} ml^{-1}

Appendix A2

Determining the parameter estimates used in Chapter 5

Parameters that were not experimentally obtained in Chapters 3 and 4 were determined using data from the literature. Values for 18, 23, 29 and 34°C were extrapolated from the data and converted to a volume of 2L to correspond with the density experiment (Chapter 4) where necessary. Extrapolation was performed by fitting a number of relationships (linear, quadratic, logarithmic) to the reported data and selecting the relationship with the highest R^2 value. These studies from the literature were conducted under different conditions, sometimes using different snail species. It would, therefore, be beneficial to obtain these parameter values using one host-parasite combination at a range of temperatures to achieve more accurate parameter estimates. However, these data are used to parameterise the model where necessary, although their limitations are recognised.

A2.1 MORTALITY RATES

1) Adult schistosome death rate (δ_P)

The adult schistosome is not subjected to significant variations in temperature as it remains within the human body for the duration of its life-span. The average life-span of the adult parasite is 5 years (Feng *et al.* 2004), which was converted to a daily rate for the model (Eq. A2.1).

$$1/\text{ (life-span in years*365)} = 5.47\text{x}10^{-4}\ \text{day}^{-1} \qquad \text{A2.1}$$

2) Miracidia death rate (δ_M)

Data on the effects of temperature on miracidial survival were obtained from Anderson *et al* (1982). The daily mortality rates were derived from the mean life-expectancy (Table A2.1) and the values needed for the model were extrapolated from a quadratic equation fitted to the data (Fig. A2.1).

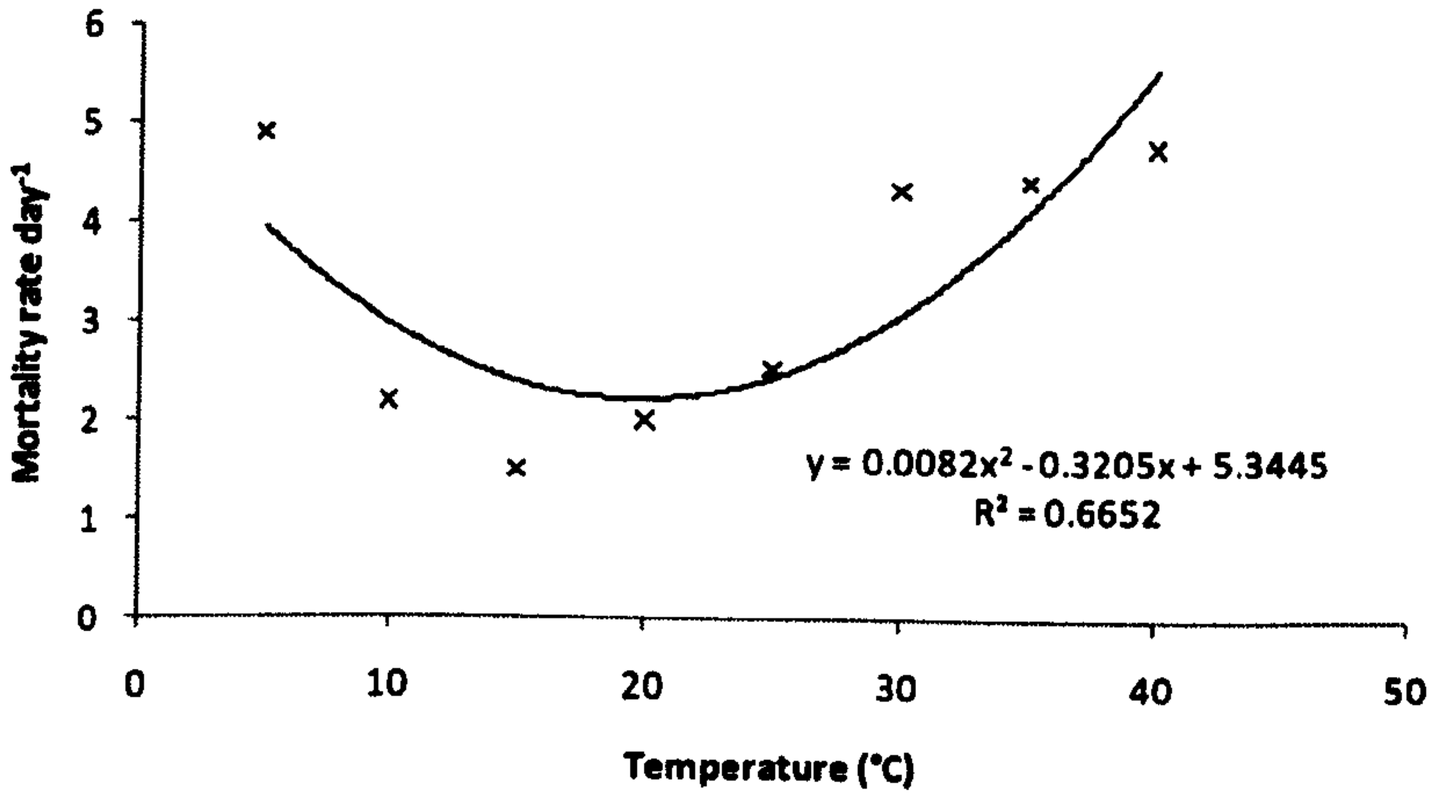

Figure A2.1 The relationship between temperature and miracidial mortality rate.

Table A2.1 Data on miracidial mortality.

The extrapolated values were obtained using the fitted quadratic relationship shown in Figure A2.1 (marked with an asterisk).

Temperature (°C)	Miracidial mortality rate
5	4.9
10	2.18
15	1.5
20	2
25	2.53
30	4.36
35	4.44
40	4.8
18	2.23*
23	2.31*
29	2.95*
34	3.93*

3) Juvenile snail mortality rate (δ_j)

El-Hassan presented mortality rates for juvenile snails at a range of temperatures over a two-week period (El Hassan 1974). These were converted into mortality rates per day using the following equation:

$$\delta_J = -\frac{\ln(N_t/N_0)}{t} \qquad \text{A2.2}$$

where N_t is the number alive at time t. The values at the four temperatures used in the model were then extrapolated from the data using the fitted quadratic relationship shown in Fig. A2.2.

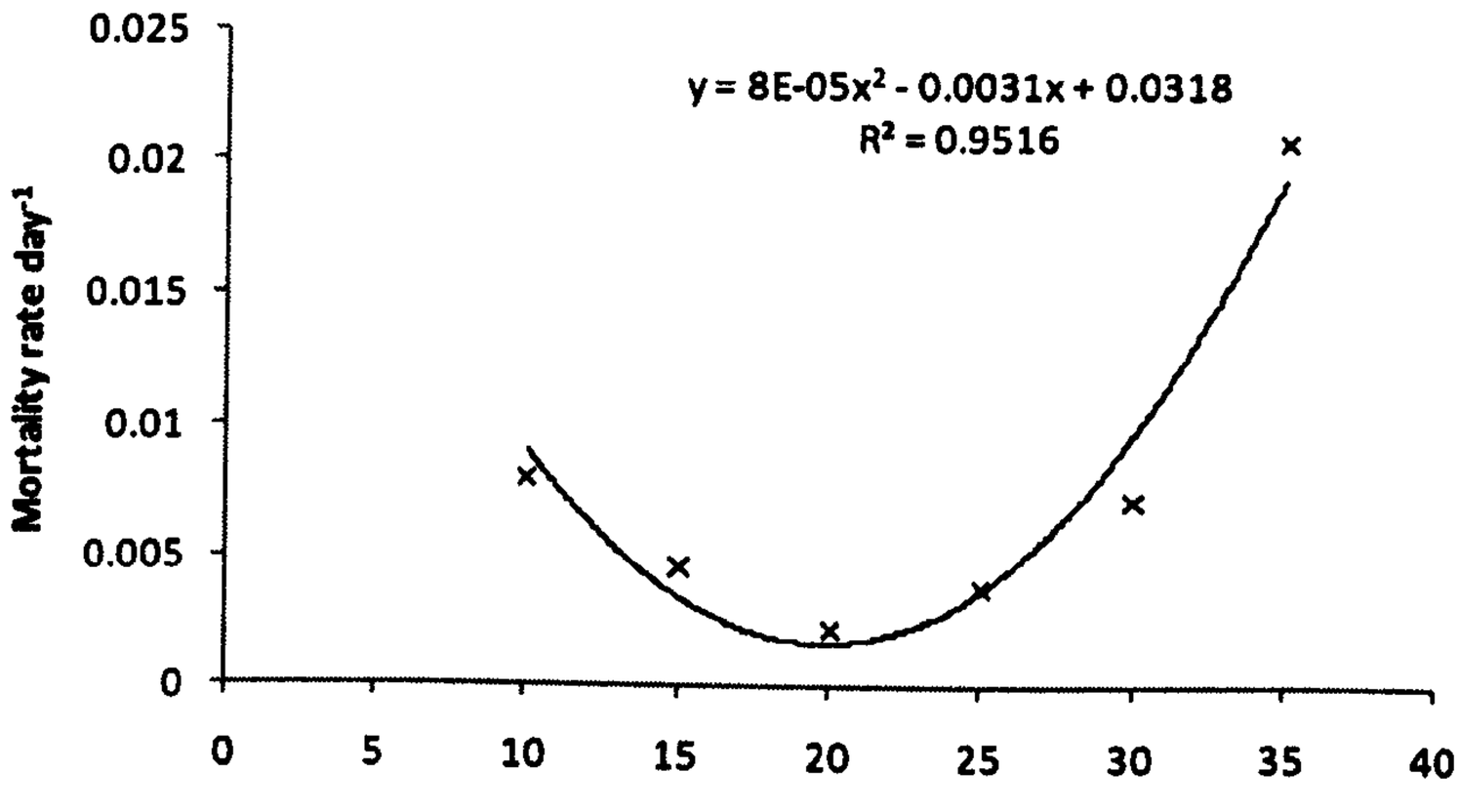

Figure A2.2 Relationship between temperature and juvenile snail mortality rate.

Table A2.2 Data on juvenile snail mortality rates.

The values were extrapolated (*) from Fig. A2.2.

Temperature (°C)	Mortality rate
10	0.008
15	0.0046
20	0.0022
25	0.0038

30	0.0071
35	0.0207
18	0.002*
23	0.003*
29	0.009*
34	0.019*

4) Snail mortality rates(δ_S, δ_L, δ_I)

These data were obtained in Chapter 3 and were calculated as the mean mortality rate per snail per day at each temperature. The values were averaged over the study period for the uninfected snails, and over the latent and patent periods for the latently and patently infected snails respectively. The parameter estimates are presented in Table A2.10.

5) Cercarial mortality rate (δ_C)

The mortality rates of cercariae at various temperatures were derived using data from Lawson and Wilson (1980) using Equation A2.2. The mortality rates obtained from the literature along with the extrapolated values for the model are presented below (Table A2.3)

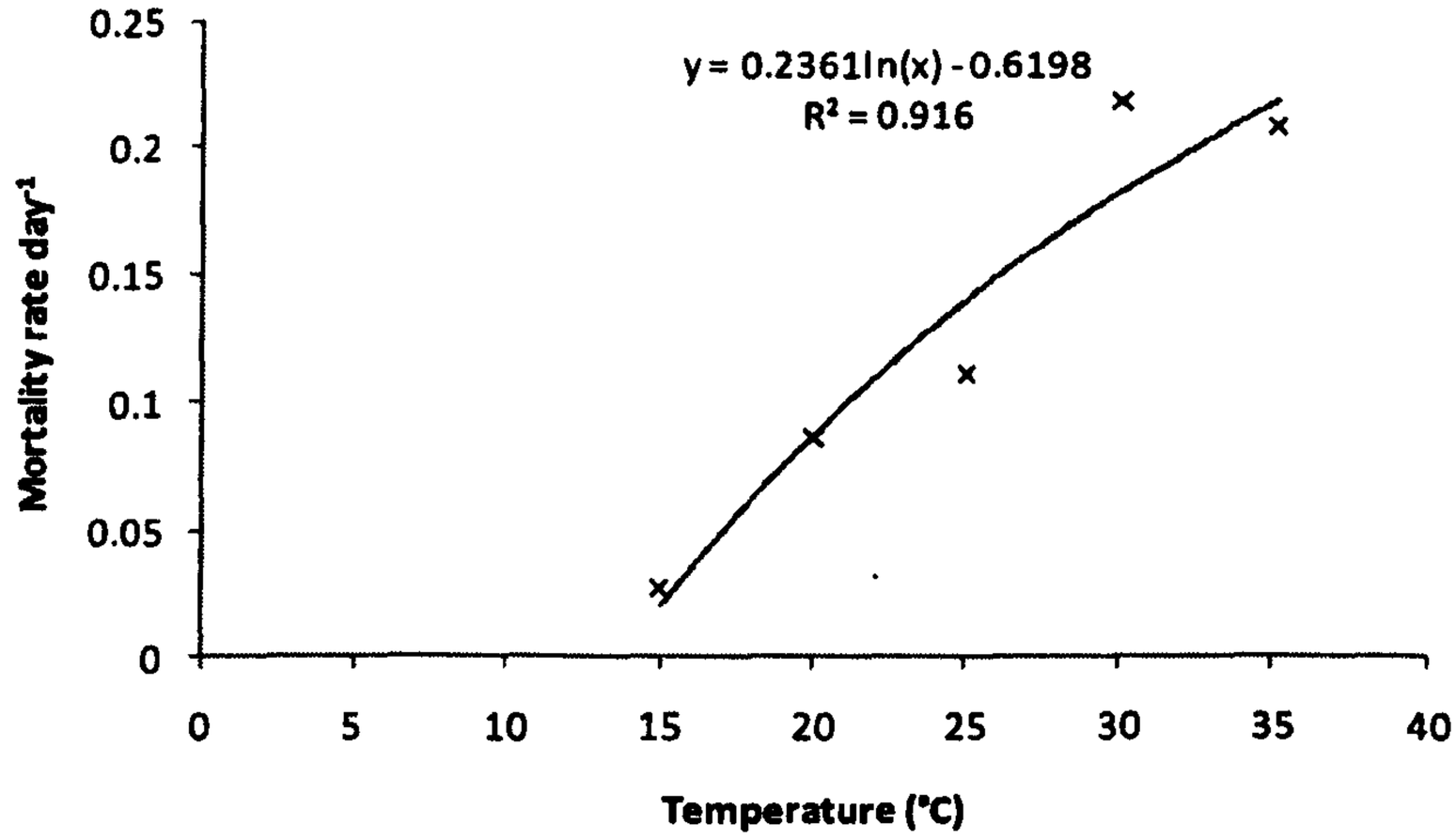

Figure A2.3 The relationship between temperature and cercarial survival.

Table A2.3 Mortality rates of cercariae and the extrapolated values (*).

Temperature (°C)	Mortality rate
15	0.026
20	0.086
25	0.11
30	0.22
35	0.21
40	0.77
18	0.063*
23	0.12*
29	0.18*
34	0.21*

A2.2 DEVELOPMENT RATES

1) Within-snail schistosome maturation rate (σ)

The time to patency for *Schistosoma mansoni* in *Biomphalaria pfeifferi* is presented by Foster (Foster 1964). The mean maturation rate was based on the minimum and maximum times to cercarial shedding (Table A2.4), and model parameters were calculated from the fitted linear relationship shown in Fig. A2.4.

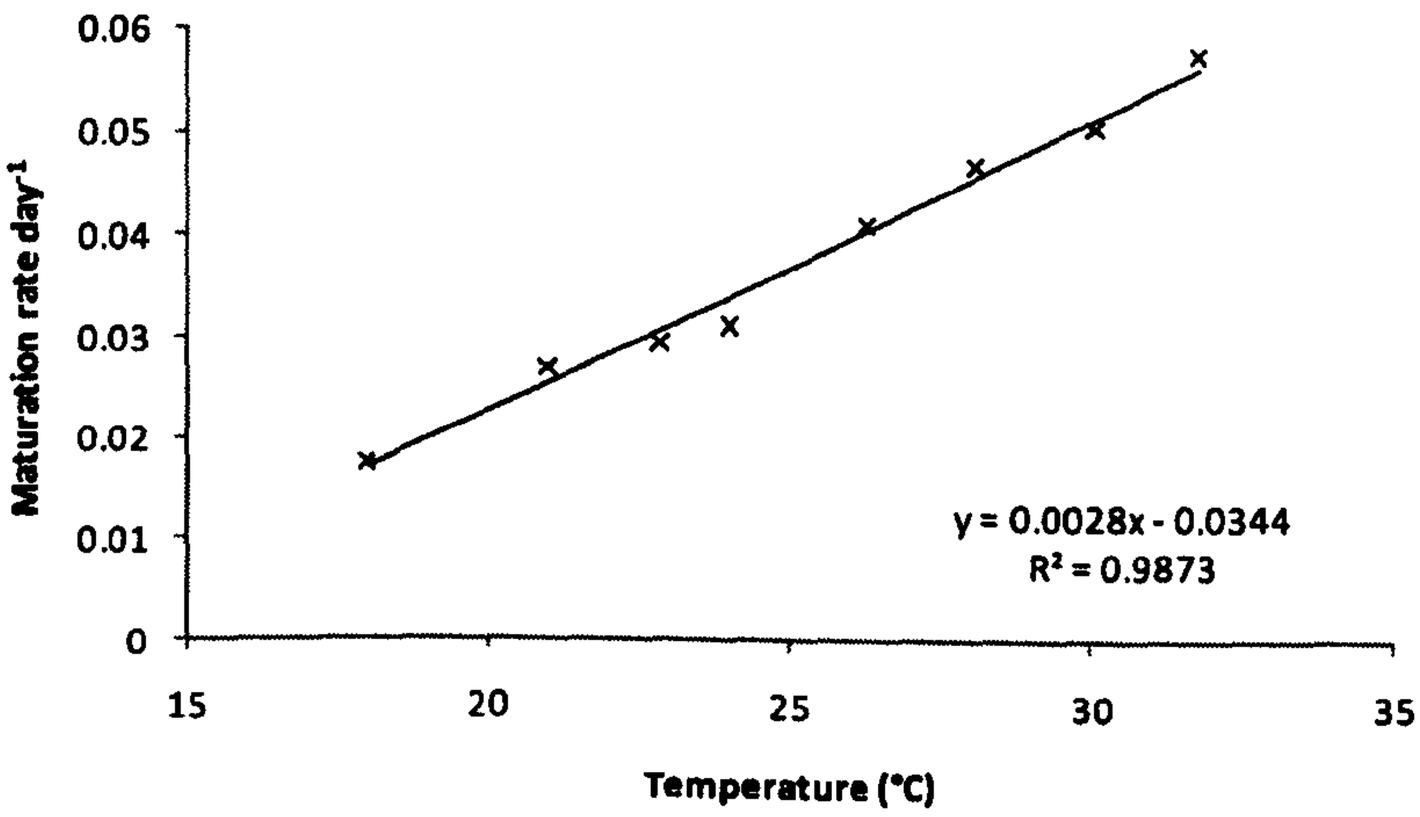

Figure A2.4 Relationship between temperature and maturation rate of *Schistosoma mansoni* within *Biomphalaria pfeifferi*.

Table A2.4 Maturation rate of schistosomes within a snail host.

The values were extrapolated for the model parameters (*).

Temperature (°C)	Average days to shedding	Maturation rate (per day)
18	57	0.017
21	37	0.027
22.85	34	0.029
24.01	32	0.031
26.26	24.5	0.041
28.07	21.5	0.047
30.04	20	0.05
31.75	17.5	0.057
18		0.016*
23		0.03*
29		0.047*
34		0.061*

2) Snail maturation rate (θ_S)

The minimum and maximum times to egg-laying were used to estimate the average maturation rate of *Biomphalaria alexandrina* (Table A2.5) (El Hassan 1974). The model parameters were calculated from the fitted quadratic relationship shown in Fig. A2.5.

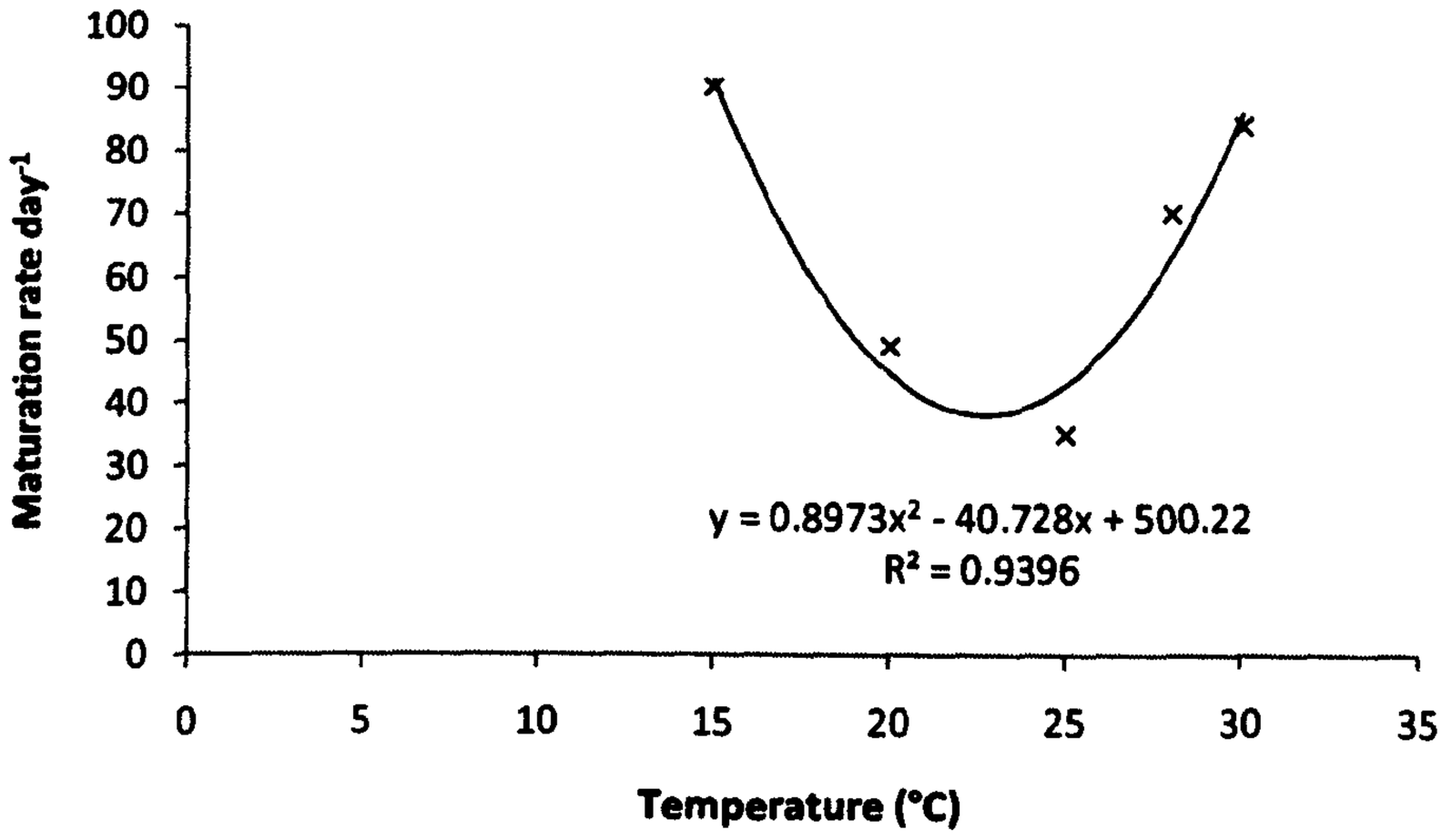

Figure A2.5 The relationship between temperature and maturation rate of snails, marked by the onset of egg-laying.

Table A2.5 The average time to the onset of egg-laying for *Biomphalaria alexandrina*. The extrapolated values for maturation rates (*).

Temperature (°C)	Average onset of egg-laying	Maturation rate day^{-1}
15	90	
20	49	
25	35	
28	70	
30	84	
18	58	0.017*
23	38	0.026*
29	74	0.014*
34	90	0.011*

A2.3 BIRTH (PRODUCTION) RATES

1) Miracidial production rate (λ_M)

Estimates for the average number of eggs produced per female adult schistosome per day range from 70 to 495 (Cheever and Anderson 1971; Cheever and Powers 1971; Powers and Cheever 1972; Damian *et al.* 1976). As a conservative estimate, a value of 250 miracidia per day per female was chosen, which takes into consideration the rate of destruction of eggs within the human host. This parameter is assumed to be independent of temperature, since schistosome reproduction will be buffered from variations in temperature within the human body.

2) Snail egg-laying rates(a_S, a_L, a_I)

The egg-laying rates for the uninfected, latently infected and patently infected snails were derived from the values obtained in Chapter 3. The mean numbers of eggs produced per snail per day were calculated for each temperature and are presented in table A2.10.

3) Snail hatching rate (θ_E)

The hatching rates for *Biomphalaria alexandrina* eggs were measured by El-Hassan (1974) over 10-37°C. These values were used to determine the values at the four temperatures used in the model by extrapolation from a fitted logarithmic function (Fig. A2.6).

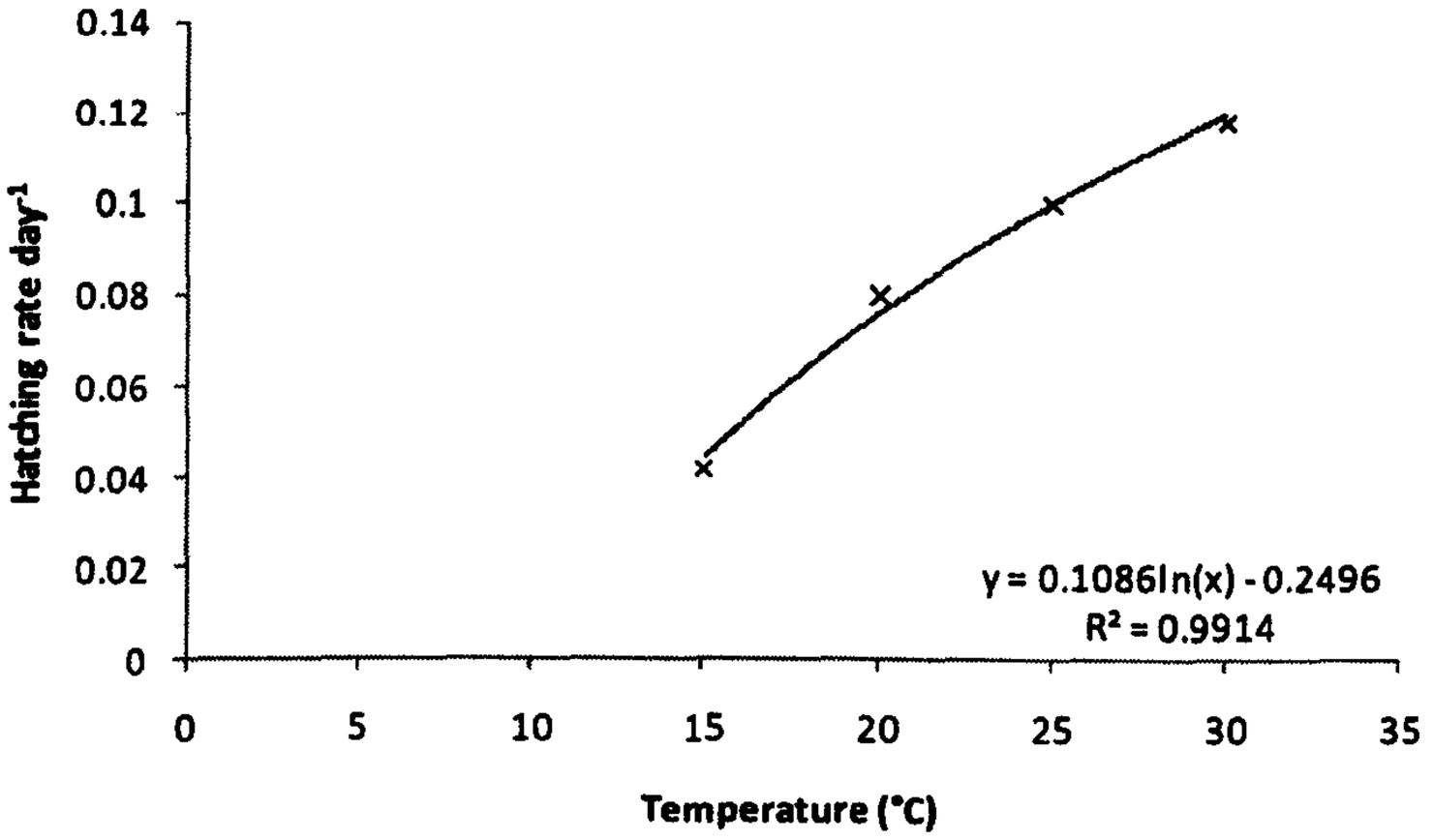

Figure A2.6 Relationship between temperature and average hatching rate of *Biomphalaria alexandrina* eggs.

Table A2.6 Average hatching rate for *Biomphalaria alexandrina* eggs.

The model parameter values derived from these data (*).

Temperature (°C)	Incubation period (days)	Hatching rate day^{-1}
15	23.5	0.042
20	12.5	0.08
25	10	0.1
30	8.5	0.118
18		0.064*
23		0.091*
29		0.116*
34		0.133*

4) Probability of hatching (v)

The probability of *Biomphalaria alexandrina* eggs hatching was added to the model in Chapter 5 as a measure of snail egg death. The data were taken from El-Hassan (1974) and plotted as a piecewise, 3 segment linear regression using SigmaPlot v.11.1 (Fig. A2.7). This method allowed the probability of hatching (y-values) to be constrained to between 0 and 1 and gave the most accurate representation of the data.

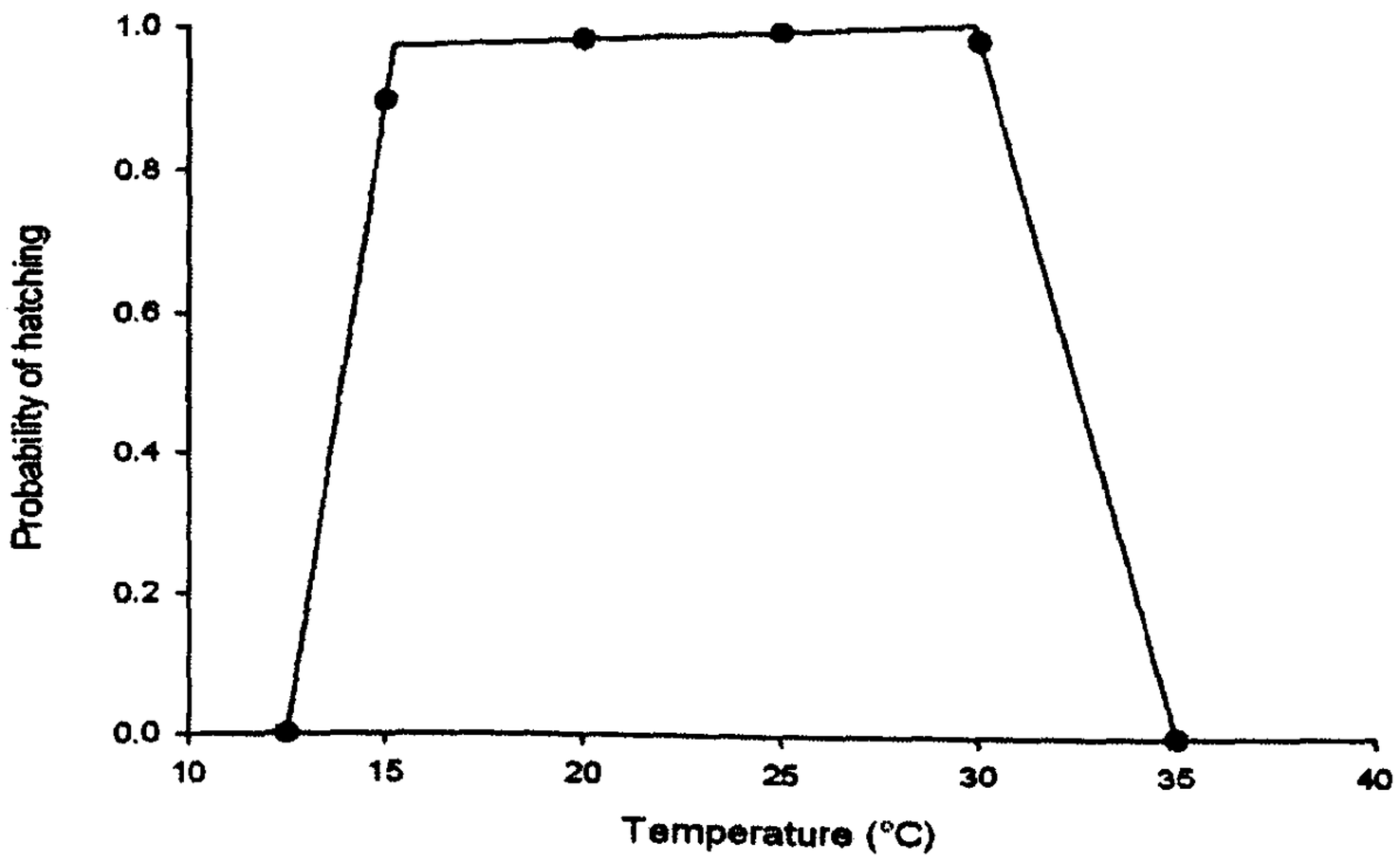

Figure A2.7 Piecewise 3 segment linear relationship between temperature and the probability of *Biomphalaria alexandrina* eggs hatching ($R^2 = 1$).

This produced a series of three equations, describing the three linear regression lines:

$$\text{region1}(t)=\frac{(1.48E-024*(15.2-t)+0.97*(t-t1))}{15.2-t1} \quad \text{A2.3}$$

$$\text{region2}(t)=\frac{(0.97*(29.9-t)+(t-15.2))}{29.9-15.2} \quad \text{A2.4}$$

$$\text{region3}(t)=\frac{((t3-t)-2.01E-26*(t-29.9))}{t3-29.9} \quad \text{A2.5}$$

If t <= 15.2079, use region1(t)

If t <= 29.8886, use region2(t)

Otherwise use region3(t)

where t1 = min(t) and t3 = max(t).

Table A2.7 Relationship between temperature and the hatching probability of *Biomphalaria alexandrina* eggs.

Temperature (°C)	% not hatching	Probability of hatching
12.5	100	0
15	10.5	0.9
20	2.1	0.98
25	1.2	0.99
30	2.3	0.98
35	100	0
18		0.93*
23		1*
29		0.91*
34		0.24*

A2.4 INFECTION RATES

1) Miracidia infection rate (β_S)

The infection rate of miracidia kept at different temperatures was documented by Anderson *et al.* (Anderson *et al.* 1982). This study exposed snails to miracidia in 5ml water and so these values were first converted to rates per 2L to correspond with the data obtained in Chapter 4. The parameter estimates for the model were then extrapolated from the quadratic relationship shown in Fig. A2.8.

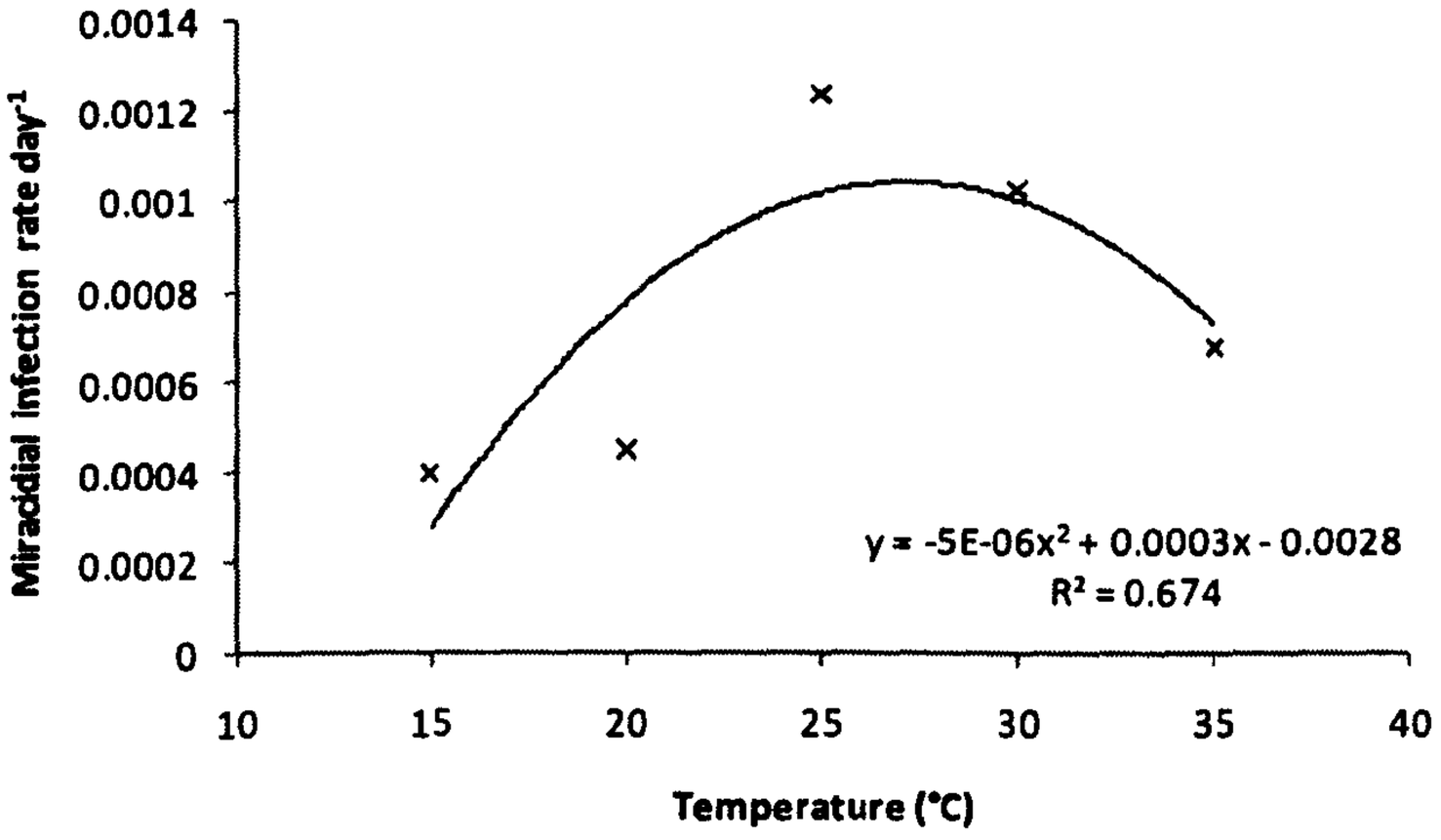

Figure A2.8. The relationship between temperature and the daily miracidia infection rate.

Table A2.8 Daily miracidia infection rates and the extrapolated values denoted by an asterisk.

Temperature (°C)	Infection rate $5ml^{-1}$	Infection rate $2L^{-1}$
15	0.16	0.0004
20	0.18	0.00045
25	0.495	0.0012
30	0.41	0.0010
35	0.27	0.00068
18		0.00057*
23		0.00089*
29		0.00094*
34		0.00068*

2) Cercarial infection rate (β_H)

The cercarial infection rates were described in Appendix A1 and were used in the same way to determine the values for the model parameters (Table A2.9 and Fig. A2.9). These data represent the best estimate available although they do not incorporate water contact patterns.

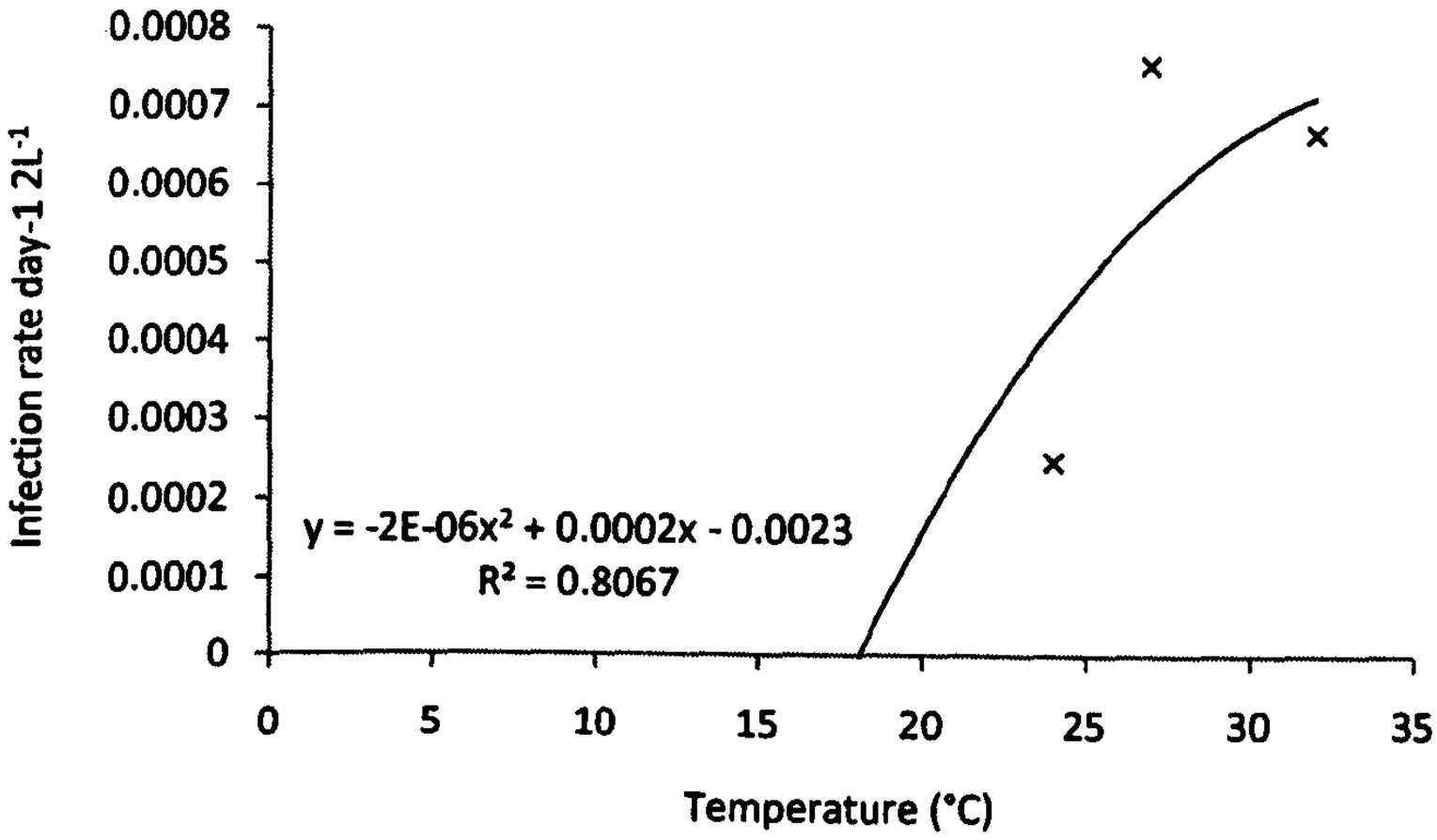

Figure A2.9 Relationship between temperature and the infection rate of cercariae.

Table A2.9 The infection rate of cercariae determined for 2L water.

Temperature (°C)	Infection rate $2L^{-1}$ day^{-1}
24	0.0002435
27	0.000749
32	0.000662
18	0.0000275
23	0.0001025
29	0.0001925
34	0.0002675

Table A2.10 Summary of the parameter estimates for the models used in Chapter 5.

Parameter	Definition	18°C	23°C	29°C	34°C	Source
δ_P	Adult schistosomes death rate	0.00055	0.00055	0.00055	0.00055	(Feng *et al.* 2004)
λ_M	Net miracidial production rate	250	250	250	250	(Cheever and Anderson 1971; Cheever and Powers 1971; Powers and Cheever 1972)
β_S	Miracidia infection rate	0.00057	0.00089	0.00094	0.00068	(Anderson *et al.* 1982)
δ_M	Miracidia death rate	2.23	2.31	2.95	3.93	(Anderson *et al.* 1982)
σ	Within-snail schistosome maturation rate	0.016	0.030	0.047	0.061	(Foster 1964)
a_S	Uninfected snail egg laying rate	3.38	12.56	6.48	2.52	Chapter 3
a_L	Latent snail egg-laying rate	11.18	10.18	8.71	2.12	Chapter 3
a_I	Infected snail egg-laying rate	3.83	2.22	0.093	0.009	Chapter 3
θ_E	Snail hatching rate	0.064	0.091	0.12	0.13	(El Hassan 1974)
δ_E	Snail egg mortality rate	0	0	0	0	
ν	Probability of hatching	0.93	1	0.91	0.24	(El Hassan 1974)
θ_S	Snail maturation rate	0.017	0.026	0.014	0.011	(El Hassan 1974)
δ_J	Snail juvenile mortality rate	0.0019	0.0028	0.0092	0.019	(El Hassan 1974)
δ_S	Uninfected snail adult mortality rate	0.01	0.0095	0.0071	0.0071	Chapter 3
δ_L	Latent snail mortality	0.01	0.0067	0.011	0.013	Chapter 3
δ_I	Infected snail mortality	0.0026	0.02	0.0038	0.006	Chapter 3
q	Strength of density dependence acting on the snail population (for Model 1, Chapter 5)	0.01	0.01	0.01	0.01	
qU	Strength of density dependence on uninfected snail population (for Model 2, Chapter 5)	0.045	0.045	0.045	0.045	Chapter 4
qI	Strength of density dependence on infected snail population (for Model 2, Chapter 5)	0.07	0.07	0.07	0.07	Chapter 4

λ_C	Cercarial production rate	416.33	540.13	378.61	410.83	Chapter 3
β_H	Cercarial infection rate	0.000028	0.0001	0.00019	0.00027	(Stirewalt 1954)
δ_C	Cercarial mortality rate	0.063	0.12	0.18	0.21	(Lawson and Wilson 1980)
k	Parasite aggregation	0.1	0.1	0.1	0.1	(Anderson and May 1982)

Appendix A3

Databases used for the models developed in Chapter 6

A3.1 Temperature and rainfall data

Temperature and rainfall data were acquired from the Food and Agriculture Organisation of the United Nation's CLIMPAG programme (http://www.fao.org/nr/climpag/data_1_en.asp). The FAO provides a global database using national meterological services, published databases and the FAO's own calculations using time-series data. This database, known as FAOCLIM, contains monthly data for up to 14 climatic parameters, including a range of daytime and night-time temperature parameters, rainfall and sunshine hours (Climatic Research Unit, CRU; Global Precipitation Climatology Center, GPCC) over the period 1960-1990. The data used in Chapter 6 were minimum, maximum and mean daytime temperatures and monthly precipitation. The table below shows the availability of data and the effective maximum distance, which is the maximum distance between recording stations:

Variable	Number of stations	Effective Maximum Distance (km^2)
Mean temperature	20828	48.36
Minimum temperature	11550	64.94
Maximum temperature	11544	64.96
Rainfall (mm)	27375	41.71

The database includes 30941 individual series of monthly data for 8 variables, with 60% of these data series relating to temperature and rainfall (Gommes 2004). The datasets are gridded with 0.5 degree resolution and are georeferenced by the FAO.

A3.2 Water temperature data

The annual predicted water temperature values were obtained using estimates by the Center for Resource and Environmental Studies (CRES) and can be interpreted as estimates of standard means for the period of 1920 to 1980 (http://www.fao.org/geonetwork/srv/en/metadata.show?id=24&currTab=simple). The data formed a grid layer comprising 1450x1380 derivative raster water temperature features with 0.05 degree resolution. The time-series data were translated from the source material in flat ASCII format and translated into Arc-Grid format for analysis and visualisation. The base grid was then translated into a shape file format in decimal degrees and this format was used for the analysis in Chapter 6. The layers available include:

Majority Monthly Water Temperature (Annual)

Maximum Monthly Water Temperature (Annual)

Median Monthly Water Temperature (Annual)

Minimum Monthly Water Temperature (Annual)

Minority Monthly Water Temperature (Annual)

Range of Monthly Water Temperature (Annual)

Monthly Water Temperature from January to December

A3.3 Estimating the Normalised Difference Vegetation Index (NDVI)

The SPOT-4 satellite was launched in March 1998 and contains a VEGETATION (VGT) sensor onboard, which is a space-borne optical sensory designed to observe vegetation and land surfaces (Xiao 2004). The VGT sensor has four spectral bands:

Band	Band Range (nm)	Band Energy
B1	430 - 470	Blue
B2	610 - 680	Red
B3	780 - 890	NIR[a]
SWIR	1580 - 1750	MIR[b]

[a] NIR = near-infrared

[b] MIR = medium infrared/short wave infrared

The blue band is used for atmospheric correction and the SWIR band records vegetation cover and leaf moisture content. Three products are produced by the VGT sensor: VGT-P (physical product), VGT-S1 (daily product) and VGT-S10 (10-day combined product). The daily product (VGT-S1) estimates the ground surface reflectance following correction for ozone, aerosols and water vapour using the Simplified Method for Atmospheric Correction (SMAC) algorithm (Rahman and Dedieu 1994). The ten-day

product, which was used in the analysis presented in Chapter 6, was produced by selecting the VGT-S1 pixels with the maximum Normalised Difference Vegetation Index (NDVI) within the defined time-period. This composite approach minimises the effects of cloud cover and atmospheric contamination.

The Global Vegetation Indices collection from University of New Hampshire, EOS-WEBSTER Earth Science Information Partner (http://eos-webster.sr.unh.edu/home.jsp) comprises three global gridded vegetation data products, normalised difference vegetation index (NDVI), enhanced vegetation index (EVI) and land surface water index (LSWI) derived from the VGT sensor onboard the SPOT-4 satellite. The data are derived from 1km data and are 10-day composites of the surface reflectance product (VGT-S10) aggregated into 0.5 degree grid cells. Each data point is an average of the daily cloud-free data over the ten-day period. The extent of the original data range from 75 degrees North to 56 degrees South latitude, and from -180 West to 180 East longitude. Mean value, standard deviation, area (km^2) and total pixel number are given for each half degree data point for all three products. The VGT-S10 data used in the model were collected during April 1998, which is the earliest date available for this dataset.

The NDVI was calculated using the near-infrared and red surface reflectance bands from the VGT-S10 data using the normalized ratio between red and near-infrared (NIR) bands as shown below:

$$NDVI = (NIR - Red) / (NIR + Red)$$

The details of the processing and calculations of vegetation indices are described by Xiao et al (2003). The production and distribution of the NDVI data is provided by Dr Xiangming Xiao, Complex Systems Research Center, Institute for the Study of Earth, Oceans, and Space, Morse Hall, University of New Hampshire, Durham, New Hampshire,

USA. The data are provided free of charge without copyright restrictions, however it is obligatory to acknowledge the provider for publications.

A3.4 Population data

The African Population Database contains data on administrative units in Africa with the associated population figures (http://na.unep.net/globalpop/africa/). The fourth version of the database was used in this study which contains decadal data on 109,000 administrative units from 1960 onwards (Center for International Earth Science Information Network, Columbia University; and Centro Internacional de Agricultura Tropical, 2004). The national boundaries and coastlines were defined by the political boundaries template of the Digital Chart of the World (DCW). The boundaries and data are correct to within 1-2km. The population figures for each administrative district represent estimated totals for the standardized years 1960, 70, 80, 90 and 2000. As historical population data are not readily available for all African countries at the same time-points, values were interpolated from published figures using the growth rate:

$$r = \frac{\ln\left(\frac{P_2}{P_1}\right)}{t}$$

where r is the average annual rate of growth, P_1 and P_2 are the population totals for two different time periods, and t is the number of years between the two time-points (see, for example, Rogers 1985). The growth rates are then used to calculate an estimate for the standardized year, e.g.

$$P_{1970} = P_{1967}.e^{3r}$$

The population data were checked against the estimates provided by the Population Division of the United Nations (2002) and national official census figures. If estimates were considerably different from the UN estimates, the growth rates were uniformly adjusted to match the UN estimates. The UN population figures were exclusively used in some instances, e.g. if no subnational data are available, or if data were only available at one time-point. The population estimates are subject to numerous sources of error, including misreporting during census, sudden population movements and government failure to disclose data. The timing of the census will also affect the population estimates in areas which experience large migration, war or famine.

The mean resolution of population data in Africa is 16km and the mean population per administrative unit is 7000. However, when you exclude data from South Africa, which comprise 77%of the total dataset, the resolution decreases to 32km and the mean population increases to 28000 people per administrative unit. This example demonstrates the uncertainty in this kind of data and the bias of data towards the more developed countries. However, this database provides the most accurate and comprehensive data on population density to date and are used with full acknowledgement of the limitations.

References

Abdel-Rahman, M. S., M. M. El-Bahy, J. B. Malone, R. A. Thompson and N. M. El Bahy (2001). Geographic information systems as a tool for control program management for schistosomiasis in Egypt. *Acta Tropica* **79**(1): 49-57.

Abellana, R., C. Ascaso, J. Aponte, F. Saute, D. Nhalungo, A. Nhacolo and P. Alonso (2008). Spatio-seasonal modeling of the incidence rate of malaria in Mozambique. *Malaria Journal* **7**.

Allen, E. J. and H. D. Victory (2003). Modelling and simulation of a schistosomiasis infection with biological control. *Acta Tropica* **87**(2): 251-267.

Anderson, R. M. (1978). Regulation Of Host Population-Growth By Parasitic Species. *Parasitology* **76**(APR): 119-157.

Anderson, R. M. (1982). Epidemiology. *Modern Parasitology*. Cox, F. E. G. Oxford, Blackwell Scientific Publications: 204-251.

Anderson, R. M. (1987). Determinants of infection in human schistosomiasis. *Bailliere's Clinical Tropical Medicine and Communicable Diseases* **2**(2): 279-300.

Anderson, R. M. and J. Crombie (1984). Experimental Studies Of Age-Prevalence Curves For *Schistosoma mansoni* Infections In Populations Of *Biomphalaria glabrata*. *Parasitology* **89**(AUG): 79-105.

Anderson, R. M. and R. M. May (1979a). Population Biology Of Infectious-Diseases 1. *Nature* **280**(5721): 361-367.

Anderson, R. M. and R. M. May (1979b). Prevalence Of Schistosome Infections Within Molluscan Populations - Observed Patterns And Theoretical Predictions. *Parasitology* **79**(AUG): 63-94.

Anderson, R. M. and R. M. May (1982). Population dynamics of human helminth infections: control by chemotherapy. *Nature* **297**(5867): 557-563.

Anderson, R. M., May, R.M. (1991). *Infectious Diseases of Humans: Dynamics and Control.* Oxford, Oxford University Press.

Anderson, R. M. and G. F. Medley (1985). Community control of helminth infections of man by mass and selective chemotherapy. *Parasitology* **90**(4): 629-660.

Anderson, R. M., J. G. Mercer, R. A. Wilson and N. P. Carter (1982). Transmission Of *Schistosoma-Mansoni* From Man To Snail - Experimental Studies Of Miracidial Survival And Infectivity In Relation To Larval Age, Water Temperature, Host Size And Host Age. *Parasitology* **85**: 339-360.

Appleton, C. C. (1977). The influence of temperature on the life-cycle and distribution of *Biomphalaria pfeifferi* (Krauss, 1948) in South-Eastern Africa. *International Journal for Parasitology* **7**(5): 335.

Appleton, C. C. and I. M. Eriksson (1984). The influence of fluctuating above-optimal temperature regimes on the fecundity of *Biomphalaria-Pfeifferi* (Mollusca, Planorbidae). *Transactions of the Royal Society of Tropical Medicine and Hygiene* **78**(1): 49-54.

Asaolu, S. O. and I. E. Ofoezie (2003). The role of health education and sanitation in the control of helminth infections. *Acta Tropica* **86**(2-3): 283-294.

Ballabeni, P. (1995). Parasite-Induced Gigantism in a Snail: A Host Adaptation? *Functional Ecology* **9**(6): 887-893.

Barbosa, F. S. and M. V. Coelho (1955). Comportamento das formas larvàlarias de Schistosoma mansoni em Australorbis glabratus (Mollusca, Planorbidae) sujeitos a estivacao. *Publ. Avulsas Inst. Aggeu Magalhaes* **4**: 51-60.

Baudoin, M. (1975). Host Castration As A Parasitic Strategy. *Evolution* **29**(2): 335-352.

Bavia, M. E., L. F. Hale, J. B. Malone, D. H. Braud and S. M. Shane (1999). Geographic information systems and the environmental risk of schistosomiasis in Bahia, Brazil. *American Journal of Tropical Medicine and Hygiene* **60**(4): 566-572.

Bavia, M. E., J. B. Malone, L. Hale, A. Dantas, L. Marroni and R. Reis (2001). Use of thermal and vegetation index data from earth observing satellites to evaluate the risk of schistosomiasis in Bahia, Brazil. *Acta Tropica* **79**(1): 79-85.

Bergquist, N. R. (2001a). A concept for the collection, consolidation and presentation of epidemiological data. *Acta Tropica* **79**(1): 3-5.

Bergquist, N. R. (2001b). Vector-borne parasitic diseases: New trends in data collection and risk assessment. *Acta Tropica* **79**(1): 13-20.

Blair, L. and J. P. Webster (2007). Dose-dependent schistosome-induced mortality and morbidity risk elevates host reproductive effort. *Journal Of Evolutionary Biology* **20**(1): 54-61.

Botros, S., H. Sayed, N. Amer, M. El-Ghannam, J. L. Bennett and T. A. Day (2005). Current status of sensitivity to praziquantel in a focus of potential drug resistance in Egypt. *International Journal for Parasitology* **35**(7): 787-791.

Boyd, H. A., W. D. Flanders, D. G. Addiss and L. A. Waller (2005). Residual spatial correlation between geographically referenced observations: A Bayesian hierarchical modeling approach. *Epidemiology* **16**(4): 532-541.

Brooker, S. (2002). Schistosomes, snails and satellites. *Acta Tropica* **82**(2): 207-214.

Brooker, S. (2007). Spatial epidemiology of human schistosomiasis in Africa: risk models, transmission dynamics and control. *Transactions of the Royal Society of Tropical Medicine and Hygiene* **101**(1): 1-8.

Brooker, S., N. B. Kabatereine, E. M. Tukahebwa and F. Kazibwe (2004). Spatial analysis of the distribution of intestinal nematode infections in Uganda. *Epidemiology and Infection* **132**(6): 1065-1071.

Brooker, S. and E. Michael (2000). The potential of geographical information systems and remote sensing in the epidemiology and control of human helminth infections. *Advances In Parasitology, Vol 47.* **47**: 245-288.

Brooker, S., E. A. Miguel, P. Waswa, R. Namunyu, S. Moulin, H. Guyatt and D. A. P. Bundy (2001). The potential of rapid screening methods for Schistosoma mansoni in western Kenya. *Annals of Tropical Medicine and Parasitology* **95**(4): 343-351.

Brooker, S., M. Rowlands, L. Haller, L. Savioli and D. A. P. Bundy (2000). Towards an atlas of human helminth infection in sub-Saharan Africa: The use of geographical information systems (GIS). *Parasitology Today* **16**(7): 303-307.

Brown, K. M., K. R. Carman and V. Inchausty (1994). Density-dependent influences on feeding and metabolism in a freshwater snail. *Oecologia* **99**(1-2): 158-165.

Carter, N. P., R. M. Anderson and R. A. Wilson (1982). Transmission Of *Schistosoma-Mansoni* From Man To Snail - Laboratory Studies On The Influence Of Snail And Miracidial Densities On Transmission Success. *Parasitology* **85**(OCT): 361-372.

Carter, T. R. (2007). General guidelines on the use of scenario data for climate impact and adaptation assessment, Intergovernmental Panel on Climate Change.

Cheever, A. W. (1968). A Quantitative Post-Mortem Study Of Schistosomiasis Mansoni In Man. *American Journal Of Tropical Medicine And Hygiene* **17**(1).

Cheever, A. W. and L. A. Anderson (1971). Rate of destruction of Schistosoma mansoni eggs in the tissues of mice. *American Journal of Tropical Medicine and Hygiene* **20**(1): 62-68.

Cheever, A. W. and K. G. Powers (1971). Rate of destruction of Schistosoma mansoni eggs and adult worms in the tissues of rhesus monkeys. *American Journal of Tropical Medicine and Hygiene* **20**(1): 69-76.

Chernin, E. (1970). Behavioral Responses Of Miracidia Of *Schistosoma-Mansoni* And Other Trematodes To Substances Emitted By Snails. *Journal Of Parasitology* **56**(2): 287-&.

Chernin, E. and E. H. Michelson (1957). Studies On The Biological Control Of Schistosome-Bearing Snails .3. The Effects Of Population Density On Growth And Fecundity In *Australorbis-Glabratus*. *American Journal Of Hygiene* **65**(1): 57-70.

Chiles, J.-P., Delfiner, P. (1999). *Geostatistics*. New York, Wiley.

Chitsulo, L., D. Engels, A. Montresor and L. Savioli (2000). The global status of schistosomiasis and its control. *Acta Tropica* **77**(1): 41-51.

Christie, J. D., Prentice, M.A. (1978). The relationship between numbers of Schistosoma mansoni daughter sporocysts and miracidia. *Ann Trop Med Parasitol* **72**(2): 197-8.

Cioli, D. (1998). Chemotherapy of schistosomiasis: An update. *Parasitology Today* **14**(10): 418-422.

Clements, A. C. A., A. Garba, M. Sacko, S. Touré, R. Dembelé, A. Landouré, E. Bosque-Oliva, A. F. Gabrielli and A. Fenwick (2008). Mapping the probability of schistosomiasis and associated uncertainty, West Africa. *Emerging Infectious Diseases* **14**(10): 1629-1632.

Clements, A. C. A., N. J. S. Lwambo, L. Blair, U. Nyandindi, G. Kaatano, S. Kinung'hi, J. P. Webster, A. Fenwick and S. Brooker (2006). Bayesian spatial analysis and disease mapping: tools to enhance planning and implementation of a schistosomiasis control programme in Tanzania. *Tropical Medicine & International Health* **11**(4): 490-503.

Clennon, J. A., P. L. Mungai, E. M. Muchiri, C. H. King and U. Kitron (2006). Spatial and temporal variations in local transmission of schistosoma haematobium in

Msambweni, Kenya. *American Journal of Tropical Medicine and Hygiene* **75**(6): 1034-1041.

Coelho, J. R. and F. S. M. Bezerra (2006). The effects of temperature change on the infection rate of *Biomphalaria glabrata* with *Schistosoma mansoni*. *Memorias Do Instituto Oswaldo Cruz* **101**(2): 223-224.

Cohen, J. E. (1977). Mathematical-Models Of Schistosomiasis. *Annual Review Of Ecology And Systematics* **8**: 209-233.

Confalonieri, U., Menne, B., Akhtar, R., Ebi, K.L., Hauengue, M., Kovats, R.S., Revich B., Woodward, A. (2007). Human health. Climate Change 2007: Impacts, Adaptation and Vulnerability. Contribution of Working Group II to the Fourth Assessment Report of the Intergovernmental Panel on Climate Change. Parry, M. L., Canziani, O.F., Palutikof, J.P., van der Linden, P.J., Hanson, C.E. Cambridge, UK: 391-431.

Craig, M., D. Le Sueur and B. Snow (1999). A climate-based distribution model of malaria transmission in sub-Saharan Africa. *Parasitology Today* **15**(3): 105-111.

Crawley, M. J. (2007). *The R Book*. Silwood Park, John Wiley & Sons, Ltd.

Crews, A. E. and T. P. Yoshino (1989). *Schistosoma-Mansoni* - Effect Of Infection On Reproduction And Gonadal Growth In *Biomphalaria-Glabrata*. *Experimental Parasitology* **68**(3): 326-334.

Cross, E. R. and R. C. Bailey (1984). Prediction of areas endemic for schistosomiasis through use of discriminant analysis of environmental data. *Military Medicine* **149**(1): 28-30.

Cross, E. R., C. Sheffield, R. Perrine and G. Pazzaglia (1984). Predicting areas endemic for schistosomiasis using weather variables and a Landsat data base. *Military Medicine* **149**(10): 542-544.

Damian, R. T., N. D. Greene and K. Fitzgerald Meyer (1976). Schistosoma mansoni in baboons. III. The course and characteristics of infection, with additional

observations on immunity. *American Journal of Tropical Medicine and Hygiene* **25**(2): 299-306.

Danso-Appiah, A. and S. J. De Vlas (2002). Interpreting low praziquantel cure rates of Schistosoma mansoni infections in Senegal. *Trends in Parasitology* **18**(3): 125-129.

Das, P., D. Mukherjee and A. K. Sarkar (2006). A study of schistosome transmission dynamics and its control. *Journal Of Biological Systems* **14**(2): 295-302.

Davies, C. M., J. P. Webster and M. E. J. Woolhouse (2001). Trade-offs in the evolution of virulence in an indirectly transmitted macroparasite. *Proceedings Of The Royal Society Of London Series B-Biological Sciences* **268**(1464): 251-257.

Dekock, K. N. (1993). The Effect Of Exposure To *Schistosoma-Mansoni* On Mortality-Rates Of Cohorts Of Different Ages Of *Biomphalaria-Pfeifferi*. *Folia Parasitologica* **40**(1): 9-12.

Deng, M. (2006). An Anisotropic Model For Spatial Processes *Monash Econometrics and Business Statistics Working Papers*, Monash University, Department of Econometrics and Business Statistics.

Dhunputh, J. (1994). Progress in the control of schistosomiasis in Mauritius. *Transactions of the Royal Society of Tropical Medicine and Hygiene* **88**(5): 507-509.

Diggle, P., R. Moyeed, B. Rowlingson and M. Thomson (2002). Childhood malaria in the Gambia: A case-study in model-based geostatistics. *Journal of the Royal Statistical Society. Series C: Applied Statistics* **51**(4): 493-506.

Diggle, P. J., J. A. Tawn and R. A. Moyeed (1998). Model-based geostatistics. *Journal of the Royal Statistical Society. Series C: Applied Statistics* **47**(3): 299-325.

Dobson, A. (2009). Climate variability, global change, immunity, and the dynamics of infectious diseases. *Ecology* **90**(4): 920-927.

Doumenge, J. P. (1987). Atlas de la répartition mondiale des schistosomiases. Doumenge, J. P., World Health Organization. Parasitic Diseases Programme. : 398.

Dunne, D. W., B. J. Vennervald, M. Booth, S. Joseph, C. M. Fitzsimmons, P. Cahen, R. F. Sturrock, J. H. Ouma, J. K. Mwatha, G. Kimani, H. C. Kariuki, F. Kazibwe, E. Tukahebwa and N. B. Kabatereine (2006). Applied and basic research on the epidemiology, morbidity, and immunology of schistosomiasis in fishing communities on Lake Albert, Uganda. *Transactions of the Royal Society of Tropical Medicine and Hygiene* **100**(3): 216-223.

El-Emam, M. A. and H. Madsen (1982). The effect of temperature, darkness, starvation and various food types on growth, survival and reproduction of *Helisoma-Duryi, Biomphalaria-alexandrina* and *Bulinus-truncatus* (Gastropoda, Planorbidae). *Hydrobiologia* **88**(3): 265-275.

El Hassan, A. A. (1974). Laboratory studies on the direct effect of temperature on *Bulinus truncatus* and *Biomphalaria alexandrina*, the snail intermediate hosts of schistosomes in Egypt. *Folia Parasitologica* **21**(2): 181.

Elkins, D. B., M. Haswell-Elkins and R. M. Anderson (1986). The epidemiology and control of intestinal helminths in the Pulicat Lake region of Southern India. I. Study design and pre- and post-treatment observations on Ascaris lumbricoides infection. *Transactions of the Royal Society of Tropical Medicine and Hygiene* **80**(5): 774-792.

Etges, F. J. and W. Gresso (1965). Effect Of *Schistosoma Mansoni* Infection Upon Fecundity In *Australorbis Glabratus. Journal Of Parasitology* **51**(5): 757-&.

Favre, T. C., T. H. P. Bogea, L. Rotenberg, H. S. Dasilva and O. S. Pieri (1995). Cercarial Emergence Of *Schistosoma-Mansoni* From *Biomphalaria-Glabrata* And *Biomphalaria-Straminea. Memorias Do Instituto Oswaldo Cruz* **90**(5): 565-567.

Feng, Z., A. Eppert, F. A. Milner and D. J. Minchella (2004). Estimation of parameters governing the transmission dynamics of schistosomes. *Applied Mathematics Letters* **17**(10): 1105-1112.

Feng, Z. L., C. C. Li and F. A. Milner (2002). Schistosomiasis models with density dependence and age of infection in snail dynamics. *Mathematical Biosciences* **177**: 271-286.

Fernandez, J. and G. W. Esch (1991). Effect of parasitism on the growth-rate of the pulmonate snail *Helisoma-anceps*. *Journal Of Parasitology* **77**(6): 937-944.

Foster, R. (1964). Effect Of Temperature On Development Of *Schistosoma Mansoni* Sambon 1907 In Intermediate Host. *Journal Of Tropical Medicine And Hygiene* **67**(12): 289.

Fried, B., R. LaTerra and Y. Kim (2002). Emergence of cercariae of *Echinostoma caproni* and *Schistosoma mansoni* from *Biomphalaria glabrata* under different laboratory conditions. *Journal Of Helminthology* **76**(4): 369-371.

Gommes, R., Grieser, J., Bernardi, M. (2004) "FAO agroclimatic databases and mapping tools." *European Society for Agronomy Newsletter*,

Greer, G. J., R. Mimpfoundi, E. A. Malek, A. Joky, E. Ngonseu and R. C. Ratard (1990). Human schistosomiasis in Cameroon. II. Distribution of the snail hosts. *American Journal of Tropical Medicine and Hygiene* **42**(6): 573-580.

Greer, G. J., P. B. Tchounwou, I. Takougang and A. Monkiedje (1996). Field tests of a village-based molluscicide programme for the control of snail hosts of human schistosomes in Cameroon. *Tropical Medicine and International Health* **1**(3): 320-327.

Grieser, J., Gommes, R., Cofield, S., Bernardi, M. (2006). Short Tabular Presentation of Koeppen Classes, The Agromet Group, FAO of the UN: 1-2.

Griffin, M., Couthino, F.A.B., Thomas, J.D. (1988). A schistosomiasis transmission model incorporating concomitant immunity,. *Rev. Bras. Biol.* **48**: 553-563.

Gryseels, B. (2000). Schistosomiasis Vaccines: A Devils' Advocate View. *Parasitology Today* **16**(2): 46-48.

Gryseels, B. and S. J. deVlas (1996). Worm burdens in schistosome infections. *Parasitology Today* **12**(3): 115-119.

Gryseels, B., A. Mbaye, S. J. De Vlas, F. F. Stelma, F. GuissÃ©, L. Van Lieshout, D. Faye, M. Diop, A. Ly, L. A. Tchuem-TchuentÃ©, D. Engels and K. Polman (2001). Are poor responses to praziquantel for the treatment of Schistosoma mansoni infections in Senegal due to resistance? An overview of the evidence. *Tropical Medicine and International Health* **6**(11): 864-873.

Gryseels, B., L. Nkulikyinka and M. H. Coosemans (1987). Field trials of praziquantel and oxamniquine for the treatment of schistosomiasis mansoni in Burundi. *Transactions of the Royal Society of Tropical Medicine and Hygiene* **81**(4): 641-644.

Gurarie, D., King, C.H. (2005). Heterogeneous model of schistosomiasis transmission and long-term control: the combined influence of spatial variation and age-dependent factors on optimal allocation of drug therapy. *Parasitology* **130**: 49-65.

Haas, W., B. Haberl, M. Kalbe and M. Korner (1995). Snail-Host-Finding By Miracidia And Cercariae - Chemical Host Cues. *Parasitology Today* **11**(12): 468-472.

Haas, W., B. Haberl, G. Schmalfuss and M. T. Khayyal (1994). *Schistosoma-Haematobium* Cercarial Host-Finding And Host-Recognition Differs From That Of *Schistosoma-Mansoni*. *Journal Of Parasitology* **80**(3): 345-353.

Hagan, P., C. C. Appleton, G. C. Coles, J. R. Kusel and L. A. Tchuem-TchuentÃ© (2004). Schistosomiasis control: Keep taking the tablets. *Trends in Parasitology* **20**(2): 92-97.

Hairston, N. G. (1961). Suggestions regarding some problems in the evaluation of molluscicides in the field. *Bull. WHO* **25**: 731.

Hales, S., N. de Wet, J. Maindonald and A. Woodward (2002). Potential effect of population and climate changes on global distribution of dengue fever: an empirical model. *Lancet* **360**(9336): 830-834.

Hay, S. I. (2000). An overview of remote sensing and geodesy for epidemiology and public health application. *Advances in Parasitology.* **47:** 1-35.

Hay, S. I. and J. J. Lennon (1999). Deriving meteorological variables across Africa for the study and control of vector-borne disease: A comparison of remote sensing and spatial interpolation of climate. *Tropical Medicine and International Health* **4**(1): 58-71.

Hay, S. I., R. W. Snow and D. J. Rogers (1998). From predicting mosquito habitat to malaria seasons using remotely sensed data: Practice, problems and perspectives. *Parasitology Today* **14**(8): 306-313.

Hisakane, N., M. Kirinoki, Y. Chigusa, M. Sinuon, D. Socheat, H. Matsuda and H. Ishikawa (2008). The evaluation of control measures against Schistosoma mekongi in Cambodia by a mathematical model. *Parasitology International* **57**(3): 379-385.

Holland, C. V., D. L. Taren, D. W. T. Crompton, M. C. Nesheim, D. Sanjur, I. Barbeau, K. Tucker, J. Tiffany and G. Rivera (1988). Intestinal helminthiases in relation to the socioeconomic environment of Panamanian children. *Social Science and Medicine* **26**(2): 209-213.

Hunter, J. M., Rey, L., Chu, K. Y., Adekolu-John, E. O., Mott, K. E. (1993). *Parasitic diseases in water resources development: the need for intersectoral negotiation.* . Geneva, World Health Organization.

Huttly, S. R. A. (1990). The impact of inadequate sanitary conditions on health in developing countries. *World Health Statistics Quarterly* **43**(3): 118-126.

IPCC (2001). Intergovernmental Panel on Climate Change. Climate Change 2001: Third Assessment Report (Volume 1). Press, C. U. Cambridge.

Ishak, M. M., Mohamed, A. M., Wafa, A., Mousa, A. H. and Ayad, N. (1970). Physiological studies on Biomphalaria alexandrina and Bulinus truncatus, the snail vectors of Schistosomiasis *Hydrobiologia* **35**(2).

Ishikawa, H., H. Ohmae, R. Pangilinan, A. Redulla and H. Matsuda (2006). Modeling the dynamics and control of *Schistosoma japonicum* transmission on Bohol island, the Philippines. *Parasitology International* **55**(1): 23-29.

Jones, J. T., P. Breeze and J. R. Kusel (1989). Schistosome Fecundity - Influence Of Host Genotype And Intensity Of Infection. *International Journal For Parasitology* **19**(7): 769-777.

Jordan, P., Webbe, G., Sturrock, R. (1993). *Human schistosomiasis.*. Wallingford, England, CAB.

Kabatereine, N. B., J. Kemijumbi, J. H. Ouma, H. C. Kariuki, J. Richter, H. Kadzo, H. Madsen, A. E. Butterworth, N. Ã˜rnbjerg and B. J. Vennervald (2004). Epidemiology and morbidity of Schistosoma mansoni infection in a fishing community along Lake Albert in Uganda. *Transactions of the Royal Society of Tropical Medicine and Hygiene* **98**(12): 711-718.

Kazembe, L. N., I. Kleinschmidt, T. H. Holtz and B. L. Sharp (2006). Spatial analysis and mapping of malaria risk in Malawi using point-referenced prevalence of infection data. *International Journal of Health Geographics* **5**.

Kazibwe, F., B. Makanga, C. Rubaire-Akiiki, J. Ouma, C. Kariuki, N. B. Kabatereine, M. Booth, B. J. Vennervald, R. F. Sturrock and J. R. Stothard (2006). Ecology of Biomphalaria (Gastropoda: Planorbidae) in Lake Albert, Western Uganda: snail distributions, infection with schistosomes and temporal associations with environmental dynamics. *Hydrobiologia* **568**(1): 433-444.

Kleinschmidt, I., M. Bagayoko, G. P. Y. Clarke, M. Craig and D. Le Sueur (2000). A spatial statistical approach to malaria mapping. *International Journal of Epidemiology* **29**(2): 355-361.

Klumpp, R. K. and K. Y. Chu (1977). Ecological studies of Bulinus rohlfsi, the intermediate host of Schistosoma haematobium in the Volta Lake. *Bulletin of the World Health Organization* **55**(6): 715-730.

Kristensen, T. K., J. B. Malone and J. C. McCarroll (2001). Use of satellite remote sensing and geographic information systems to model the distribution and abundance of snail intermediate hosts in Africa: a preliminary model for *Biomphalaria pfeifferi* in Ethiopia. *Acta Tropica* **79**(1): 73-78.

Kuntz, R. E. (1947). Effect of Light and Temperature on Emergence of *Schistosoma mansoni* Cercariae. *Transactions of the American Microscopical Society* **66**(1): 37-49.

Lande, R., Engen, S., Saether, B.E. (2002). Estimating density dependence in time-series of age-structured populations. *Philos Trans R Soc Lond B Biol Sci.* **357**(1425): 1179-84.

Lawson, J. R. and R. A. Wilson (1980). The Survival Of The Cercariae Of *Schistosoma-Mansoni* In Relation To Water Temperature And Glycogen Utilization. *Parasitology* **81**(OCT): 337-348.

Leonardo, L. R., P. T. Rivera, B. A. Crisostomo, J. N. Sarol, N. C. Bantayan, W. U. Tiu and N. R. Bergquist (2005). A study of the environmental determinants of malaria and schistosomiasis in the Philippines using Remote Sensing and Geographic Information Systems. *Parassitologia* **47**(1): 105-114.

Lewis, F. A., M. A. Stirewalt, C. P. Souza and G. Gazzinelli (1986). Large-Scale Laboratory Maintenance Of *Schistosoma-Mansoni*, With Observations On 3 Schistosome Snail Host Combinations. *Journal Of Parasitology* **72**(6): 813-829.

Loker, E. S. (1983). A Comparative-Study Of The Life-Histories Of Mammalian Schistosomes. *Parasitology* **87**(OCT): 343-369.

Loreau, M. and B. Baluku (1987). Population dynamics of the freshwater snail Biomphalaria pfeifferi in Eastern Zaire. *Journal of Molluscan Studies* **53**: 249-265.

Mabaso, M. L. H., M. Craig, A. Ross and T. Smith (2007). Environmental predictors of the seasonality of malaria transmission in Africa: The challenge. *American Journal of Tropical Medicine and Hygiene* **76**(1): 33-38.

Macdonal.G (1965). Dynamics Of Helminth Infections With Special Reference To Schistosomes. *Transactions Of The Royal Society Of Tropical Medicine And Hygiene* **59**(5): 489-&.

Macdonald, G. (1965). The dynamics of helminth infections, with special reference to schistosomes. *Transactions of the Royal Society of Tropical Medicine and Hygiene* **59**(5): 489-506.

Magnussen, P. (2003). Treatment and re-treatment strategies for schistosomiasis control in different epidemiological settings: a review of 10 years' experiences. *Acta Tropica* **86**(2-3): 243-254.

Mahmoud, A. A. (2001). *Schistosomiasis*, Imperial College Press.

Malenganisho, W. L. M., P. Magnussen, H. Friis, J. Siza, G. Kaatano, M. Temu and B. J. Vennervald (2008). Schistosoma mansoni morbidity among adults in two villages along Lake Victoria shores in Mwanza District, Tanzania. *Transactions of the Royal Society of Tropical Medicine and Hygiene* **102**(6): 532-541.

Malone, J. B., M. S. AbdelRahman, M. M. ElBahy, O. K. Huh, M. Shafik and M. Bavia (1997). Geographic information systems and the distribution of *Schistosoma mansoni* in the Nile delta. *Parasitology Today* **13**(3): 112-119.

Malone, J. B., N. R. Bergquist, O. K. Huh, M. E. Bavia, M. Bernardi, M. M. El Bahy, M. V. Fuentes, T. K. Kristensen, J. C. McCarroll, J. M. Yilma and X. N. Zhou (2001a). A

global network for the control of snail-borne disease using satellite surveillance and geographic information systems. *Acta Tropica* **79**(1): 7-12.

Malone, J. B., J. M. Yilma, J. C. McCarroll, B. Erko, S. Mukaratirwa and X. Y. Zhou (2001b). Satellite climatology and the environmental risk of *Schistosoma mansoni* in Ethiopia and east Africa. *Acta Tropica* **79**(1): 59-72.

Mangal, T. D., S. Paterson and A. Fenton (2008). Predicting the impact of long-term temperature changes on the epidemiology and control of schistosomiasis: a mechanistic model. *PLoS ONE* **3**(1): e1438.

Martens, W. J. M., T. H. Jetten and D. A. Focks (1997). Sensitivity of malaria, schistosomiasis and dengue to global warming. *Climatic Change* **35**(2): 145-156.

Martens, W. J. M., T. H. Jetten, J. Rotmans and L. W. Niessen (1995). Climate-Change And Vector-Borne Diseases - A Global Modeling Perspective. *Global Environmental Change-Human And Policy Dimensions* **5**(3): 195-209.

Mas-Coma, S., Valero, M.A., Bargues, M.D. (2009). Climate change effects on trematodiases, with emphasis on zoonotic fascioliasis and schistosomiasis. *Veterinary Parasitology* **[in press]**.

Mascie-Taylor, C. G. N. and E. Karim (2003). The burden of chronic disease. *Science* **302**(5652): 1921-1922.

May, R. M. (1977). Togetherness among Schistosomes: its effects on the dynamics of the infection. *Mathematical Biosciences* **35**(3-4): 301-343.

May, R. M. and R. M. Anderson (1979). Population Biology Of Infectious-Diseases .2. *Nature* **280**(5722): 455-461.

McCullough, F. S. (1972). The distribution of Schistosoma mansoni and S. haematobium in East Africa. *Tropical and Geographical Medicine* **24**(3): 199-207.

McCullough, F. S., Gayral, P., Duncan, J., Christie, J. D. (1980). Molluscicides in schistosomiasis control. *Bulletin of the World Health Organization* **58**(5): 681-689.

Medley, G., Anderson, R.M. (1985). Density-dependent fecundity in Schistosoma mansoni infections in man. *Trans R Soc Trop Med Hyg.* **79**(4): 532-4.

Moodley, I., I. Kleinschmidt, B. Sharp, M. Craig and C. Appleton (2003). Temperature-suitability maps for schistosomiasis in South Africa. *Annals Of Tropical Medicine And Parasitology* **97**(6): 617-627.

Mouchet, F., A. Theron, P. Bremond, E. Sellin and B. Sellin (1992). Pattern Of Cercarial Emergence Of *Schistosoma-Curassoni* From Niger And Comparison With 3 Sympatric Species Of Schistosomes. *Journal Of Parasitology* **78**(1): 61-63.

Nasell, I. (1977). On transmission and control of schistosomiasis, with comments on Macdonald's model. *Theoretical Population Biology* **12**(3): 335-365.

Ohlweiler, F. P. and T. Kawano (2002). Biomphalaria tenagophila (Orbigny, 1835) (Mollusca): adaptation to desiccation and susceptibility to infection with Schistosoma mansoni Sambon, 1907. *Revista do Instituto de Medicina Tropical de São Paulo* **44**: 191-201.

Ostfeld, R. S. (2009). Climate change and the distribution and intensity of infectious diseases. *Ecology* **90**(4): 903-905.

Ottersen, G., B. Planque, A. Belgrano, E. Post, P. C. Reid and N. C. Stenseth (2001). Ecological effects of the North Atlantic Oscillation. *Oecologia* **128**(1): 1-14.

Pages, J. R. and A. Theron (1990). *Schistosoma-Intercalatum* From Cameroon And Zaire - Chronobiological Differentiation Of Cercarial Emergence. *Journal Of Parasitology* **76**(5): 743-745.

Pan, C. T. (1965). Studies On Host-Parasite Relationship Between *Schistosoma Mansoni* And Snail *Australorbis Glabratus*. *American Journal Of Tropical Medicine And Hygiene* **14**(6): 931-&.

Patz, J. A., D. Campbell-Lendrum, T. Holloway and J. A. Foley (2005). Impact of regional climate change on human health. *Nature* **438**(7066): 310-317.

Patz, J. A., T. K. Graczyk, N. Geller and A. Y. Vittor (2000). Effects of environmental change on emerging parasitic diseases. *International Journal For Parasitology* **30**(12-13): 1395-1405.

Peel, M. C., B. L. Finlayson and T. A. McMahon (2007). Updated world map of the Koeppen-Geiger climate classification. *Hydrology and Earth System Sciences* **11**(5): 1633-1644.

Pfluger, W. (1980). Experimental epidemiology of Schistosomiasis. 1. The Pre-patent period and cercarial production of *Schistosoma-mansoni* in *Biomphalaria* snails at various constant temperatures. *Zeitschrift Fur Parasitenkunde-Parasitology Research* **63**(2): 159-169.

Pimentel-Souza, F., N. D. Barbosa and D. F. Resende (1990). Effect of temperature on the reproduction of the snail *Biomphalaria glabrata*. *Brazilian Journal of Medical and Biological Research* **23**(5): 441.

Polderman, A. M. (1984). Cost-effectiveness of different ways of controlling intestinal schistosomiasis: A case study. *Social Science & Medicine* **19**(10): 1073-1080.

Poulin, R. (2006). Global warming and temperature-mediated increases in cercarial emergence in trematode parasites. *Parasitology* **132**: 143-151.

Powers, K. G. and A. W. Cheever (1972). Comparison of geographical strains of Schistosoma mansoni in the rhesus monkey. *Bulletin of the World Health Organization* **46**(3): 295-300.

Prah, S. K. and C. James (1978). The influence of physical factors on the behavior and infectivity of miracidia of Schistosoma mansoni and S. haematobium. II. Effect of light and depth. *Journal of Helminthology* **52**(2): 115-120.

Purnell, R. E. (1966). Host-Parasite Relationships In Schistosomiasis .3. Effect Of Temperature On Survival Of *Schistosoma Mansoni* Miracidia And On Survival And Infectivity Of *Schistosoma Mansoni* Cercariae. *Annals Of Tropical Medicine And Parasitology* **60**(2): 182-&.

Rahman, H. and G. Dedieu (1994). SMAC: a simplified method for the atmospheric correction of satellite measurements in the solar spectrum. *International Journal of Remote Sensing* **15**(1): 123-143.

Raso, G., B. Matthys, E. K. N'Goran, M. Tanner, P. Vounatsou and J. Utzinger (2005). Spatial risk prediction and mapping of Schistosoma mansoni infections among schoolchildren living in western CÃ´te d'Ivoire. *Parasitology* **131**(1): 97-108.

Robinson, T. P. (2000). Spatial statistics and geographical information systems in epidemiology and public health. *Advances in Parasitology.* **47:** 81-128.

Rogers, D. J. and S. E. Randolph (1991). Mortality-Rates And Population-Density Of Tsetse-Flies Correlated With Satellite Imagery. *Nature* **351**(6329): 739-741.

Rogers, D. J. and S. E. Randolph (1993). Distribution Of Tsetse And Ticks In Africa - Past, Present And Future. *Parasitology Today* **9**(7): 266-271.

Rogers, D. J., S. E. Randolph, R. W. Snow and S. I. Hay (2002). Satellite imagery in the study and forecast of malaria. *Nature* **415**(6872): 710-715.

Rogers, D. J. and B. G. Williams (1993). Monitoring Trypanosomiasis In Space And Time. *Parasitology* **106**: S77-S92.

Scherrer, A. U., M. K. Sjöberg, A. Allangba, M. Traoré, L. K. Lohourignon, A. B. Tschannen, E. K. N'Goran and J. Utzinger (2009). Sequential analysis of helminth egg output

in human stool samples following albendazole and praziquantel administration. *Acta Tropica* **109**(3): 226-231.

Seto, E., B. Xu, S. Liang, P. Gong, W. Wu, G. Davis, D. Qiu, X. Gu and R. Spear (2002). The use of remote sensing for predictive modeling of schistosomiasis in China. *Photogrammetric Engineering and Remote Sensing* **68**(2): 167-174.

Shiff, C. J. (1964). Studies on Bulinus (Physopsis) globosus in Rhodesia. 3. Bionomics of a natural population existing in a temporary habit. *Annals of Tropical Medicine and Parasitology* **58**: 240-255.

Shuval, H. I., R. L. Tilden, B. H. Perry and R. N. Grosse (1981). Effect of investments in water supply and sanitation on health status: A threshold-saturation theory. *Bulletin of the World Health Organization* **59**(2): 243-248.

Sibly, R. M., Barker, D., Denham, M.C., Hone, J., Pagel, M. (2005). On the regulation of populations of mammals, birds, fish, and insects. *Science* **309**(5734): 607-10.

Smith, G., Guerrero, J. (1993). Mathematical models for the population biology of Ostertagia ostertagi and the significance of aggregated parasite distributions. *Vet Parasitol.* **46**: 243-57.

Snow, J. (1856). The mode of propagation of cholera. *The Lancet* **67**(1694): 184.

Stenseth, N. C., A. Mysterud, G. Ottersen, J. W. Hurrell, K. S. Chan and M. Lima (2002). Ecological effects of climate fluctuations. *Science* **297**(5585): 1292-1296.

Stensgaard, A. S., A. JÃ‚rgensen, N. B. Kabatereine, J. B. Malone and T. K. Kristensen (2005). Modeling the distribution of Schistosoma mansoni and host snails in Uganda using satellite sensor data and Geographical Information Systems. *Parassitologia* **47**(1): 115-125.

Stirewalt, M. A. (1954). Effect Of Snail Maintenance Temperatures On Development Of *Schistosoma-Mansoni*. *Experimental Parasitology* **3**(6): 504-516.

Sturrock, B. M. (1966a). Influence Of Infection With *Schistosoma Mansoni* On Growth Rate And Reproduction Of *Biomphalaria Pfeifferi*. *Annals Of Tropical Medicine And Parasitology* **60**(2): 187-&.

Sturrock, B. M. and R. F. Sturrock (1970). Laboratory Studies Of Host-Parasite Relationship Of *Schistosoma-Mansoni* And *Biomphalaria-Glabrata* From St-Lucia, West-Indies. *Annals Of Tropical Medicine And Parasitology* **64**(3): 357-&.

Sturrock, R. F. (1966b). The influence of temperature on the biology of Biomphalaria pfeifferi (Krauss), an intermediate host of Schistosoma mansoni. *Annals of Tropical Medicine and Parasitology* **60**(1): 100-105.

Sturrock, R. F. (1973a). Field studies on the population dynamics of *Biomphalaria-glabrata* intermediate host of *Schistosoma-mansoni* on the West-Indian island of St-Lucia. *International Journal for Parasitology* **3**(2): 165-174.

Sturrock, R. F. (1973b). Field studies on the transmission of Schistosoma-mansoni and the bionomics of its intermediate host Biomphalaria-glabrata on St-Lucia West-Indies. *International Journal for Parasitology* **3**(2): 175-194.

Sturrock, R. F. (1993). The intermediate hosts and host-parasite relationships. *Human Schistosomiasis*. Jordan, P. W., G.; Sturrock, R.F. Wallingford, CAB International.

Sturrock, R. F., G. Barnish and E. S. Upatham (1974). Snail findings from an experimental molluscicide programme to control Schistosoma mansoni transmission on St. Lucia. *International Journal for Parasitology* **4**(3): 231-240.

Sturrock, R. F., R. K. Klumpp, J. H. Ouma, A. E. Butterworth, A. J. C. Fulford, H. C. Kariuki, F. W. Thiongo and D. Koech (1994). Observations On The Effects Of Different Chemotherapy Strategies On The Transmission Of *Schistosoma-Mansoni* In Machakos District, Kenya, Measured By Long-Term Snail Sampling And Cercariometry. *Parasitology* **109**: 443-453.

Sturrock, R. F. and E. S. Upatham (1973). An investigation of the interactions of some factors influencing the infectivity of Schistosoma-mansoni miracidia to Biomphalaria-glabrata. *International Journal for Parasitology* **3**(1): 35-41.

Sukwa, T. Y., Bulsara, M.K., Wurapa, F.K. (1986). The relationship between morbidity and intensity of Schistosoma mansoni infection

in a rural Zambian community. *International Journal of Epidemiology* **15**(2): 248-51.

Tanser, F. C., B. Sharp and D. Le Sueur (2003). Potential effect of climate change on malaria transmission in Africa. *Lancet* **362**(9398): 1792-1798.

TDR (2000). Artemether protects against schistosome infection. *TDR News* **62**: 13.

Theron, A. (1984). Early And Late Shedding Patterns Of *Schistosoma-Mansoni* Cercariae - Ecological Significance In Transmission To Human And Murine Hosts. *Journal Of Parasitology* **70**(5): 652-655.

Thomas, J. D. (1987). A holistic view of schistosomiasis and snail control. *Memorias do Instituto Oswaldo Cruz* **82 Suppl 4**: 183-192.

Thomas, J. D. and M. Benjamin (1974). The effects of population density on growth and reproduction of Biomphalaria glabrata (Say) (Gastropoda: Pulmonata). *Journal of Animal Ecology* **43**: 31-50.

Thomas, J. D., M. Benjamin, A. Lough and R. H. Aram (1974). The effects of calcium in the external environment on the growth and natality rates of Biomphalaria glabrata (Say). *J. Anim. Ecol.* **43**: 839-860.

Thornhill, J. A., J. T. Jones and J. R. Kusel (1986). Increased Oviposition And Growth In Immature *Biomphalaria-Glabrata* After Exposure To *Schistosoma-Mansoni*. *Parasitology* **93**: 443-450.

Touassem, R., Théron, A. (1989). Schistosoma rodhaini: dynamics and cercarial production for mono- and pluri-miracidial infections of Biomphalaria glabrata. *J Helminthol.* **63**(2): 79-83.

Upatham, E. S. (1973). The effect of water temperature on the penetration and development of St. Lucian *Schistosoma mansoni* miracidia in local *Biomphalaria glabrata*. *Southeast Asian J Trop Med Public Health.* **4**(3): 367-70.

Utzinger, J., E. K. N'Goran, A. N'Dri, C. Lengeler, X. Shuhua and M. Tanner (2000). Oral artemether for prevention of Schistosoma mansoni infection: Randomised controlled trial. *Lancet* **355**(9212): 1320-1325.

Utzinger, J., X. Shuhua, E. K. N'Goran, R. Bergquist and M. Tanner (2001). The potential of artemether for the control of schistosomiasis. *International Journal for Parasitology* **31**(14): 1549-1562.

Vennervald, B. J. and D. W. Dunne (2004). Morbidity in schistosomiasis: an update. *Current Opinion In Infectious Diseases* **17**(5): 439-447.

Watts, S., K. Khallaayoune, R. Bensefia, H. Laamrani and B. Gryseels (1998). The study of human behavior and schistosomiasis transmission in an irrigated area in Morocco. *Social Science & Medicine* **46**(6): 755-765.

Webbe, G. (1964). Biology of intermediate hosts of schistosomiasis, with particular reference to control of transmission. *Ann. Trop. Med. Parasitol.* **58**: 228-233.

Webbe, G. and R. F. Sturrock (1964). Laboratory tests of some new molluscicides in Tanganyika. *Am. Trop. Med. Parasit.* **58**: 234-239.

Webster, J. P., C. M. Gower and L. Blair (2004). Do hosts and parasites coevolve? Empirical support from the *Schistosoma* system. *American Naturalist* **164**(5): S33-S51.

Webster, J. P. and M. E. J. Woolhouse (1999). Cost of resistance: relationship between reduced fertility and increased resistance in a snail-schistosome host-parasite system. *Proceedings Of The Royal Society Of London Series B-Biological Sciences* **266**(1417): 391-396.

WHO (2002). Prevention and control of schistosomiasis and soil-transmitted helminthiasis; report of a WHO Expert Committee. . *WHO Technical Report Series No. 912*. Geneva, World Health Organization.

WHO (2003). WHO. Climate Change and Human Health - Risks and Responses. Geneva, World Health Organization.

Wilkins, H. A. (1989). Reinfection After Treatment Of Schistosome Infections. *Parasitology Today* **5**(3): 83-88.

Williams, G. M., A. C. Sleigh, Y. S. Li, Z. Feng, G. M. Davis, H. G. Chen, A. G. P. Ross, R. Bergquist and D. P. McManus (2002). Mathematical modelling of *schistosomiasis japonica*: comparison of control strategies in the People's Republic of China. *Acta Tropica* **82**(2): 253-262.

Woolhouse, M. E. J. (1989). The Effect Of Schistosome Infection On The Mortality-Rates Of *Bulinus-Globosus* And *Biomphalaria-Pfeifferi*. *Annals Of Tropical Medicine And Parasitology* **83**(2): 137-141.

Woolhouse, M. E. J. (1991). On The Application Of Mathematical-Models Of Schistosome Transmission Dynamics. 1. Natural Transmission. *Acta Tropica* **49**(4): 241-270.

Woolhouse, M. E. J. (1992). On The Application Of Mathematical-Models Of Schistosome Transmission Dynamics. 2. Control. *Acta Tropica* **50**(3): 189-204.

Woolhouse, M. E. J. (1994). Epidemiology of Human Schistosomes. *Parasitic and Infectious Diseases : Epidemiology and Ecology*. Scott, M. E., Smith, G., Academic Press, Inc.: 197-217.

Woolhouse, M. E. J. and S. K. Chandiwana (1990a). The Epidemiology Of Schistosome Infections Of Snails - Taking The Theory Into The Field. *Parasitology Today* **6**(3): 65-70.

Woolhouse, M. E. J. and S. K. Chandiwana (1990b). Temporal Patterns In The Epidemiology Of Schistosome Infections Of Snails - A Model For Field Data. *Parasitology* **100**: 247-253.

Woolhouse, M. E. J. and S. K. Chandiwana (1992). A Further Model For Temporal Patterns In The Epidemiology Of Schistosome Infections Of Snails. *Parasitology* **104**: 443-449.

Xiao, X., Braswell, B., Zhang, Q., Boles, S., Frolking, S., Moore, B. (2003). Sensitivity of vegetation indices to atmospheric aerosols: Continental-scale observations in Northern Asia. *Remote Sensing of Environment* **84**: 385-392.

Xiao, X., Hollinger, D., Aber, J., Goltz, M., Davidson, E., Zhang, Q., Moore, B. (2004). Satellite-based modeling of gross primary production in an evergreen needleleaf forest. *Remote Sensing of Environment:* **89**: 519-534.

Yang, G. J., A. Gemperli, P. Vounatsou, M. Tanner, X. N. Zhou and J. Utzinger (2006). A growing degree-days based time-series analysis for prediction of Schistosoma japonicum transmission in Jiangsu province, China. *American Journal of Tropical Medicine and Hygiene* **75**(3): 549-555.

Yang, G. J., P. Vounatsou, X. N. Zhou, M. Tanner and J. Utzinger (2005a). A Bayesian-based approach for spatio-temporal modeling of county level prevalence of *Schistosoma japonicum* infection in Jiangsu province, China. *International Journal For Parasitology* **35**(2): 155-162.

Yang, G. J., P. Vounatsou, X. N. Zhou, M. Tanner and J. Utzinger (2005b). A potential impact of climate change and water resource development on the transmission of Schistosoma japonicum in China. *Parassitologia* **47**(1): 127-134.

Yang, H. M. (2003). Comparison between schistosomiasis transmission modelings considering acquired immunity and age-structured contact pattern with infested water. *Mathematical Biosciences* **184**(1): 1-26.

Yang, H. M. and A. C. Yang (1998). The stabilizing effects of the acquired immunity on the schistosomiasis transmission modeling - The sensitivity analysis. *Memorias Do Instituto Oswaldo Cruz* **93**: 63-73.

Zhao, R., Milner, F.A. (2008). A Mathematical model of Schistosoma mansoni in Biomphalaria glabrata with control strategies. . *Bulletin of Mathematical Biology* **70**(7): 1886-1905.

Zhou, X., L. Dandan, Y. Huiming, C. Honggen, S. Leping, Y. Guojing, H. Qingbiao, L. Brown and J. B. Malone (2002). Use of landsat TM satellite surveillance data to measure the impact of the 1998 flood on snail intermediate host dispersal in the lower Yangtze River Basin. *Acta Tropica* **82**(2): 199-205.

Zhou, X. N., J. B. Malone, T. K. Kristensen and N. R. Bergquist (2001). Application of geographic information systems and remote sensing to schistosomiasis control in China. *Acta Tropica* **79**(1): 97-106.

Zhou, X. N., L. Y. Wang, M. G. Chen, X. H. Wu, Q. W. Jiang, X. Y. Chen, Z. Jiang and J. Utzinger (2005). The public health significance and control of schistosomiasis in China - Then and now. *Acta Tropica* **96**(2-3): 97-105.

Zhou, X. N., G. J. Yang, K. Yang, X. H. Wang, Q. B. Hong, L. P. Sun, J. B. Malone, T. K. Kristensen, N. R. Bergquist and J. Utzinger (2008). Potential impact of climate change on schistosomiasis transmission in China. *American Journal of Tropical Medicine and Hygiene* **78**: 188-194.